ADAPTIVE POWER SYSTEM CONTROL

by

Edgardo Celestino Manansala

Dissertation submitted to the Faculty of the

Virginia Polytechnic Institute and State University

in partial fulfillment of the requirements for the degree of

Doctor of Philosophy

in

Electrical Engineering

APPROVED:

Prof. Arun Phadke, Chairman

Prof. Saifur Rahman

Prof. Kwa-Sur Tam

Prof. William Baumann

Prof. Werner Kohler

August 1989

Blacksburg, Virginia

ADAPTIVE POWER SYSTEM CONTROL

by

Edgardo Celestino Manansala

Prof. Arun Phadke, Chairman

Electrical Engineering

(ABSTRACT)

This work presents a centralized control scheme applied to a power system. The scheme has adaptive characteristics which allow the controller to keep track of the changing power system operating point and to control nonlinear functions of state variables. Feedback to the controller is obtained from phasor measurements at chosen power system buses, generator field voltage measurements, and state estimators. Control effort is aimed at minimizing the oscillations and influencing the power system state trajectory through the control of linear and nonlinear functions of state variables during a power system disturbance.

The main contributions of this dissertation are the simultaneous introduction and utilization of measurement based terms in the state and output equations in the derivation and implementation of the control law, the study of limits on controller performance as the state residual vector becomes very large, and the simulation of the performance of local state estimators to prove the need for faster phasor measurement systems.

The test system is a hypothetical 39-Bus AC power system consisting of typical components which have been sufficiently modelled for the simulation of power system performance in a dynamic stability study.

Acknowledgements

"Vanity obscures good things."

-Thomas Aquinas

The author would like to thank his academic advisor, Professor Arun G. Phadke, for the full support he received during the entire duration of this research work. He would also like to thank the four other members of his advisory committee for their genuine interest in the research work : Professors Saifur Rahman, Kwa-Sur Tam and William Baumann of the Electrical Engineering Department and Professor Werner Kohler of the Mathematics Department. The help of of Cornell University in dealing with some theoretical aspects of the investigation is also truly appreciated.

This work was sponsored by the National Science Foundation.

Table of Contents

List of Illustrations

List of Tables

Chapter 1

Introduction

The dynamic stability of an electric power system can be enhanced substantially through the application of appropriate control input signals during a disturbance. The control input signals are normally applied to the excitation and speed-governing systems of each generator. An adaptive control scheme will be studied in this work. An essential component of this planned adaptive scheme are the phasor measurement systems located at appropriately chosen power system buses. Real-time phasor measurements performed on the power system allow the presently existing power system state to be known at any time. Results of these phasor measurements, together with those of the state estimators and field voltage measurement systems, are brought to a power system control center through fast communication links. The control input signals are then computed by a controller situated in this centralized location and brought back to the appropriate control elements.

This work is about a new development on optimal controllers applied to a nonlinear power system. Much of the past work on optimal controllers assumed a linear regulator acting on a very small power system. In the present work, a system-wide centralized controller acting on a reasonably large AC power system will be studied. The controller has mechanisms to keep track of changing power system operating point and to control nonlinear functions of the state variables. Unlike the optimal regulator approach, the present formulation has adaptive characteristics which allow the postfault steady-state condition of the power system to be different from the prefault operating point.

The optimal controller assumes the following system equations :

$$\dot{\underline{X}}(t) = \underline{A}\underline{X}(t) + \underline{B}\underline{U}(t) + \underline{f}(t)$$

$$\underline{Y}(t) = \underline{C}\underline{X}(t) + \underline{s}(t)$$

The cost function is

$$J(\underline{U}) = \frac{1}{2}\int_{t_o}^{\infty} [\underline{U}^T\underline{R}\underline{U} + (\underline{Y} - \underline{Y}_d)^T\underline{Q}(\underline{Y} - \underline{Y}_d)]\ \mathrm{dt}$$

where $\underline{Y}_d(t)$ is the target trajectory for the output vector $\underline{Y}(t)$.

A recent work [77] has taken into account the existence of the state residual $\underline{f}(t)$ but with $\underline{s}(t) = \underline{0}$. With the introduction of the output residual $\underline{s}(t)$, control of nonlinear power system state variables and their functions become possible. The residual vectors $\underline{f}(t)$ and $\underline{s}(t)$ represent power system nonlinearities (such as the higher order terms in the Taylor's series expansion) and possible changes in power system configuration and operating point during a disturbance.

Using the results of phasor and field voltage measurements, the value of any element of $\underline{X}(t)$ at any time is known either from direct measurements or from state estimators which make use of the measurements. Mathematical models of the system components are assumed to be known and are used to compute the real-time value of $\dot{\underline{X}}(t)$. Elements of $\underline{Y}(t)$ are measurable quantities (such as bus voltages) which are to be controlled, hence, they are also known in real time. The residual terms are thereby effectively "measured" through the power system equations :

$$\underline{f}(t) = \dot{\underline{X}}(t) - \underline{A}\underline{X}(t) - \underline{B}\underline{U}(t)$$

$$\underline{s}(t) = \underline{Y}(t) - \underline{C}\underline{X}(t)$$

Two figures illustrate the control scheme to be studied in this work. Figure 1.1 is drawn from a functional viewpoint while Figure 1.2 is drawn from a more dynamical perspective. In both cases, a centralized controller is assumed which continually communicates with the control elements and measurement systems through fast communication links [67]. The control elements consist of devices which apply the control input signals to the generator excitation and speed-governing systems. The measurement systems consist of the phasor and field voltage measurements, and the state estimators whose outputs are used for feedback to the controller.

In this work, controller performance will be evaluated and studied through simulation. A typical, medium-sized AC power system will be assumed in the simulations. Subsequent chapters will deal with some details pertaining to the simulation procedure itself and with some important questions related to the centralized controller and the state estimators. In many of the simulation studies in this work, the output vector $\underline{Y}$ will contain nonlinear functions of the controller state variables (i.e., generator terminal

voltages). In the chapter on the centralized controller, power system response to various types of optimal controllers will be studied. Variations are mainly in the choice of variables for the control input vector $\underline{U}(t)$, for the state vector $\underline{X}(t)$, and for the output vector $\underline{Y}(t)$. In two cases, a different feedback matrix $\underline{A}$ was chosen to induce large state residual terms. In another case, power system response to several local controllers (instead of one centralized controller) is dealt with. In two more cases, the effects of varying the elements of the $\underline{Q}$ matrix in the cost function are studied. In the chapter on state estimators, interaction between the centralized controller and decentralized state estimators is assumed. As stated earlier, feedback to the centralized controller is provided by the measurement systems and the output of the state estimators. An interesting question which arises is the effect of reducing the phasor measurement rate on the controller feedback and power system response. This question is motivated by the upper limits on measurement rates imposed by presently existing measurement systems. The chapter on state estimators will determine if detrimental effects are introduced by the reduced phasor measurement rate. The last chapter of this work will deal with conclusions based on the results of this work and some recommendations for future work.

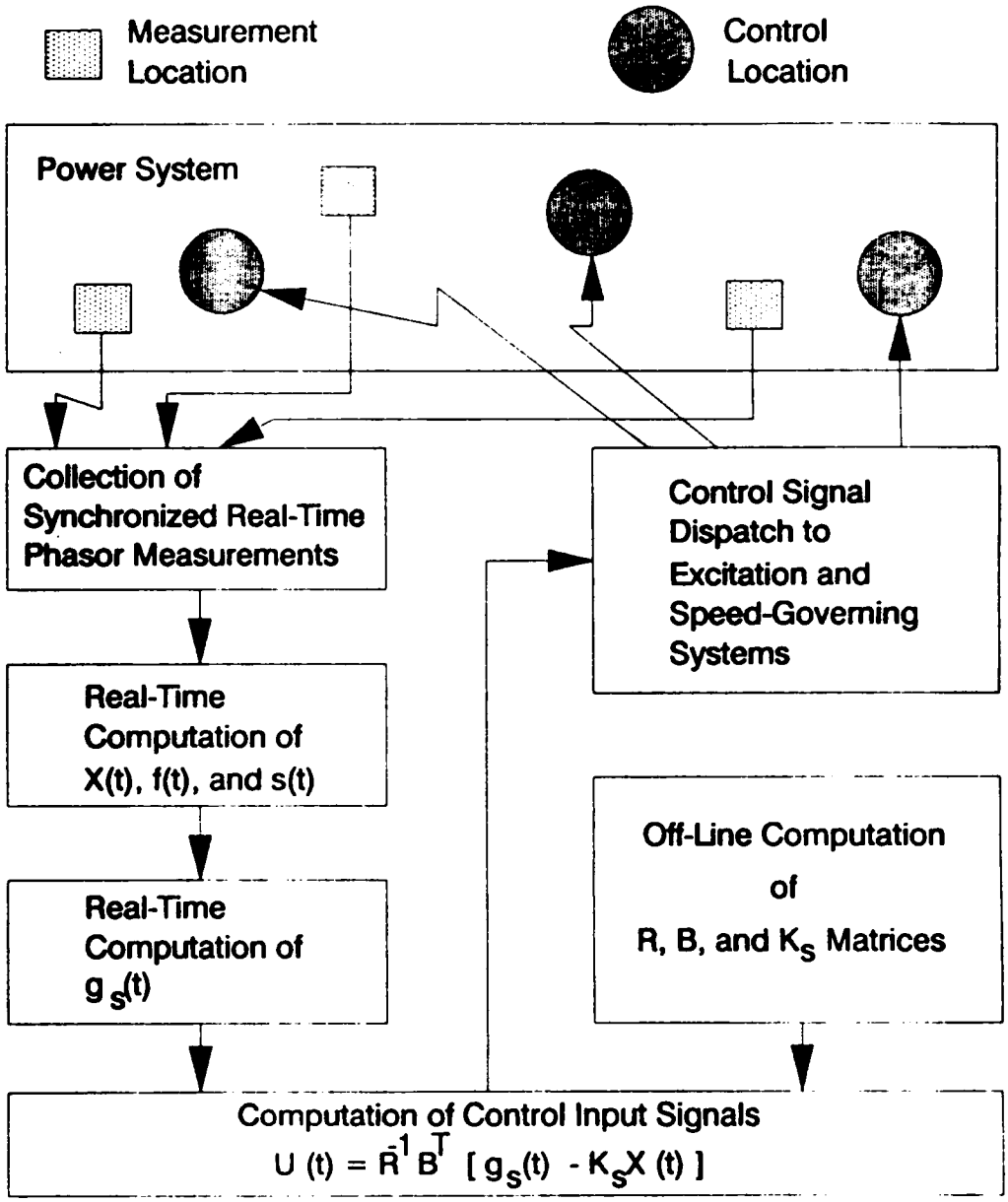

Figure 1.1. Centralized Controller Representation

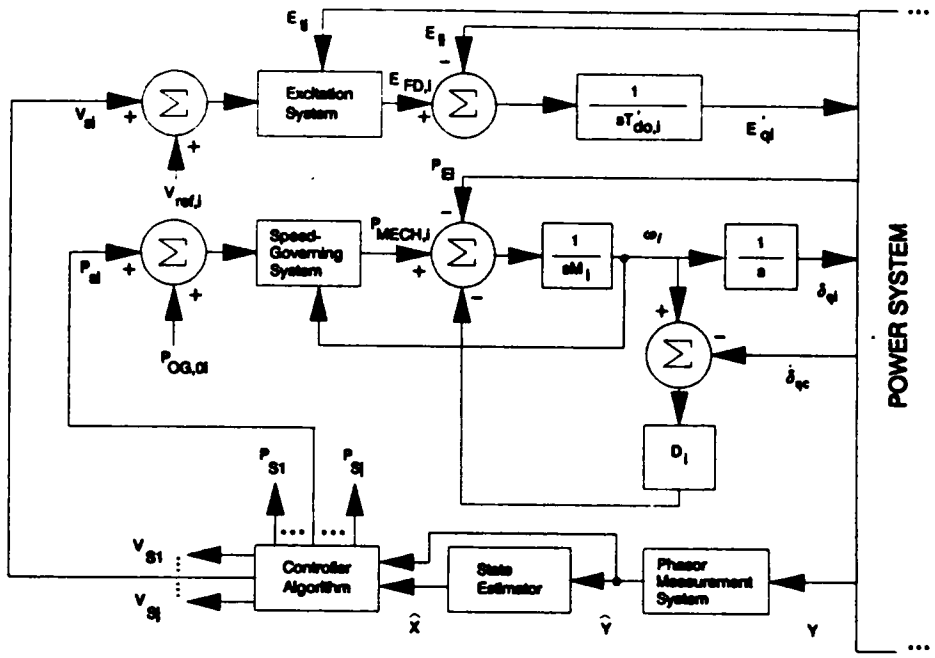

$$u_i = [\, V_{si} \;\; P_{si} \,]^T$$

$$u = [\, u_1^T \; u_2^T \ldots \; u_i^T \ldots \; u_g^T \,]^T$$

Figure 1.2. Representation of Generator Subject to Controller

Chapter 2

Literature Review

The use of excitation systems in the automatic voltage regulation of synchronous generators under varying load conditions has been a widely accepted practice for decades [78, 79]. Due to the relative slowness of the dynamics of these systems, their effects on the transient stability of a power system were not considered great. Transient stability studies (covering a time span of one second or less) normally represented generators by voltages behind their respective transient reactances [78, 79]. Dynamic stability studies (covering a time span of several seconds), however, which went beyond the first power system swing following a disturbance normally included existing excitation systems in the generator representations.

The significant capability of excitation systems to enhance or destroy the dynamic stability of the power system has caused great active research efforts to be expended on them. Initially, research has been in the direction of studying the benefits and potential harm provided by excitation systems with fixed reference signals [1]. Later on, research

was directed towards various methods to derive appropriate input signals to the excitation systems which were superimposed on the reference signals for at least a period of time [1-33 , 40, 42, 43, 45, 47, 49, 50, 52, 53, 57-60, 65-67, 69, 73, 75-77]. The methods were aimed not only to counteract the potential dangers but to turn their existence to advantage by using them to enhance power system dynamic stability.

DeMello and Concordia [1] carried out a detailed study of the effects of an excitation system applied to a single machine connected to an infinite bus. The influence of the voltage-regulator-exciter system on the synchronizing and damping torques of the machine under various operating conditions was dealt with. Using a linearized system model about the nominal operating point, they have shown that the excitation system contributed substantial positive synchronizing torques under most conditions while contributing negligible negative synchronizing torques in rare situations. An important result shown was the existence of substantial negative damping torques originating from a high-gain excitation system under easily attainable conditions. These resulted in either a highly oscillatory or unstable power system behavior following a disturbance. The authors pointed out the use of suitable input signals derived from either the machine speed, terminal frequency, or terminal power to provide a sufficient amount of positive damping during a disturbance. Using the linearized model, they have established some basic observations and guidelines in the choice of a transfer function (single-input single-output) for the power system stabilizer (PSS). In particular, they simulated the performance of some speed-sensitive PSS's. Parameter settings in the PSS transfer functions were determined by trial and error.

Systematic determination of PSS transfer function parameters using shaft speed, electrical power, or frequency as input signals to the stabilizers has been proposed

[2-12,16-22]. Many of these methods used an infinite bus to represent the part of the power system external to the generator to be equipped with a stabilizer. Root locus [4], frequency response [4,6,7,10], and optimal output feedback pole assignment [8,9] methods have been tested in off-line studies. On-line fine tuning of stabilizer settings have also been carried out [6,7]. Laboratory implementation of a digital controller designed using s-domain and mapping techniques to derive the stabilizing signal applied to the generator exciter has also been reported [10]. These design methods were aimed mainly at damping out local electromechanical modes of oscillations.

Some papers have appeared on stabilizers designed to damp out tie-line power oscillations [11,12] as well. Bollinger, et.al. [11] determined first the external plant transfer function G(s) from the bode plot obtained using conventional frequency response techniques. G(s) assumed the signal to the automatic voltage regulator (stabilizer output) as its input and the generator electric power (stabilizer input) as its output. The root locus method was then used to determine the parameters of the controller transfer function H(s) for improved system damping. Bollinger and Windsor [12] measured the tie-line power and fed it to the stabilizer through a frequency modulated communication link. The transfer function relating the disturbance and stabilizer-derived signal to the tie-line power was used to obtain the closed-loop characteristic equation

$$1 + G_{\mathrm{TLS}}(s)G_{\mathrm{pt}}(s)H_t(s) = 0 \tag{2.1}$$

Stabilizer parameters were chosen to maintain stability of the control loop within acceptable gain and phase margins.

Although these papers considered overall system performance to some degree, they assumed specific stabilizer locations in the power system without justifying them.

Hence, they did not necessarily represent the most effective form of power system stabilization. Out of economic, practical, and theoretical considerations, it was not deemed appropriate to install a PSS at every generator location in a multimachine system [13-21]. In most cases, it was sufficient to install a single PSS for an entire inertia group of generators. Moreover, an inertia group did not necessarily require a stabilizer.

DeMello, et.al. [13] proposed a sequential procedure, backed up by power system simulations, to address the problem of PSS site selection in a multimachine system. The method was applied to a multimachine system which exhibited dynamic instability and poor damping of several inter-machine modes of oscillation. A machine represented either a single unit or an inertia group. The effectiveness of placing a PSS at a particular machine location was evaluated by observing the improvement in damping of the lower frequency modes associated with the machine swing equations. An ideal PSS was introduced as one where the gain

$$g_i = \frac{E'_{qi}}{f_i} \tag{2.2}$$

was constant. The first stabilizer location was determined by placing an ideal PSS with nonzero gain at various locations, one machine at a time. The most effective location was one where the greatest improvement in the damping of the lowest frequency mechanical mode was achieved. Assuming a realistic speed-sensitive PSS installed at the newest location, a simulation of power system behavior was performed to determine the need for additional stabilizers. If so, the process was repeated for machines which still did not have a PSS while observing the damping of the next lower frequency mechanical mode of oscillation. Power system simulation was once more performed, taking into

account the existence of new and previously established PSS locations. The process was terminated when simulation results showed adequate damping characteristics.

Hiyama [14] presented a coherency-based scheme for the identification of optimum sites for PSS applications. Arguing that use of a stabilizer in a generator belonging to a certain coherent group did not improve modes of oscillations exhibited by a different coherent group, he proposed the use of a single stabilizer in each group placed at an optimally chosen generator location. Using the coherency index

$$J_{ij} = \sum_{k=1}^{m} |\Delta\delta_i(j\omega_k) - \Delta\delta_j(j\omega_k)| \tag{2.3}$$

where ω_k denoted one of the m generator electromechanical modes and $\Delta\delta_j$ the rotor angle deviation, coherent inertia groups of generators in the power system were identified. The best PSS location in each coherent group was then identified using the performance index

$$I_{Gi} = \int_0^{\infty} \sum_{j \varepsilon G_i} \Delta\omega_j^2 dt \tag{2.4}$$

Based on the results for a 39-Bus power system, it was concluded that the best way to stabilize the poorly damped modes of oscillation in each of the four coherent groups was to attach the PSS to the central generator (i.e., the generator that was "most" coherent to every other generator in the group).

Abdalla, et.al. [15] presented an alternative sequential procedure for the selection of the "best" machines to be equipped with a power system stabilizer. The objective of

placing a PSS in a machine location was to apply an input signal which created a positive damping torque (in-phase with the speed) in the corresponding swing equation. The criteria used in the selection was the amount of leftward shift in the complex plane location of the eigenvalues related to the rotor oscillations as damping terms were systematically introduced in increasing magnitudes in the swing equations, one machine at a time. Two quantities were defined in the paper.

$$\text{NRP} = \frac{\text{Real Part of Eigenvalue With } K_d \text{ Positive}}{\text{Real Part of Eigenvalue With } K_d \text{ Zero}} \tag{2.5}$$

$$K_d = \text{Coefficient of Damping Introduced in the Swing Equation} \tag{2.6}$$

Assuming an initially stable system, the value of NRP for a given K_d was a measure of the effectiveness of placing a PSS in the machine where additional damping was introduced in terms of damping out the mechanical mode associated with the computed NRP. Stabilizers were installed as long as improvements in the mechanical mode eigenvalue locations were significant. The process was terminated as the NRP's approached the value of unity regardless of PSS location.. In the computation of system eigenvalues for a PSS location being tested, previously installed PSS's were accounted for (thus increasing system size) . Settings for the PSS's were determined by trial and error, as a compromise between improvement in damping of critical eigenvalues and the deterioration in damping of other system eigenvalues.

The next problem in the stabilization of multimachine systems using a number of PSS's was the coordinated tuning of parameters [16-21]. Solutions have been proposed either to assign resulting closed-loop eigenvalues to specific locations or specific domains in the complex s-plane or to cause the machines to exhibit desired damping characteristics.

Fleming, et.al. [16] utilized the small signal transfer function from the voltage regulator reference Δe_{tri} of the machine where the stabilizer was to be applied to the speed deviation $p\delta_i$ of that machine. Mutual machine interactions were not explicitly included in the local closed-loop transfer functions which were used mainly to compute for the parameters of the stabilizer in the corresponding locations. Stabilizer locations were chosen using the sequential procedure suggested in reference [13].

Gooi, et.al. [17] proposed an iterative procedure based on complex frequency analysis in which the parameter settings of all PSS's in the power system were coordinated so as to yield desired effective damping coefficients in each machine. Mutual machine interactions were taken into account, thus avoiding the rightward drift in the complex plane of the mechanical mode eigenvalues. The drift characterized procedures which determined PSS settings without including mutual machine interactions [16]. The paper by Gooi assumed a speed sensitive PSS with the generalized transfer function denoted by

$$\frac{\Delta V_{si}}{\Delta \omega_i} = G_{Fi}(s) \tag{2.7}$$

In each machine, the mutual interactions were represented through a linearized model which extended the one originally used by DeMello and Concordia [1]. The model used for machine 'i' in block diagram form is shown in Figure 2.1. Every machine was represented by the given block diagram whose values were partial derivatives evaluated at the nominal operating point. To determine the synchronizing and damping torque contribution to every machine from every source in the system, the system signal flow graph had to be constructed and the general gain formula

$$G = \frac{y_{out}}{y_{in}} = \sum_{k=1}^{N} \frac{G_k \Omega_k}{\Omega} \tag{2.8}$$

had to be used. A truth table to map interactions of various nodes in the system was used to facilitate the use of the preceding formula. Assuming known mechanical mode eigenvalues within each iteration, each electrical torque contribution to every machine was decomposed into a synchronizing and a damping component (with s = λ_i). Thus, each machine was described by a second-order differential equation with modified synchronizing and damping torque coefficients. These coefficients were the composite sums of the damping and synchronizing components of the electrical torques from every source in the system. For each machine, the torque component produced by the regulator-exciter action in response to the speed-derived signal was

$$\begin{aligned} \Delta T_{ei} &= K_{2,ii} G_{ri}(s) \Delta V_{si} \\ &= K_{2,ii} G_{ri}(s) G_{fi}(s) \Delta \omega_i \\ &= D_{ei} \Delta \omega_i \end{aligned} \tag{2.9}$$

where

$G_{ri}(s)$ = transfer function of the ith reactive loop (2.10)

D_{ei} = desired positive damping coefficient from ith stabilizer (2.11)

For maximum positive damping, ΔT_{ei} must be in-phase with $\Delta \omega_i$. This requirement, imposed on each machine at every iteration was expressed by

$$\angle G_{ri}(s) + \angle G_{Fi}(s) = 0 \tag{2.12}$$

The procedure was repeated at every iteration until the desired damping coefficients were obtained.

Doi and Abe [18] proposed the use of eigenvalue sensitivity analysis and linear algebra to assign the resulting closed-loop eigenvalues to specified regions in the complex s-plane. These regions were determined such that each open-loop eigenvalue λ_k was shifted by at least $\Delta\sigma_k$ to the left, while vertical movements were limited to at most $\pm\gamma\omega_k$. The minimized objective function was the weighted sum of individual PSS gains. The proposed method allowed the simultaneous determination of the most effective PSS location and synthesis of the required transfer functions. It also tended to damp out all local and inter-area modes of oscillations. Its drawback was its reliance on a linearization which assumed small changes in the eigenvalues (caused by corresponding changes in PSS parameters).

Lim and Elangovan [19] used the complex frequency approach to determine the appropriate PSS parameters that would set the mechanical mode eigenvalues to specified locations in the complex plane. The state vector x consisted of rotor angles and speeds. Each stabilizer was assumed to have two unknown parameters. After incorporating the PSS transfer functions into the original system of equations, closed-loop system equations became

$$[sI - \overline{A}(s)]x = 0 \tag{2.13}$$

where $\overline{A}(s)$ was an operational transfer matrix. Assuming k PSS's to be installed, it was shown that the condition

$$|sI - \overline{A}(s)| = 0\ ,\ s = s_1, s_1^*, \ldots, s_j, s_j^*, \ldots, s_k, s_k, s_k^* \tag{2.14}$$

was equivalent to k second-order characteristic equations

$$s_j^2 + f_{1j}s_j + f_{2j} = f_{3j}s_j b_j F_j(s_j) \ , j = 1,...,k \tag{2.15}$$

where $F_j(s)$ was the transfer function of the jth stabilizer. The problem was posed such that the k eigenvalue pair (s_j, s_j^*) were known while the parameters T_{1j} and K_j of each stabilizer were to be determined. Moreover, the terms $f_{1j}, f_{2j}, f_{3j}, b_j$ in the jth characteristic equation were constants if all other PSS settings except those of $F_j(s)$ were known. An iterative procedure was developed from these observations. Initial estimates for the T_{1j}'s and K_j's were assumed. Iteration steps then consisted of improving the estimates T_{1j}, K_j by using the second-order characteristic equations and current estimated values of the other parameters. The procedure was terminated until convergence was achieved for all values of PSS parameters.

Chen and Hsu [21] proposed an efficient solution to the exact eigenvalue assignment problem. Assuming known PSS locations, each transfer function used had four parameters of which two were unknown (stabilizer gain K_j and a numerator parameter T_{1j}). These parameters were determined to assign m eigenvalue pairs corresponding to the electromechanical modes to specified locations. The authors succeeded in decomposing the known eigenvalue requirements through a decentralized modal control algorithm into 2m simultaneous equations for the 2m unknowns. Thus,

$$f_i(K_1, T_{11}, K_2, T_{12}, \ldots K_m, T_{1m}) = 0 \ , \qquad i = 1,2,...,2m \tag{2.16}$$

A numerical iterative procedure (e.g.,the Newton-Raphson method) was then used to solve the 2m simultaneous equations.

Lefebvre [20] used a linear algebra approach to solve the coordinated PSS tuning problem. The question of parameter optimization was posed as an eigenvalue assignment problem. The form of the PSS transfer function was assumed known with the parameters still to be optimized. The parameters to be set were defined as elements of a real matrix K_d . State variables arising from the introduction of PSS's were included in the state vector. The linearized equations which included the effects of the stabilizers were described by

$$\begin{aligned} \dot{X} &= AX + BU = AX + BK_dX \\ &= (A + BK_dC)X \end{aligned} \tag{2.17}$$

U was the vector of input signals to the excitation systems while Y was the vector of machine speeds. An algorithm was derived based on the parametrization of the vector of specified eigenvalues $\vec{\Lambda}$ and required settings K_d .

$$\vec{\Lambda}_r(r) = \vec{\Lambda}_o + r(\vec{\Lambda} - \vec{\Lambda}_o) \tag{2.18}$$

$$K_d(r) = \text{matrix of PSS settings giving rise to } \vec{\Lambda}_r(r) \tag{2.19}$$

There, $\vec{\Lambda}_o$ was the vector of eigenvalues corresponding to $K_d(0)$, the matrix of initially assumed settings. The submatrix K(r) was defined to consist of the nonzero rows and columns of $K_d(r)$ (only k < NG machines will have installed PSS's). The paper has shown the following relation to be true:

$$K(r) = K(0) + \int_0^r [P^+(s)(\vec{\Lambda} - \vec{\Lambda}_o) + V(s)\alpha(s)]ds \tag{2.20}$$

where $P^{+}(r)$ was the Moore-Penrose pseudo- inverse (general right inverse) of P(r) derived from the system eigenvectors at $K_d(r)$. The term $V(r)\alpha(r)$, which could be arbitrarily set to zero, allowed the optimization of a cost function under the specified constraint of eigenvalue assignment. Lefebvre selected $\alpha(r)$ to minimize the shifting of the eigenvalues that were not specified in the problem formulation.

The previously described fixed-parameter controllers have been designed to operate best under a given nominal power system operating point. Under a given disturbance (permanent or temporary) from this operating point the performance of the controllers may get degraded. The use of digital adaptive controllers to stabilize a power system has been a subject of research for some years now [23-31]. In particular, the self-tuning type has received substantial attention with generator excitation control being the intended application [23-31]. A block diagram of a self-tuning adaptive regulator taken from reference [25] is shown in Figure 2.2. In self-tuning adaptive control studies, a model was assumed for the system to be controlled. This model had parameters which were identified at every sampling instant based on output and input measurements using a suitable algorithm (e.g., a form of recursive least squares) [23-35]. The updated parameters were then used to synthesize the control input signal to satisfy some criteria (e.g., pole-shifting or minimum output variance) [23-27,29-31,33-35]. Hsu and Liou [28] proposed adaptive techniques to derive the equivalent parameters of a proportional-integral-derivative (PID) PSS in real time. Cheng, et.al. [29] simulated adaptive controllers which stabilized a multimachine power system. Model parameters of a particular unit were identified using purely local measurements of the input and output signals. Stating that present measurements actually reflected existing power conditions, the authors were able to justify their method. Malik, et.al. [27] proposed a multi-microcomputer based dual-rate self-tuning scheme to increase the control rate five times which

in turn improved controller performance. Use of a lower identification rate helped in eliminating unmodeled system dynamics in the parameter estimates. At every instant that the control input signal had to be updated, the controller used the most recent value of these estimates. Improvements were reported over the single-board implementation which used identical rates for estimation and control.

At present, the use of adaptive excitation control techniques for power system stabilization are still in the simulation stage.

The above schemes employing single-input single-output transfer functions have been referred to as conventional controllers. Controllers employing multiple-input multiple-output transfer functions derived from Optimal Control Theory have produced other schemes referred to as optimal controllers. Although some of these devices are admittedly sub-optimal, the term has been applied to the entire class of controllers.

This literature review will now consider optimal controllers which aim at minimizing the deviations of defined power system "state" variables from some nominal or target values over time by applying control input signals to either or both excitation and speed-governing systems of each generator [42-45, 47-54, 57-60, 65-67, 73, 75-77]. In particular, stabilizers with control laws derived from quadratic cost functions will be dealt with. Optimal controllers employing other means or other performance criteria [36-41, 55, 56] will not be considered.

Yu,et.al. [47] was the first to propose the use of an optimal controller for power system dynamic stabilization. The method presented by the authors was applied to a single salient-pole synchronous machine connected to an infinite bus. The machine was assumed to have a second-order exciter-voltage-regulator system where the first input sig-

nal was applied, a third-order governor-hydraulic system where the second input signal was applied, and a third-order synchronous machine (including the swing equations). These models determined the choice and size of the state vector used to design the optimal controller. The scheme made use of complete state vector feedback and a linear control law. Given the system of equations

$$\dot{x} = Ax + Bu \tag{2.21}$$

where x was the vector of state deviations from their nominal values and a quadratic cost functional

$$J = \frac{1}{2}\int_0^T (x'Qx + u'Ru)\mathrm{dt} \tag{2.22}$$

the optimal control input signals were given by the control law

$$u = -R^{-1}B'Kx \tag{2.23}$$

where K was the solution to the steady-state Riccati equation

$$-A'K - KA + KBR^{-1}B'K - Q = 0 \tag{2.24}$$

The closed-loop system was thus given by

$$\dot{x} = (A - BR^{-1}B'K)x \tag{2.25}$$

The matrix Q in the cost functional was determined using a trial and error approach. Elements of the matrices for Q and R were varied until the "best" optimal performance was achieved.

Fosha and Elgerd [48] shortly applied the previous principles to the two-area megawatt-frequency control problem. Each coherent area was assumed to have a turbine control arrangement such that the control input signal could be defined as the incremental change in the speed changer position. The complete state and control input vectors were

$$X = [x_1\ x_2\ \dots\ x_9]^T \tag{2.26}$$

$$U = [u_1\ u_2]^T \tag{2.27}$$

where

$$\begin{aligned}
x_1 &= \int \Delta P_{\text{tie},1}\,dt = \int T_{12}^{*}(x_2 - x_6)dt \\
x_2 &= \int \Delta f_1\,dt & x_6 &= \int \Delta f_2\,dt \\
x_3 &= \Delta f_1 & x_7 &= \Delta f_2 \\
x_4 &= \Delta P_{G1} & x_8 &= \Delta P_{G2} \\
x_5 &= \Delta X_{GV1} & x_9 &= \Delta X_{GV2} \\
u_1 &= \Delta P_{C1} & u_2 &= \Delta P_{C2}
\end{aligned} \tag{2.28}$$

Here, ΔP_{Gi} was the incremental change in generated power in area i, Δf_i the incremental change in frequency, ΔX_{GVi} the incremental change in speed governor position, and $\Delta P_{tie,i}$ the incremental change in tie-line power from area i. The system equations were then expressed as

$$\dot{X} = AX + BU + \Gamma \Delta P_d \tag{2.29}$$

where ΔP_d was the vector of incremental changes in demand power. For the direct application of results from the optimal linear regulation problem, the state vector was redefined as the deviation from its steady-state value.

$$X^1 = X - X_{ss} \tag{2.30}$$

Thus,

$$\dot{X}^1 = AX^1 + BU \quad , X^1(0) = -X_{ss} \tag{2.31}$$

Several cases corresponding to changes in relative values of nonzero elements of Q and R were then presented. In one of the cases, the performance measure (cost function) was the expression

$$J = (\Delta f_1)^2 + (\Delta f_2)^2 + (\Delta P_{tie,1})^2 + (\int \Delta f_1 dt)^2 + \int (\Delta f_2 dt)^2 + u_1^2 + u_2^2 \tag{2.32}$$

from which the appropriate Q and R matrices were deduced. The paper stated that controller performance can be improved by using all available information from the state vector as opposed to using only the information on tie-line power and frequency deviations (as in most control strategies that were then presently existing). Moreover, for weakly coupled coherent areas, independent individual suboptimal controllers may be used in each area with satisfactory results. This was demonstrated by Feliachi in a much later paper [54].

In the paper by Yu and Siggers [49], comparison was made between the performance of two types of conventional stabilizers, power-derived and speed-derived, and that of an optimally derived controller. All three methods substantially improved system

damping and thus established optimal control as a serious alternative to the use of conventional stabilizing signals. Comparison was made both for the single-machine and multimachine systems. For each machine, twelve state variables were used in the simulation program arising from a fifth-order machine model, a third-order exciter, and a fourth-order speed governor. The design of the optimal controller, however, assumed constant shaft power and defined only four measurable state variables in each machine given by the vector $[\Delta\omega\ \Delta V_t\ \Delta V_F\ \Delta T_e]^T$. The linear control law was derived to minimize a quadratic performance index J for several cases using various weighting factors for Q and R.

In the first of two joint papers by Yu and Moussa [42], a new formula for the sensitivity of the real and imaginary parts of the stable eigenvalues of the 2n x 2n matrix M with respect to changes in the diagonal elements Δq of the Q matrix in the quadratic performance measure was developed. The matrix M was given by

$$M = \begin{bmatrix} A & -BR^{-1}B' \\ -Q & -A' \end{bmatrix} \tag{2.33}$$

and use was made of its properties and eigenvectors to derive the sensitivity expressions $S(i,j) = \partial\lambda_i/\partial q_j$. Denoting the number of distinct real parts in the set of closed-loop eigenvalues by m and the shift in the ith distinct real part by $\Delta\xi(i)$, a weighted total real shift Σ was defined.

$$\Sigma = \beta_1\Delta\xi(1) + \beta_2\Delta\xi(2) + \ldots + \beta_m\Delta\xi(m) = \phi'\Delta q \tag{2.34}$$

The positive β's were chosen so as to implement a leftward shift of the dominant eigenvalues (stable eigenvalues closest to the right-hand side of complex plane) while

basically maintaining the locations of the other eigenvalues. The adjustments of the diagonal elements of Q were in the direction of steepest descent,

$$\Delta q = -k\phi \ , \ k > 0 \tag{2.35}$$

The process of updating the diagonal elements of Q was repeated until a satisfactory eigenvalue shift was made or until practical controller limits were reached (e.g. extremely large elements in the gain matrix K). This method of determining the diagonal elements of the matrix Q was then used to study several cases of optimal controller applications. All this applications pertained to a single machine connected to an infinite bus. The cases covered included:

1.Optimal excitation control without optimal governor control

2.Optimal governor control (without optimal excitation control) with and without dashpot

3.Combined excitation and speed-governor control

The authors arrived at the following conclusions:

1.Optimal governor control without dashpot provided a comparable quality of control to that of optimal excitation control.

2.Combined excitation and speed-governor control provided an even better controller performance.

Utilizing the results of their first joint paper, Yu and Moussa [50] considered the question of including complete system dynamics in the design of the optimal controller.

Various possibilities were considered for a three-machine system. The first two cases included system dynamics at all locations in the power system to design the controller. In the first case, the control input signal was assumed to exist in one machine only while in the second case, control input signals were applied at every machine. The third (one independent controller) and fourth (independent controller in each machine) cases captured local dynamics only in the design of the controllers, i.e., the rest of the power system outside each machine was assumed to be an infinite bus.

It was found that the controller of Case 2 performed better than that of Case 1 while that of Case 1 performed better than that of Case 3. The last case which made use of individual machine controllers designed locally was detrimental to overall system stability. The paper showed the need to include machine dynamic couplings in the design of the optimal controller (as a linear regulator) for the multimachine system considered.

Formulation assumed static transmission networks, a seventh-order machine model (including swing equations and machine flux equations), second-order exciter and voltage regulator system, and a fourth-order governor-hydraulic system. Thirteen state variables for each machine were defined. In each formulation, the state equations were written in the form

$$\dot{Y} = AY + BU \tag{2.36}$$

In the linearization process, use was made of all machine fluxes and transmission line and generator currents resolved along the d-q axes of the individual machines, the displacements of which with respect to the system d-q axis were obtained by solving the equations at the nominal system operating point.

Davison, et.al. [51] utilized output feedback from measurable quantities (machine speed and angle) to study optimal decentralized regulators utilizing two forms of control law:

a) $\bar{u} = Ky_m$

b) $\bar{u} = K_1 y_m + K_2 \dot{y}_m$

The vector y_m denoted measurable output variables thus eliminating the need to estimate the nonmeasurable states. The gain matrices K, K_1, K_2 were computed to minimize the performance index:

$$J(k) = \int_0^\infty (y'Qy + \bar{u}'R\bar{u})dt \tag{2.37}$$

where k was a vector of relevant elements of the gain matrix(ces), Q and R positive definite matrices, and y a vector of desired outputs not necessarily identical to y_m. An interaction index was also used to predict unfavourable interactions among the decentralized controllers.

$$I^3(k_1,k_2) = D^3(k_1,k_2) - D^3(0,0) \tag{2.38}$$

Contrary to the results obtained by Yu [50], Davison obtained results which showed satisfactory performance by localized controllers (for the three-machine system studied).

Habibullah and Yu [43] attempted to design an optimal controller which would perform satisfactorily under varying load conditions. The study system was a single-machine connected to an infinite bus. Starting with machine fluxes and rotor angle and

speed as state variables, the order of the machine model used was reduced by neglecting stator transients, an initial step justified through eigenvalue analysis. Initially, the state vector was defined as

$$X = [\Delta\delta\ \Delta\omega\ \Delta\psi_f\ \Delta\psi_D\ \Delta\psi_Q\ \Delta E_{fd}]^t \tag{2.39}$$

The transformation matrix M utilizing linearized terms was then calculated such that the resultant state vector consisted of physically measurable quantities.

$$Z = MX = [\Delta\delta\ \Delta\omega\ \Delta V_t\ \Delta P\ \Delta i_f\ \Delta E_{fd}]^t \tag{2.40}$$

An algorithm was then presented to enable the system equation to be expressed in canonical form through the transformation matrix T

$$Y = T^{-1}Z \tag{2.41}$$

$$\dot{Y} = F_o Y + G_o U \tag{2.42}$$

where U was the input to the generator excitation system. A performance index (cost function) J was then defined to design an optimal controller

$$J = \frac{1}{2}\int_0^\infty [Y^t Q_o Y + U^t R U]dt \tag{2.43}$$

where $Q_o = qI_n$ and $R = r$. Appropriate values (q/r) were then determined by examining the effects of the ratio on the combined optimal state and costate (adjoint) eigenvalues and implementing as much leftward shift on the complex plane as is reasonable on the mechanical mode eigenvalues. A suitable controller was thus found for the equivalent performance index

$$J = \frac{1}{2}\int_0^\infty (Z^t QZ + U^t RU)\mathrm{dt} \tag{2.44}$$

where

$$Q = q(TT^t)^{-1} \tag{2.45}$$

The controller was designed using full-load condition assumptions. While it performed satisfactorily at lighter loads, the authors stated that possible difficulties may arise at heavier loads because of reduced damping.

In a similar paper, Habibullah [44] used speed-governor control to test the principles developed in the preceding paper.

Raina, et.al. [65] used an integral control law to derive the control input signal to the excitation system. The state vector included state variables from a conventional stabilizer which may also be present. The formulation assumed a single machine connected to an infinite bus. A vector Δu_2 which represented unknown disturbances external to the generator was defined. The state equations were then rewritten in terms of output and input variables derived from deviations of the original state variables from their desired steady-state incremental changes. The desired incremental changes were assumed known from the disturbance. The control law was derived to minimize the performance index

$$J = \int_0^\infty \{\Delta\bar{y}^T Q_1 \Delta\bar{y} + h^T Q_2 h + \Delta\bar{u}_1^T R \Delta\bar{u}_1\}\mathrm{dt} \tag{2.46}$$

subject to

$$\begin{bmatrix} \Delta\dot{\bar{y}} \\ \dot{h} \end{bmatrix} = \begin{bmatrix} A & 0 \\ 0 & 0 \end{bmatrix} \begin{bmatrix} \Delta\bar{y} \\ h \end{bmatrix} + \begin{bmatrix} B \\ 1 \end{bmatrix} \Delta\bar{u}_1 \tag{2.47}$$

The resultant integral control law was

$$u_1 = u_{1e} + K_1(y - y_o) - K_1 M_1(u_{1e} - u_1^o) + K_2 \int_0^t (u_1 - u_{1e})dt \tag{2.48}$$

where the superscript "o" denoted nominal values while the subscript "e" denoted desired values at steady-state.

Wilson and Aplevich [53] employed the linear regulator with full state feedback approach to derive the local control input signals for multimachine stabilization. Local generator state variables were chosen such that they were directly measurable while the external power system was represented by a dynamic equivalent the states variables of which were calculated by a state estimator. The state vector of the local controller included both the generator local and external state variables. The proposed method had adaptive properties while minimizing the need for state estimators and eliminating the need for a centralized controller with a very large number of state variables.

Ohtsuka, et.al. [52] reported an actual implementation of an optimal controller with adaptive properties. The local generator controller was designed using discrete-time formulation with the rest of the power system represented by a time-varying reactance and voltage. During transient conditions, the precalculated controller gains were used. Longer control periods, however, allowed the gains to be updated approximately after

every four seconds. By augmenting the controller state vector to include set point variations, model and measurement errors were taken into account.

Abdel-Magid and Aly [57] proposed the use of a two-level stabilizer in place of a single, centralized (integrated) controller. A subsystem was defined for each plant (equivalent machine). State equations for each of the N subsystems were written neglecting the coupling terms in the complete system matrix. Individual controllers (suboptimal linear regulators) were then designed in the usual manner with local input signals computed through local state feedback ,i.e.,

$$u_i^{\ell} = - K_i X_i \tag{2.49}$$

where

$$K_i = R_i^{-1} B_{ii}^T P_i \tag{2.50}$$

$$P_i A_{ii} + A_{ii}^T P_i - P_i B_{ii} R_i^{-1} B_{ii}^T P_i + Q_i = 0 \tag{2.51}$$

and

$$\dot{X}_i = A_{ii} X_i + B_{ii} u_i^{\ell} \text{ , i = 1,2,...,N} \tag{2.52}$$

For a strongly coupled system, a global control u^g was introduced to reduce the effect of coupling, i.e.

$$u_i(t) = u_i^{\ell} + u_i^g \tag{2.53}$$

u^g was a component of the global vector signal u^g which was determined such that

$$Bu^g + CX = 0 \tag{2.54}$$

The CX vector represented the mutual machine interaction terms in the original complete state equations. Thus,

$$u = u^\ell + u^g = u^\ell - B'CX \tag{2.55}$$

There, B' was the pseudo-inverse of B. The complete state equations were given by

$$\dot{X} = AX + Bu \tag{2.56}$$

Savings in computational effort at the subsystem level was achieved at the cost of some deterioration in performance as compared to linear integrated optimal formulation.

In the paper by Chan and Hsu [66] , an optimal variable structure stabilizer was designed with low sensitivity to plant parameter changes and external disturbances. The results of single-machine and multimachine system simulations showing reduced overshoot and settling time of the torque angles following a disturbance reflected the reduced sensitivity. After defining a similarity transformation of the original state vector, the switching vector was determined by minimizing a quadratic performance index with respect to transformed variables in the switching mode. This was accomplished by formulating the equations in the sliding mode as an optimal control problem. The linear state feedback law was a piecewise constant function, the constants determined through a trial and error approach. The solution presented was based on a slight modification of the theory presented by Utkin and Yang [68]. One input signal was defined for each generator and was applied to the excitation systems. The linear state feedback parameters were chosen such that the controller was sensitive only to the angular and speed deviations of the machines. The solution as presented in the paper follows.

Given that

$$\dot{x} = Ax + Bu \tag{2.57}$$

where A and B are n x n and n x m matrices, define a similarity transformation $y = Mx$ such that

$$MB = \begin{bmatrix} 0 \\ B_2 \end{bmatrix} \tag{2.58}$$

where B_2 has rank m and is square. Then,

$$\begin{bmatrix} \dot{y}_1 \\ \dot{y}_2 \end{bmatrix} = \begin{bmatrix} A_{11} & A_{12} \\ A_{21} & A_{22} \end{bmatrix} \begin{bmatrix} y_1 \\ y_2 \end{bmatrix} + \begin{bmatrix} 0 \\ B_2 \end{bmatrix} u \tag{2.59}$$

The motion of the system in the sliding mode is given by

$$\dot{y}_1 = A_{11}y_1 + A_{12}y_2 \tag{2.60}$$

$$\sigma(y) = c_{11}y_1 + c_{12}y_2 = 0 \tag{2.61}$$

The switching vector C^T has the property $\sigma(x) = C^T x = 0$. Hence,

$$[C_{11} \quad C_{12}] = C^T M^{-1} \tag{2.62}$$

Without loss of generality, C_{12} was set equal to I_m in the paper. The subsystem described by $\dot{y}_1$ and $\sigma(y)$ was regarded as an open loop control system with state vector y_1 and control vector y_2. The form of control was given by

$$y_2 = -C_{12}C_{11}y_1 = -C_{11}y_1 \tag{2.63}$$

Elements of C_{11} were optimized by minimizing the performance index

$$J = \frac{1}{2}\int_{t_s}^{\infty} y^T Q y \, dt \tag{2.64}$$

with respect to y_2 where the sliding mode of operation starts at t_s. An alternative expression for the performance index was

$$J = \frac{1}{2}\int_{t_s}^{\infty} (y_1^T Q_{11} y_1 + 2y_1^T Q_{12} y_2 + y_2^T Q_{22} y_2) dt \tag{2.65}$$

Using the well-known results for a linear optimal regulator, if

1. Q_{22} is positive-definite

2. (A,B) is controllable

3. $(A_{11} - A_{12}Q_{22}^{-1}Q_{12}^T, D)$ is observable where $D^T D = Q_{11} - Q_{12}Q_{22}^{-1}Q_{12}^T$

then the optimal control law was given by

$$y_2 = -(Q_{22}^{-1}A_{12}^T P + Q_{22}^{-1}Q_{12}^T)y_1 = -C_{11}y_1 \tag{2.66}$$

where

$$PA' + (A')^T P - PB'(R')^{-1}(B')^T P + Q' = 0 \tag{2.67}$$

$$A' = A_{11} - A_{12}Q_{22}^{-1}Q_{12}^T \tag{2.68}$$

$$R' = Q_{22} \tag{2.69}$$

$$B' = A_{12} \tag{2.70}$$

$$Q' = D^T D = Q_{11} - Q_{12}Q_{22}^{-1}Q_{12}^T \tag{2.71}$$

Thus,

$$C^T = [C_{11} \;\; I_m]M \tag{2.72}$$

$$\sigma_i(x) = C_i^T x = 0 \tag{2.73}$$

where C_i was the ith column of C. The control input signals of the original system were computed as

$$u_i = -\Psi_i^T x = -\sum_{j=1}^{n} \psi_{ij} x_j \tag{2.74}$$

with i = 1,2,...,m and j = 1,2,...,n. The feedback elements were

$$\psi_{ij} = \begin{cases} \alpha_{ij} \;\; , \text{if } x_j \sigma_i \geq 0 \\ -\alpha_{ij} \;\; , \text{if } x_j \sigma_i < 0 \end{cases} \tag{2.75}$$

The α_{ij} elements were determined using a trial and error approach while satisfying some inequality constraints. Another paper by the same authors [69] showed these constraints for a single machine system. $\alpha_{ij} = 0$ if j did not correspond to machine angle and speed, thus removing the need for a state estimator. If physical constraints existed in the system, the gains α_{ij} were reduced to maintain stability. In the performance index, Q was assumed known. Selection of its elements depended on the criterion that the dominant

closed-loop eigenvalues of the system in the sliding mode be shifted leftward as far as possible to obtain maximum stability.

Chen and Kusic [45] presented a paper which dealt with the efficient determination of an appropriate weighting matrix Q in the cost function to assign some closed-loop system eigenvalues to prescribed locations. Although the system considered was a multimachine system with an impedanceless transmission network, the technique presented to compute the feedback gain matrix K and weighting matrix Q is easily extended to other systems. The state variables defined were all measurable quantities and were linear combinations of the incremental changes in the original system variables by assumption. This was accomplished through the usual linearization about the nominal operating point. With the new n-state vector denoted by X,

$$\dot{X} = AX + BU \tag{2.76}$$

An initial choice Q_o for the quadratic performance measure was used to compute the initial feedback gain matrix K_o, producing the closed loop system

$$\dot{X} = (A + BK_o)X \tag{2.77}$$

The eigenvalues of $(A + BK_o)$ were then investigated to determine r, the number of eigenvalues λ_i which will have to be reassigned to specific values S_i. A real transformation matrix T derived from a modal matrix of A was then used such that

$$X = TY \tag{2.78}$$

A further transformation $Z = HY$ where

$$H = [I_r \ \ 0] \ \text{, an r x n matrix} \tag{2.79}$$

was used to finally arrive at

$$\dot{Z} = \Lambda'_r Z + HT^{-1}BU = FZ + GU \tag{2.80}$$

The reduced form for Z was subjected to an appropriate pole assignment technique [46] such that the closed loop system

$$\dot{Z} = (F + GK_r)Z \tag{2.81}$$

had eigenvalues exactly equal to the r specified values S_i. With Q_r being the weighting matrix in the quadratic cost function J_r of the reduced system, the original system matrices were computed as

$$K = K_r HT^{-1} + K_o \tag{2.82}$$

$$Q = (HT^{-1})^T Q_r (HT^{-1}) + Q_o \tag{2.83}$$

Hsu and Hsu [58] used the suboptimal approach with output (rotor angle and speed) feedback to determine the parameters K_P and K_I of Proportional Integral (PI) PSS's placed at each machine location. Supporting technical literature [61-63] has been utilized. The speed-sensitive PSS's had the transfer function

$$G(s) = K_P + \frac{K_I}{s} \tag{2.84}$$

In the suboptimal regulator approach used, the input signals were derived as linear combinations of the measurable output variable ($\Delta\delta$and $\Delta\omega$ from each machine), i.e.,

$$U^*(t) = -F^* Y(t) \tag{2.85}$$

Local suboptimal regulators designed for each machine then yielded the equivalent parameters K_P and K_I of each PI PSS (since the integral of the speed was the angle). Performance of the equivalent PI PSS's were also compared to that obtained using state regulators with complete state feedback (global and local) and global suboptimal regulators. For the latter case, the complete closed-loop system became

$$\dot{X} = (A - BF^{*}C)X = A^{*}X \tag{2.86}$$

The cases considered (single-machine and multimachine systems) have shown the suboptimal regulator to perform better than conventional stabilizers in spite of some limitations inherent in the suboptimal approach [61, 64]. As expected, the optimal regulators with complete state feedback yielded the best results.

As shown in another paper [61] , the statement of and solution to the global analog suboptimal state regulator problem were as follows:

Given

$$\begin{aligned} \dot{X}(t) &= AX(t) + BU(t) \\ Y(t) &= CX(t) \end{aligned} \tag{2.87}$$

Minimize the performance measure

$$J = \frac{1}{2}\int_0^{\infty} (X^T QX + U^T RU)\mathrm{dt} \tag{2.88}$$

by applying signals

$$U^{*}(t) = -F^{*}Y(t) \quad , \text{ i.e., find } F^{*}. \tag{2.89}$$

The solution is given by the set of matrix equations

$$F^* = R^{-1}B^T K^* L^* C^T [CL^* C^T]^{-1} \tag{2.90}$$

$$0 = K^* A^* + (A^*)^T K^* + Q + C^T (F^*)^T R F^* C \tag{2.91}$$

$$0 = L^* (A^*)^T + A^* L^* + I \tag{2.92}$$

Feliachi, et.al. [60] derived a control law using a reduced-order model for the power system. The stabilization problem was cast as a linear regulator problem. State variables in the reduced-order model corresponded to rotor speeds and torque angles. The reduced order model was chosen so as to retain modes which contributed most to the steady-state mean squared error J_* if deleted. The error was defined as the deviation from the approximate state variables $\hat{z}$ of the actual state variables z, i.e.,

$$e = z - \hat{z} \tag{2.93}$$

With the original system described by

$$\dot{x} = Ax + Bu \tag{2.94}$$

a reduced-order model of the form

$$\dot{\hat{z}} = F\hat{z} + Gu \tag{2.95}$$

was derived where $\hat{z}$ was an m x 1 vector which approximated the desired vector of torque angles and rotor speeds. There,

$$F = D_1 \Lambda_1 D_1^{-1} \tag{2.96}$$

where Λ_1 was a diagonal matrix containing eigenvalues of the retained modes while D_1 was an m x m matrix relating the retained modes to the desired state variables. They were determined after performing a similarity transformation on the original system of equations. The reduced control matrix was given by

$$G = K + \Lambda^{-1}\Omega B \tag{2.97}$$

where Λ and Ω were Lagrange multipliers defined in the expression for J_s. Moreover,

$$K = D_1\Gamma_1 + D_2\Gamma_2 \tag{2.98}$$

where D_1,D_2 and Γ_1,Γ_2 were the feedback and control matrices obtained from the similarly transformed system of equations. Using the reduced system of equations, the authors then proceeded to derive the linear control law which minimized the cost function

$$J = \frac{1}{2}\int_0^\infty \{\hat{z}^T Q\hat{z} + u^T Ru\}\mathrm{dt} \tag{2.99}$$

Rostamkolai, et.al. [67] derived a control law for an HVDC system described by state equations with residual terms

$$\dot{X} = AX + BU + f(t) \tag{2.100}$$

and an output equation

$$Y = CX \tag{2.101}$$

while minimizing the cost function

$$J = \frac{1}{2}\int_0^{\infty} \{(Y - Y_d)^T Q(Y - Y_d) + U^T RU\}\mathrm{dt} \tag{2.102}$$

The vector $(Y - Y_d)$ replaced the usual X vector in the cost function of the linear regulator problem. This modification and the residual term allowed the controller to act tightly even in the presence of a permanent change in the structure or operating condition of the power system. The vector Y_d representing the target output vector trajectory was computed in real time. The control law was given by

$$U(t) = R^{-1}B^T[g(t) - KX(t)] \tag{2.103}$$

where

$$g(t) = -[A^T - KBR^{-1}B^T]^{-1}\{C^T QY_d - Kf(t)\} \tag{2.104}$$

and K was the steady-state solution to the matrix Riccati equation

$$0 = -A^T K - KA + KBR^{-1}B^T K - C^T QC \tag{2.105}$$

The control law was seen to consist of a structure-dependent term $g(t)$ and a full state feedback term KX. It therefore assumed some kind of a fast dynamic estimator interacting with the controller in real time.

Substantial amounts of research efforts have been devoted to the subject of real-time power system dynamic state estimation, a miniscule proportion of which is shown in [70-76]. However, much of this work dealt with the very slow dynamics of a power system [70-72]. State vector was defined as the set of complex node voltages of a system in a quasi-steady-state condition. Sets of measurements were normally the real and re-

active power injections at the nodes. Simulation studies were concerned with power system behavior over a period of hours or days. Estimates of the power system state were updated in matters of minutes or even hours, and were the basis for the slow application of controls to achieve minimal costs and optimal security of operation. The techniques presented were not at all suited to the needs of a fast-acting controller (which must update control input signals in matters of milliseconds) aimed at improving the transient and dynamic stability of a power system immediately following a disturbance. A few technical publications have addressed this need to some degree [73, 75, 76].

Handschin and Galiana [73] presented a real-time state estimation scheme featuring a slow centralized tracking estimator and fast local dynamic estimators based on Kalman-Bucy filtering. The centralized tracking estimator assumed a quasi-steady-state power system condition and used the update equation

$$\hat{\underline{x}}(t_{k+1}) = \hat{\underline{x}}(t_k) + (H^T R^{-1} H)^{-1} H^T R^{-1} [\underline{z}_s(t_{k+1}) - \underline{h}(\hat{\underline{x}}(t_k))] \tag{2.106}$$

There, $\hat{x}$, represented the estimates of the power system state vector while z, represented the measurements. A detailed linearized model of a power plant was used to design its dynamic estimator. The dynamic estimator allowed the estimate of the power plant state to be updated much more frequently than the power system state vector itself. THe power plant state estimate was given by the equation

$$\dot{\hat{\underline{x}}}(t) = A\hat{\underline{x}} + \underline{b}u(t) + \underline{c}P_e(t) + \underline{K}[z_f(t) - \underline{h}^T\hat{\underline{x}}(t)] \tag{2.107}$$

where K was the steady-state Kalman-Bucy filter gain. $z_f(t)$ corresponded to the measured frequency deviation while $P_e(t)$, the electrical power, and u(t) were known inputs to the filter. By comparing the statistical properties of the filter residual

$$e_f(t) = z_f(t) - \underline{h}^T \hat{\underline{x}}(t) \tag{2.108}$$

at any time with the known values under normal operating conditions, detection of power plant disturbances was made possible. The plant dynamic estimator was then made to interact with the central tracking estimator through the generator terminal voltage estimate $\hat{V}_{k|}\hat{\theta}_k$. The availability of the voltage estimate allowed the estimation of the machine rotor angle, and thus of $\hat{P}_e(t_{k+1})$ by the tracking estimator. Statistical analysis of the difference between the measured $P_e(t)$ and $\hat{P}_e(t_{k+1})$ allowed network disturbances to be determined.

Two related papers [75, 76] reported on-line laboratory implementation results of an optimal controller and estimator to improve the stability of a generator. A fixed-gain optimal regulator with full state feedback was used in conjunction with a Kalman-Bucy observer to synthesize the control input signals. The estimator equations were formulated to include all non-linear terms in the system. For an n-dimensional system with equations:

$$\dot{X} = AX + BU + \Gamma \quad \text{and } y = CX \tag{2.109}$$

the dynamics of the estimator was:

$$\dot{\overline{X}} = A\dot{X} + BU + \Gamma + K(Y - C\overline{X}) \tag{2.110}$$

where Γ represented all of the non-linear terms in the system. K was a time-varying matrix obtained by solving the following equations:

$$AQ + QA^T + V_{11} - QC^T V_{11}^{-1} CQ = 0 \tag{2.111}$$

$$K = QC^T V_{22}^{-1} \tag{2.112}$$

where V_{11} and V_{22} were matrices of assumed white noise intensities. Thus, K was a time-varying matrix for time-varying noise intensities.

This ends the literature review which has been restricted basically to coordinated multimachine stabilization using conventional stabilizers and the use of optimal controllers to derive appropriate control input signals to the generator excitation and/or speed-governing system(s) of a power system.

The subsequent chapters of this work will attempt to extend Rostamkolai's work [67,77] while incorporating the use of discrete-time fast dynamic state estimators , thus allowing the full state feedback required by the control law.

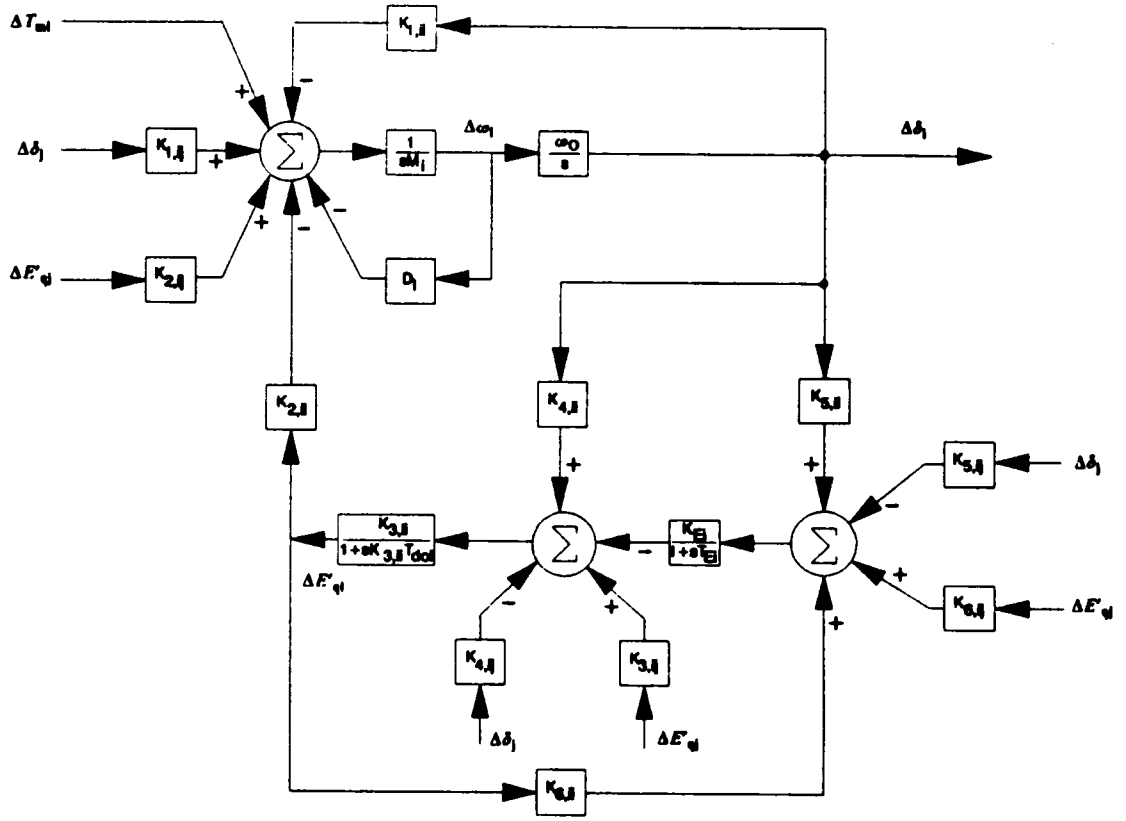

Figure 2.1. Block Diagram of Machine i Showing Multimachine Interaction

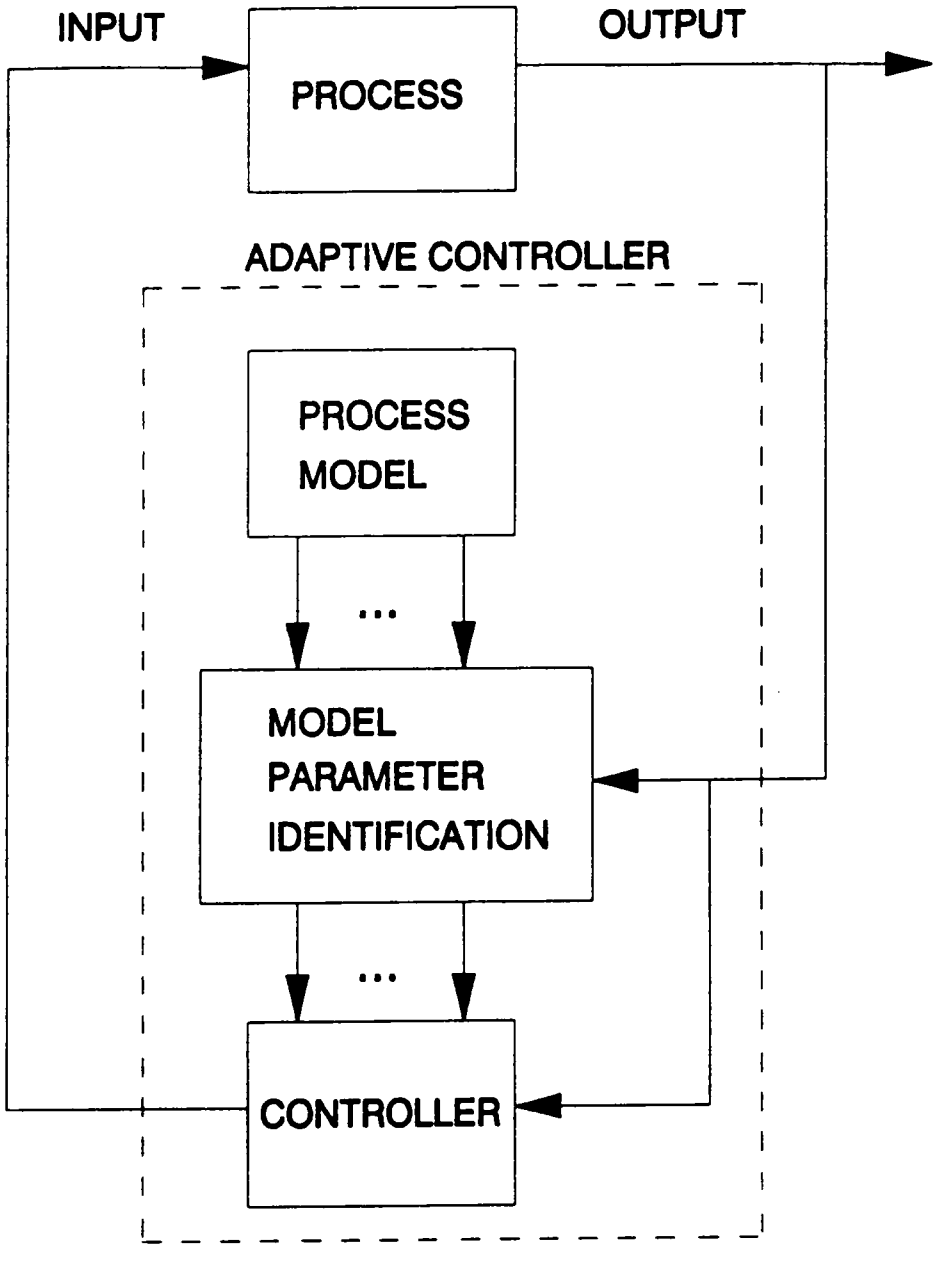

Figure 2.2. Block Diagram of a Self-Tuning Adaptive Regulator

Chapter 3

Study System

A 39-Bus multimachine system will be used to test and analyze the performance of the proposed controller. A single-line diagram of the test system is shown on Figure 3.1. It consists of 34 transmission lines, 12 transformers, and 10 generators. This chapter will present the required data for the parameters of the system components. Data on excitation and speed-governing systems were obtained from references [85,86,87] which are all in reference [78]. Most of the power system data came from reference [91]. Chapter 5 will discuss the controller algorithm including the choice of target trajectory for the power system following a disturbance. The disturbance to be considered is a symmetrical fault in one of the transmission lines followed by instantaneous clearing without breaker reclosing. The transmission line chosen for this purpose is Line 20 (from Bus 15 to Bus 16) which transports the largest amount of reactive power under normal operating conditions. To prepare for this, the power system states corresponding to the prefault, immediate postfault, and steady-state postfault conditions will be given in this chapter.

The system has 34 transmission lines each of which is characterized by a lumped series resistance, a series reactance, and a shunt susceptance. Transmission line data (in per unit) is shown in Table 3.1. The numbers given under the column "ωC" correspond to the total line susceptance, i.e., half of each value is placed at the end of each line (for an equivalent π representation).

Table 3.2 shows the data for the 12 system transformers. Fixed transformer tap ratios are assumed in the study. The series resistances and reactances (in per unit) shown on the table are those seen from the unity side of each transformer.

Generator data in per-unit is shown in Table 3.3. As suggested in references [79,88], a third-order model will be used to represent each generator in the following dynamic stability study. Figure 3.2 shows the phasor diagram derived from the model. Stator winding resistances are neglected as they are much smaller in magnitude compared to the reactance values. Moreover, neglecting them yields conservative results in a dynamic stability study as they tend to increase generator damping. The original damping coefficients shown on the first column of Table 3.4 do not account for the effects of the generator damper windings. However, it is well-known that damper (amortisseur) windings enhance the damping of the generator electromechanical modes [79,97]. Reference [79] gives an equivalent of about 25 per-unit damping torque to account for these effects. These effects which enhance electromechanical damping are captured by using the modified damping coefficients shown on the second part of Table 3.3.

Tables 3.4 shows the data for the excitation systems. Each generator except Generator 10 is assumed to operate with an equivalent IEEE Type 1 Excitation System. The block diagram corresponding to this excitation system model is shown on Figure 3.3. Generator 10 has a constant field excitation. All parameter values (gains, time constants, $A_{,,}$

B_e) are assumed to be constants independent of the operating point. Finally, the quantity S_{E_0} denotes the prefault value of the saturation function S_E.

Table 3.5 shows the speed-governor data obtained from reference [86]. The mechanical-hydraulic, nonreheat steam turbine is assumed for each generator. A block diagram representation of the combined speed-governor and turbine is shown on Figure 3.4.

The system operating point data corresponding to the three conditions mentioned earlier will be presented next. A load factor of 1.13 is used over the nominal values given in reference [91]. For the same fault, a heavier loading corresponds to a more severe disturbance and a more appropriate test for the controller.

Tables 3.6, 3.7, and 3.8 show the values of each bus voltage (magnitude and angle), and each state variable under prefault conditions. These prefault conditions correspond to a stable equilibrium point for the power system. Table 3.6 shows the prefault bus voltages (per unit, degrees) and injected powers (per unit) obtained after solving the loadflow problem. Generator contributions are not accounted for in the values shown in columns 3 and 4. Note that the last ten system buses (30-39) are generator terminal buses.

Table 3.7 shows prefault values for the internal voltage E'_q (per unit), internal angle δ_q (degrees) and the real and reactive powers (per unit) from each generator.

Table 3.8 shows the prefault values of the state variables and the value of the reference signal in each of the excitation systems. Values for V_t are not shown as they are equal to the corresponding generator terminal voltages shown in Table 3.6.

Table 3.8 also shows the prefault values of the state variables and the value of the reference signal in each of the generator speed-governor system. All values given are in per unit power.

Table 3.9 shows the system conditions immediately after the occurrence of the disturbance in terms of the 39 bus voltages. State variables retain their prefault values as they do not change instantaneously. The loads are assumed to draw the same amount of real and reactive powers under all conditions considered. Thus, the same values are to be found in columns 3 and 4 as those of Table 3.6.

Tables 3.10 and 3.11 show the target steady-state power system condition corresponding to the post-fault transmission line configuration. It is the solution to the loadflow problem with generator terminal buses 30-38 treated as P-V buses. The voltage magnitudes and generated real powers chosen for these buses were set equal to their prefault values. Bus 39 was treated as a slack bus.

Details pertaining to the simulation program will be discussed in the next chapter. Preliminary simulation results, however, will be presented in this chapter. Figures 3.5 to 3.7 show six sets of post-fault time curves without the application of the optimal controller. Figure 3.5A shows the voltage at Bus 15, one of the terminal buses of transmission line 20, as the most badly affected bus in the entire system. The remaining figures reveal sustained oscillations for a substantial amount of time following the disturbance. These voltage magnitude and rotor angle oscillations endanger power system stability. Thus, the objective of the optimal controller will be to reduce these oscillations and to bring the power system to a safe steady-state postfault operating point.

Table 3.1. Transmission Line Data

From	To	R	X	ωC
1	2	0.0035	0.0411	0.6987
1	30	0.0010	0.0250	0.7500
2	3	0.0013	0.0151	0.2572
2	25	0.0070	0.0086	0.1460
3	4	0.0013	0.0213	0.2214
3	18	0.0011	0.0133	0.2138
4	5	0.0008	0.0128	0.1342
4	14	0.0008	0.0129	0.1382
5	6	0.0002	0.0026	0.0434
5	8	0.0008	0.0112	0.1476
6	7	0.0006	0.0092	0.1130
6	11	0.0007	0.0082	0.1389
7	8	0.0004	0.0046	0.0780
8	9	0.0023	0.0363	0.3804
9	30	0.0010	0.0250	1.2000
10	11	0.0004	0.0043	0.0729
10	13	0.0004	0.0043	0.0729
13	14	0.0009	0.0101	0.1723
14	15	0.0018	0.0217	0.3660
15	16	0.0009	0.0094	0.1710
16	17	0.0007	0.0089	0.1342
16	19	0.0016	0.0195	0.3040
16	21	0.0008	0.0135	0.2548
16	24	0.0003	0.0059	0.0680
17	18	0.0007	0.0082	0.1319
17	27	0.0013	0.0173	0.3216
21	22	0.0008	0.0140	0.2565
22	23	0.0006	0.0096	0.1846
23	24	0.0022	0.0350	0.3610
25	26	0.0032	0.0323	0.5130
26	27	0.0014	0.0147	0.2396
26	28	0.0043	0.0474	0.7802
26	29	0.0057	0.0625	1.0290
28	29	0.0014	0.0151	0.2490

Table 3.2. Transformer Data

From	To	R	X	Tap Ratio
12	11	0.0016	0.0435	1.006
12	13	0.0016	0.0435	1.006
6	31	0.0000	0.0250	1.070
10	32	0.0000	0.0200	1.070
19	33	0.0007	0.0142	1.070
20	34	0.0009	0.0180	1.009
22	35	0.0000	0.0143	1.025
23	36	0.0005	0.0272	1.000
25	37	0.0006	0.0232	1.025
2	39	0.0000	0.0181	1.025
29	38	0.0008	0.0156	1.025
19	20	0.0007	0.0138	1.060

Table 3.3. Generator Data

Unit	H	X_d	X'_d	X_q
1	42.0	0.1000	0.0310	0.0690
2	30.3	0.2950	0.0697	0.2820
3	35.8	0.2495	0.0531	0.2370
4	28.6	0.2620	0.0436	0.2580
5	26.0	0.6700	0.1320	0.6200
6	34.8	0.2540	0.0500	0.2410
7	26.4	0.2950	0.0490	0.2920
8	24.3	0.2900	0.0570	0.2800
9	34.5	0.2106	0.0570	0.2050
10	500.0	0.0200	0.0006	0.0190

Unit	D (original)	D (modified)
1	4.0000	24.000
2	9.7500	29.750
3	10.000	30.000
4	10.000	30.000
5	3.0000	23.000
6	10.000	30.000
7	8.0000	28.000
8	9.0000	29.000
9	14.000	34.000
10	10.000	30.000

Table 3.4. Excitation System Data

Unit	K_A	T_A	K_F	T_F
1	5.0	0.06 s.	0.0400	1.000 s.
2	6.2	0.05 s.	0.0570	0.500 s.
3	5.0	0.06 s.	0.0800	1.000 s.
4	5.0	0.06 s.	0.0800	1.000 s.
5	40.0	0.02 s.	0.0300	1.000 s.
6	5.0	0.02 s.	0.0754	1.246 s.
7	40.0	0.02 s.	0.0300	1.000 s.
8	5.0	0.02 s.	0.0845	1.260 s.
9	40.0	0.02 s.	0.0300	1.000 s.

Unit	T_R	V_{RMAX}	V_{RMIN}	S_{EO}
1	0.006 s.	1.0	-1.0	0.0519
2	0.006 s.	1.0	-1.0	0.6694
3	0.006 s.	1.0	-1.0	0.0469
4	0.006 s.	1.0	-1.0	0.0680
5	0.006 s.	10.0	-10.0	0.7589
6	0.006 s.	1.0	-1.0	0.0496
7	0.006 s.	6.5	-6.5	0.4396
8	0.006 s.	1.0	-1.0	0.0549
9	0.006 s.	10.5	-10.5	0.3975

Unit	K_E	T_E	A_E	B_E
1	-.0485	0.250 s.	0.0229000	0.5136
2	-.6330	0.405 s.	0.4007000	0.1943
3	-.0198	0.500 s.	0.0000158	3.1945
4	-.0525	0.500 s.	0.0060000	1.0368
5	1.0000	0.785 s.	0.2674000	0.2339
6	-.0419	0.471 s.	0.0089000	0.6975
7	1.0000	0.730 s.	0.1947000	0.3574
8	-.0470	0.528 s.	0.0120000	0.7416
9	1.0000	1.400 s.	0.2406000	0.2224

Table 3.5. Speed-Governor Data

Unit	C_G	T_{1G}	T_{3G}	T_{CH}
1	20.00	0.2500 s.	0.1000 s.	0.3500 s.
2	20.00	0.2500 s.	0.1000 s.	0.3500 s.
3	20.00	0.2500 s.	0.1000 s.	0.3500 s.
4	20.00	0.2500 s.	0.1000 s.	0.3500 s.
5	20.00	0.2500 s.	0.1000 s.	0.3500 s.
6	20.00	0.2500 s.	0.1000 s.	0.3500 s.
7	20.00	0.2500 s.	0.1000 s.	0.3500 s.
8	20.00	0.2500 s.	0.1000 s.	0.3500 s.
9	20.00	0.2500 s.	0.1000 s.	0.3500 s.

Table 3.6. Prefault Bus Voltages and Externally Injected Powers

Bus k	V_k	δ_k	P_k	Q_k
1	1.0448	−10.387°	0.0000	0.0000
2	1.0427	−07.419°	0.0000	0.0000
3	1.0193	−10.709°	-3.6386	-0.0271
4	0.9890	−11.647°	-5.6500	-2.0792
5	0.9914	−10.270°	0.0000	0.0000
6	0.9944	−9.457°	0.0000	0.0000
7	0.9820	−12.014°	-2.6419	-0.9492
8	0.9810	−12.602°	-5.8986	-1.9956
9	1.0220	−12.384°	0.0000	0.0000
10	1.0057	−6.701°	0.0000	0.0000
11	1.0003	−7.640°	0.0000	0.0000
12	0.9795	−7.658°	-0.0961	-0.9944
13	1.0018	−7.525°	0.0000	0.0000
14	0.9979	−9.457°	0.0000	0.0000
15	1.0014	−9.953°	-3.6160	-1.7289
16	1.0202	−8.332°	-3.7222	-0.3650
17	1.0217	−9.475°	0.0000	0.0000
18	1.0191	−10.440°	-1.7854	-0.3390
19	1.0436	−3.038°	0.0000	0.0000
20	0.9853	−4.657°	-7.6840	-1.1639

Table 3.6. Prefault Bus Voltages and Externally Injected Powers

Bus k	V_k	δ_k	P_k	Q_k
21	1.0204	−5.558°	-3.0962	-1.2995
22	1.0425	−0.447°	0.0000	0.0000
23	1.0368	−0.675°	-2.7967	-0.9560
24	1.0265	−8.195°	-3.4872	1.0419
25	1.0523	−5.873°	-2.5312	-0.5334
26	1.0416	−7.314°	-1.5707	-0.1921
27	1.0253	−9.638°	-3.1753	-0.8531
28	1.0409	−3.294°	-2.3278	-0.3119
29	1.0427	−0.141°	-3.2036	-0.3040
30	1.0300	−12.159°	-12.4752	-2.8250
31	0.9820	0.592°	-0.1040	-0.0520
32	0.9830	2.448°	0.0000	0.0000
33	0.9970	2.884°	0.0000	0.0000
34	1.0120	1.240°	0.0000	0.0000
35	1.0490	5.203°	0.0000	0.0000
36	1.0630	8.273°	0.0000	0.0000
37	1.0280	1.825°	0.0000	0.0000
38	1.0260	7.884°	0.0000	0.0000
39	1.0480	−4.596°	0.0000	0.0000

Table 3.7. Prefault Generator Conditions

Unit	E'_q	δ_q	P_E	Q_E
1	1.0852	21.528°	-1.1752	-1.2483
2	1.1385	47.289°	6.3698	2.6298
3	1.0577	49.718°	7.3450	2.7076
4	0.8900	55.862°	7.1416	1.5331
5	1.3145	58.799°	5.7404	1.9969
6	1.0774	50.498°	7.3450	2.7038
7	0.9458	58.478°	6.3280	1.4016
8	0.8627	58.017°	6.1020	0.3121
9	1.0086	65.791°	9.3790	0.7469
10	1.0582	−1.812°	2.9009	1.8507

Table 3.8. Prefault Excitation System and Speed-Governor State Variables

Unit	V_r	V_z	E_{FD}	V_{ref}
1	0.005411	0.0000	1.5929	1.0311
2	0.096218	0.0000	2.6413	0.9975
3	0.067738	0.0000	2.5027	0.9965
4	0.036243	0.0000	2.3413	1.0042
5	7.843456	0.0000	4.4594	1.2081
6	0.018919	0.0000	2.4625	1.0528
7	3.280284	0.0000	2.2786	1.1450
8	0.016275	0.0000	2.0513	1.0313
9	3.154916	0.0000	2.2575	1.1049
10	----------	----------	1.0847	----------

Unit	P_W	P_{GV}	P_{MECH}	P_{OG}
1	0.0000	11.3000	11.3000	11.3000
2	0.0000	6.4738	6.4738	6.4738
3	0.0000	7.3450	7.3450	7.3450
4	0.0000	7.1416	7.1416	7.1416
5	0.0000	5.7404	5.7404	5.7404
6	0.0000	7.3450	7.3450	7.3450
7	0.0000	6.3280	6.3280	6.3280
8	0.0000	6.1020	6.1020	6.1020
9	0.0000	9.3790	9.3790	9.3790
10	0.0000	2.9009	2.9009	2.9009

Table 3.9. Immediate Postfault Bus Voltages and Injected Powers

Bus k	V_k	δ_k	P_k	Q_k
1	1.0066	−11.659°	0.0000	0.0000
2	1.0133	−8.086°	0.0000	0.0000
3	0.9718	−12.001°	-3.6386	-0.0271
4	0.8862	−16.116°	-5.6500	-2.0792
5	0.8865	−14.423°	0.0000	0.0000
6	0.8885	−13.473°	0.0000	0.0000
7	0.8781	−16.442°	-2.6419	-0.9492
8	0.8788	−17.061°	-5.8986	-1.9956
9	0.9546	−15.136°	0.0000	0.0000
10	0.8905	−10.693°	0.0000	0.0000
11	0.8879	−11.661°	0.0000	0.0000
12	0.8603	−11.948°	-0.0961	-0.9944
13	0.8821	−12.041°	0.0000	0.0000
14	0.8686	−15.326°	0.0000	0.0000
15	0.8127	−21.472°	-3.6160	-1.7289
16	1.0274	−6.442°	-3.7222	-0.3650
17	1.0109	−8.635°	0.0000	0.0000
18	0.9939	−10.407°	-1.7854	-0.3390
19	1.0516	−1.684°	0.0000	0.0000
20	0.9937	−3.376°	-7.6840	-1.1639

Table 3.9. Immediate Postfault Bus Voltages and Injected Powers

Bus k	V_k	δ_k	P_k	Q_k
21	1.0282	−3.942°	-3.0962	-1.2995
22	1.0501	0.856°	0.0000	0.0000
23	1.0444	0.616°	-2.7967	-0.9560
24	1.0339	−6.378°	-3.4872	1.0419
25	1.0285	−6.377°	-2.5312	-0.5334
26	1.0252	−7.240°	-1.5707	-0.1921
27	1.0115	−9.255°	-3.1753	-0.8531
28	1.0260	−3.234°	-2.3278	-0.3119
29	1.0285	−0.035°	-3.2036	-0.3040
30	0.9880	−13.844°	-12.4752	-2.8250
31	0.8945	−0.865°	-0.1040	-0.0520
32	0.8894	1.094°	0.0000	0.0000
33	1.0032	3.896°	0.0000	0.0000
34	1.0209	2.292°	0.0000	0.0000
35	1.0554	6.210°	0.0000	0.0000
36	1.0688	9.094°	0.0000	0.0000
37	1.0078	1.708°	0.0000	0.0000
38	1.0138	8.107°	0.0000	0.0000
39	1.0408	−4.859°	0.0000	0.0000

Table 3.10. Steady-State Postfault System Bus Conditions

Bus k	V_k	δ_k	P_k	Q_k
1	1.0415	−11.747°	0.0000	0.0000
2	1.0371	−7.537°	0.0000	0.0000
3	1.0081	−11.053°	-3.6386	-0.0271
4	0.9617	−15.429°	-5.6500	-2.0792
5	0.9714	−14.292°	0.0000	0.0000
6	0.9753	−13.545°	0.0000	0.0000
7	0.9635	−16.034°	-2.6419	-0.9492
8	0.9629	−16.560°	-5.8986	-1.9956
9	1.0145	−15.216°	0.0000	0.0000
10	0.9822	−11.305°	0.0000	0.0000
11	0.9782	−12.082°	0.0000	0.0000
12	0.9532	−12.300°	-0.0961	0.0000
13	0.9727	−12.360°	0.0000	0.0000
14	0.9553	−14.933°	0.0000	0.0000
15	0.9067	−19.942°	-3.6160	-1.7289
16	1.0326	−4.200°	-3.7222	-0.3650
17	1.0255	−6.859°	0.0000	0.0000
18	1.0166	−8.939°	-1.7854	-0.3390
19	1.0482	1.044°	0.0000	0.0000
20	0.9878	−0.558°	-7.6840	-1.1639

Table 3.10. Steady-State Postfault System Bus Conditions

Bus k	V_k	δ_k	P_k	Q_k
21	1.0292	−1.470°	-3.0962	-1.2995
22	1.0472	3.588°	0.0000	0.0000
23	1.0416	3.361°	-2.7967	-0.9560
24	1.0377	−4.063°	-3.4872	1.0419
25	1.0517	−5.679°	-2.5312	-0.5334
26	1.0435	−5.924°	-1.5707	-0.1921
27	1.0284	−7.683°	-3.1753	-0.8531
28	1.0419	−1.911°	-2.3278	-0.3119
29	1.0434	1.238°	-3.2036	-0.3040
30	1.0300	−14.261°	-12.4752	-2.8250
31	0.9820	−3.297°	-0.1040	-0.0520
32	0.9830	−1.936°	0.0000	0.0000
33	0.9970	6.952°	0.0000	0.0000
34	1.0120	5.331°	0.0000	0.0000
35	1.0490	9.213°	0.0000	0.0000
36	1.0630	12.273°	0.0000	0.0000
37	1.0280	2.023°	0.0000	0.0000
38	1.0260	9.260°	0.0000	0.0000
39	1.0480	−4.596°	0.0000	0.0000

Table 3.11. Steady-State Postfault Generator Conditions

Unit	E'_q	δ_q	P_E	Q_E
1	1.1010	18.702°	-1.1752	-1.2483
2	1.2029	40.246°	6.3698	2.6298
3	1.1397	41.058°	7.3450	2.7076
4	0.8641	61.492°	7.1416	1.5331
5	1.2931	63.889°	5.7404	1.9969
6	1.0520	55.869°	7.3450	2.7038
7	0.9278	63.518°	6.3280	1.4016
8	0.8657	58.037°	6.1020	0.3121
9	1.0052	67.360°	9.3790	0.7469
10	1.0600	−1.727°	2.9009	1.8507

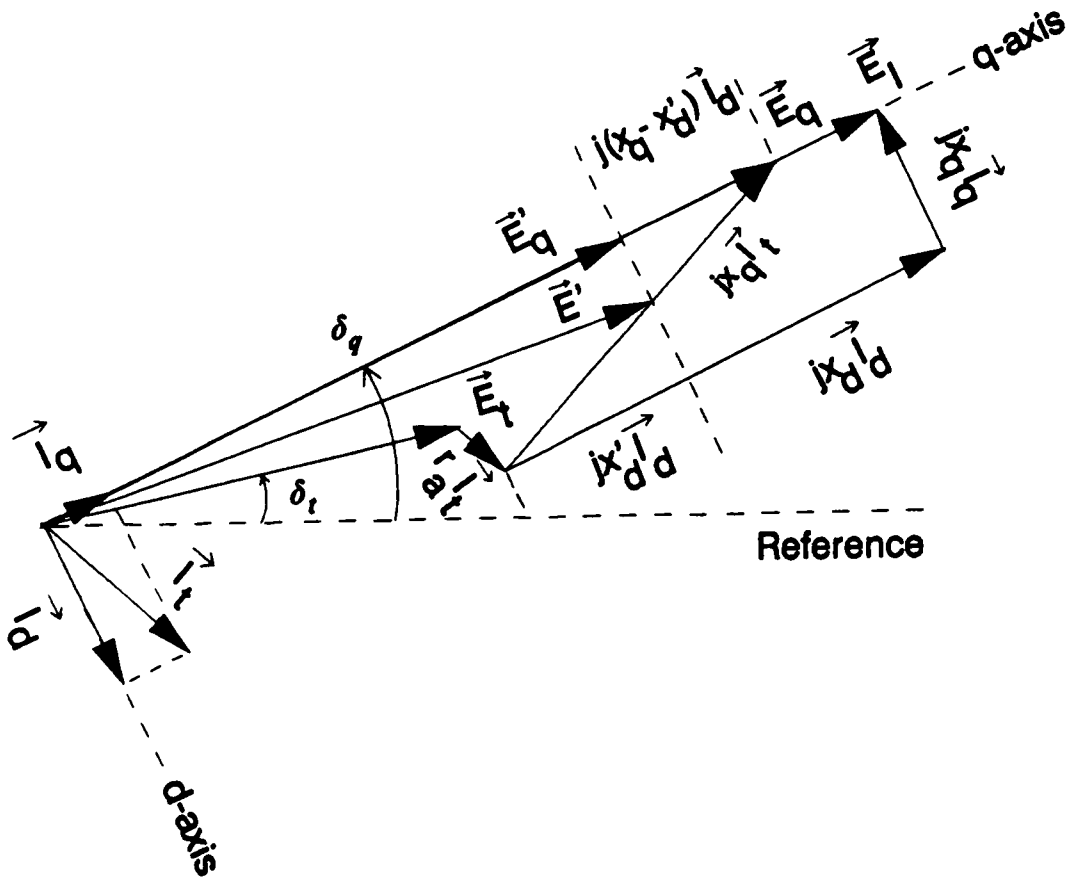

Figure 3.1. Synchronous Generator Phasor Diagram

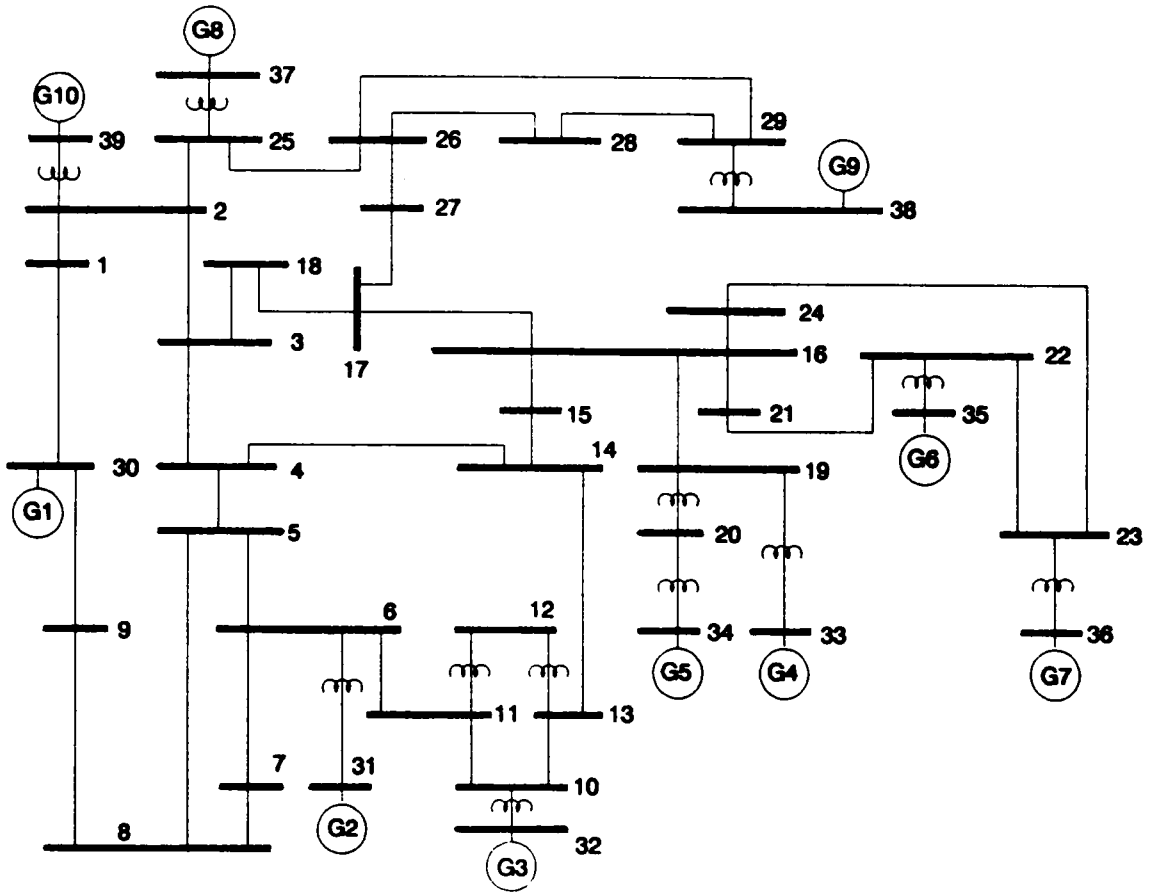

Figure 3.2. New England 10-Unit 39-Bus Test System

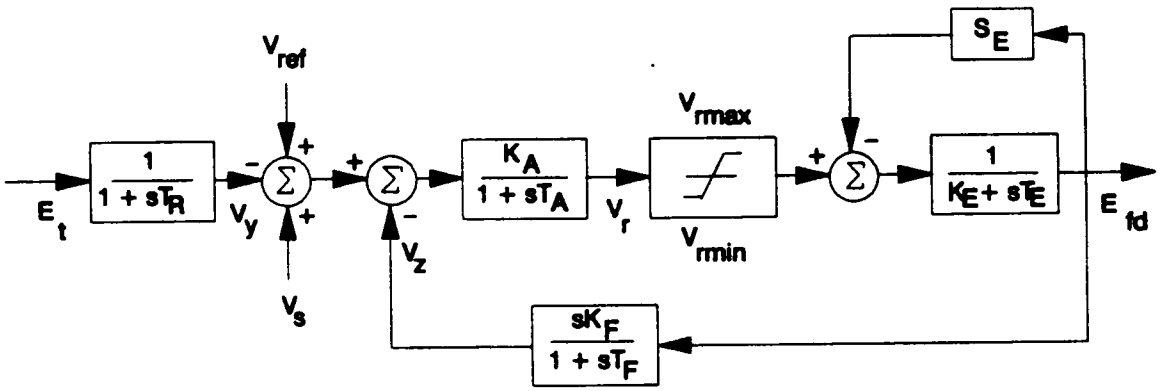

Figure 3.3. Representation of IEEE Type 1 Excitation System

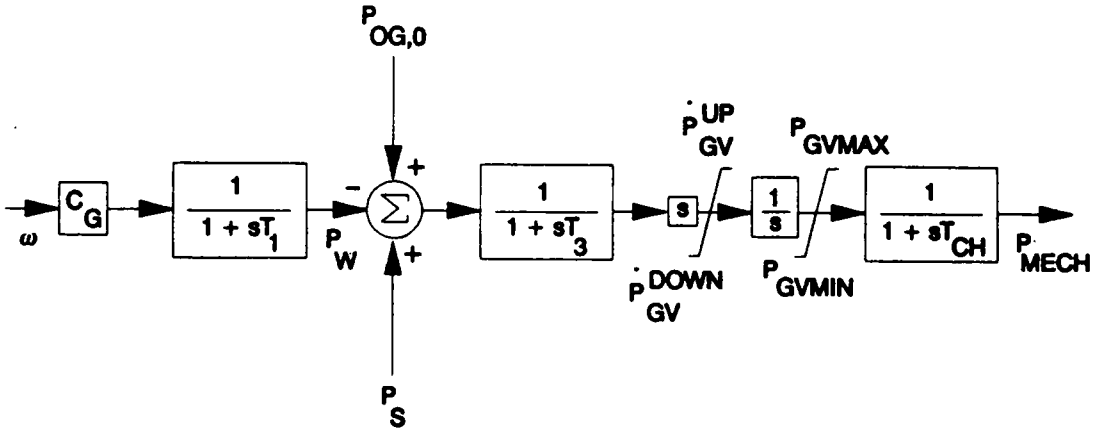

Figure 3.4. Representation of Combined Speed-Governor and Turbine

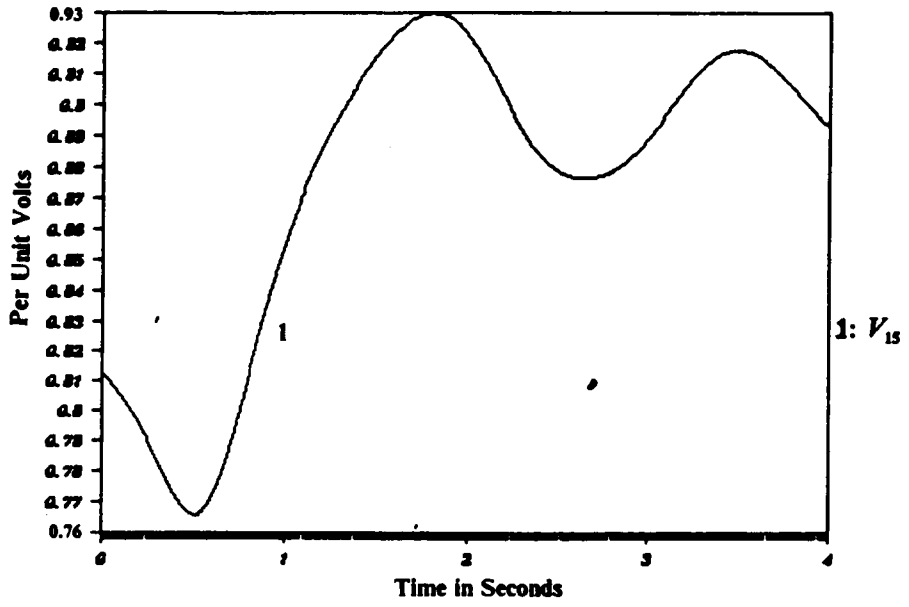

A. Voltage at Bus 15

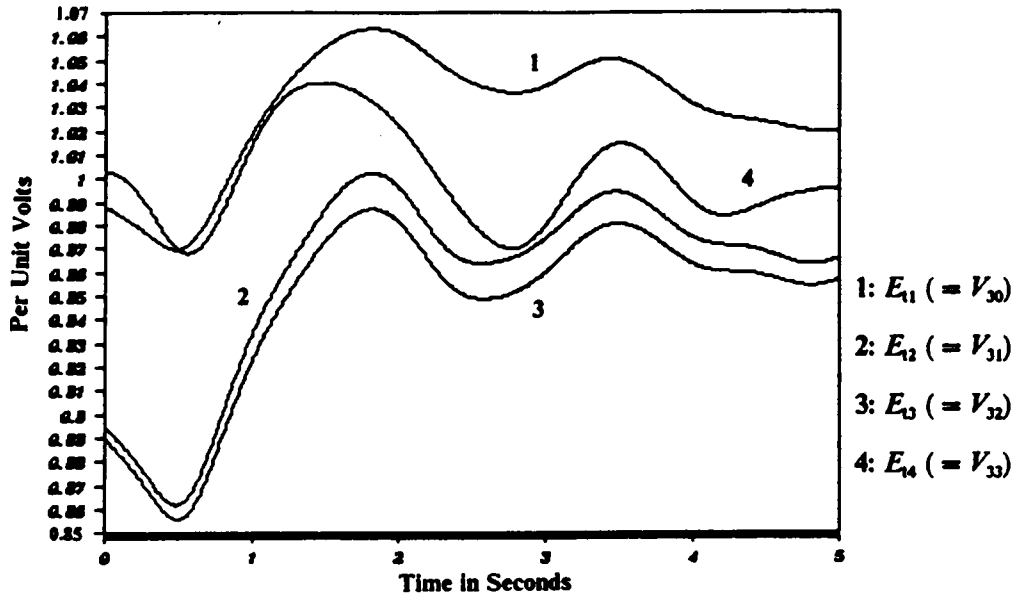

B. Some Generator Terminal Voltages

Figure 3.5. Bus Voltages (No Controller Case)

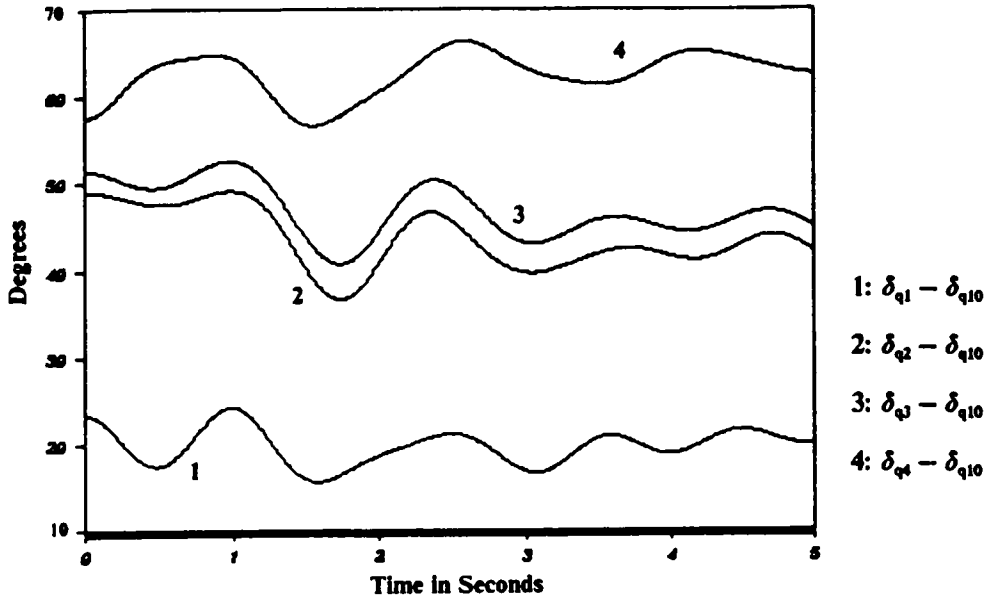

A. Generators 1 to 4

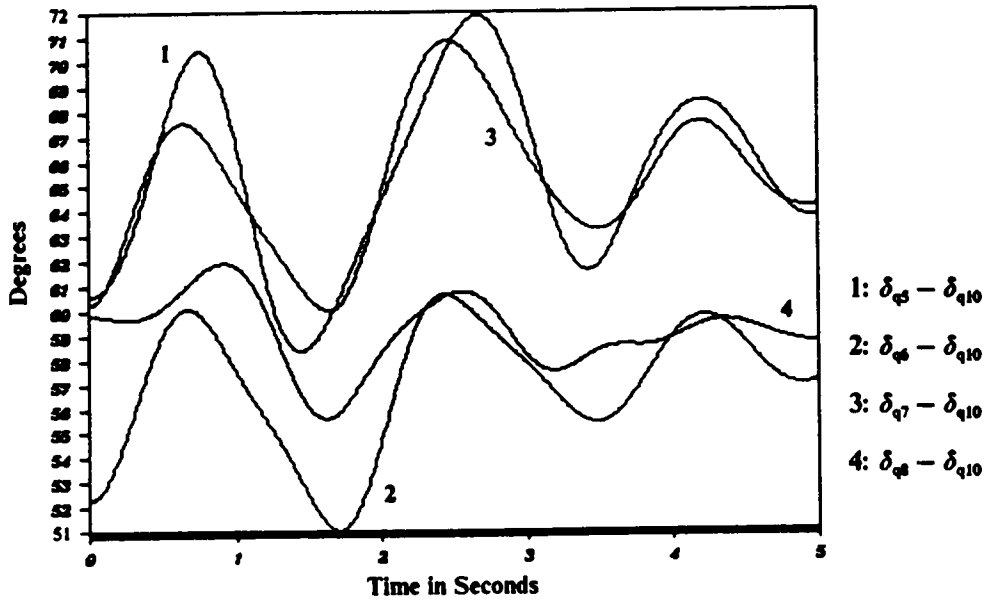

B. Generators 5 to 8

Figure 3.6. Internal Rotor Angles (No Controller)

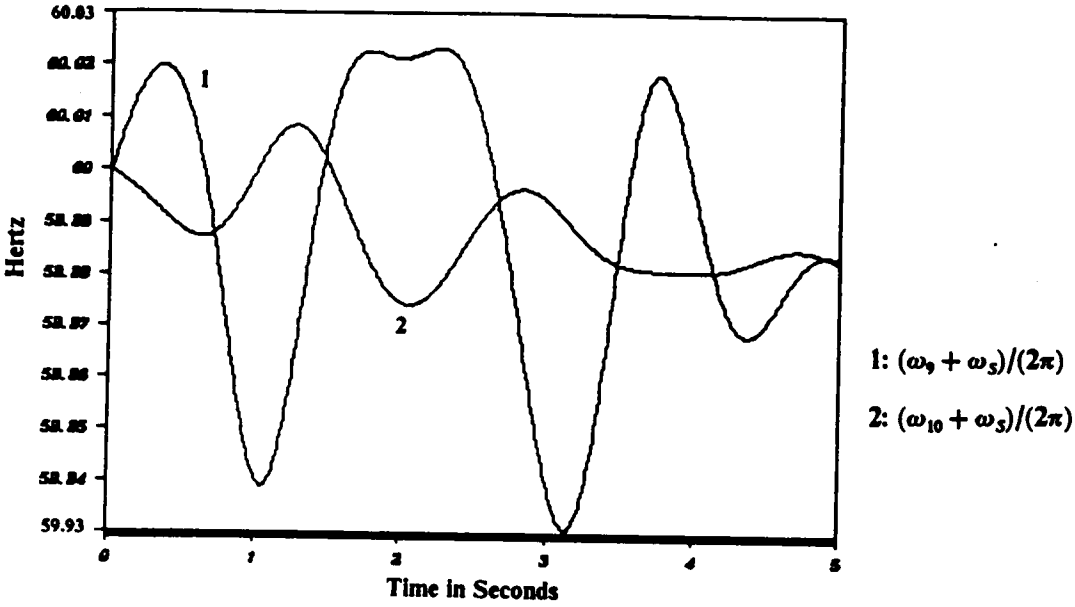

A. Generators 9 to 10

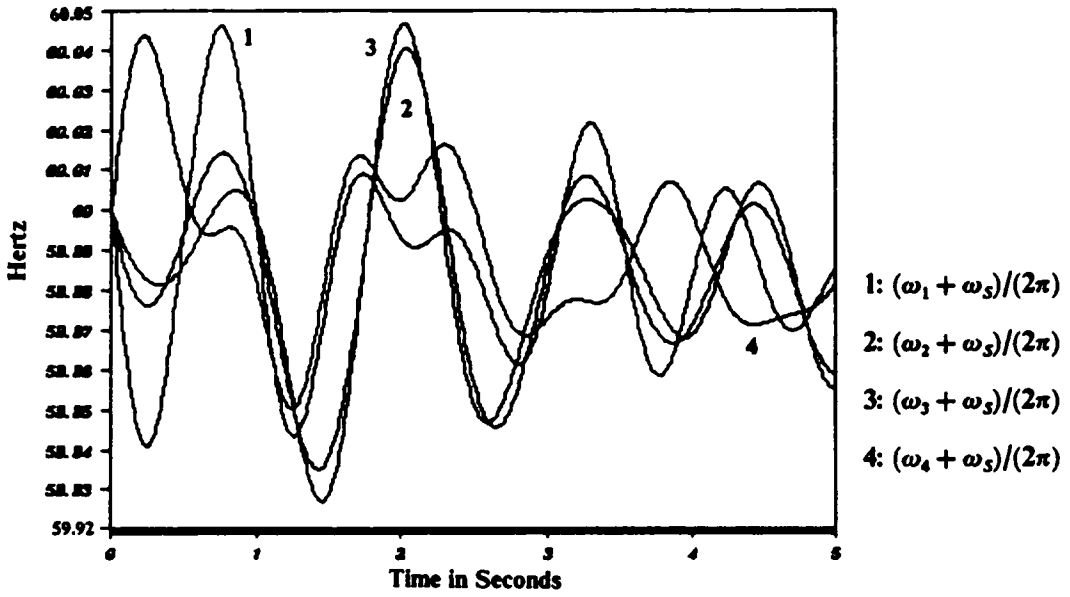

B. Generators 1 to 4

Figure 3.7. Rotor Speeds (No Controller)

Chapter 4

Simulation Program

Introduction

To study the response of the power system subject to the proposed controller, a mathematical description of various power system components is required. A mechanism to represent the interaction among these components is also necessary. The amount of detail placed on these component models depends to a large extent on the purpose of the study. Here, a dynamic stability study is being performed on a power system subject to the proposed controller. Thus, models involving changes occurring in short periods of time (of the order of milliseconds) or changes implemented on the power system or its components over extended periods of time (of the order of minutes) are not of major importance here. These very fast or very slow changes are assumed to occur either instantaneously or not at all over the time interval being studied (of the order of seconds). The component models required by the simulation program are those of the

excitation and speed-governing systems, the synchronous generators, system transformers, and transmission lines. The excitation and speed-governing system models are described mainly by nonlinear differential equations which are solved through a Runge-Kutta integration scheme. For the synchronous generators, the model used is suited for dynamic stability studies. In this model, fast transients are neglected, and only synchronous currents and voltages are taken into account in the armature circuits. This synchronous generator model is consistent with the transformer and transmission line models used in the study.

The test system, which data is shown in the preceding chapter, represents a typical power system. Action of the excitation and speed-governing systems on a generator is reflected in the instantaneous value of synchronous voltages and currents in the generator phasor diagram. Nonlinear interaction among the generators occurs across the complex transmission network. The loadflow solution to the network at any step in the simulation provides a measure of this interaction.

The remainder of this chapter provides a detailed explanation and justification of the simulation program used in the study.

Component Modelling

Excitation System Model. Inclusion of excitation system behavior in a dynamic stability study allows a more realistic and accurate machine representation which goes beyond the simpler model of constant voltage behind the transient reactance. With the

exception of Generator 10 which has a constant field excitation, an equivalent IEEE Type 1 excitation system will be assumed for each of the generators. This model corresponds to a continuously acting regulator and exciter. The control and state estimation problems which will be discussed in the next two chapters will be formulated based on the assumed excitation system model. Use of a different model necessarily requires the reformulation of these two problems. However, the general methodology would still apply.

A block diagram of an IEEE Type 1 exciter was shown on Chapter 3. Two nonlinearities are accounted for, namely, the upper and lower ceiling voltages on the regulator output, and the saturation function which depends nonlinearly on the field voltage. The first transfer function will be a matter of interest in the chapter on state estimation. It is a simple time constant T_R representing the rectifier system and regulator input filtering. T_R is usually very small and may be considered to be zero under certain conditions.

The following nomenclature will be used in this paper to denote the state variables and other quantities in the ith excitation system.

V_{yi} = output voltage of input filter

V_{ri} = main regulator output voltage

V_{zi} = excitation major damping loop signal

$E_{fd,i}$ = field voltage

S_{Ei} = saturation function

$V_{ref,i}$ = constant reference signal

V_{si} = control input signal

The differential equations relating the above quantities to one another are given by :

$$\dot{V}_{yi} = \frac{1}{T_{ri}}(E_{ti} - V_{yi}) \tag{4.1}$$

$$\dot{V}_{ri} = \frac{1}{T_{ai}}[-V_{ri} + (-V_{yi} - V_{zi} + V_{refi} + V_{si})K_{ai}] \tag{4.2a}$$

In situations where the regulator voltage is at its upper or lower limit,

$$\dot{V}_{ri} = 0 \tag{4.2b}$$

$$\dot{V}_{zi} = \frac{1}{T_{fi}}\left\{\frac{K_{fi}}{T_{ei}}[V_{ri} - (S_{Ei} + K_{Ei})E_{fdi}] - V_{zi}\right\} \tag{4.3}$$

$$\dot{E}_{fdi} = \frac{1}{T_{Ei}}[V_{ri} - (S_{Ei} + K_{Ei})E_{fdi}] \tag{4.4}$$

The saturation is a nonlinear monotonically increasing function of the field voltage $E_{fd,i}$. In this paper, the function was assumed to be exponential, i.e.,

$$S_{Ei} = f(E_{fd,i}) = A_{ei} \exp(B_{ei} \cdot E_{fd,i}) \tag{4.5}$$

The constants A_{ei} and B_{ei} were determined using the base data (100% loading and generation levels and (1/1.13) of the corresponding values shown in Chapter 3). Once computed, they were used to simulate power system performance at 113% level of loading and generation. For each of the nine generators with variable field excitation,

the base case field voltage $E_{fdo,i}$ was computed from base case data and used in the following manner to solve for A_{ei} and B_{ei}:

Self-Excited Exciter. Assuming known $S_{Emax,i}$ and $V_{Rmax,i}$ from input data and an exponential saturation function,

$$V_{Rmax,i} - (K_{Ei} + S_{Emax,i})E_{fdmax,i:ef.} = 0 \tag{4.6}$$

Computation of $E_{fdmax,i}$ from the preceding yields two equations for A_{ei} and B_{ei}.

$$S_{Emax,i} = A_{ei} \exp(B_{ei} \cdot E_{fdmax,i}) \tag{4.7}$$

$$K_{Ei} + A_{ei} \exp(B_{ei} \cdot E_{fdo,i}) = 0 \tag{4.8}$$

The last equation is justified by the argument that at the initial value $E_{fdo,i}$, the shunt field exactly compensates for the exciter saturation and no regulator output is required [85]. It also reveals that $K_{Ei} < 0$ for a self-excited exciter. As can be seen from the excitation system data of Chapter 2, generators 1,2,3,4,6,8 have this kind of excitation system.

Separately-Excited Exciter. The values of the saturation function at $E_{fdmax,i}$ and $0.75E_{fdmax,i}$ are given as $S_{Emax,i}$ and $S_{E0.75max,i}$ from the input data together with $V_{Rmax,i}$. As before, $E_{fdmax,i}$ is computed from

$$V_{Rmax,i} - (K_{Ei} + S_{Emax,i})E_{fdmax,i:ef.} = 0 \tag{4.9}$$

Then, the following equations were solved for A_{ei} and B_{ei}.

$$S_{Emax,i} = A_{ei} \exp(B_{ei} \cdot E_{fdmax,i}) \tag{4.10}$$

$$S_{E0.75max,i} = A_{ei} \exp(B_{ei} \cdot 0.75E_{fdmax,i}) \tag{4.11}$$

Speed-Governor Model. Figure 4.1 shows a functional block diagram showing the location of the speed-governing system and turbine of a generator relative to the complete system. An input signal is provided to the Governor Speed Changer by Automatic Generation Control. This input representing a composite load and speed reference is normally assumed constant over the interval of a stability study. Figure 4.2A shows a model of a speed-governing system for a steam turbine using either electro-hydraulic or mechanical-hydraulic control. The time constant T_2 represents steam feedback which exists in an electro-hydraulic control scheme. Assuming a mechanical-hydraulic control scheme, the time constant is set to zero. In the following power system study, nonlinearities will be neglected except for the rate and position limits represented in Figure 4.2A. Provided that rate limits $\dot{P}_{GV}^{UP}$ and $\dot{P}_{GV}^{DOWN}$ on P_{GV} are recognized, the speed-governor model reduces to that shown in Figure 4.2B. The existence of a control input signal P_S will be assumed by the controller to be studied in this paper.

The speed-governor basically works in the following manner. The speed signal is subtracted from the reference input SR and the resulting error signal ω is fed into the speed relay (with time constant T_1) where it is amplified and converted into a position signal. Thus, the control input signal is superimposed on this position signal. A second stage amplifier (with time constant T_3) is provided by the servo-motor which operates the steam valves. The steam flow through these valves produces a torque which is opposed by the load and loss torques. The net remaining torque is used to accelerate the rotating mass of the shaft which feeds the speed signal back to the speed governor.

Between the governor-controlled valves and the high-pressure turbine is a steam bowl or chest. This vessel introduces a time delay T_{CH} between changes in valve steam flow and steam flow in the high-pressure turbine as shown in Figure 4.3. The fraction F re-

presents the effective gain of the governor-controlled valves. In this paper, the small boiler tube drop will be ignored (i.e., F = 1). The block diagram of Figure 4.3 corresponds to the simple nonreheat steam turbine. Many of the more complicated models arising from the other steam turbine types essentially reduce to the nonreheat type when the large time constants (7.5 seconds on the average) are neglected.

Combination of the block diagrams in Figures 4.2 and 4.3 results in the speed-governor diagram shown in Chapter 3 with the following nomenclature:

ω_i = error signal, speed deviation from rated value

C_{Gi} = speed relay gain

T_{1i} = speed relay time constant (seconds)

P_{Wi} = speed relay output

$P_{OG,i}$ = servo-motor reference signal

P_{Si} = control input signal

T_{3i} = servo-motor time constant (seconds)

$P_{GV,i}$ = servo-motor output

$T_{CH,i}$ = charging time constant

$P_{MECH,i}$ = mechanical power output

The differential equations relating governor-turbine state variables to one another are given by:

$$\dot{P}_{Wi} = \frac{1}{T_{1i}}(C_{Gi}\omega_i - P_{Wi}) \tag{4.12}$$

$$\dot{P}_{GV,i} = \frac{1}{T_{3i}}(P_{Si} + P_{OG,i} - P_{Wi} - P_{GV,i}) \tag{4.13a}$$

In cases where $P_{GV,i}$ is at its upper or lower limit,

$$\dot{P}_{GV,i} = 0 \tag{4.13b}$$

Physical constraints are also imposed on the time rate of change of $\dot{P}_{GV,i}$. At these operating points, the time rate is constant, i.e.

$$\dot{P}_{GV,i} = \dot{P}_{GVi}^{UP} \tag{4.13c}$$

or

$$\dot{P}_{GV,i} = \dot{P}_{GVi}^{DOWN} \tag{4.13d}$$

whichever is applicable.

$$\dot{P}_{MECH,i} = \frac{1}{T_{CH,i}}(P_{GV,i} - P_{MECH,i}) \tag{4.14}$$

Synchronous Generator Model. Figure 4.4 shows the phasor diagram corresponding to the synchronous generator model to be used in this paper. It assumes steady-state conditions in the armature stator windings of the generator and includes the effects of three windings (generator field winding and the equivalent d-q armature windings) only

[79,88,97]. The damper winding circuits are neglected because they involve time constants much shorter than periods of time normally associated with dynamic stability studies. The phasor equations are given by :

$$\vec{E}_{qi} = \vec{E}_{ti} + r_{ai}\vec{I}_{ti} + jx_{qi}\vec{I}_{ti} \tag{4.15}$$

$$\vec{E}_{Ii} = \vec{E}_{ti} + r_{ai}\vec{I}_{ti} + jx_{di}\vec{I}_{di} + jx_{qi}\vec{I}_{qi} \tag{4.16}$$

The algebraic equations are:

$$E'_{qi} = E_{qi} - (x_{qi} - x'_{di})I_{di} \tag{4.17}$$

$$E_{Ii} = E_{qi} + (x_{di} - x_{qi})I_{di} \tag{4.18}$$

$$E_{Ii} = E'_{qi} + (x_{di} - x'_{di})I_{di} \tag{4.19}$$

Reference [79] has shown the following differential equation to be applicable under the same assumptions:

$$\dot{E}'_{qi} = \frac{1}{T'_{do,i}}(E_{fd,i} - E_{Ii}) \tag{4.20}$$

where

E'_{qi} = voltage proportional to field flux linkages

E_{Ii} = voltage proportional to field current

$E_{fd,i}$ = voltage proportional to field voltage

Appendix A derives the following expressions for the generated real and reactive power directly from the phasor diagram:

$$P_{Ei} = \frac{E'_{qi}E_{ti}}{x'_{di}} \sin(\delta_{qi} - \delta_{ti}) - \frac{E_{ti}^2(x_{qi} - x'_{di})}{2x'_{di}x_{qi}} \sin(2\delta_{qi} - 2\delta_{ti}) \tag{4.21}$$

$$Q_{Ei} = \frac{E'_{qi}E_{ti}}{x'_{di}} \cos(\delta_{qi} - \delta_{ti}) - \frac{E_{ti}^2}{x'_{di}x_{qi}} [x_{qi}\cos^2(\delta_{qi} - \delta_{ti}) + x'_{di}\sin^2(\delta_{qi} - \delta_{ti})] \tag{4.22}$$

The electromechanical behavior of generator "i" is described by the following swing equations.

$$M_i\ddot{\delta}_{qi} + D_i(\dot{\delta}_{qi} - \dot{\delta}_{qc}) = P_{Mi} - P_{Ei} \tag{4.23}$$

$$\dot{\delta}_{qi} = \omega_i \tag{4.24}$$

where, δ_{qc}, the center-of-angle is given by

$$\delta_{qc} = \frac{\sum_{i=1}^{i=NG} M_i\delta_{qi}}{\sum_{i=1}^{i=NG} M_i} \tag{4.25}$$

Transformer Model. As shown in Figure 4.5, the transformer equivalent circuit with a per-unit turns ratio a:1 can be converted into an equivalent π circuit using the following admittance transformation :

$$Y_A = Y\left(\frac{1}{a}\right)$$
$$Y_B = Y\left(\frac{1-a}{a^2}\right) \tag{4.26}$$
$$Y_C = Y\left(\frac{a-1}{a}\right)$$

Here it is noted that transformer data given in the preceding chapter provide the series per-unit impedance as seen from the unity side of the transformer. The admittance Y shown in Figure 4.5A is the reciprocal of the given series impedance.

System Network and Transmission Line Models. Each of the transmission lines will be represented by its π network equivalent. The values of the transmission line parameters evaluated at the nominal frequency were given in Chapter 3 and are used to compute the elements of the power system admittance matrix. This method of representation neglects the network transients characterized by very small time constants and is consistent with the steady-state assumptions made for the generator armature windings [97,98].

Treating the synchronous generators for the moment as components external to the network, the following discussion applies. Let an element $\vec{Y}_{kn}$ of the complex admittance matrix be denoted by Y_{kn}/θ_{kn}. The current $\vec{I}_k$ injected into bus k is given by

$$\vec{I} = \vec{Y}\vec{V} \tag{4.27}$$

where

$\vec{I}$ = vector of injected bus current phasors

$\vec{Y}$ = complex admittance matrix

$\vec{V}$ = vector of bus voltage phasors

Thus, letting NBUS denote the total number of system buses,

$$\vec{I}_k = \sum_{n=1}^{\text{NBUS}} \vec{Y}_{\text{kn}}\, \vec{V}_n = \sum_{n=1}^{\text{NBUS}} (Y_{\text{kn}} \angle\theta_{\text{kn}})\,(V_n \angle\delta_n) \tag{4.28}$$

The complex power injected into bus k is

$$\vec{S}_k = \vec{V}_k \vec{I}_k^{*} = V_k \angle\delta_k \sum_{n=1}^{\text{NBUS}} (Y_{\text{kn}} \angle -\theta_{\text{kn}})\,(V_n \angle -\delta_n) \tag{4.29}$$

$$\vec{S}_k = \sum_{n=1}^{\text{NBUS}} V_k V_n Y_{\text{kn}} \angle(\delta_k - \delta_n - \theta_{\text{kn}}) \tag{4.30}$$

The injected real power is given by

$$P_k = Re\,[\vec{S}_k] = \sum_{n=1}^{\text{NBUS}} V_k V_n Y_{\text{kn}} \cos(\delta_k - \delta_n - \theta_{\text{kn}}) \tag{4.31}$$

while the injected reactive power is

$$Q_k = Im\,[\vec{S}_k] = \sum_{n=1}^{\text{NBUS}} V_k V_n Y_{\text{kn}} \sin(\delta_k - \delta_n - \theta_{\text{kn}}) \tag{4.32}$$

The above equations apply to any of the NBUS system buses not directly connected to a generator. The admittance matrix $\vec{Y}$ used in the preceding equations was formed without regard to the generator parameters. The power quantities P_k and Q_k above implicitly include the contributions from attached generators for cases where the system bus corresponds to a generator terminal. Let P_{kload} and Q_{kload} denote the power drawn by an external load from the generator terminal bus. Then, letting "i" denote the corresponding generator

$$-P_{\text{kload}} = P_k = \sum_{n=1}^{\text{NBUS}} V_k V_n Y_{\text{kn}} \cos(\delta_k - \delta_n - \theta_{\text{kn}}) - P_{\text{Ei}} \tag{4.33}$$

$$-Q_{\text{kload}} = Q_k = \sum_{n=1}^{\text{NBUS}} V_k V_n Y_{\text{kn}} \sin(\delta_k - \delta_n - \theta_{\text{kn}}) - Q_{\text{Ei}} \tag{4.34}$$

where P_{Ei} and Q_{Ei} are the real and reactive power contributions from the ith generator mentioned in the preceding section.

Simulation Program Flowchart

Figure 4.6 shows the general flowchart followed in the simulation program.

As mentioned in Chapter 3, the disturbance assumed in the study is the instantaneous and permanent outage of one of the system transmission lines. The change in network topology therefore occurs once only (at the very start of the simulation).

In the proposed field implementation of the optimal controller, necessary bus voltage quantities required by the controller and the state estimators will be provided by the phasor measurement systems. Real-time computation of the loadflow solution will be performed once only at the very start of the control time interval to determine a target steady-state operating condition for the power system. Thus, the loadflow calculations performed in the simulation of power system behavior following the disturbance take the place of real-time phasor and auxiliary measurements performed on the power system. The solution to the loadflow problem yields the power system bus voltage magnitudes and angles under given load and machine internal voltage conditions and allows direct computation of the ith generator quantities P_{Ei} and E_{Ii} for use in the machine swing and excitation system equations.

Computation of the control input signals to the excitation and speed-governing systems consists of state estimation and the application of the control law. Chapter 6 will discuss the problem of state estimation to calculate the state variables in the exciter and speed-governor of each generator under assumed levels of measurement noise and state disturbances. Chapter 5 will deal the control algorithm itself. These aspects of the program will not be discussed in detail in this chapter.

The next step in the simulation is the numerical integration of the differential equations arising from the assumed models for the system components. Each generator has ten state variables (four from the excitation system, three from the speed-governor, one from the generator model itself, and two from the swing equations) except the largest generator which has six (since it has a constant field excitation). Thus, for the ten-machine system being studied, the stability program must numerically integrate ninety-six (96) differential equations. A fixed-time step fourth-order Runge-Kutta

scheme is used to accomplish the integration. At each time step, the nonlinear quantities on the right-hand of some differential equations are provided by the solution to the loadflow problem.

A period of five seconds will be simulated in the various cases to be considered (Chapters 5 and 6). This is about the amount of time needed by the power system to approach a steady-state condition upon application of the optimal controller under the best conditions.

The last section of this chapter will discuss in some detail the loadflow subroutine of the simulation program.

The Loadflow Subroutine (Multiple $V-\delta$ Bus Formulation). The following formulation of the loadflow problem and its solution assumes constant power (real and reactive) loads. The (2*NBUS) unknown quantities to be computed are the voltage magnitudes and angles of the system buses which satisfy the known P,Q conditions on the same buses and the known internal machine voltages $\vec{E}'_q$. The loadflow computations are performed at every time step. Thus, the $\vec{E}'_{qi}$'s correspond to the current solutions to the differential equations.

In the conventional loadflow problem, the only $V-\delta$ bus is the slack bus. In the present case, there are effectively NG (NG = number of generators in the system) slack buses corresponding to the NG internal machine buses containing the voltages $\vec{E}'_q$. Let

$$P_L = [P_1 \;\; P_2 \;\; \cdots \;\; P_k \;\; \cdots \;\; P_{\text{NBUS}}]^T \tag{4.35}$$

$$Q_L = [Q_1 \;\; Q_2 \;\; \cdots \;\; Q_k \;\; \cdots \;\; Q_{\text{NBUS}}]^T \tag{4.36}$$

$$\underline{V}_L = [V_1 \;\; V_2 \;\; \cdots \;\; V_k \;\; \cdots \;\; V_{\mathrm{NBUS}}]^T \tag{4.37}$$

$$\underline{\delta}_L = [\delta_1 \;\; \delta_2 \;\; \cdots \;\; \delta_k \;\; \cdots \;\; \delta_{\mathrm{NBUS}}]^T \tag{4.38}$$

$$\underline{\vec{E}'}_q = [\vec{E}'_{\mathrm{q1}} \;\; \vec{E}'_{\mathrm{q2}} \;\; \cdots \;\; \vec{E}'_{\mathrm{qi}} \;\; \cdots \;\; \vec{E}'_{\mathrm{q,NG}}]^T \tag{4.39}$$

$$\underline{E'}_q = [E'_{\mathrm{q1}} \;\; E'_{\mathrm{q2}} \;\; \cdots \;\; E'_{\mathrm{qi}} \;\; \cdots \;\; E'_{\mathrm{q,NG}}]^T \tag{4.40}$$

$$\underline{\delta}_q = [\delta_{\mathrm{q1}} \;\; \delta_{\mathrm{q2}} \;\; \cdots \;\; \delta_{\mathrm{qi}} \;\; \cdots \;\; \delta_{\mathrm{q,NG}}]^T \tag{4.41}$$

$$\underline{E}_t = [E_{\mathrm{t1}} \;\; E_{\mathrm{t2}} \;\; \cdots \;\; E_{\mathrm{ti}} \;\; \cdots \;\; E_{\mathrm{t,NG}}]^T \tag{4.42}$$

$$\underline{\delta}_t = [\delta_{\mathrm{t1}} \;\; \delta_{\mathrm{t2}} \;\; \cdots \;\; \delta_{\mathrm{ti}} \;\; \cdots \;\; \delta_{\mathrm{t,NG}}]^T \tag{4.43}$$

Then, for a generator terminal bus, using Eqs.(4.33)-(4.34),

$$P_k = P_k(\underline{V}_L, \underline{\delta}_L, E'_{\mathrm{qi}}, \delta_{\mathrm{qi}}) \tag{4.44}$$

$$Q_k = Q_k(\underline{V}_L, \underline{\delta}_L, E'_{\mathrm{qi}}, \delta_{\mathrm{qi}}) \tag{4.45}$$

where k = NBUS - NG + i.

For a system bus not attached to any generator,

$$P_k = P_k(\underline{V}_L, \underline{\delta}_L) \qquad \mathrm{k} = 1, 2, \ldots, \mathrm{NBUS} \tag{4.46}$$

$$Q_k = Q_k(\underline{V}_L, \underline{\delta}_L) \qquad \mathrm{k} = 1, 2, \ldots, \mathrm{NBUS} \tag{4.47}$$

where 1 < k < (NBUS-NG). As pointed out in Chapter 3, the last ten system buses correspond to the ten generator terminal buses.

At a given instant of time, the internal voltage phasor

$$\vec{E}'_{qi} = E'_{qi} \angle \delta_{qi} \tag{4.48}$$

is treated as a given constant. Thus,

$$\Delta P_k = \frac{\partial P_k}{\partial \underline{V}_L} \Delta \underline{V}_L + \frac{\partial P_k}{\partial \underline{\delta}_L} \Delta \underline{\delta}_L \tag{4.49}$$

$$\Delta Q_k = \frac{\partial Q_k}{\partial \underline{V}_L} \Delta \underline{V}_L + \frac{\partial Q_k}{\partial \underline{\delta}_L} \Delta \underline{\delta}_L \tag{4.50}$$

and

$$\begin{bmatrix} \Delta \underline{P}_L \\ \Delta \underline{Q}_L \end{bmatrix} = \begin{bmatrix} \underline{J}_{11} & \underline{J}_{12} \\ \underline{J}_{21} & \underline{J}_{22} \end{bmatrix} \begin{bmatrix} \Delta \underline{V}_L \\ \Delta \underline{\delta}_L \end{bmatrix} \tag{4.51}$$

Eqs.(4.46) and (4.47) are solved for $\underline{V}_L$ and $\underline{\delta}_L$ by using the well-known Newton-Raphson iterative method. In this method, the Jacobian matrix of Eq.(4.51)

$$\underline{J} = \begin{bmatrix} \underline{J}_{11} & \underline{J}_{12} \\ \underline{J}_{21} & \underline{J}_{22} \end{bmatrix} \tag{4.52}$$

with rank and size of (2*NBUS) is reevaluated at every iteration. From Eq.(4.51),

$$\begin{bmatrix} \Delta \underline{V}_L \\ \Delta \underline{\delta}_L \end{bmatrix} = \underline{J}^{-1} \begin{bmatrix} \Delta \underline{P}_L \\ \Delta \underline{Q}_L \end{bmatrix} \tag{4.53}$$

The improved estimate to $[\underline{V}_L^T \ \underline{\delta}_L^T]^T$ based on the estimate $[\underline{V}_L^{(k)} \ \underline{\delta}_L^{(k)}]^T$ at the kth iteration is

$$\begin{bmatrix} \underline{V}_L^{(k+1)} \\ \underline{\delta}_L^{(k+1)} \end{bmatrix} = \begin{bmatrix} \underline{V}_L^{(k)} \\ \underline{\delta}_L^{(k)} \end{bmatrix} + \underline{J}^{-1} \begin{bmatrix} \underline{P}_L^{(sch)} - \underline{P}_L^{(k)} \\ \underline{Q}_L^{(sch)} - \underline{Q}_L^{(k)} \end{bmatrix} \tag{4.54}$$

In the last equation, $\underline{P}_L^{(sch)}$ and $\underline{Q}_L^{(sch)}$ are the vectors of the known constant P,Q loads while $\underline{P}_L^{(k)}$ and $\underline{Q}_L^{(k)}$ are the computed injected powers corresponding to the bus voltage estimates at the kth iteration. The estimate $[\underline{V}_L^{(k+1)} \ \underline{\delta}_L^{(k+1)}]^T$ is considered the solution to Eqs.(4.46) and (4.47) if the corresponding differences between the elements of the two estimates at the kth and (k + 1)th iterations are less than a predetermined convergence criteria. Once the loadflow solution is determined for the current instant of time, the quantities P_{Ei} and E_{Ii} for each generator "i" can be computed and used in the next step of the numerical integration.

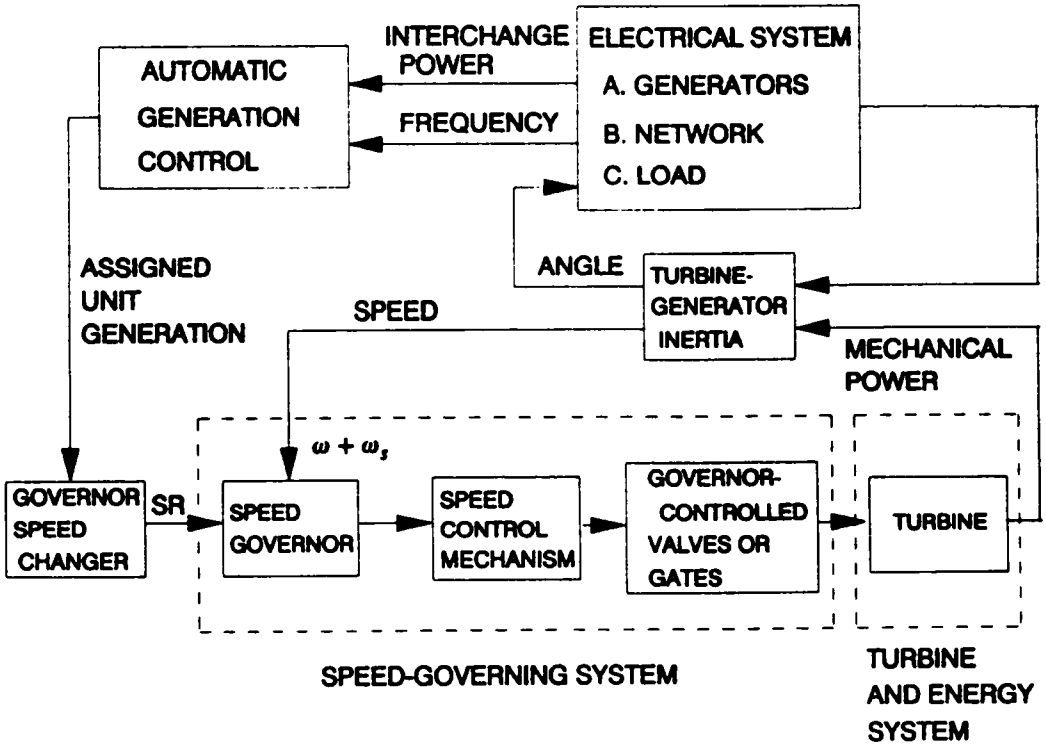

Figure 4.1. Relative Location of Generator Speed-Governing System

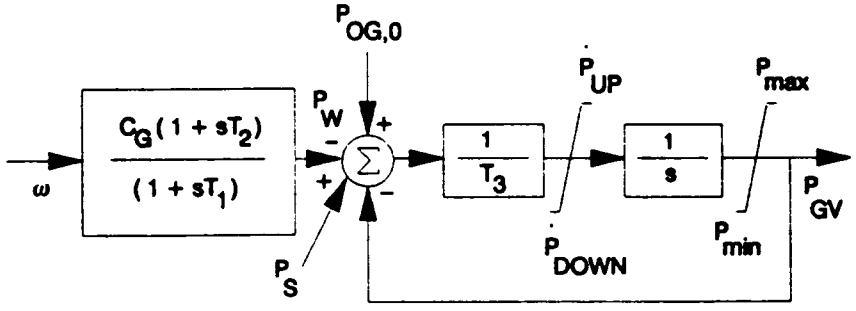

A.General Model of Speed-Governing System

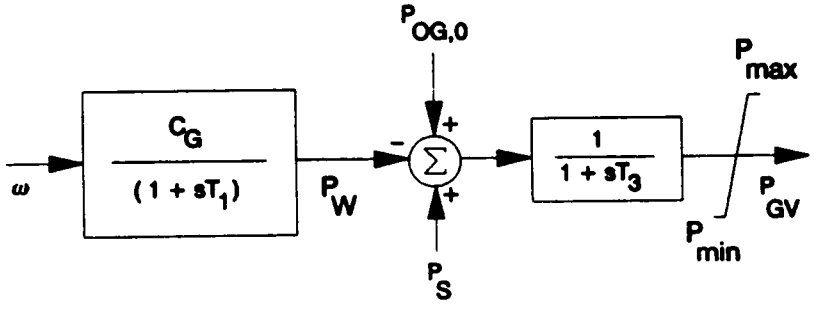

B.Speed-Governing System with Mechanical-Hydraulic Control

Figure 4.2. Evolution of Speed-Governing System Model

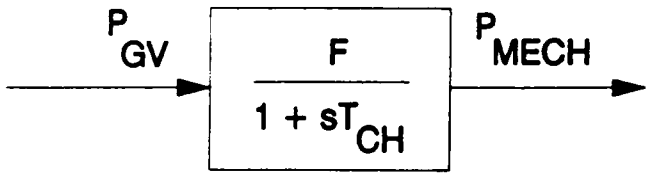

Figure 4.3. Nonreheat Steam Turbine Model

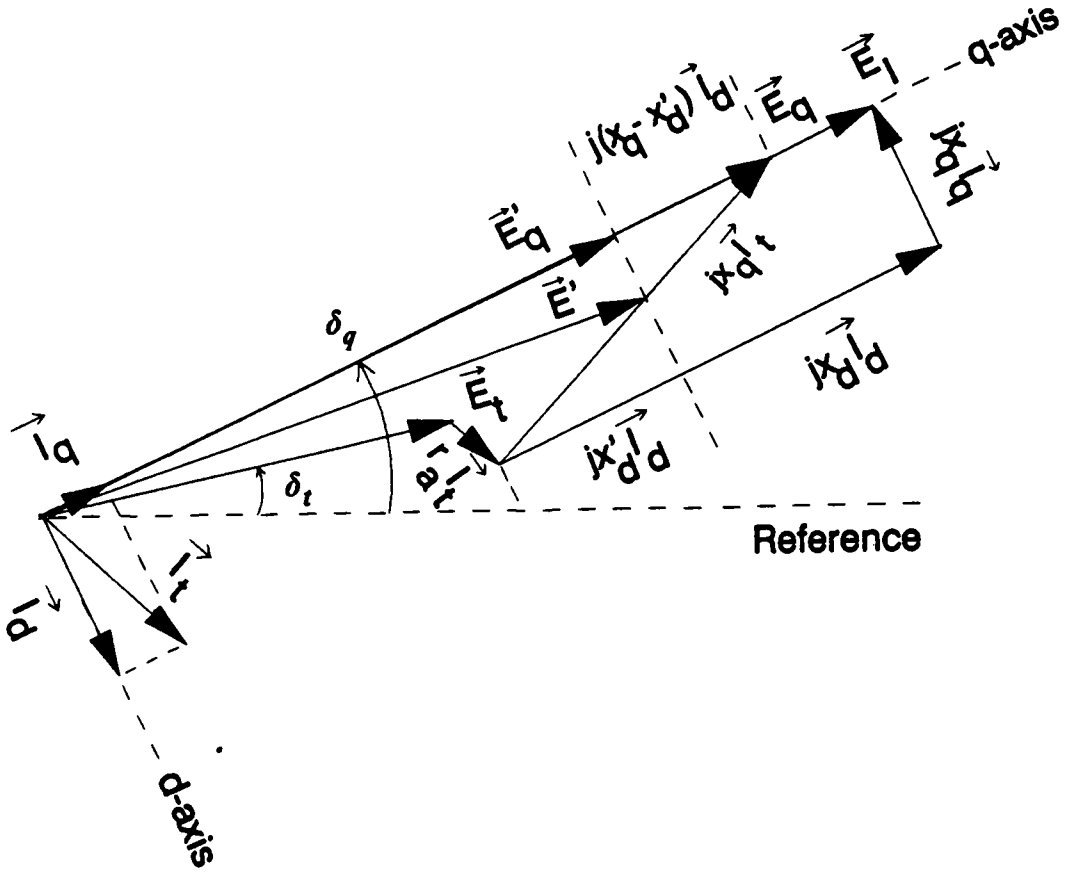

Figure 4.4. Synchronous Generator Phasor Diagram (Overexcited Case)

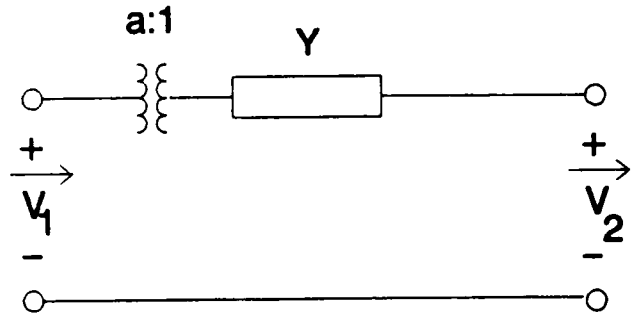

A.Nonunity Turns Ratio Transformer Model

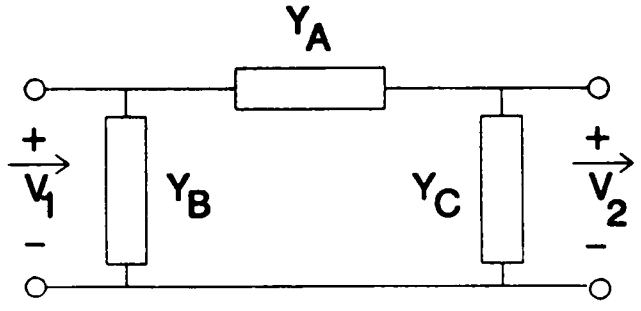

B.Equivalent Transformer Model

Figure 4.5. Per-Unit Transformer Models for Admittance Matrix Calculations

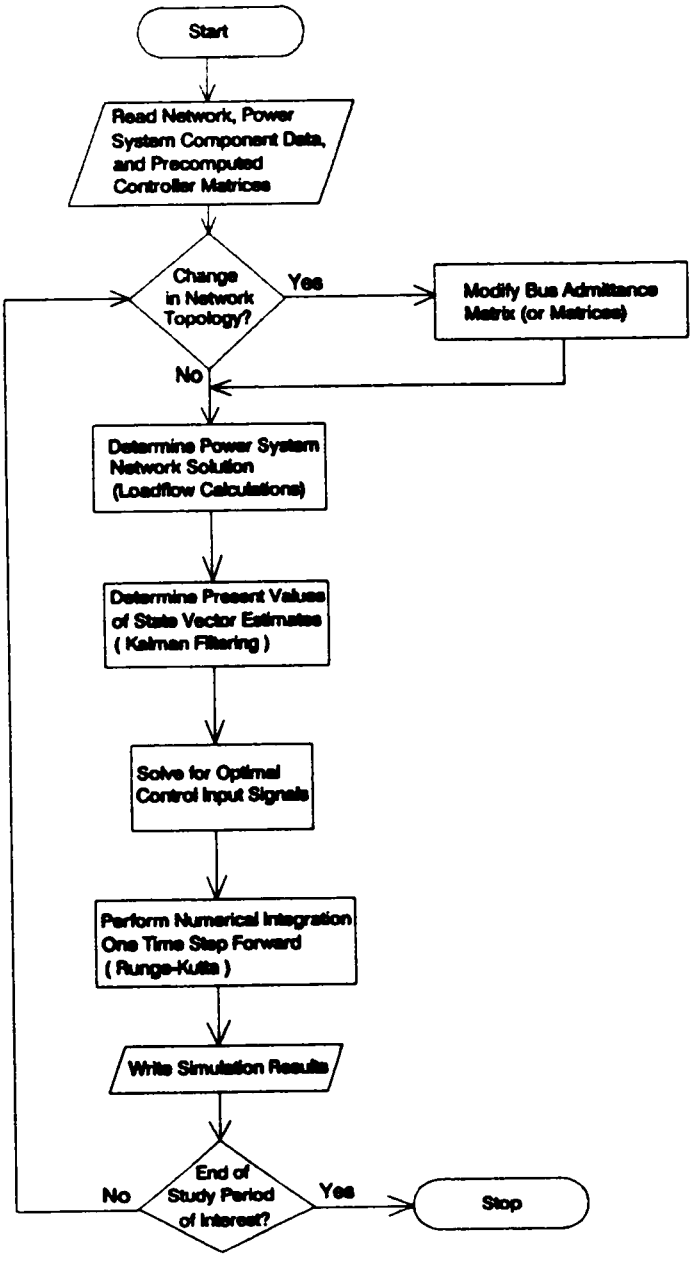

Figure 4.6. General Flowchart of Simulation Program

Chapter 5

The Centralized Controller

Introduction

In this chapter, the performance of the centralized controller will be evaluated by simulating its behavior under various conditions. Discussion will first cover the formulation of the control problem, the solution, and minimum requirements for successful control action. Related questions will then be considered through simulation studies. Questions to be answered include the adequacy of excitation system control (without speed-governor control), minimum amount of power system measurements that need to be made to satisfy controller requirements, effects of large state residuals on controller performance, use of local controllers (instead of the centralized controller), methods used in the computation of $\underline{g}_S(t)$ in the control law, and choice of elements for the weighting matrix $\underline{Q}$ in the cost function.

Simulation studies assume ideal state estimators which provide feedback to the centralized controller. The next chapter will deal with the interaction between practical state estimators and the centralized controller.

Control Equations

At this point, the control problem will be formally stated. Given the following state equation

$$\dot{\underline{X}}(t) = \underline{A}\underline{X}(t) + \underline{B}\underline{U}(t) + \underline{f}(t) \tag{5.1}$$

where $\underline{X}(t)$ is the state n-vector, $\underline{U}(t)$ the control input r-vector, and $\underline{f}(t)$ is the state residual n-vector representing all inaccuracies in the linearization and the output equation

$$\underline{Y}(t) = \underline{C}\underline{X}(t) + \underline{s}(t) \tag{5.2}$$

where $\underline{Y}(t)$ is the q-vector of variables to be controlled and $\underline{s}(t)$ is the output residual q-vector representing all inaccuracies in linearization of the output equation, find the optimal control input signal $\underline{U}^*(t)$ such that the scalar $J(\underline{U}^*(t))$ is the minimum of the cost function

$$J(\underline{U}) = \frac{1}{2}[\underline{e}^T(t_f)\underline{H}\underline{e}(t_f)] + \frac{1}{2}\int_{t_o}^{t_f}\{[\underline{e}^T(t)\underline{Q}\underline{e}(t)] + [\underline{U}^T(t)\underline{R}\underline{U}(t)]\}dt \tag{5.3}$$

with respect to $\underline{U}(t)$. In the above equations,

$$\underline{e}(t) = \underline{Y}(t) - \underline{Y}_d(t) \tag{5.4}$$

where $\underline{e}(t)$ is the error vector and $\underline{Y}_d(t)$ is the target trajectory for the output vector $\underline{Y}(t)$. The controller is assumed to act over a control time interval $[t_o, t_f]$. The output error weighting matrices H and $\underline{Q}$ are semi-positive matrices while the control effort weighting matrix R is positive-definite. All of the weighting matrices are assumed to be time-invariant.

Reference [77] has derived the solution to the control problem stated above with the output residual vector $\underline{s} = \underline{0}$. It is an extension of the linear output tracking problem solution given in reference [80]. The solution to the present control problem is intuitively obvious (i.e., replace all terms corresponding to $\underline{Y}_d(t)$ with $\underline{Y}_d(t) - \underline{s}(t)$). Appendix C of this paper presents a formal proof of the solution which will be presented shortly. The proof has been presented along the lines of references [77,80].

The optimal control law is given by

$$\underline{U}^*(t) = R^{-1}B^T[\underline{g}(t) \dot{-} K(t)\underline{X}(t)] \tag{5.5}$$

where the Kalman gain matrix $K(t)$ is the solution to the matrix Riccati equation

$$\dot{K}(t) = -A^T K(t) - K(t)A + K(t)BR^{-1}B^T K(t) - C^T \underline{Q} C \tag{5.6}$$

and $\underline{g}(t)$ is the solution to the auxiliary differential equation

$$\dot{\underline{g}}(t) = -[A^T - K(t)BR^{-1}B^T]\underline{g}(t) - C^T \underline{Q}[\underline{Y}_d(t) - \underline{s}(t)] + K(t)\underline{f}(t) \tag{5.7}$$

Here it is noted that for $\underline{Y}_d(t) = \underline{s}(t) = \underline{0}$ and $\underline{f}(t) = \underline{0}$, $\underline{g}(t) = \underline{0}$, even after taking into account the final condition of Eq.(5.9). Thus, $\underline{g}(t)$ is the adaptive term in the optimal control law and is the mechanism by which the controller keeps track of changing power system conditions. The two preceding differential equations have the following final conditions at the end t_f of the control time interval:

$$\underline{K}(t_f) = \underline{C}^T \underline{H} \underline{C} \tag{5.8}$$

$$\underline{g}(t_f) = \underline{C}^T \underline{H}[\underline{Y}_d(t_f) - \underline{s}(t_f)] \tag{5.9}$$

Thus, $\underline{K}(t)$ and $\underline{g}(t)$ are solved using backward numerical integration schemes. A special situation occurs when $t_f = \infty$. Physically, this may imply that the controller is allowed to act for an indefinite amount of time to achieve a target value for the output vector. "Steady-state" solutions to the differential equations are then used. In the Riccati Eq.(5.6), $\underline{K}(t)$ becomes a constant matrix $\underline{K}_S$ and is the solution to the matrix algebraic equation

$$\underline{0} = -\underline{A}^T \underline{K}_S - \underline{K}_S \underline{A} + \underline{K}_S \underline{B} \underline{R}^{-1} \underline{B}^T \underline{K}_S - \underline{C}^T \underline{Q} \underline{C} \tag{5.10}$$

The corresponding steady-state solution for $\underline{g}(t)$ is given by

$$\dot{\underline{g}}_S(t) = -[\underline{A}^T - \underline{K}_S \underline{B} \underline{R}^{-1} \underline{B}^T] \underline{g}_S(t) - \underline{C}^T \underline{Q}[\underline{Y}_d(t) - \underline{s}(t)] + \underline{K}_S \underline{f}(t) \tag{5.11}$$

Here it is noted that $\underline{g}_S$ remains a function of time since $\underline{Y}_d(t)$, $\underline{s}(t)$, and $\underline{f}(t)$ are not time-invariant vectors. Integration of the preceding differential equation is also implied. However, a good approximation to $\underline{g}_S(t)$ was used in reference [77]. This approximation avoids the backward numerical integration implied by Eqs.(5.7) and (5.9) by assuming that $\dot{\underline{g}}_S(t) = \underline{0}$.

$$\underline{g}_S(t) = -[\underline{A}^T - \underline{K}_S\underline{B}\underline{R}^{-1}\underline{B}^T]^{-1}\{\underline{C}^T\underline{Q}[\underline{Y}_d(t) - \underline{s}(t)] - \underline{K}_S\underline{f}(t)\} \tag{5.12}$$

Thus, with $t_f = \infty$, and using the approximation of Eq.(5.12), computation of the "steady-state" matrices $\underline{K}_S$ and $\underline{g}_S(t)$ become independent of the final conditions given by Eqs.(5.8)-(5.9). Also, the cost function is now equivalent to

$$J(\underline{U}) = \frac{1}{2}\int_{t_o}^{\infty}\{[\underline{e}^T(t)\underline{Q}\underline{e}(t)] + [\underline{U}^T(t)\underline{R}\underline{U}(t)]\}dt \tag{5.13}$$

During actual controller implementation, the controller state and output variables are either measured or estimated from the measurements. Thus, the nonlinear vector function $\dot{\underline{X}}(t)$ can be directly computed. Elements of the output vector $\underline{Y}(t)$ are all directly measured. The state and output residual terms $\underline{f}(t)$ and $\underline{s}(t)$ can then be computed as

$$\underline{f}(t) = \dot{\underline{X}}(t) - \underline{A}\underline{X}(t) - \underline{B}\underline{U}(t) \tag{5.14}$$

and

$$\underline{s}(t) = \underline{Y}(t) - \underline{C}\underline{X}(t) \tag{5.15}$$

Definition of Controller Vectors

This chapter will study and consider different types of controllers employing either or both excitation system and speed-governor control. The section on "Simulation Studies" enumerates and describes the different cases considered in this chapter. This

section and the following will assume the controller of Case 1 using both excitation system and speed-governor control, with measurement and control of field and generator terminal voltages. Modification of the control problem for the other cases will be discussed in the latter sections of this chapter.

The controller state vector will now be defined. As discussed in Chapter 3, the study system has ten generators with the largest generator, generator 10, having a constant field excitation. Also, relative angular values will be used in the controller formulation to make the resulting feedback matrix A nonsingular. The section entitled "Comments on the Riccati Equation" will explain the necessity of using a nonsingular feedback matrix. The principle is identical to that used in the solution to the conventional loadflow problem in which the slack bus angle is set to a constant value (normally zero) and all the other bus angles are solved with respect to the slack bus angle. In the present case, the q-axis of the largest generator is chosen to be the reference bus. Only nine relative angular values determined from the actual positions of the q-axis of each machine are necessary to determine the state of the power system. Moreover, the largest generator may in fact be a single machine representation of an external system. The present formulation will use incremental changes in the original state variables of the transient stability program for the controller variables. These changes are the deviations from the nominal prefault operating point values presented in Chapter 3.

For the excitation system of generator i, the contribution to the controller state vector is

$$X_{EXC,i} = [\Delta V_{yi} \;\; \Delta V_{ri} \;\; \Delta V_{Zi} \;\; \Delta E_{FD,i}]^T \tag{5.16a}$$

The speed-governing system of the same generator contributes

$$X_{SP,i} = [\Delta P_{Wi} \;\; \Delta P_{GV,i} \;\; \Delta P_{MECH,i}]^T \tag{5.16b}$$

The generator itself gives rise to the vector

$$X_{Gi} = [\Delta E'_{qi} \;\; (\Delta\delta_{qi} - \Delta\delta_{q10}) \;\; (\omega_{qi} - \omega_{q10})]^T \tag{5.16c}$$

In the last expression, E'_{qi} is the internal machine voltage, δ_{qi} is the position of the ith machine q-axis with respect to the a synchronously rotating frame of reference, and ω_i is the speed of the ith machine rotor with respect to the synchronous frame of reference. The q-axis position of Generator 10 is used as the reference axis for controller itself. The state vector contribution from the ith generator is therefore given by the 10-element vector

$$X_i = [X_{Gi}^T \;\; X_{EXC,i}^T \;\; X_{SP,i}^T]^T \tag{5.17}$$

For the centralized controller, the complete state vector has 91 elements given by

$$X = [X_1^T \;\; X_2^T \;\; \ldots \;\; X_i^T \;\; \ldots \;\; X_9^T \;\; \Delta E'_{q10}]^T \tag{5.18}$$

The control input vector will be defined next. As described in the excitation and speed-governing system models of Chapter 4 and the accompanying block diagrams, at most two control input signals are defined for generator i, V_{si} and P_{si}. They are applied to the excitation and speed-governing systems respectively. Thus,

$$U_i = [V_{si} \;\; P_{si}]^T \tag{5.19}$$

For the centralized controller, the complete control input vector is

$$U = [U_1^T \;\; U_2^T \;\; \ldots \;\; U_i^T \;\; \ldots \;\; U_9^T]^T \tag{5.20}$$

Here it is noted that no control input signals were assumed for the largest generator and $\underline{U}(t)$ has 18 elements.

The controller output vector will be defined next. The elements of this vector correspond to the variables that are being controlled and measured directly. With the exception of the field voltages, they define the dynamic state of the power system itself. The output vector contribution from generator i is given by the 4-element vector

$$\underline{Y}_i = [\Delta E_{ti} \;\; (\Delta\delta_{qi} - \Delta\delta_{q10}) \;\; (\omega_{qi} - \omega_{q10}) \;\; \Delta E_{FD,i}]^T \tag{5.21}$$

In the above expression, ΔE_{ti} is the incremental change in the ith generator terminal voltage magnitude from its nominal operating point value and is a nonlinear function of the controller state variables. The complete controller output vector is

$$\underline{Y} = [\underline{Y}_1^T \;\; \underline{Y}_2^T \;\; \ldots \;\; \underline{Y}_i^T \;\; \ldots \;\; \underline{Y}_9^T \;\; \Delta E_{t10}]^T \tag{5.22}$$

and has 37 elements.

At this point, the target trajectory $\underline{Y}_d(t)$ for the output vector $\underline{Y}(t)$ will be given some attention. The expression for the cost function defines the output error vector as

$$\underline{e}(t) = \underline{Y}_d(t) - \underline{Y}(t) \tag{5.23}$$

In the above expression, $\underline{Y}_d(t)$ is chosen to be an exponential function of time, i.e.,

$$\underline{Y}_d(t) = \underline{Y}_{df} + (\underline{Y}_{do} - \underline{Y}_{df}) \exp(-t/\tau) \tag{5.24a}$$

$\underline{Y}_{do}$, $\underline{Y}_{df}$, and τ are all time-invariant quantities.

The preceding equation for $\underline{Y}_d(t)$ is applicable to its elements corresponding to ΔE_{ti}, $(\Delta\delta_{qi} - \Delta\delta_{q10})$, and $\Delta E_{FD,i}$. However, it must be noted that ω_i is the time derivative of $\Delta\delta_{qi}$. Therefore, the same relationship must hold true for their target trajectories. Use of a time-invariant (zero) trajectory for the relative rotor speed and an exponential time-varying trajectory for the relative rotor angle would impose obviously contradictory conditions on the controller and the power system. Denoting target trajectories by the subscript "d", and quantities with respect to the largest generator by the subcript "r",

$$\begin{aligned} \omega_{ri,d} &= \frac{d}{dt}(\Delta\delta_{qr,id}) \\ \omega_{ri,d} &= -(1/\tau)(\Delta\delta_{qr,ido} - \Delta\delta_{qr,idf})\exp(-t/\tau) \end{aligned} \qquad (5.24b)$$

assuming that ω_{ri} and $\Delta\delta_{qr,i}$ have consistent units (e.g., radians/sec. and radians).

The vector $\underline{Y}_{do}$ is the immediate postfault value (t=0+) of the output vector and is directly dependent on the nature of the disturbance. The immediate post-disturbance power system state is shown in Chapter 3 (Table 3.1). Of the four output variables corresponding to generator i, only the incremental change in the generator terminal voltage ΔE_{ti} is nonzero since the fault clearance is assumed to be instantaneous and only the generator terminal voltages are immediately affected by the sudden change in the transmission network configuration. In each generator i, the real state variables E'_{qi}, δ_{qi} , ω_{qi}, and $E_{FD,i}$ do not change instantaneously. Thus, the corresponding incremental changes at t=0+ are zero. The values of $\underline{Y}_{do}$ are shown on the second column of Table 5.1 to four significant digits.

The final value $\underline{Y}_{df}$ of the output vector is the target steady-state condition for the power system based on an assumed postfault configuration. The data presented in Chapter 3 was based on the instantaneous clearance and permanent dropping of the

faulted transmission line 20 (Bus 15-Bus 16). Thus, the elements of $\underline{Y}_{df}$ are the corresponding incremental changes obtained from the power system network and individual machine equation solutions at steady-state. The elements of $\underline{Y}_{df}$ are given on the third column of Table 5.1.

The time constant τ in the expression for $\underline{Y}_d(t)$ was determined from an examination of the post-fault time curves with no controller some of which are shown in Chapter 3 (Figures (3.5)-(3.10)). In this study, a single value was chosen for all elements of the target trajectory ($\tau = 0.8$ second).

The Controller Matrices

The purpose of this section is to illuminate on the procedure used to compute the linearized controller matrices shown in Eqs.(5.1)-(5.2).

The power system and equipment model equations of Chapter 4 will be the starting point of the derivations. Most of the equations are repeated here for clarity while some of them have been modified to suit the state variables defined for the controller. The following differential equations apply to the large-signal state variables of the controller.

$$\dot{E}'_{qi} = \frac{1}{T'_{do,i}}(E_{fd,i} - E_{li}) \tag{5.25}$$

$$\dot{\delta}_{qi} - \dot{\delta}_{q10} = \omega_i - \omega_{10} \tag{5.26}$$

$$\dot{\omega}_i - \dot{\omega}_{10} = \frac{1}{M_i}(P_{\mathrm{Mi}} - P_{\mathrm{Ei}} - D_{\mathrm{i}}(\omega_i - \omega_c)) - \frac{1}{M_{10}}(P_{\mathrm{M10}} - P_{\mathrm{E10}} - D_{10}(\omega_{10} - \omega_c)) \tag{5.27a}$$

where, ω_c, the speed of the center-of-angle with respect to the synchronous frame is given by

$$\omega_c = \frac{\sum_{i=1}^{i=10} M_{\mathrm{i}}\omega_i}{\sum_{i=1}^{i=10} M_{\mathrm{i}}} \tag{5.27b}$$

$$\dot{V}_{yi} = \frac{1}{T_{ri}}(E_{ti} - V_{yi}) \tag{5.28}$$

$$\dot{V}_{ri} = \frac{1}{T_{ai}}[-V_{ri} + (-V_{yi} - V_{zi} + V_{\mathrm{refi}} + V_{si})K_{ai}] \tag{5.29}$$

$$\dot{V}_{zi} = \frac{1}{T_{fi}}\left\{\frac{K_{fi}}{T_{ei}}[V_{ri} - (S_{Ei} + K_{Ei})E_{fdi}] - V_{zi}\right\} \tag{5.30}$$

$$\dot{E}_{fdi} = \frac{1}{T_{Ei}}[V_{ri} - (S_{Ei} + K_{Ei})E_{fdi}] \tag{5.31}$$

$$\dot{P}_{\mathrm{Wi}} = \frac{1}{T_{1\mathrm{i}}}(C_{\mathrm{Gi}}\omega_i - P_{\mathrm{Wi}}) \tag{5.32}$$

$$\dot{P}_{\mathrm{GV,i}} = \frac{1}{T_{3\mathrm{i}}}(P_{\mathrm{Si}} + P_{\mathrm{OG,i}} - P_{\mathrm{Wi}} - P_{\mathrm{GV,i}}) \tag{5.33}$$

$$\dot{P}_{MECH,i} = \frac{1}{T_{CH,i}}(P_{GV,i} - P_{MECH,i}) \tag{5.34}$$

An examination of the differential equations above show some nonlinear terms on the right-hand side of some of the equations. It is seen that these nonlinear terms can be expressed in terms of the controller state variables and generator terminal voltages (magnitude and angle). Thus, in the differential equation for $\dot{E}'_{qi}$,

$$E_{Ii} = E'_{qi}\left(\frac{x_{di}}{x'_{di}}\right) - \left(\frac{x_{di}}{x'_{di}} - 1\right)E_{ti}\cos[(\delta_{qi} - \delta_{q10}) - (\delta_{ti} - \delta_{q10})] \tag{5.35}$$

In the differential equation for $(\dot{\omega}_i - \dot{\omega}_{i0})$, the electrical power output is given by

$$\begin{aligned} P_{Ei} = {} & \frac{E'_{qi}E_{ti}}{x'_{di}}\sin[(\delta_{qi} - \delta_{q10}) - (\delta_{ti} - \delta_{q10})] \\ & - \frac{E_{ti}^2}{2x'_{di}x_{qi}}(x_{qi} - x'_{di})\sin[2(\delta_{qi} - \delta_{q10}) - 2(\delta_{ti} - \delta_{q10})] \end{aligned} \tag{5.36}$$

Lastly, in the excitation system equations, the saturation function is given by

$$S_{Ei} = A_{Ei}\exp(B_{Ei} \bullet E_{fdi}) \tag{5.37}$$

The state of a power system (the bus voltage magnitudes and angles) is directly determined by the generator state variables E'_{qi} and δ_{qi}. Knowledge of this state variable pair for all the generators define a stable solution to the loadflow problem provided that the network and load behavior is known. As stated in the previous chapter, loads external to the network are assumed to draw a constant amount of real and reactive power. Thus, letting

$$E_t = [E_{t1} \;\; E_{t2} \;\; \cdots \;\; E_{ti} \;\; \cdots \;\; E_{t10}]^T \tag{5.38}$$

and

$$\underline{\delta}_{tr} = [(\delta_{t1} - \delta_{q10})\ \ (\delta_{t2} - \delta_{q10})\ \ \cdots\ \ (\delta_{ti} - \delta_{q10})\ \ \cdots\ \ (\delta_{t10} - \delta_{q10})]^T \tag{5.39}$$

they can be written symbolically as

$$\begin{aligned} \underline{E}_t &= \underline{E}_t(\underline{\chi}(t)) \\ \underline{\delta}_{tr} &= \underline{\delta}_{tr}(\underline{\chi}(t)) \end{aligned} \tag{5.40}$$

where

$$\underline{\chi}(t) = \underline{\chi}_o + \underline{X}(t) \tag{5.41}$$

is the vector of large-signal controller state variables and $\underline{X}(t)$ is the corresponding small-signal vector defined in the preceding section. $\underline{\chi}_o$ is the prefault value of $\underline{\chi}(t)$. The nonlinear differential Eqs.(5.25)-(5.34) can then be written in compact form as

$$\dot{\underline{\chi}}(t) = \underline{G}(\ \underline{\chi}(t),\ \underline{U}(t),\ \underline{E}_t(\underline{\chi}(t)),\ \underline{\delta}_{tr}(\underline{\chi}(t))\ ) \tag{5.42}$$

Assuming that the functional $\underline{G}$ is evaluated for the prefault network configuration, the stable prefault equilibrium operating point is described by

$$\underline{0} = \underline{G}(\ \underline{X}_o,\ \underline{0},\ \underline{E}_t(\underline{\chi}_o),\ \underline{\delta}_{tr}(\underline{\chi}_o)) = \underline{G}_o \tag{5.43}$$

From Eq.(5.41),

$$\dot{\underline{\chi}}(t) = \dot{\underline{\chi}}_o + \dot{\underline{X}}(t) = \dot{\underline{X}}(t) \tag{5.44}$$

since $\underline{\chi}_o$ is a time-invariant vector. Thus,

$$\dot{\underline{X}}(t) = \underline{G}(\ \underline{\chi}_o + \underline{X}(t),\ \underline{U}(t),\ \underline{E}_t(\underline{\chi}_o + \underline{X}(t)),\ \underline{\delta}_{tr}(\underline{\chi}_o + \underline{X}(t))\ ) \tag{5.45}$$

Applying a first order Taylor's series expansion to the preceding equation and the chain rule,

$$\dot{\underline{X}}(t) = \underline{G}_o + \left[\frac{\partial \underline{G}}{\partial \underline{\chi}} + \frac{\partial \underline{G}}{\partial \underline{E}_t} \frac{\partial \underline{E}_t}{\partial \underline{\chi}} + \frac{\partial \underline{G}}{\partial \underline{\delta}_{tr}} \frac{\partial \underline{\delta}_{tr}}{\partial \underline{\chi}} \right] \underline{X}(t) + \frac{\partial \underline{G}}{\partial \underline{U}} \underline{U}(t) + \underline{f}(\underline{\chi}(t)) \tag{5.46}$$

Noting that $\underline{G}_o = \underline{0}$,

$$\dot{\underline{X}}(t) = \underline{A}\underline{X}(t) + \underline{B}\underline{U}(t) + \underline{f}(\underline{\chi}(t)) \tag{5.47}$$

The partial derivatives are evaluated at the stable prefault equilibrium point of the power system. The vector $\underline{f}(\underline{\chi}(t))$ represents the second and higher order terms in the Taylor's series expansion. Here, it is noted that the partial derivatives of $\underline{G}$ with respect to $\underline{\chi}$, $\underline{E}_t$, $\underline{\delta}_{tr}$, and $\underline{U}$ can be computed directly, some of them visually for the linear terms, through Eqs.(5.25)-(5.34). This observation is particularly true for the elements of the control matrix $\underline{B}$. Appendix D shows the necessary expressions needed in the computation of the partial derivatives. Computation of the partial derivatives of the generator terminal quantities $\underline{E}_t$ and $\underline{\delta}_{tr}$ with respect to the state vector $\underline{\chi}$ is not straightforward because of the absence of closed form expressions for Eqs.(5.40). In fact, the determination of generator terminal quantities for given values of generator state variables is the equivalent of the loadflow problem itself as discussed in Chapter 4. Evaluation of the partial derivatives

$$\frac{\partial \underline{E}_t}{\partial \underline{\chi}} \quad \text{and} \quad \frac{\partial \underline{\delta}_{tr}}{\partial \underline{\chi}} \tag{5.48}$$

at the prefault operating point will be accomplished in an indirect way by utilizing the external transmission network configuration. This configuration also determines the manner of interaction among the generators of the system.

Define the vector of incremental internal machine voltages as

$$\Delta \underline{E'_q} = [\Delta E'_{q1} \;\; \Delta E'_{q2} \;\; \ldots \Delta E'_{qi} \;\; \ldots \Delta E'_{q10}]^T \tag{5.49}$$

Also, let the vector of incremental relative angular values be

$$\Delta \underline{\delta}_{qr} = [(\Delta\delta_{q1} - \Delta\delta_{q10}) \;\; (\Delta\delta_{q2} - \Delta\delta_{q10}) \;\; \ldots \;\; \Delta\delta_{qr,i} \;\; \ldots \;\; (\Delta\delta_{q9} - \Delta\delta_{q10})]^T \tag{5.50}$$

where

$$\Delta\delta_{qr,i} = (\Delta\delta_{qi} - \Delta\delta_{q10})$$

The vector of incremental changes in the bus voltage magnitudes is

$$\Delta \underline{V_L} = [\Delta V_{L1} \;\; \Delta V_{L2} \;\; \ldots \Delta V_{Lk} \;\; \ldots \Delta V_{L39}]^T \tag{5.51}$$

and the vector of incremental changes in relative angular values of the bus voltages is given by

$$\Delta \underline{\delta}_{Lr} = [(\Delta\delta_{L1} - \Delta\delta_{q10})(\Delta\delta_{L2} - \Delta\delta_{q10}) \;\; \ldots \;\; \Delta\delta_{Lr,k} \;\; \ldots \;\; (\Delta\delta_{L39} - \Delta\delta_{q10})]^T \tag{5.52}$$

where

$$\Delta\delta_{Lr,k} = (\Delta\delta_{Lk} - \Delta\delta_{q10})$$

Further, let the vectors of incremental changes in the injected real and reactive bus powers be defined as

$$\Delta \underline{P} = [\Delta P_1 \;\; \Delta P_2 \;\; \ldots \Delta P_k \;\; \ldots \Delta P_{39}]^T \tag{5.53}$$

and

$$\Delta \underline{Q} = [\Delta Q_1 \;\; \Delta Q_2 \;\; \ldots \Delta Q_k \;\; \ldots \Delta Q_{39} \;\;]^T \tag{5.54}$$

For a generator terminal bus k corresponding to generator i (k = 29 + i), P_{Ei} and Q_{Ei} are negative components of P_k and Q_k respectively. Eq.(5.36) gives the expression for P_{Ei} while Q_{Ei} is given by

$$\begin{aligned} Q_{Ei} = & \frac{E'_{qi}E_{ti}}{x'_{di}}\cos(\delta_{qr,i} - \delta_{tr,i}) \\ & - \frac{E_{ti}^2}{x'_{di}x_{qi}}[x_{qi}\cos^2(\delta_{qr,i} - \delta_{tr,i}) + x'_{di}\sin^2(\delta_{qr,i} - \delta_{tr,i})] \end{aligned} \tag{5.55}$$

Then, P_k and Q_k are given by

$$P_k = \sum_{n=1}^{NBUS} V_{Lk}V_{Ln}Y_{kn}\cos(\delta_{Lr,k} - \delta_{Lr,n} - \theta_{kn}) - P_{Ei} \tag{5.56}$$

$$Q_k = \sum_{n=1}^{NBUS} V_{Lk}V_{Ln}Y_{kn}\sin(\delta_{Lr,k} - \delta_{Lr,n} - \theta_{kn}) - Q_{Ei} \tag{5.57}$$

Noting that ΔE_{ti} and $\Delta\delta_{tr,i}$ are components of $\Delta\underline{V}_L$ and $\Delta\underline{\delta}_{Lr}$ respectively,

$$\begin{aligned} P_k &= P_k(\underline{V}_L, \underline{\delta}_{Lr}, \underline{E'}_q, \underline{\delta}_{qr}) \\ Q_k &= Q_k(\underline{V}_L, \underline{\delta}_{Lr}, \underline{E'}_q, \underline{\delta}_{qr}) \end{aligned} \tag{5.58}$$

and

$$\begin{aligned} \underline{P} &= \underline{P}(\underline{V}_L, \underline{\delta}_{Lr}, \underline{E'}_q, \underline{\delta}_{qr}) \\ \underline{Q} &= \underline{Q}(\underline{V}_L, \underline{\delta}_{Lr}, \underline{E'}_q, \underline{\delta}_{qr}) \end{aligned} \tag{5.59}$$

where $\underline{P}$ and $\underline{Q}$ are the vectors of injected real and reactive bus powers. Linearizing using a first-order Taylor's series expansion yields

$$\begin{bmatrix} \Delta\underline{P} \\ \Delta\underline{Q} \end{bmatrix} = \underline{J}_A \begin{bmatrix} \Delta\underline{V}_L \\ \Delta\underline{\delta}_{Lr} \end{bmatrix} + \underline{J}_B \begin{bmatrix} \Delta\underline{E'}_q \\ \Delta\underline{\delta}_{qr} \end{bmatrix} \tag{5.60}$$

Appendix D shows the appropriate expressions for the elements of $\underline{J}_A$ and $\underline{J}_B$. Under the assumption of constant P-Q loads,

$$\begin{bmatrix} \Delta\underline{V}_L \\ \Delta\underline{\delta}_{Lr} \end{bmatrix} = -\underline{J}_A^{-1}\underline{J}_B \begin{bmatrix} \Delta\underline{E'}_q \\ \Delta\underline{\delta}_{qr} \end{bmatrix} = \underline{C}_1 \begin{bmatrix} \Delta\underline{E'}_q \\ \Delta\underline{\delta}_{qr} \end{bmatrix} \tag{5.61}$$

Thus, by choosing the appropriate row of $\underline{C}_1$, ΔE_{ti} and $(\Delta\delta_{ti} - \Delta\delta_{q10})$ may be expressed in terms of the elements of $\Delta\underline{E'}_q$ and $\Delta\underline{\delta}_{qr}$. In other words, the matrix $\underline{C}_1$ contains all of the elements required by the matrix of partial derivatives of $\underline{E}_t$ and $\underline{\delta}_{tr}$ with respect to $\underline{\chi}$, given by expressions (5.48).

The procedure just outlined to express the generator terminal quantities $\Delta\underline{E}_t$ and $\Delta\underline{\delta}_{tr}$ as linear combinations of the state variables $\delta\underline{E'}_q$ and $\Delta\underline{\delta}_{qr}$ allows the direct determination of elements of the output matrix $\underline{C}$. Each row of the output matrix corresponding to an incremental change in generator terminal voltage contains elements which are either from the $\underline{C}_1$ matrix or zeroes. Each row corresponding to a state variable in the controller has an element "1" placed at the appropriate column. Otherwise, the element is zero.

Comments on the Riccati Equation

The Riccati differential equation given by Eq.(5.6) is repeated here.

$$\dot{K}(t) = -A^T K - KA + KBR^{-1}B^T K - C^T Q C \tag{5.62}$$

Reference [89] points out that if the matrix pair (A, B) is controllable, a steady-state solution K_S exists for the preceding Riccati equation. Reference [90] has weakened the existence condition to the stabilizability of the matrix pair (A, B), i.e., the steady-state solution K_S exists if all unstable eigenvalues of the feedback matrix A are controllable. In the present problem formulation, linearization of the differential Eqs.(5.25)-(5.34) was performed about the stable prefault equilibrium point of the power system, consequently producing a stable feedback matrix (all eigenvalues have negative real parts). Thus, A has no unstable eigenvalues and the pair (A, B) is stabilizable regardless of the value chosen for the control matrix B. Therefore, K_S exists which satisfies the algebraic Riccati equation :

$$0 = -A^T K_S - K_S A + K_S B R^{-1} B^T K_S - C^T Q C \tag{5.63}$$

At this point, it will be shown that two minimum requirements must be satisfied by the resulting K_S matrix for succesful control action :

1) K_S must be positive-definite.

2) The closed-loop feedback matrix $(A - BR^{-1}B^T K_S)$ must be stable.

The need for the first condition will be proved in two steps. Firstly, it will be shown that the linear output regulator problem is a special case of the present problem formulation and therefore, a requirement for the linear output regulator is also a requirement for the more general nonlinear output tracking controller. Secondly, it will be shown that the linear output regulator problem requires K_S to be positive-definite.

The first step is easily accomplished by noting that for $\underline{f}(t) = \underline{0}$, $s(t) = \underline{0}$, and $\underline{Y}_d(t) = \underline{0}$, the system is described by the equations :

$$\begin{aligned} \dot{\underline{X}}(t) &= \underline{A}\underline{X}(t) + \underline{B}\underline{U}(t) \\ \underline{Y}(t) &= \underline{C}\underline{X}(t) \end{aligned} \tag{5.64}$$

with cost function

$$J(\underline{U}) = \frac{1}{2}\int_{t_o}^{\infty} (\underline{U}^T \underline{R}\underline{U} + \underline{Y}^T \underline{Q}\underline{Y})\mathrm{dt} \tag{5.65}$$

The steady-state solution to the auxiliary differential Eq.(5.12) subject to the linear regulator conditions is

$$g_S(t) = \underline{0} \tag{5.66}$$

with the resulting control law

$$\underline{U}^*(t) = -\underline{R}^{-1}\underline{B}^T K_S \underline{X}(t) \tag{5.67}$$

The second step will be accomplished by invoking the Hamilton-Jacobi equation which must be satisfied by the optimal cost function $J(\underline{U}^*)$. Reference [89] shows a derivation

of the Hamilton-Jacobi equation which is stated below for an infinite control time interval.

Define the performance index as

$$V(\underline{X}(t), \underline{U}(t), t) = 2J(U) = \int_{t_o}^{\infty} \ell(\underline{X}(t), \underline{U}(t), t)\mathrm{dt} \tag{5.68}$$

where

$$\ell(\underline{X}(t), \underline{U}(t), t) = \underline{U}^T(t)\underline{R}\underline{U}(t) + \underline{Y}^T(t)\underline{Q}\underline{Y}(t) \tag{5.69}$$

Also, let

$$\dot{\underline{X}}(t) = \underline{F}(\underline{X}(t), \underline{U}(t), t) \tag{5.70}$$

If $V^*(\underline{X}(t), t)$ satisfies the following Hamilton-Jacobi equation,

$$\frac{\partial V^*}{\partial t} = -\min\left\{\ell(\underline{X}(t), \underline{U}(t), t) + \left(\frac{\partial V^*}{\partial \underline{X}}\right)^T \underline{F}(\underline{X}(t), \underline{U}(t), t)\right\} \tag{5.71}$$

where minimization is performed with respect to the control input vector $\underline{U}(t)$, then

$$V^*(\underline{X}(t), t) = V(\underline{X}(t), \underline{U}^*(t), t) = 2J(\underline{U}^*) \tag{5.72}$$

and is the optimal performance index.

A solution will now be assumed for $V^*(\underline{X}(t), t)$ and shown to satisfy the Hamilton-Jacobi Eq.(5.71). Assume that

$$V^*(\underline{X}(t), t) = \underline{X}^T(t)\underline{K}_S\underline{X}(t) \tag{5.73}$$

Hence,

$$\frac{\partial V^*}{\partial t} = \underline{X}^T(t)\left(\frac{\mathrm{d}}{\mathrm{dt}}\underline{K}_S\right)\underline{X}(t) = 0 \tag{5.74}$$

since $\underline{K}_S$ is time-invariant. Moreover,

$$\left(\frac{\partial V^*}{\partial \underline{X}(t)}\right)^T = 2\underline{X}^T(t)\underline{K}_S \tag{5.75}$$

since $\underline{K}_S$ is symmetric. Using Eq.(5.65) which defines the cost function for the linear regulator problem and the last two equations,

$$\begin{aligned}
&\ell(\underline{X}(t), \underline{U}(t), t) + \left(\frac{\partial V^*}{\partial \underline{X}(t)}\right)^T \underline{E}(\underline{X}(t), \underline{U}(t), t) \\
&\qquad = \underline{U}^T\underline{R}\underline{U} + \underline{Y}^T\underline{Q}\underline{Y} + 2\underline{X}^T\underline{K}_S(\underline{A}\underline{X} + \underline{B}\underline{U}) \\
&\qquad = \underline{U}^T\underline{R}\underline{U} + (\underline{X}^T\underline{C}^T)\underline{Q}(\underline{C}\underline{X}) + 2\underline{X}^T\underline{K}_S(\underline{A}\underline{X} + \underline{B}\underline{U}) \\
&\qquad = (\underline{U} + \underline{R}^{-1}\underline{B}^T\underline{K}_S\underline{X})^T\underline{R}(\underline{U} + \underline{R}^{-1}\underline{B}^T\underline{K}_S\underline{X}) \\
&\qquad\quad + \underline{X}^T[\underline{C}^T\underline{Q}\underline{C} - \underline{K}_S\underline{B}\underline{R}^{-1}\underline{B}^T\underline{K}_S + \underline{K}_S\underline{A} + \underline{A}^T\underline{K}_S]\underline{X}
\end{aligned} \tag{5.76}$$

The last part of the equation above has been obtained through the use of a matrix identity applied to an analogous expression in reference [89]. The right-hand side of the equation is to be minimized with respect to the control input vector $\underline{U}(t)$. Since $\underline{R}$ is specified to be positive-definite, and the second term in the last part of the equation is independent of $\underline{U}$, the optimal control input vector is given by

$$\underline{U}^* = -\underline{R}^{-1}\underline{B}^T\underline{K}_S\underline{X} \tag{5.77}$$

which is the control law of Eq.(5.67). Moreover, since K_S is the steady-state solution to the Riccati equation, it satisfies Eq.(5.10) which is repeated here after a rearrangement of terms.

$$\underline{0} = \underline{C}^T \underline{Q} \underline{C} - K_S B R^{-1} B^T K_S + K_S A + A^T K_S \tag{5.78}$$

Thus, the second term is simply zero and

$$\ell(\underline{X}(t), \underline{U}^*(t), t) + \left(\frac{\partial V^*}{\partial \underline{X}(t)} \right)^T E(\underline{X}(t), \underline{U}^*(t), t) = \underline{0} \tag{5.79}$$

Therefore, the assumed $V^*(\underline{X}(t), t) = \underline{X}^T(t) K_S \underline{X}(t)$ satisfies the Hamilton-Jacobi equation and is the optimal performance index for the linear output regulator problem. This most recent result shows that for a non-positive definite K_S, minimization of $J(\underline{U})$ with respect to $\underline{U}$ does not necessarily imply the regulation of the vectors $\underline{Y}$ and $\underline{X}$. On the other hand, with a positive definite K_S, minimization necessarily implies regulation.

The second requirement on the steady-state Kalman gain matrix K_S is the stability of the closed-loop feedback matrix $(A - BR^{-1}B^T K_S)$. As shown in Eq.(5.5), the control law for the nonlinear output tracking problem is given by

$$\underline{U}^*(t) = R^{-1} B^T [\underline{g}_S(t) - K_S \underline{X}(t)] \tag{5.80}$$

Once more, for the linear output regulator problem, Eq.(5.11) gives the solution

$$\underline{g}_S(t) = \underline{0} \tag{5.81}$$

and

$$\underline{U}^*(t) = - R^{-1} B^T K_S \underline{X}(t) \tag{5.82}$$

The state equations then reduce to

$$\begin{aligned}\dot{X} &= AX - BR^{-1}B^T K_S X \\ &= (A - BR^{-1}B^T K_S)X\end{aligned} \tag{5.83}$$

The output regulator control action ($\underline{Y}_d(t) = \underline{0}$) can occur in a practical power system during conditions where the system is being returned to its initial prefault operating point. In these cases, however, $\underline{f}(t)$ and $\underline{s}(t)$ represent the higher-order terms in the Taylor's series expansion and are small nonzero quantities. Thus, even in these conditions, the controller still remains nonlinear. On the other hand, as argued earlier, the stability of the closed-loop feedback matrix $(A - BR^{-1}B^T K_S)$ for the special case of linear output regulation must be a requirement for the more general nonlinear output tracking problem.

In a paper by Kalman [81], an analogous algebraic Riccati equation was studied and given by

$$\underline{0} = -A^T K_S - K_S A + K_S B R^{-1} B^T K_S - D^T D \tag{5.84}$$

where the matrix $(D^T D)$ was semi-positive definite. In that paper, it was pointed out that if the matrix pair (A, B) is controllable and the matrix pair (A, D) is observable, then the resulting steady-state solution K_S is positive-definite and the closed-loop feedback matrix $(A - BR^{-1}B^T K_S)$ is stable.

In the nonlinear output tracking formulation, the Riccati equation is given by Eq.(5.10). Thus, by comparison,

$$C^T Q C = D^T D \tag{5.85}$$

Given that the matrices $\underline{Q}$ to be used in the following study cases are real, diagonal, and positive definite, observability of the matrix pair $(\underline{A}, \underline{D})$ can be evaluated through the matrix pair $(\underline{A}, \underline{C})$ itself. Thus, observability of the linearized system of equations is directly related to the number of assumed measurements in the power system. Inadequate number of measurements is reflected by a non-positive definite (singular) $\underline{K}_S$. Some of the cases to be studied in the following sections are aimed at determining the minimum number of required measurements for successful control action.

Using the assumed control input signals, controllability based on the linearized system of equations only can be shown for a very small analogous AC system. However, to a much larger system, this conclusion regarding controllability cannot be automatically extended. In addition, the choice of control input signals in the following study cases is limited to presently existing control methods (excitation system and speed-governor control). Availability of new arbitrary control signals is not assumed. Hence, conclusions regarding controllability of the large nonlinear power system being presently studied will be based on simulation results. Stability of the linear closed-loop feedback matrix $(\underline{A} - \underline{B}\underline{R}^{-1}\underline{B}^T\underline{K}_S)$ will be monitored closely in all cases.

Simulation Studies

Controller performance under various conditions has been evaluated through a number of simulation case studies. In the case studies of this chapter, ideal state estimators are assumed. An ideal state estimator is defined here as a device which feeds to the controller the exact values of state variables for computation of $\underline{g}_S(t)$ and control input

signal vector $\underline{U}(t)$. Interaction between practical state estimators and the centralized controller will be considered in the next chapter. In the following paragraphs, the base case study (Case 1) is presented first. The succeeding case studies are then described as variations from Case 1. The differential Riccati Eq.(5.6) is re-solved where necessary.

Case 1. This case involves combined excitation system and speed-governor control in each generator, with field voltage measurement and control, and accurate linearization. As stated earlier, the state, control input, and output vectors are given by

$$\underline{X}_i = [\underline{X}_{Gi}^T \ \underline{X}_{EXC,i}^T \ \underline{X}_{SP,i}^T]^T \tag{5.86}$$

where

$$\underline{X}_{Gi} = [\Delta E'_{qi} \ (\Delta\delta_{qi} - \Delta\delta_{q10}) \ (\omega_{qi} - \omega_{q10})]^T \tag{5.87a}$$

$$\underline{X}_{EXC,i} = [\Delta V_{yi} \ \Delta V_{ri} \ \Delta V_{Zi} \ \Delta E_{FD,i}]^T \tag{5.87b}$$

$$\underline{X}_{SP,i} = [\Delta P_{Wi} \ \Delta P_{GV,i} \ \Delta P_{MECH,i}]^T \tag{5.87c}$$

$$\underline{U}_i = [V_{si} \ P_{si}]^T \tag{5.88}$$

$$\underline{Y}_i = [\Delta E_{ti} \ (\Delta\delta_{qi} - \Delta\delta_{q10}) \ (\omega_{qi} - \omega_{q10}) \ \Delta E_{FD,i}]^T \tag{5.89}$$

and for the centralized controller

$$\underline{X} = [\underline{X}_1^T \ \underline{X}_2^T \ \dots \ \underline{X}_i^T \ \dots \ \underline{X}_9^T \ \Delta E'_{q10}]^T \tag{5.90}$$

$$\underline{U} = [\underline{U}_1^T \ \underline{U}_2^T \ \dots \ \underline{U}_i^T \ \dots \ \underline{U}_9^T]^T \tag{5.91}$$

$$\underline{Y} = [\underline{Y}_1^T \ \underline{Y}_2^T \ \cdots \ \underline{Y}_i^T \ \cdots \ \underline{Y}_9^T \ \Delta E_{t10}]^T \tag{5.92}$$

Related time curves obtained for this case are shown in Figures 5.1 to 5.6 and Figure 5.10.

Case 2. This case is intended to study the adequacy of excitation system control alone (without speed-governor control) in accomplishing the centralized control task. It has been observed that the time derivatives corresponding to the speed governor state variables tended to be small. Thus, the state vector as defined in this case does not include the speed governor state variables. Their effects in a generator are reflected in the changing instantaneous value of $P_{MECH,i}$, as captured by the residual term in one of the swing equations. Therefore,

$$\underline{X}_i = [\underline{X}_{Gi}^T \ \underline{X}_{EXC,i}^T]^T \tag{5.93}$$

$$\underline{U}_i = [V_{si}]^T \tag{5.94}$$

$$\underline{X} = [\underline{X}_1^T \ \underline{X}_2^T \ \cdots \ \underline{X}_i^T \ \cdots \ \underline{X}_9^T \ \Delta E'_{q10}]^T \tag{5.95}$$

$$\underline{U} = [V_{s1} \ V_{s2} \ \cdots \ V_{si} \ \cdots \ V_{s9}]^T \tag{5.96}$$

The controller output vector is the same as in Case 1. Related time curves for this case are shown in Figures 5.7 and 5.1.

Case 3. This case shows the need for field voltage measurement and control. The state and control input vectors $\underline{X}$ and $\underline{U}$ are the same as in Case 1. Here, however, the output vector $\underline{Y}_i$ does not include the element $\Delta E_{FD,i}$ and is given by

$$Y_i = [\Delta E_{ti} \ (\Delta\delta_{qi} - \Delta\delta_{q10}) \ (\omega_{qi} - \omega_{q10})]^T \tag{5.97}$$

$$Y = [Y_1^T \ Y_2^T \ \ldots \ Y_i^T \ \ldots \ Y_9^T \ \Delta E_{t10}]^T \tag{5.98}$$

Related time curves for this case are shown in Figure 5.1 and Figures 5.8 to 5.9.

Case 4. In this case, the effects on controller performance of a large state residual vector $f(t)$ will be studied. The state, control input, and output vectors used are identical to those in Case 1. However, the feedback matrix to be used in Case 4 is

$$A_{30} = 0.30^* A_{100} \tag{5.99}$$

where A_{100} is the feedback matrix of Case 1. Use of A_{30} induces large values to appear for the state residual vector $f(t)$. Although A_{100} itself is a stable matrix (obtained by linearizing about the prefault operating point), A_{30} may or may not be stable. This was checked and A_{30} was found to be stable, thus ensuring the existence of a steady-state solution to the corresponding Riccati equation. Here, the scalar quantity r_f is defined.

$$r_f = \frac{|f(t)|}{|AX|} \tag{5.100}$$

where

$$|f(t)|^2 = \sum_{i=1}^{91} f_i^2(t)$$

and

$$|AX|^2 = \sum_{i=1}^{91}\left[\sum_{j=1}^{91} A_{ij}x_j(t)\right]^2$$

Thus, r_f is a measure of the relative magnitudes of the elements of $\underline{f}(t)$ relative to the time derivatives of the controller state vector. It is found to be about twice larger in Case 4 than in Case 1. Related time curves for this case are shown in Figures 5.10 to 5.13.

Case 5. The controller as formulated in this case is an attempted improvement over that of Case 4. The same feedback matrix A_{30} as used in Case 4 will be utilized here, thereby retaining the large state residual terms. However, the controller state and output vectors will be altered slightly such that for the new controller,

$$\begin{aligned} \underline{Y}_{d,new}(t) &= \underline{0} \\ \underline{s}_{new}(t) &= \underline{0} \end{aligned} \tag{5.101}$$

The last two conditions are motivated by the equations used to compute $\underline{g}_S(t)$ and the control input vector $\underline{U}(t)$ in Case 4:

$$\begin{aligned} \dot{\underline{g}}_S(t) &= -[A^T - K_S B R^{-1} B^T] - \underline{C}^T \underline{Q}[\underline{Y}_d(t) - \underline{s}(t)] + K_S \underline{f}(t) \\ \underline{U}^*(t) &= R^{-1} B^T [\underline{g}_S(t) - K_S X(t)] \end{aligned} \tag{5.102}$$

The differential equation above shows that the forcing function

$$\underline{C}^T \underline{Q}[\underline{Y}_d(t) - \underline{s}(t)] + K_S \underline{f}(t)$$

is dominated by $K_S\underline{f}(t)$ as $\underline{f}(t)$ gets larger. It is noted that typically, elements of the Kalman gain matrix K_S are two or three orders of magnitude larger than the elements

of the weighting matrix $\underline{Q}$ itself. Thus, for large state residuals, the controller becomes relatively insensitive to the target trajectory $\underline{Y}_d(t)$ and the output residual term $\underline{s}(t)$. In the controller of Case 5, the burden of $\underline{Y}_d(t)$ and $\underline{s}(t)$ will be shifted to $\underline{f}(t)$.

Define the controller output vector temporarily as

$$\underline{Y}_i = [\Delta E'_{qi} \;\; (\Delta\delta_{qi} - \Delta\delta_{q10}) \;\; (\omega_{qi} - \omega_{q10}) \;\; \Delta E_{FD,i}]^T \tag{5.103}$$

$$\underline{Y} = [\underline{Y}_1^T \;\; \underline{Y}_2^T \;\; \cdots \;\; \underline{Y}_i^T \;\; \cdots \;\; \underline{Y}_9^T \;\; \Delta E'_{q10}]^T \tag{5.104}$$

Then,

$$\underline{s}(t) = \underline{0} \tag{5.105}$$

since the output variables are all elements of the controller state vector. Now, let

$$\begin{aligned} \underline{Y}_{old}(t) &= \underline{Y}(t) \\ \underline{Y}_{new}(t) &= \underline{Y}_{old}(t) - \underline{Y}_{d,old}(t) \\ \underline{Y}_{d,new}(t) &= \underline{Y}_{d,old}(t) - \underline{Y}_{d,old}(t) = \underline{0} \end{aligned} \tag{5.106}$$

where $\underline{Y}_{d,old}(t)$ is computed from the immediate postfault and steady-state postfault values of the controller state vector $\underline{X}(t)$. Thus, if the new output vector is defined as the deviation of the old output vector $\underline{Y}_{old}(t)$ from its target trajectory $\underline{Y}_{d,old}(t)$, the new output target trajectory would simply be zero. Define the new output vector for generator "i" as :

$$\underline{Y}_{i,new} = \begin{bmatrix} \Delta E'_{qi} - \Delta E'_{qi,d} \\ \Delta\delta_{qi} - \Delta\delta_{qi,d} - \Delta\delta_{q10} + \Delta\delta_{q10,d} \\ \omega_i - \omega_{10} \\ \Delta E_{FDi} - \Delta E_{FDi,d} \end{bmatrix} \tag{5.107}$$

and for the centralized controller as

$$\underline{Y}_{new} = [\underline{Y}_{1,new}^T \ \underline{Y}_{2,new}^T \ \cdots \ \underline{Y}_{i,new}^T \ \cdots \ \underline{Y}_{9,new}^T \ (\Delta E'_{q10} - \Delta E'_{q10,d})]^T \tag{5.108}$$

Here, it is noted that

$$\omega_{i,d} - \omega_{10,d} = 0 \tag{5.109}$$

Since the condition $\underline{s}_{new}(t) = \underline{0}$ requires the output variables to be state variables also, the new controller state vector is defined in Case 5 as:

$$\underline{X}_{new} = [\underline{X}_{1,new}^T \ \underline{X}_{2,new}^T \ \cdots \ \underline{X}_{i,new}^T \ \cdots \ \underline{X}_{9,new}^T \ (\Delta E'_{q10} - \Delta E'_{q10,d})]^T \tag{5.110}$$

where

$$\underline{X}_{i,new} = \begin{bmatrix} \Delta E'_{qi} - \Delta E'_{qi,d} \\ \Delta\delta_{qi} - \Delta\delta_{qi,d} - \Delta\delta_{q10} + \Delta\delta_{q10,d} \\ \omega_i - \omega_{10} \\ \Delta V_{yi} \\ \Delta V_{ri} \\ \Delta V_{zi} \\ \Delta E_{FDi} - \Delta E_{FDi,d} \\ \Delta P_{Wi} \\ \Delta P_{GV,i} \\ \Delta P_{MECH,i} \end{bmatrix} \tag{5.111}$$

Using the above formulation allows the computation

$$\dot{\underline{g}}_{S,new}(t) = -[\underline{A}^T - \underline{K}_{S,new}\underline{B}\underline{R}^{-1}\underline{B}^T]\underline{g}_{S,new}(t) + \underline{K}_{S,new}\underline{f}(t) \tag{5.112}$$

without dependence on $\underline{Y}_{d,new}(t)$ or $\underline{s}_{new}(t)$. The new cost function for this case is given by

$$J_{new}(\underline{U}) = \frac{1}{2}\int_{t_o}^{\infty} (\underline{U}^T \underline{R}\underline{U} + \underline{Y}_{new}^T \underline{Q}\underline{Y}_{new}^T)dt \tag{5.113}$$

Related time curves for this case are shown in Figures 5.11 to 5.13.

Case 6. This case study is intended to show the importance of coordinating the control action in each individual generator. Here, the control input signals are computed from local measurements and local feedback only. The Riccati equation is solved for each generator and used in individual decentralized controllers. Each controller is described by the following equations:

$$\begin{aligned}
&\dot{\underline{X}}_i(t) = \underline{A}_i\underline{X}_i(t) + \underline{B}_i\underline{U}_i(t) + \underline{f}_i(t) \\
&\underline{Y}_i(t) = \underline{C}_i\underline{X}_i(t) + \underline{s}_i(t) \\
&\underline{U}_i^*(t) = \underline{R}_i^{-1}\underline{B}_i^T[\underline{g}_{Si}(t) - \underline{K}_{Si}\underline{X}_i(t)]
\end{aligned} \tag{5.114}$$

where

$$\begin{aligned}
&\underline{Q} = -\underline{A}_i^T\underline{K}_{Si} - \underline{K}_{Si}\underline{A}_i + \underline{K}_{Si}\underline{B}_i\underline{R}_i^{-1}\underline{B}_i^T\underline{K}_{Si} - \underline{C}_i^T\underline{Q}_i\underline{C}_i \\
&\underline{g}_{Si}(t) = -[\underline{A}_i^T - \underline{K}_{Si}\underline{B}_i\underline{R}_i^{-1}\underline{B}_i^T]^{-1}\left[\underline{C}_i^T\underline{Q}_i[\underline{Y}_{di}(t) - \underline{s}_i(t)] - \underline{K}_{Si}\underline{f}_i(t)\right]
\end{aligned} \tag{5.115}$$

Individual controller vectors are defined as

$$\underline{X}_i = [\underline{X}_{Gi}^T \;\; \underline{X}_{EXC,i}^T \;\; \underline{X}_{SP,i}^T]^T \tag{5.116}$$

where

$$
\begin{aligned}
X_{Gi} &= [\Delta E'_{qi} \;\; (\Delta\delta_{qi} - \Delta\delta_{q10}) \;\; (\omega_{qi} - \omega_{q10})]^T \\
X_{EXC,i} &= [\Delta V_{yi} \;\; \Delta V_{ri} \;\; \Delta V_{Zi} \;\; \Delta E_{FD,i}]^T \\
X_{SP,i} &= [\Delta P_{Wi} \;\; \Delta P_{GV,i} \;\; \Delta P_{MECH,i}]^T
\end{aligned}
\tag{5.117}
$$

$$
\underline{X}_i = [\Delta E_{ti} \;\; (\Delta\delta_{qi} - \Delta\delta_{q10}) \;\; (\omega_{qi} - \omega_{q10}) \;\; \Delta E_{FD,i}]^T \tag{5.118}
$$

$$
\underline{U}_i = [V_{si} \;\; P_{si}]^T \tag{5.119}
$$

$$
\underline{e}_i(t) = \underline{X}_i(t) - \underline{X}_{di}(t) \tag{5.120}
$$

Each controller attempts to minimize the cost function

$$
J_i(\underline{U}_i) = \frac{1}{2}\int_{t_o}^{\infty} \{[\underline{e}_i^T(t)\underline{Q}_i\underline{e}_i(t)] + [\underline{U}_i^T(t)\underline{R}_i\underline{U}_i(t)]\}\mathrm{dt} \tag{5.121}
$$

Thus, there is no attempt to control the terminal voltage of the largest generator. Time curves related to Case 6 are shown in Figure 5.14.

Cases 7 and 8. In an earlier section of this chapter, the controller equations have been discussed. As stated in that section, an infinite control time interval ($t_f = \infty$) is assumed in formulating the solution to the control problem. Therefore, in the control law

$$
\underline{U}^*(t) = R^{-1}B^T(\underline{g}_S(t) - K_S\underline{X}(t)) \tag{5.122}
$$

the time-invariant solution to the algebraic Riccati Eq.(5.10) was used. However, the vector $\underline{g}_S(t)$ remains a function of time because the steady-state solution $\underline{g}_S(t)$ to the differential equation

$$\dot{\underline{g}}(t) = -[\underline{A}^T - \underline{K}_S\underline{B}\underline{R}^{-1}\underline{B}^T]\underline{g}(t) - \underline{C}^T\underline{Q}[\underline{Y}_d(t) - \underline{s}(t)] + \underline{K}_S\underline{f}(t) \tag{5.123}$$

is dependent on $\underline{Y}_d(t)$, $\underline{s}(t)$, and $\underline{f}(t)$. In fact, the backward numerical integration of the differential equation above from ($t_f = \infty$) to the instantaneous value of time (t) requires a knowledge of the future values (from t to t_f) of $\underline{Y}_d(t)$, $\underline{s}(t)$, and $\underline{f}(t)$. This is not a problem as far as the target trajectory $\underline{Y}_d(t)$ is concerned since it is determined at the very start of the control time interval. However, the residual vectors $\underline{f}(t)$ and $\underline{s}(t)$ are determined only as the measurements come using Eqs.(5.14) and (5.15). Thus, only the past and present values of the vectors are known. A solution to this dilemma was suggested and tested in references [77,67] for a small HVDC system using an approximate solution for $\underline{g}_S(t)$:

$$\underline{g}_S(t) = -[\underline{A}^T - \underline{K}_S\underline{B}\underline{R}^{-1}\underline{B}^T]^{-1}\left\{\underline{C}^T\underline{Q}[\underline{Y}_d(t) - \underline{s}(t)] - \underline{K}_S\underline{f}(t)\right\} \tag{5.124}$$

The equation above is identical to Eq.(5.12) and is used in all the study cases of this paper except Case 8 of this chapter.

A less practical, not necessarily optimal scheme, has been tested through simulation in the same reference [77] for the same HVDC system. The scheme follows from the differential equation itself and assumes that all future values of $\underline{f}(t)$ are equal to the average of the last four measurements, i.e.,

$$\underline{f}(t_k) = \frac{1}{4}\sum_{i=1}^{4} \underline{f}(t_{j+1-i}) \tag{5.125}$$

where t_j denotes the time of the most recent measurements and $t_k > t_j$. Extension of the previous formula to the output residual vector gives

$$\underline{s}(t_k) = \frac{1}{4}\sum_{i=1}^{4} \underline{s}(t_{j+1-i}) \tag{5.126}$$

Using the assumed future values of $\underline{f}(t)$ and $\underline{s}(t)$, the differential Eq.(5.123) is integrated backwards in time at every value of t. This integration is performed over a reasonably long interval of time to ensure that the resultant value of $\underline{g}(t)$ is the "steady-state" solution $\underline{g}_s(t)$. Obviously, both the simulation and real-time implementation of the controller using this scheme require a substantial amount of time to compute $\underline{g}_s(t)$ and $\underline{U}(t)$.

The purpose of Cases 7 and 8 is to compare controller performance using these two schemes, one described by the approximate Eq.(5.124) (Case 7) and the other using backward numerical integration based on assumed values for $\underline{f}(t)$ and $\underline{s}(t)$ (Case 8). In these two study cases, the controller vectors $\underline{X}$, $\underline{U}$, $\underline{Y}$ and matrices $\underline{A}$, $\underline{B}$, $\underline{C}$, $\underline{K}_S$ are identical to those of Case 1. The main difference is in the assumed behavior of some power system components. Loads are assumed to act as constant impedances during the transient period and the largest generator is assumed to have an infinite mass. These assumptions should not impair the comparison between the two schemes, as can be seen in the definition of the cost function and the chosen output vector for Case 1. Since the simulation studies of Chapter 6 on the state estimators also assume constant impedance loads, Case 7 can be looked on as the result of the interaction between the centralized controller and ideal state estimators. Lastly, it is recognized that since the loads are assumed to behave differently from Case 1, the final value of $\underline{Y}_d(t)$ must be recomputed. For Cases 7 and 8, the vector $\underline{Y}_{df}$ together with the initial value $\underline{Y}_{do}$ is shown in Table 5.2.

Time curves related to Cases 7 and 8 are shown in Figures 5.15 to 5.17.

Choice of $\underline{Q}$ and $\underline{R}$ Matrices for Cases 1 to 8. The cost function corresponding to the controller formulation of Eqs.(5.1)-(5.15) with ($t_f = \infty$) is given by

$$J(\underline{U}) = \frac{1}{2}\int_{t_o}^{\infty} [(\underline{Y} - \underline{Y}_d)^T \underline{Q}(\underline{Y} - \underline{Y}_d) + \underline{U}^T \underline{R}\underline{U}]dt \tag{5.127}$$

where $\underline{Q}$ and $\underline{R}$ are diagonal positive-definite penalty matrices. Except for Cases 2, 3, and 6 where the sizes of state, control input, and output vectors are different from Case 1, the matrix $\underline{Q}$ (q = 37) is given by (Cases 1,4,5,7,8) :

$$\begin{aligned} &\underline{Q}(k, k) = 10^4 \\ &\underline{Q}(i, i) = 10^2 \\ &\underline{Q}(k, j) = 0 \quad , j \neq k \\ &\underline{Q}(i, j) = 0 \quad , i \neq k \end{aligned} \tag{5.128}$$

The subscript "k" corresponds to ΔE_{fi} or $(\Delta E'_{qi} - \Delta E'_{qi,d})$, i.e., k = 1, 5, 9, 13, 17, 21, 25, 29, 33, 37. The subscript "i" corresponds to rotor angles, rotor speeds, and field voltages , i.e., i = 2, 3, 4, 6, 7, 8,..., 36. The matrix $\underline{R}$ is given by (Cases 1,4,5,7,8) :

$$\begin{aligned} &\underline{R}(i\ , i) = 1.0 \quad , i = 1, 2, ..., 18 \\ &\underline{R}(i\ , j) = 0.0 \quad , j \neq i \end{aligned} \tag{5.129}$$

For Case 2 (no speed-governor control), $\underline{Q}$ is identical to that of Case 1 shown above. Since r = 9 in this case,

$$\begin{aligned} &\underline{R}(i\ , i) = 1.0 \quad , i = 1, 2, ..., 9 \\ &\underline{R}(i\ , j) = 0.0 \quad , j \neq i \end{aligned} \tag{5.130}$$

For Case 3 (no field voltage control), $\underline{R}$ (r = 18) is identical to that of Case 1. However, q = 28 in this case, i.e.,

$$\begin{aligned}
&\underline{Q}(k, k) = 10^4 \\
&\underline{Q}(i, i) = 10^2 \\
&\underline{Q}(k, j) = 0 \quad , j \neq k \\
&\underline{Q}(i, j) = 0 \quad , i \neq k
\end{aligned} \tag{5.131}$$

where k = 1, 4, 7, 10, 13, 16, 19, 22, 25, 28 and i = 2, 3, 5, 6, ..., 27.

Finally, for Case 6 (local controllers), each controller has q = 4 and r = 2. The $\underline{Q}_i$ and $\underline{R}_i$ matrices are given by

$$\begin{aligned}
\underline{Q}_i &= \begin{bmatrix} 10^4 & 0 & 0 & 0 \\ 0 & 10^2 & 0 & 0 \\ 0 & 0 & 10^2 & 0 \\ 0 & 0 & 0 & 10^2 \end{bmatrix} \\
\underline{R}_i &= \begin{bmatrix} 1.0 & 0 \\ 0 & 1.0 \end{bmatrix}
\end{aligned} \tag{5.132}$$

Cases 9 and 10. These cases are almost identical to Case 1 from the viewpoint of formulation. Identical controller vectors are used with linearization about prefault operating point performed as accurately as possible. The variation from Case 1 is in the choice of slightly different output penalty matrices $\underline{Q}$. The matrix $\underline{R}$ is unchanged.

For Case 9,

$$\underline{Q}(i\ , i) = 10^2 \quad , \ i = 1, 2, ..., 37 \tag{5.133}$$

For Case 10,

$$\underline{Q}(i\,,\,i) = 10^4 \quad , \; i = 1, 2, ..., 37 \tag{5.134}$$

Time curves related to these two cases are shown in Figures 5.18 to 5.19.

Simulation Results

This section will state some practical observations based on results of simulation of controller performance for the cases described in the previous section.

Case 1 (Base Case). This case provided the best controller performance of the first six cases. The power system approached the postfault steady-state condition after about five seconds. There were minimal voltage magnitude oscillations as expected since the generator terminal voltages were given the priority in the controller. Machine rotor oscillations were damped out substantially within the first second of operation.

Case 2 (No Speed-Governor Control). In this case, both voltage magnitude and rotor angle oscillations have been reduced substantially. The power system seems to approach the postfault steady-state condition much slower than in Case 1. Persistent low amplitude oscillations are present even towards the end of the simulation study period (5 seconds).

Case 3 (No Field Voltage Control). This case reveals the need for field voltage control as in Case 1. In Case 3, the solution K_s to the Riccati equation was very close to

singularity. Low-frequency large-amplitude oscillations characterized some of the output variables, particularly those associated with Generator 2.

Case 4 (Large State Residuals). Power system response to the controller was characterized by minimal oscillations on the output variables coupled with the relative insensitivity of the controller to the target trajectory (the generator voltages in particular). Some of the output variables were far from the intended target values for most of the time interval under study.

Case 5 (Large State Residuals with Regulator Formulation) . This case is marked by an increase in the sensitivity of the controller to the chosen output target trajectory. However, oscillation amplitudes larger than those in Case 1 is observed for most of the output variables.

Case 6 (Local Controllers). The voltages were controlled very poorly. The rotor angles and speeds failed to stabilize to steady-state values. In general, the combined performance of the individual controllers was very poor.

Cases 7 and 8 (Comparison Between Two Methods of Computation of $\underline{g}_5(t)$). In both cases, the controller performed satisfactorily. Case 8 employing the backward numerical integration scheme showed some additional oscillations during the early transient period. In general, performance of the two schemes appear to be comparable.

Case 9 (Reduced Weighting Factor for Voltages). In this case, the controller performed much more poorly than in Case 1. Power system response was characterized by larger amplitude and more persistent oscillations during the earlier stages of the time interval

of interest. The reduced control on the generator terminal voltages caused these quantities to move away from their desired trajectories.

Case 10 (Increased Weighting Factor for Rotor Angles). This case reveals the practical impossibility of making all output variables follow the target trajectory. With more weight assigned to the angles, the generator terminal voltages did not closely follow their corresponding target trajectories for most of the time interval under study. Still, controller performance in this respect is better than in Case 9. The angles themselves followed their target trajectories more closely. Increasing the elements of $\underline{Q}$ from that given in Case 1 did not significantly improve controller performance.

Conclusions

This chapter has dealt with the evaluation of the performance of the centralized controller under various conditions. Some very important questions have been answered.

Results of Case 1 indicate that the proposed controller utilizing excitation system and speed-governor control performs excellently as long as the minimum requirements of positive definiteness and linear closed loop stability with accurate linearization are satisfied.

Comparison between the results of Cases 1 and 2 show that excitation system control alone produces a reasonable, though not totally satisfactory controller performance.

Comparison between Cases 1 and 3 show the need for field voltage measurement and control.

Cases 4 and 5 show that in the presence of large state residuals, the controller performs better if operated as an output regulator ($\underline{Y}_{new,d}(t) = \underline{0}$) with zero output residuals ($\underline{s}_{new}(t) = \underline{0}$). However, the increase in oscillation amplitudes between Cases 1 and 5 show that there is a practical limit to the size of the state residual vector with which the controller can perform well. With very large state residual terms, the computed control input signals can become unusually large such that the excitation system regulator voltages simply move back and forth from their lower to upper limit values and vice-versa. In certain situations, it is necessary to neglect these ceiling values in the computation of the state residual terms (i.e., the computed time derivative is not set equal to zero) since their inclusion causes the computed residuals to increase in magnitude unnecessarily. Moreover, with $\underline{s}_{new}(t) = \underline{0}$, an important capability of the controller is taken away. Only state variables or their linear combinations can be controlled, thus excluding the control of nonlinear quantities such as voltage magnitudes at generator terminals or any other power system bus.

Case 6 shows that inspite of the presence of residual terms in the state and output equations (which are included in the control law) and coordinated trajectories, individual controllers which derive generator control input signals from local measurements only fail to perform satisfactorily as a group.

Cases 7 and 8 show that the use of the time-saving approximation of Eq.(5.12) to compute $\underline{g}_S(t)$ is highly acceptable.

Cases 9 and 10 show that some care must be exercised in the choice of elements for the $\underline{Q}$ matrix. Use of small values (Case 9) reduces the effectiveness of the controller and fails to damp out oscillations in a reasonably short amount of time. Use of large values above a certain level (Case 10) does not necessarily improve controller performance and only makes the computation of the solution to the Riccati equation more difficult.

All of the study cases in this chapter assumed ideal state estimators for controller feedback. Simulation of practical state estimators, and study of the interaction between the estimators and the centralized controller will be dealt with in the next chapter.

Table 5.1. Nonzero Initial and Final Values of Target Trajectory for Case 1

i	$Y_{do,i}$	$Y_{df,i}$
1	-4.195×10^{-2}	0.0000
2	0.0000	-5.080×10^{-2}rad
4	0.0000	$+3.517 \times 10^{-2}$p.u.
5	-8.751×10^{-2}	0.0000
6	0.0000	-1.244×10^{-1}rad
8	0.0000	$+1.489 \times 10^{-1}$p.u.
9	-9.357×10^{-2}	0.0000
10	0.0000	-1.526×10^{-1}rad
12	0.0000	$+1.932 \times 10^{-1}$p.u.
13	$+6.219 \times 10^{-3}$	0.0000
14	0.0000	$+9.677 \times 10^{-2}$rad
16	0.0000	-4.615×10^{-2}p.u.
17	$+8.903 \times 10^{-3}$	0.0000
18	0.0000	$+8.735 \times 10^{-2}$rad
20	0.0000	-4.748×10^{-2}p.u.
21	$+6.366 \times 10^{-3}$	0.0000
22	0.0000	$+9.225 \times 10^{-2}$rad
24	0.0000	-5.584×10^{-2}p.u.
25	$+5.801 \times 10^{-3}$	0.0000
26	0.0000	$+8.648 \times 10^{-2}$rad
28	0.0000	-3.353×10^{-2}p.u.
29	-2.016×10^{-2}	0.0000
30	0.0000	-1.133×10^{-3}rad
32	0.0000	$+4.225 \times 10^{-3}$p.u.
33	-1.224×10^{-2}	0.0000
34	0.0000	$+2.590 \times 10^{-2}$rad
36	0.0000	-4.695×10^{-3}p.u.
37	-7.180×10^{-3}	0.0000

Table 5.2. Nonzero Initial and Final Values of Target Trajectory for Cases 7 and 8

i	$Y_{do,i}$	$Y_{df,i}$
1	-4.195×10^{-2}	0.0000
2	0.0000	-2.107×10^{-1}rad
4	0.0000	$+8.165 \times 10^{-2}$p.u.
5	-8.751×10^{-2}	0.0000
6	0.0000	-3.511×10^{-1}rad
8	0.0000	$+3.029 \times 10^{-1}$p.u.
9	-9.357×10^{-2}	0.0000
10	0.0000	-3.785×10^{-1}rad
12	0.0000	$+3.462 \times 10^{-1}$per unit
13	$+6.219 \times 10^{-3}$	0.0000
14	0.0000	-3.151×10^{-2}rad
16	0.0000	-2.861×10^{-2}p.u.
17	$+8.903 \times 10^{-3}$	0.0000
18	0.0000	-3.444×10^{-2}rad
20	0.0000	-3.300×10^{-2}p.u.
21	$+6.366 \times 10^{-3}$	0.0000
22	0.0000	-3.582×10^{-2}rad
24	0.0000	-3.423×10^{-2}p.u.
25	$+5.801 \times 10^{-3}$	0.0000
26	0.0000	-3.909×10^{-2}rad
28	0.0000	-2.073×10^{-2}p.u.
29	-2.016×10^{-2}	0.0000
30	0.0000	-1.381×10^{-1}rad
32	0.0000	$+5.090 \times 10^{-2}$p.u.
33	-1.224×10^{-2}	0.0000
34	0.0000	-1.045×10^{-1}rad
36	0.0000	$+1.113 \times 10^{-2}$p.u.
37	-7.180×10^{-3}	0.0000

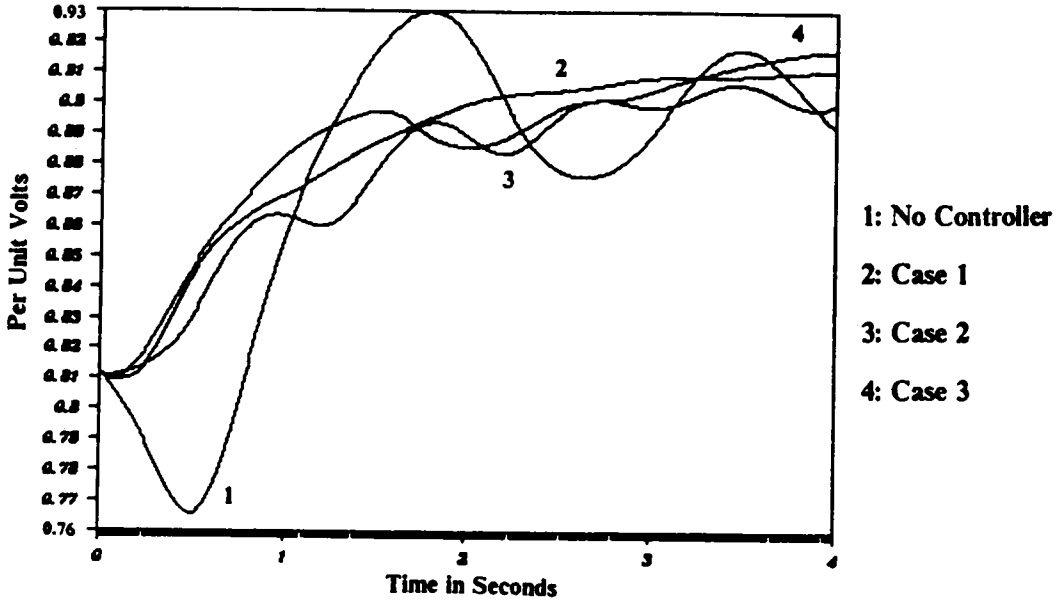

Figure 5.1. Voltage at Bus 15 (No Controller and Cases 1,2,3)

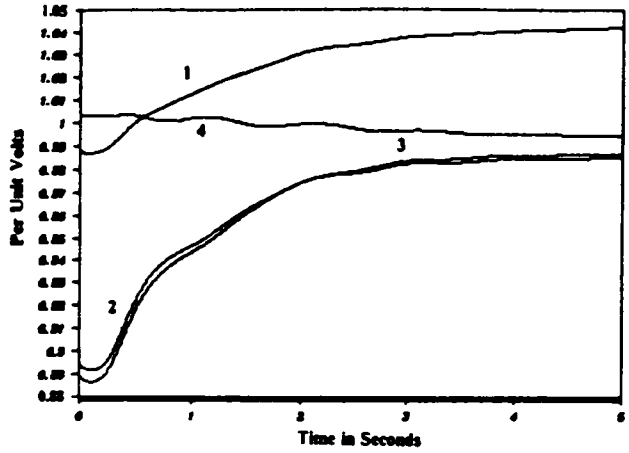

1: E_{11}

2: E_{12}

3: E_{13}

4: E_{14}

A. Generators 1 to 4

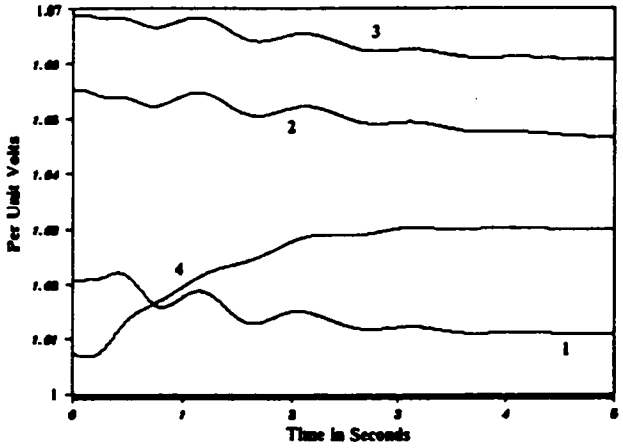

1: E_{15}

2: E_{16}

3: E_{17}

4: E_{18}

B. Generators 5 to 8

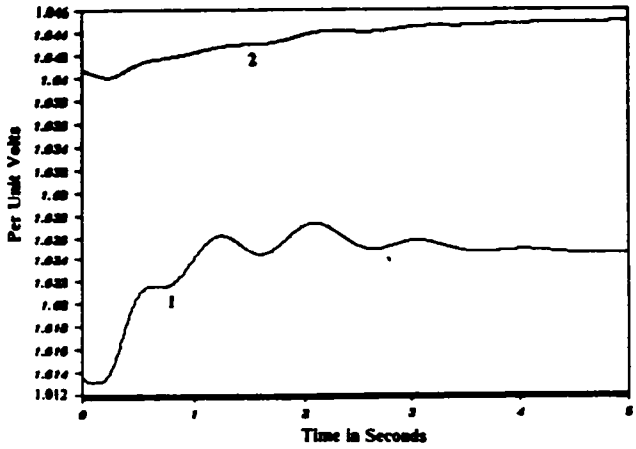

1: E_{19}

2: E_{110}

C. Generators 9 and 10

Figure 5.2. Generator Terminal Voltages (Case 1)

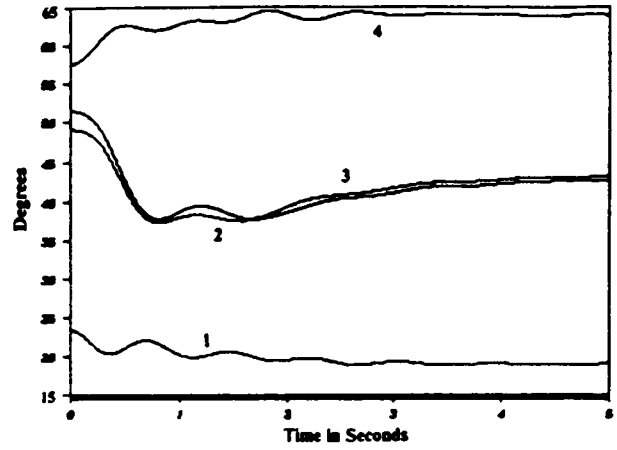

A. Generators 1 to 4

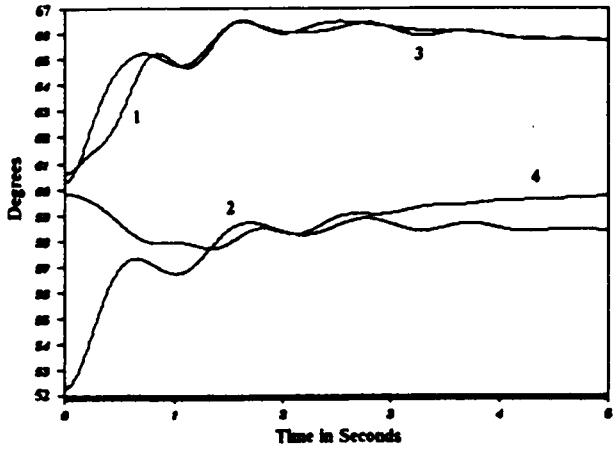

B. Generators 5 to 8

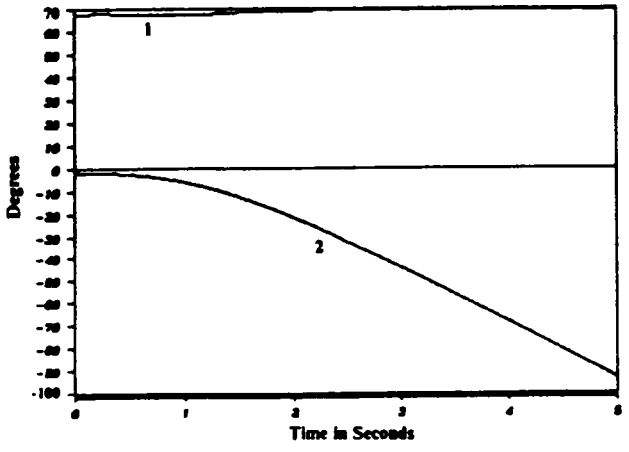

C. Generators 9 and 10

Figure 5.3. Internal Rotor Angles (Case 1)

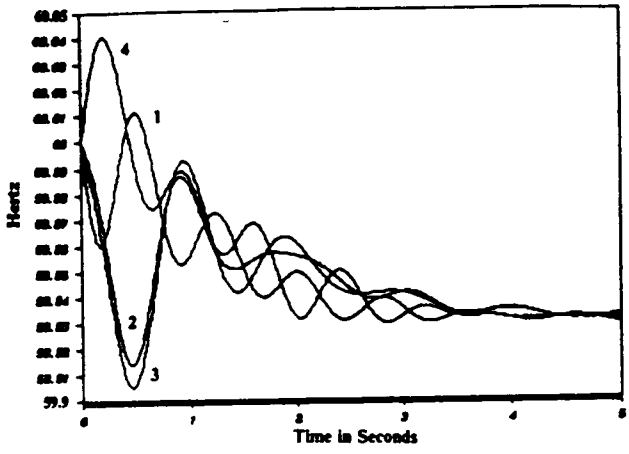

1: $(\omega_1 + \omega_S)/(2\pi)$

2: $(\omega_2 + \omega_S)/(2\pi)$

3: $(\omega_3 + \omega_S)/(2\pi)$

4: $(\omega_4 + \omega_S)/(2\pi)$

A. Generators 1 to 4

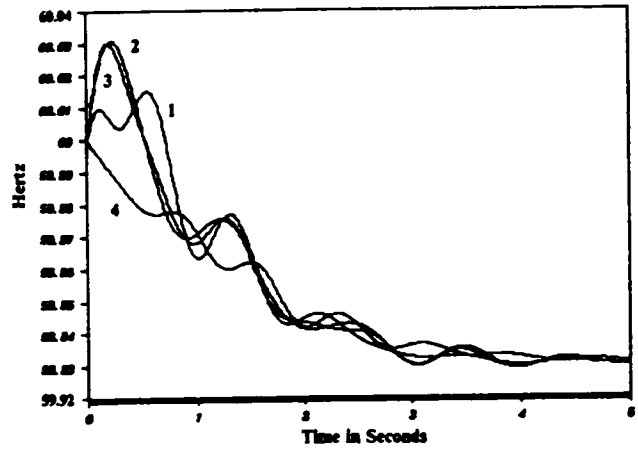

1: $(\omega_5 + \omega_S)/(2\pi)$

2: $(\omega_6 + \omega_S)/(2\pi)$

3: $(\omega_7 + \omega_S)/(2\pi)$

4: $(\omega_8 + \omega_S)/(2\pi)$

B.Generators 5 to 8

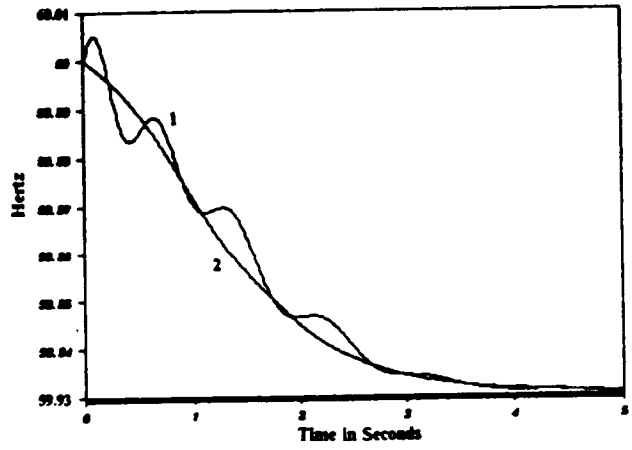

1: $(\omega_9 + \omega_S)/(2\pi)$

2: $(\omega_{10} + \omega_S)/(2\pi)$

C. Generators 9 and 10

Figure 5.4. Rotor Speeds (Case 1)

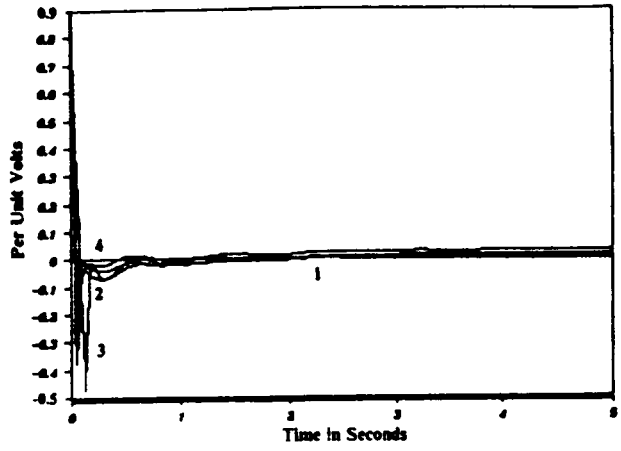

1: V_{S1}

2: V_{S2}

3: V_{S3}

4: V_{S4}

A. Generators 1 to 4

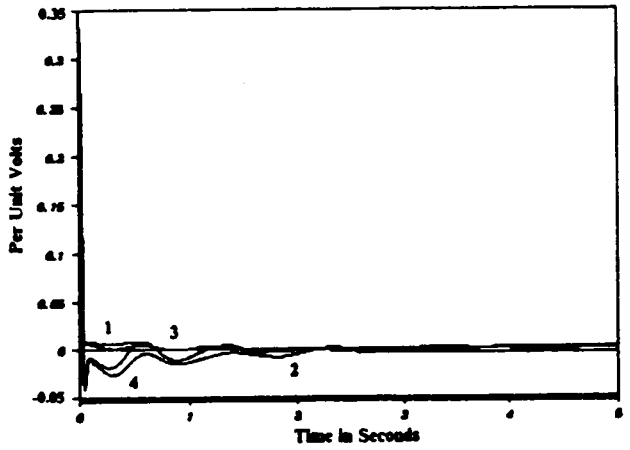

1: V_{S5}

2: V_{S6}

3: V_{S7}

4: V_{S8}

B. Generators 5 to 8

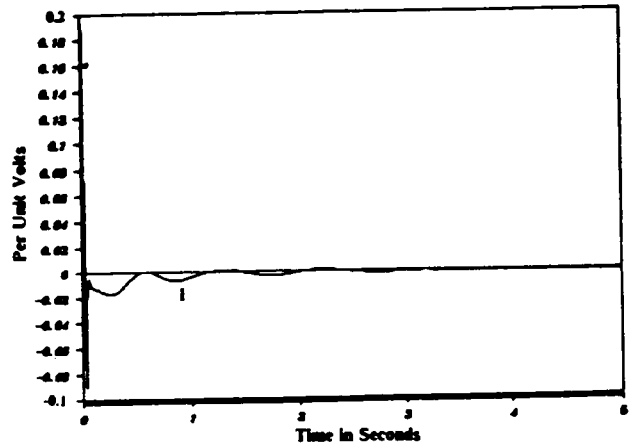

1: V_{S9}

C. Generator 9

Figure 5.5. Excitation System Input Signals (Case 1)

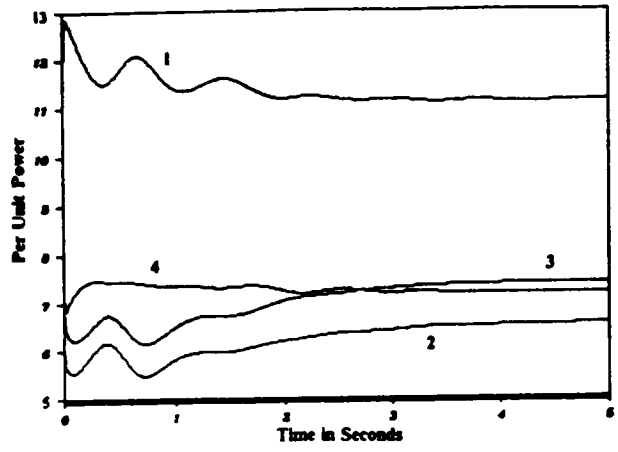

1: $P_{S1} + P_{OG0,1}$

2: $P_{S2} + P_{OG0,2}$

3: $P_{S3} + P_{OG0,3}$

4: $P_{S4} + P_{OG0,4}$

A. Generators 1 to 4

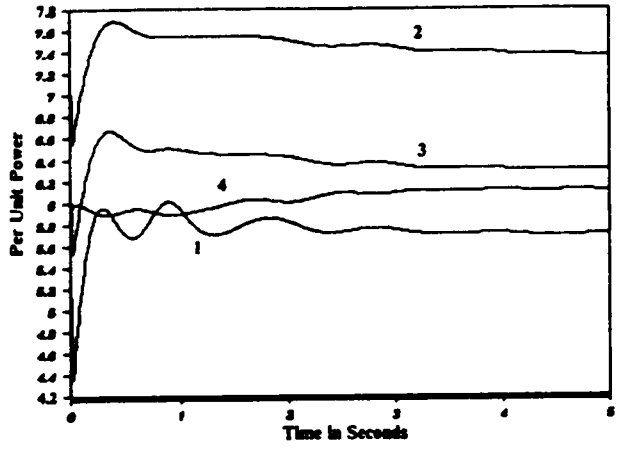

1: $P_{S5} + P_{OG0,5}$

2: $P_{S6} + P_{OG0,6}$

3: $P_{S7} + P_{OG0,7}$

4: $P_{S8} + P_{OG0,8}$

B. Generators 5 to 8

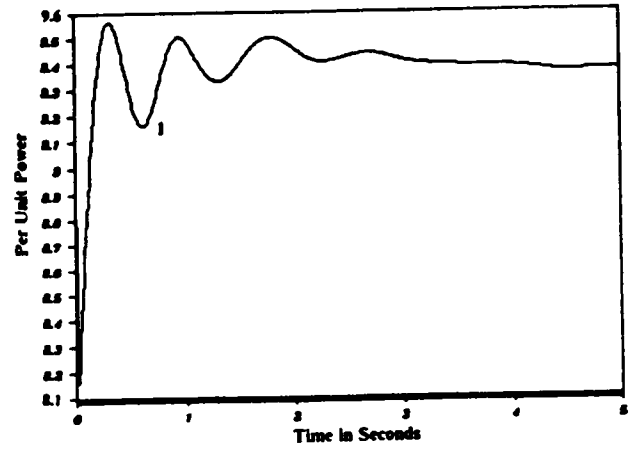

1: $P_{S9} + P_{OG0,9}$

C. Generator 9

Figure 5.6. Speed-Governor Input Signals (Case 1)

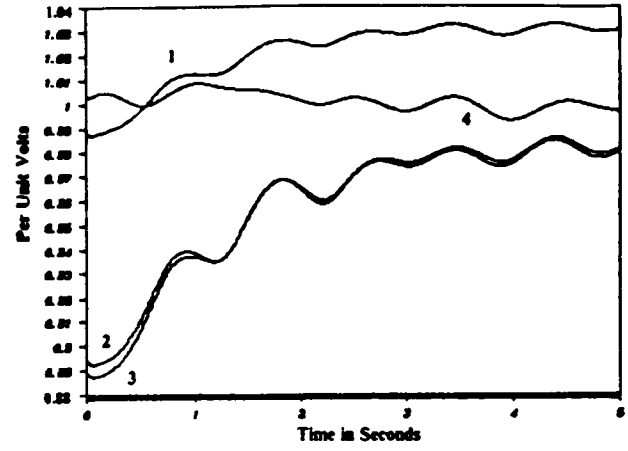

A. Generator Terminal Voltages

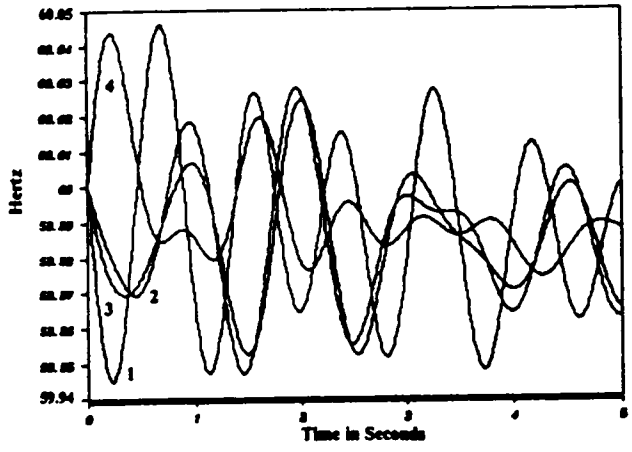

B. Rotor Speeds

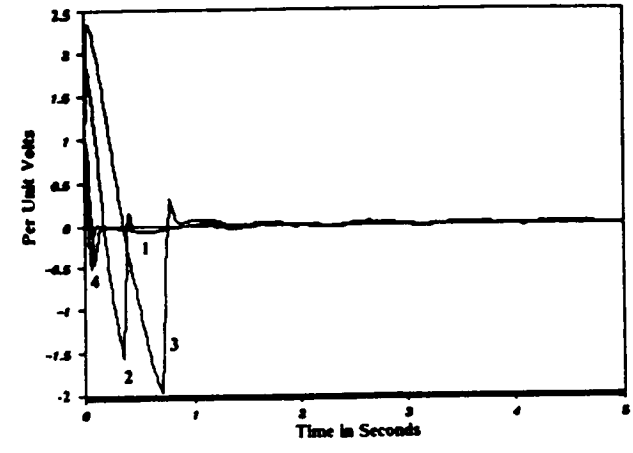

C. Control Input Signals

Figure 5.7. Time Curves for Case 2 (No Speed Governor Control)

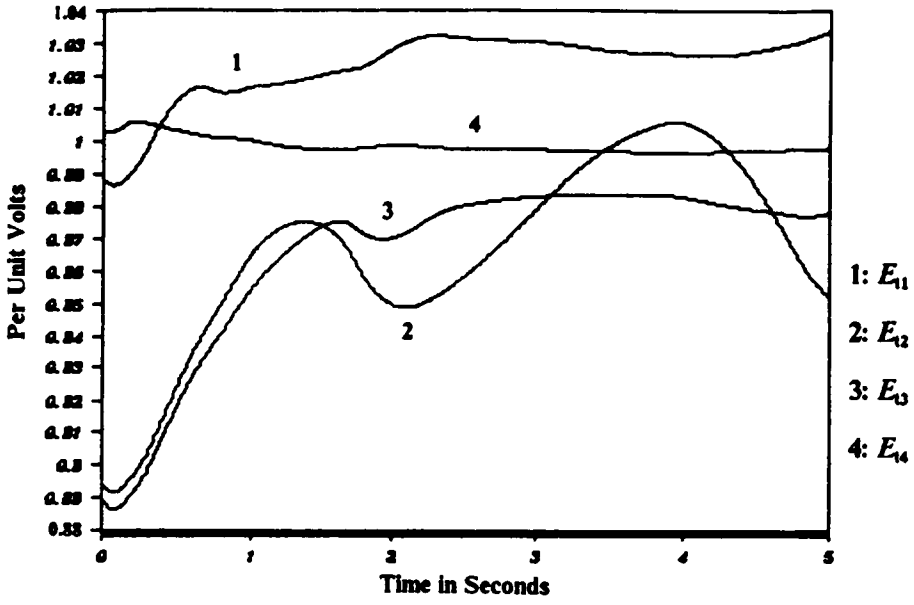

A. Generator Terminal Voltages

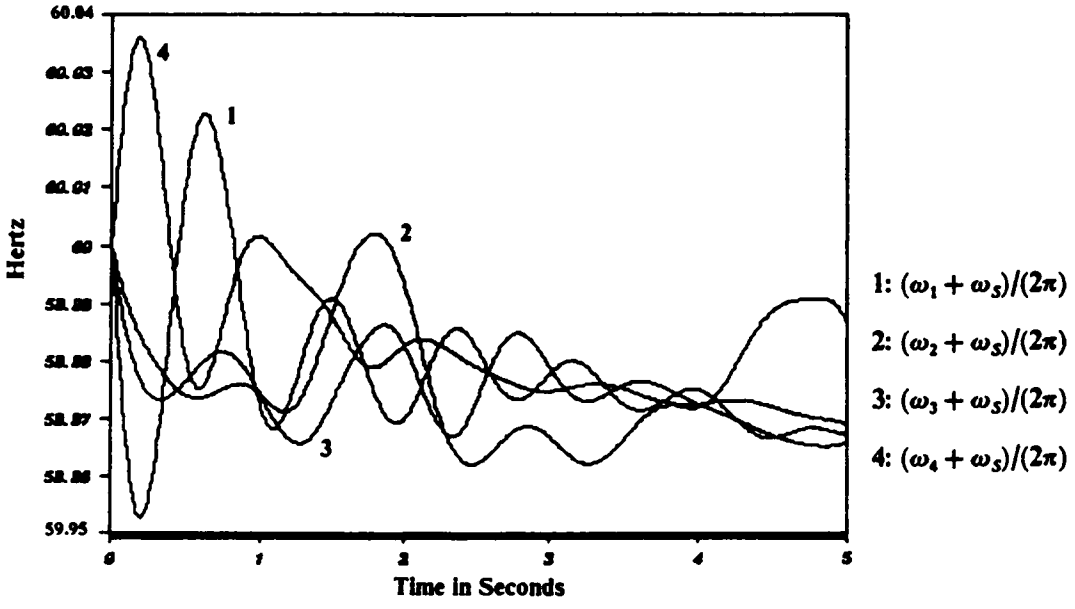

B. Rotor Speeds

Figure 5.8. Time Curves for Case 3 (No Field Voltage Control)

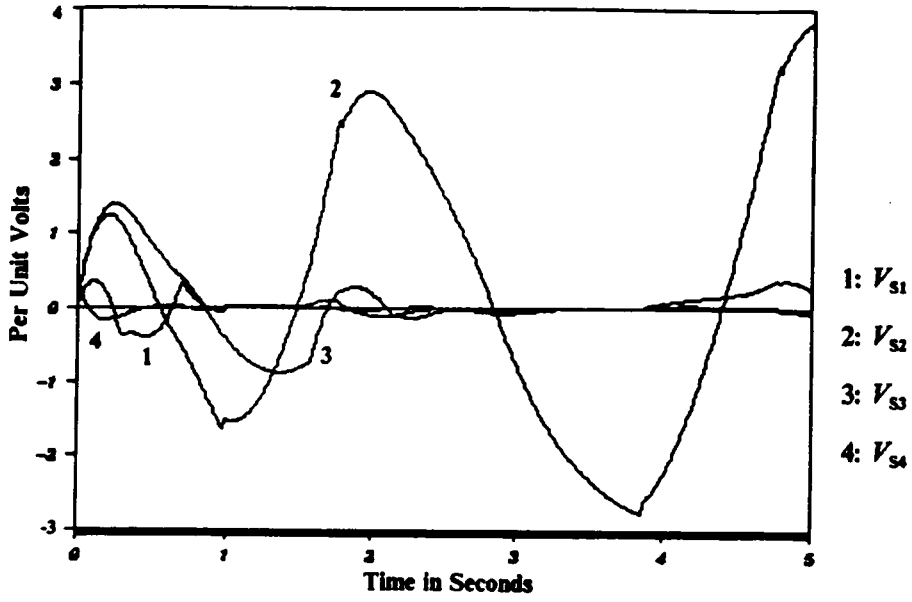

A. Excitation System Input Signals

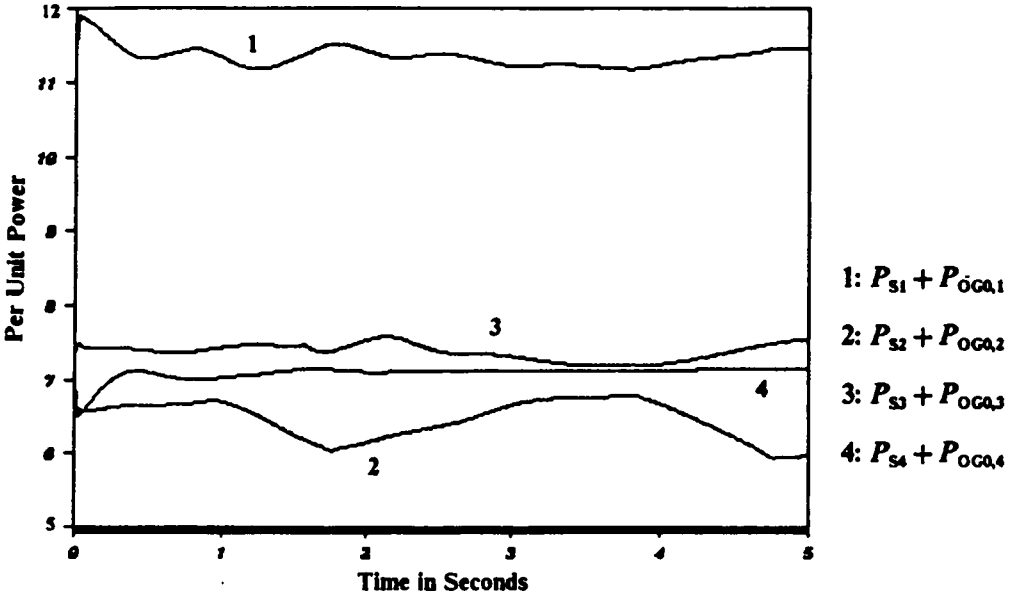

B. Speed-Governor Input Signals

Figure 5.9. Control Input Signals (Case 3)

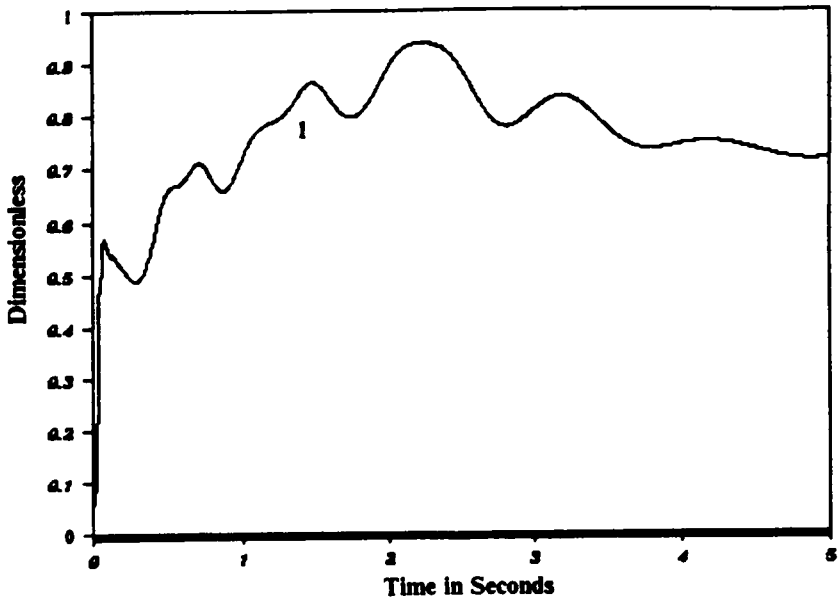

A. r_f (Case 1)

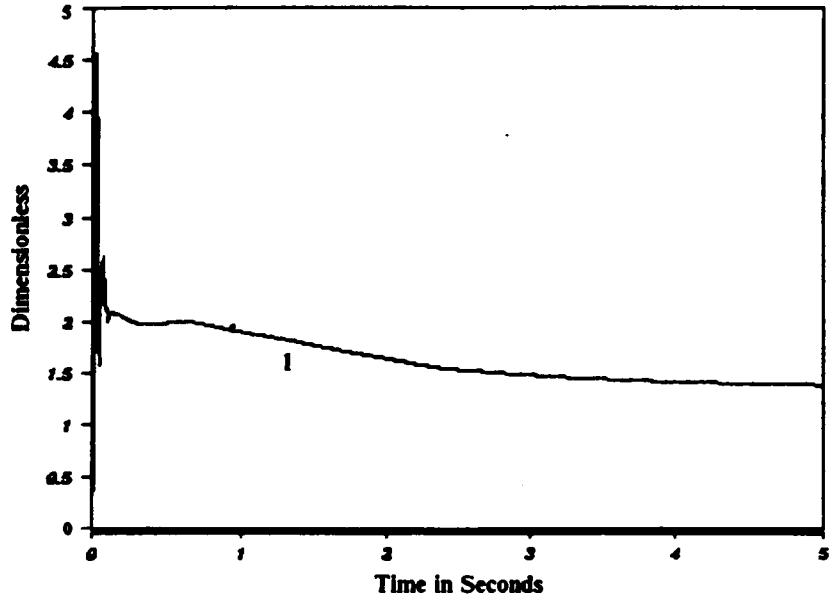

B. r_f (Case 4)

Figure 5.10. Measure of State Residual Vector

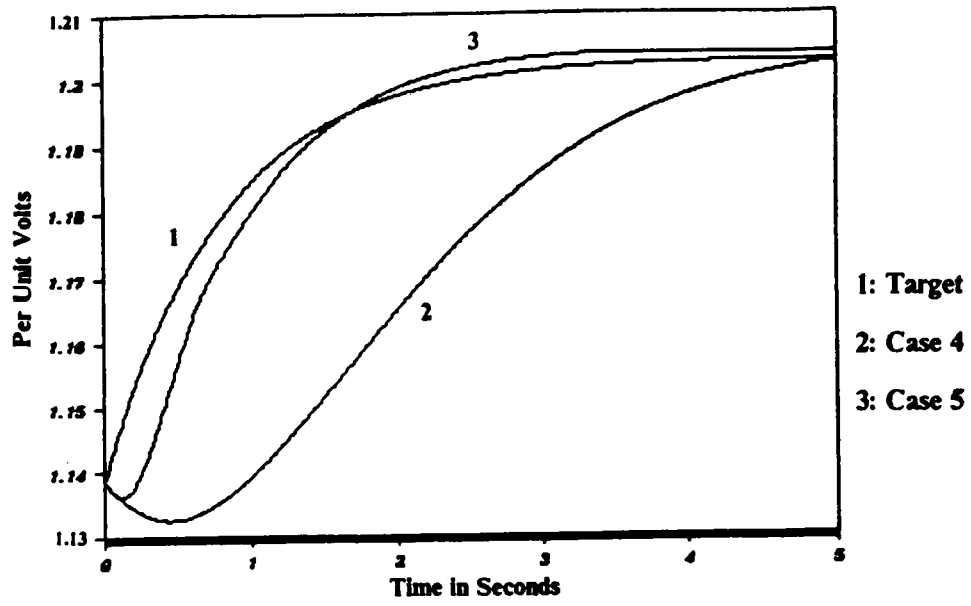

A. E'_{q2}

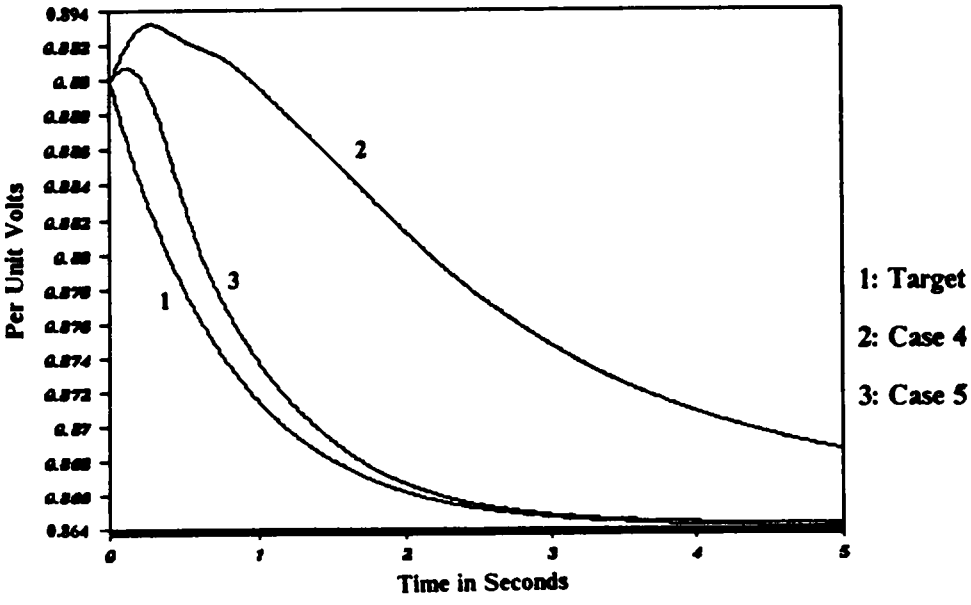

B. E'_{q4}

Figure 5.11. Internal Machine Voltages (Cases 4 and 5)

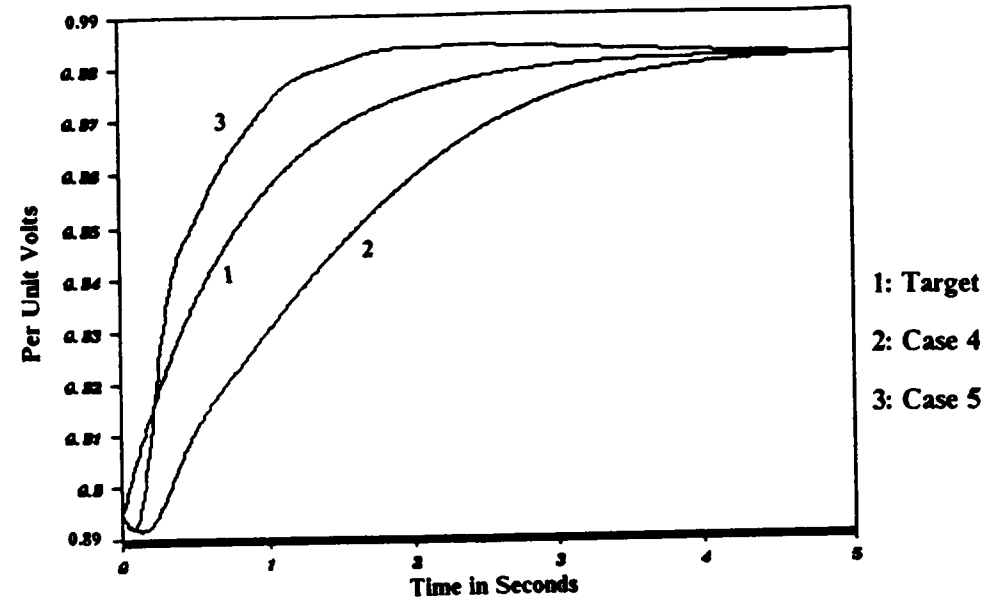

A. E_{12}

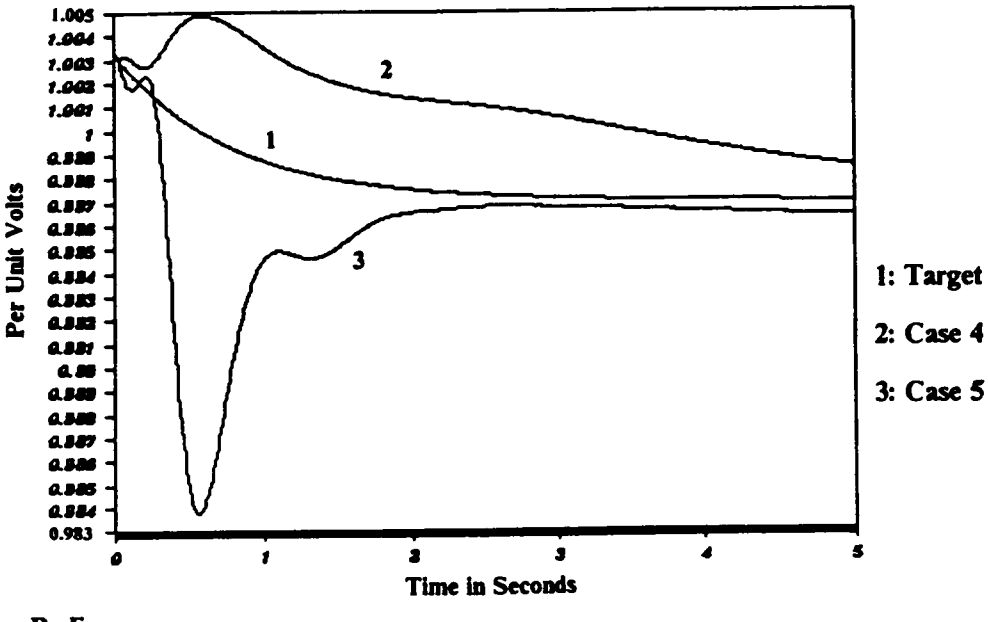

B. E_{14}

Figure 5.12. Generator Terminal Voltages (Cases 4 and 5)

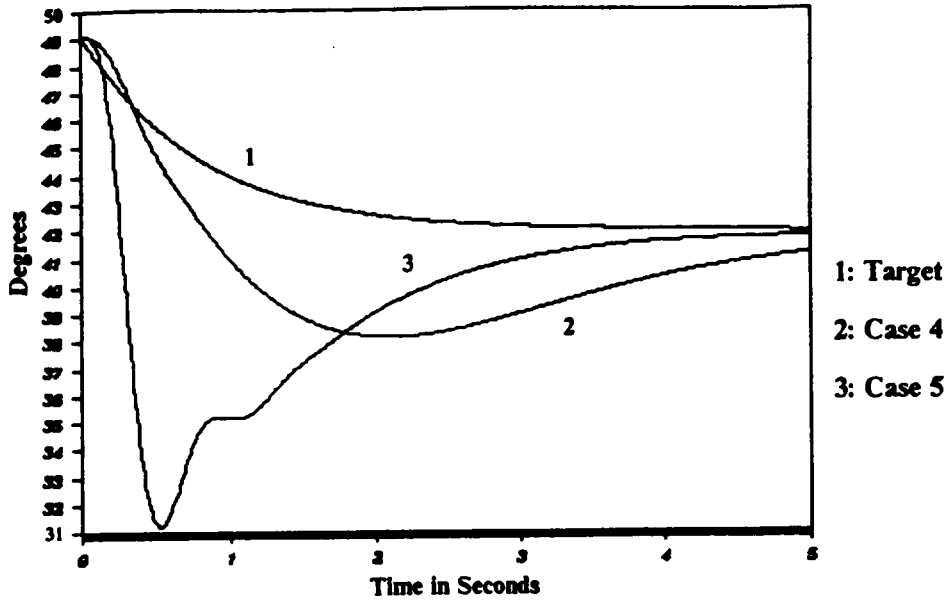

A. $(\delta_{q2} - \delta_{q10})$

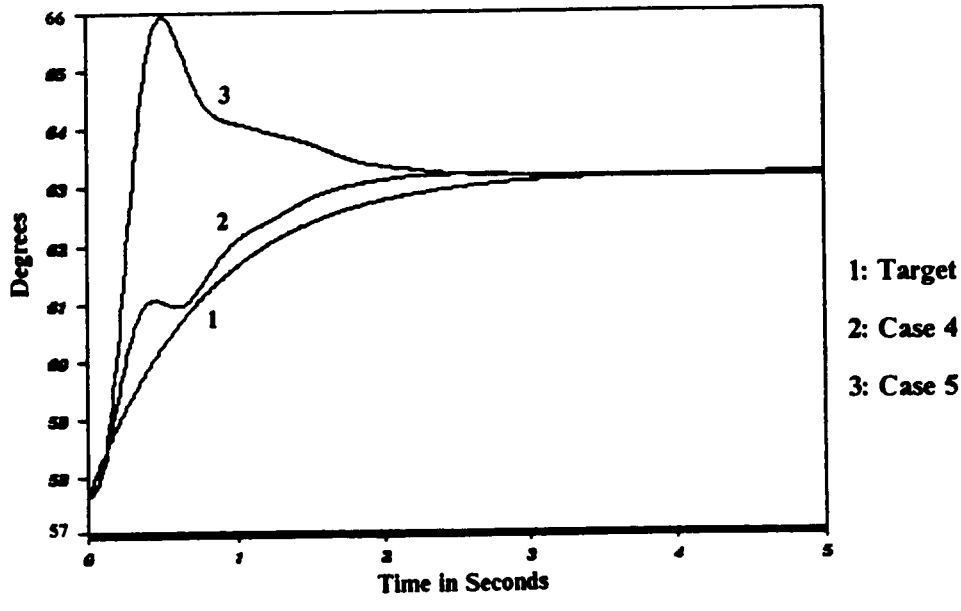

B. $(\delta_{q4} - \delta_{q10})$

Figure 5.13. Internal Rotor Angles (Cases 4 and 5)

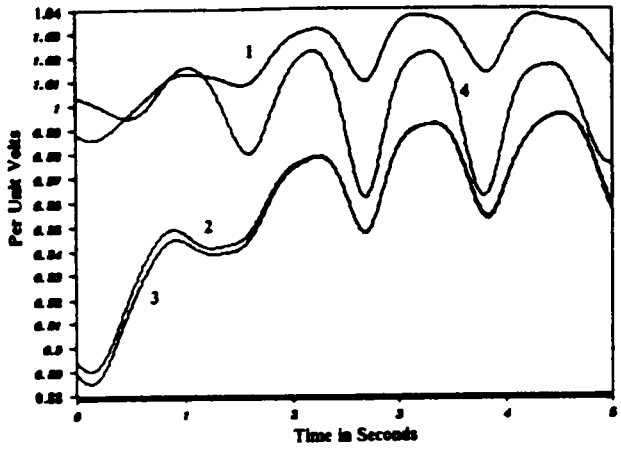

1: E_{t1}

2: E_{t2}

3: E_{t3}

4: E_{t4}

A. Generator Terminal Voltages

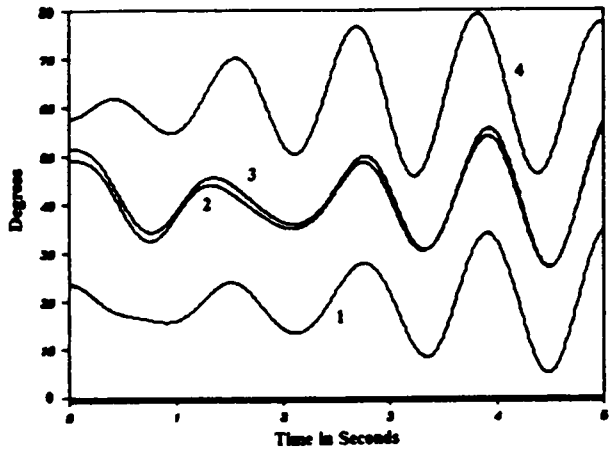

1: $(\delta_{q1} - \delta_{q10})$

2: $(\delta_{q2} - \delta_{q10})$

3: $(\delta_{q3} - \delta_{q10})$

4: $(\delta_{q4} - \delta_{q10})$

B. Internal Rotor Angles

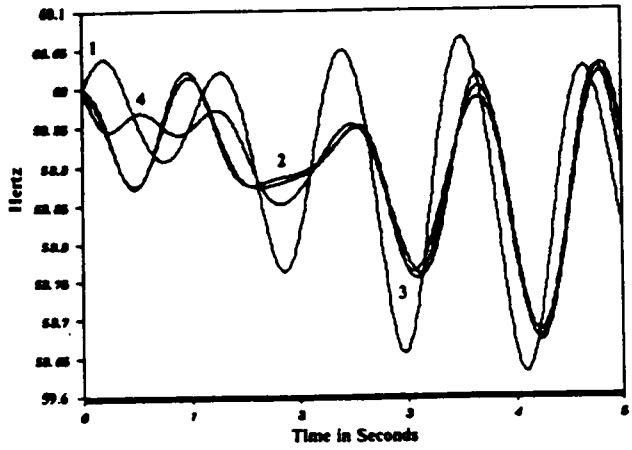

1: $(\omega_1 + \omega_S)/(2\pi)$

2: $(\omega_2 + \omega_S)/(2\pi)$

3: $(\omega_3 + \omega_S)/(2\pi)$

4: $(\omega_4 + \omega_S)/(2\pi)$

C. Rotor Speeds

Figure 5.14. Time Curves for Case 6 (Local Controllers)

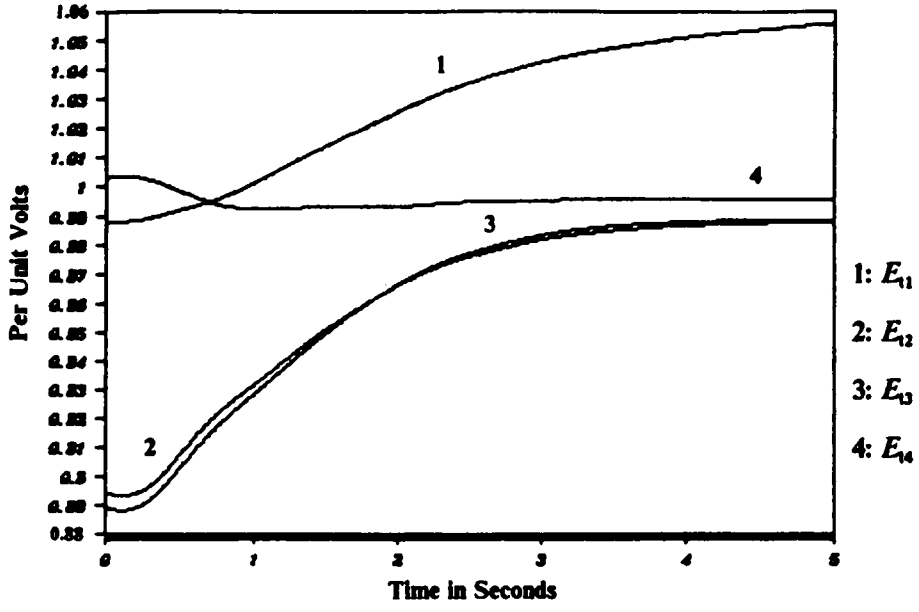

A. $\dot{g}_S(t) = \underline{0}$ (Case 7)

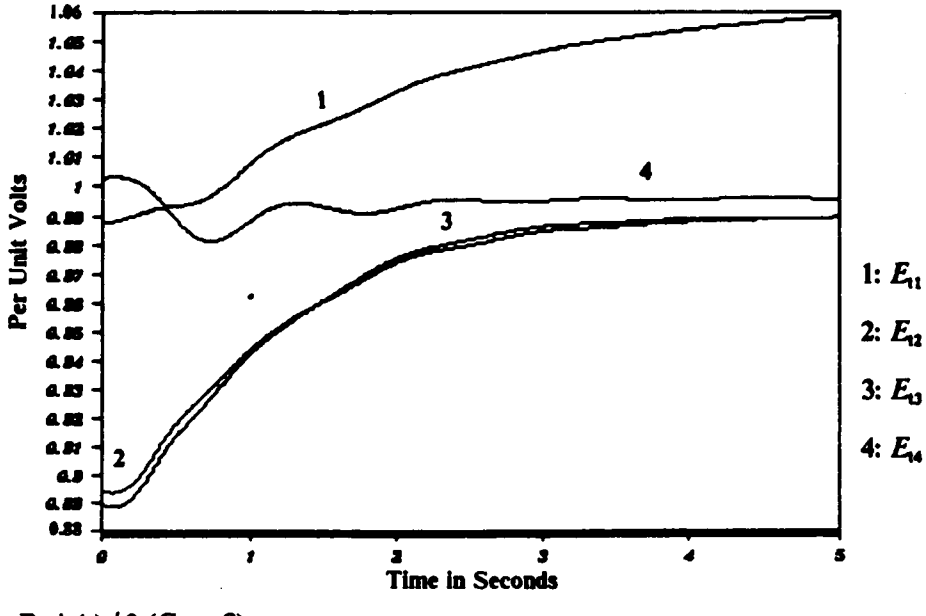

B. $\dot{g}_S(t) \neq \underline{0}$ (Case 8)

Figure 5.15. Generator Terminal Voltages (Cases 7 and 8)

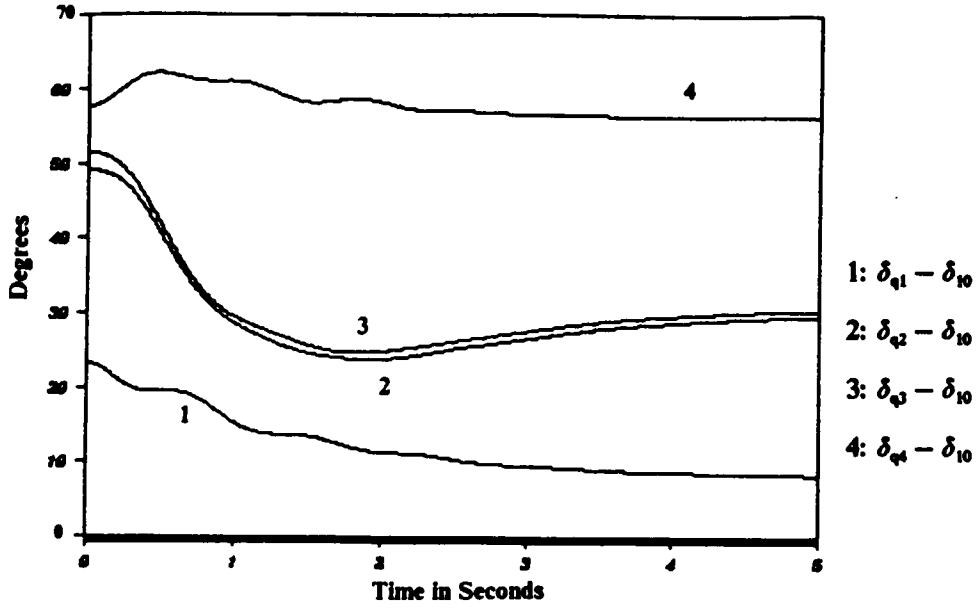

A. $\dot{g}_S(t) = \underline{0}$ (Case 7)

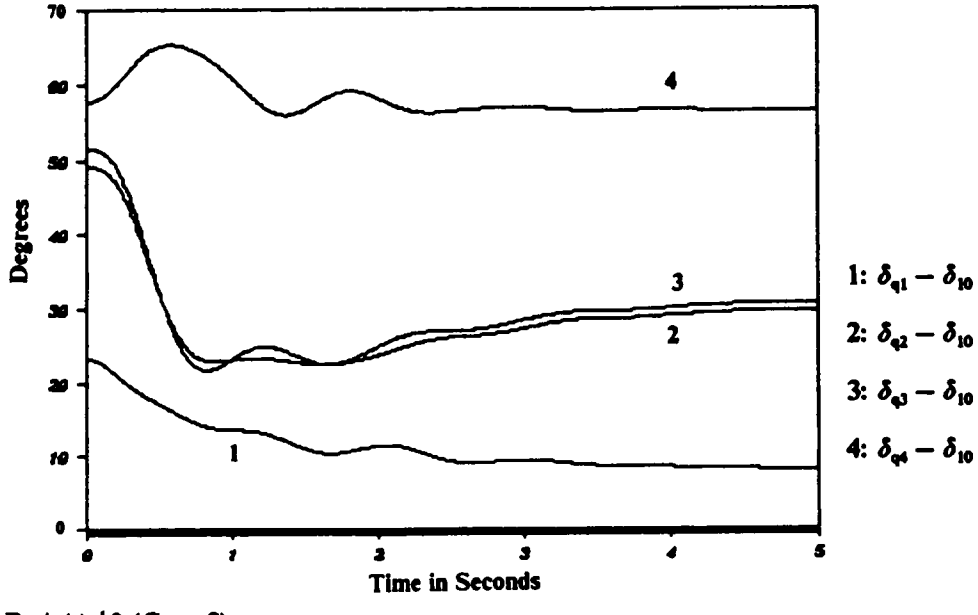

B. $\dot{g}_S(t) \neq \underline{0}$ (Case 8)

Figure 5.16. Internal Rotor Angles (Cases 7 and 8)

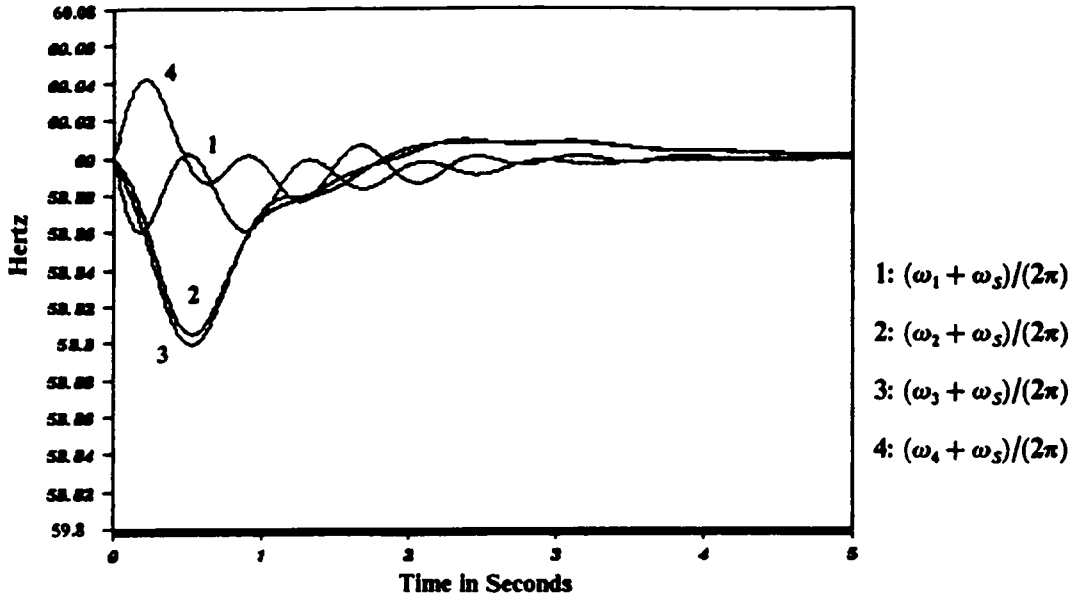

A. $\dot{g}_S(t) = \underline{0}$ (Case 7)

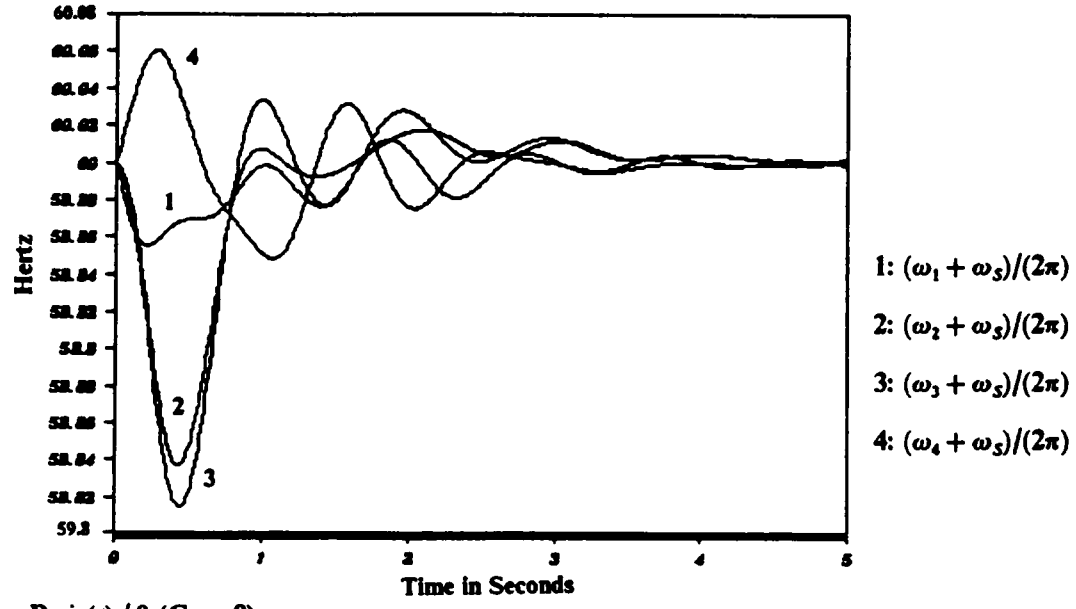

B. $\dot{g}_S(t) \neq \underline{0}$ (Case 8)

Figure 5.17. Rotor Speeds (Cases 7 and 8)

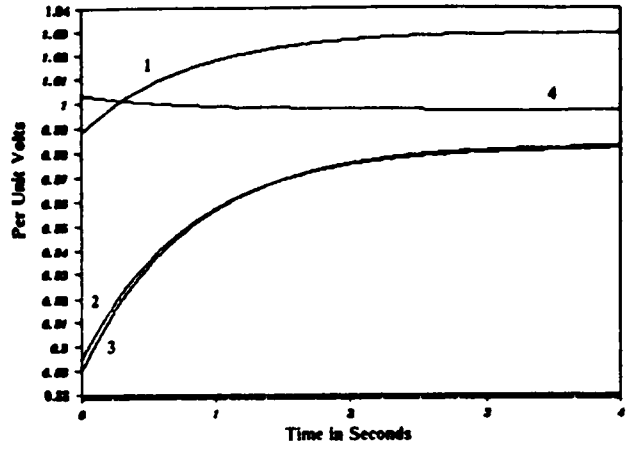

1: E_{t1}

2: E_{t2}

3: E_{t3}

4: E_{t4}

A. Target

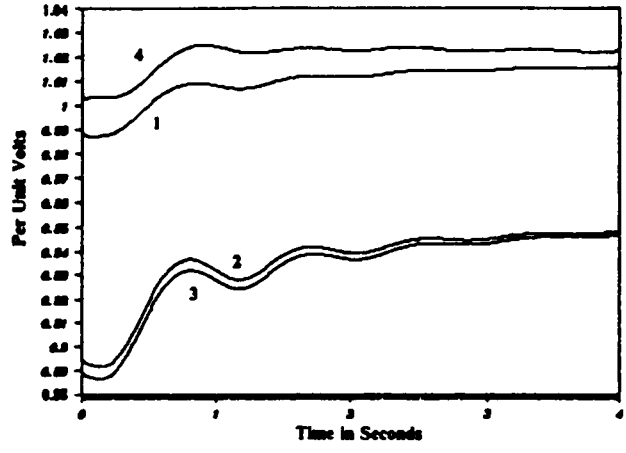

1: E_{t1}

2: E_{t2}

3: E_{t3}

4: E_{t4}

B. Case 9 (Reduced Voltage Control)

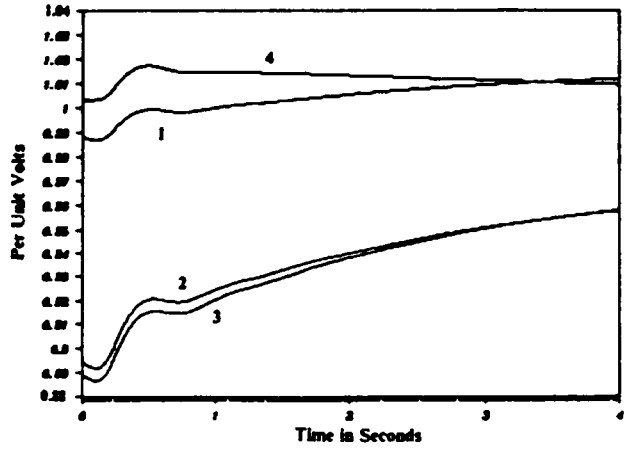

1: E_{t1}

2: E_{t2}

3: E_{t3}

4: E_{t4}

C. Case 10 (Increased Angular Control)

Figure 5.18. Generator Terminal Voltages (Cases 9 and 10)

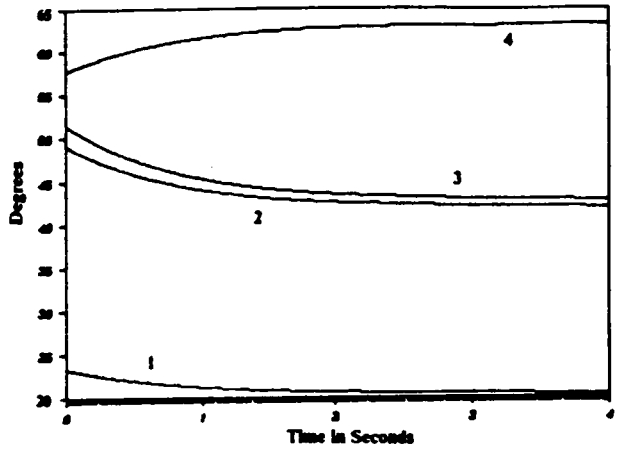

1: $\delta_{q1} - \delta_{q10}$

2: $\delta_{q2} - \delta_{q10}$

3: $\delta_{q3} - \delta_{q10}$

4: $\delta_{q4} - \delta_{q10}$

A. Target

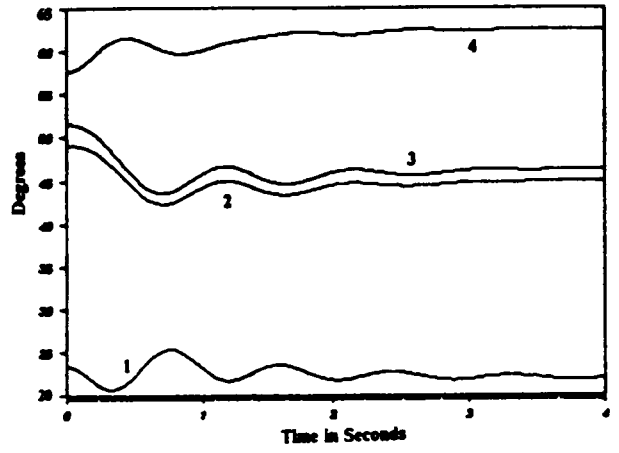

1: $\delta_{q1} - \delta_{q10}$

2: $\delta_{q2} - \delta_{q10}$

3: $\delta_{q3} - \delta_{q10}$

4: $\delta_{q4} - \delta_{q10}$

B. Case 9 (Reduced Voltage Control)

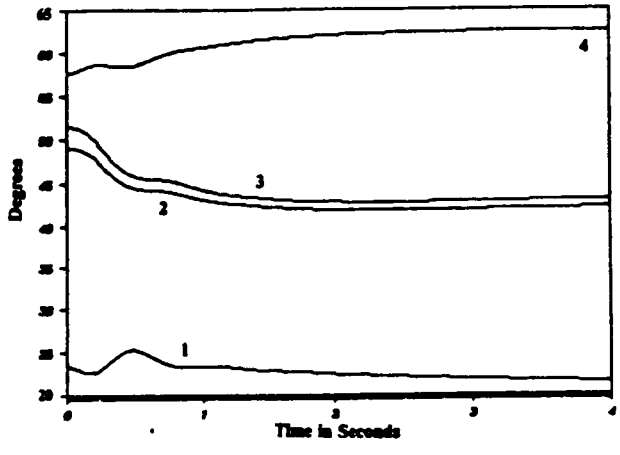

1: $\delta_{q1} - \delta_{q10}$

2: $\delta_{q2} - \delta_{q10}$

3: $\delta_{q3} - \delta_{q10}$

4: $\delta_{q4} - \delta_{q10}$

C. Case 10 (Increased Angular Control)

Figure 5.19. Internal Rotor Angles (Cases 9 and 10)

Chapter 6

Fast Dynamic State Estimation

Introduction

This chapter will deal with the problem of fast dynamic state estimation for the excitation and speed-governing systems. The previous chapter dealt with the controller behavior and performance assuming an ideal estimator, i.e., state feedback and computation of the adaptive vector term made use of the exact values of the state variables at all times. In the actual implementation of the controller, however, direct measurements are limited to the elements of the output vector and to the controller state variables contributed by the largest generator. The remaining state variables must be estimated in real time from the results of phasor and field voltage measurements. In this chapter, the performance of a decentralized state estimator scheme will be evaluated through simulation. Some background theory will also be presented.

The use of decentralized state estimators has been proposed earlier in reference [73] where fast dynamic estimators were required for control purposes. Also, extension of the linear Kalman filter theory to the nonlinear estimation problem by including the state residual vectors in the prediction step has been implemented earlier in actual laboratory set-ups [75,76].

The question of varying the phasor measurement rate as it affects the combined controller-estimator will be addressed in particular. This is motivated by the apparent conflict between the need for high estimation rates and upper limits imposed by present measurement devices. Time curves from the simulations involving actual state variables and their estimates will be presented at the end of the chapter.

Time-Discretization of a Continuous-Time System

Consider a continuous-time system described by the following matrix differential and algebraic equations:

$$\dot{X} = AX + BU + L_n f \tag{6.1}$$

$$Z = HX \tag{6.2}$$

where

X = n state vector

U = r control vector

$\underline{f}$ = n residual vector

$\underline{Z}$ = q measurement vector

$\underline{A}$ = n x n constant feedback matrix

$\underline{B}$ = n x r constant control matrix

$\underline{I}_n$ = n x n identity matrix

$\underline{H}$ = q x n constant measurement matrix

A direct extension of the discussion in reference [82] shows that an equivalent discrete-time representation can be found as given by the following state transition and output measurement equations:

$$\underline{X}(k+1) = \underline{\Phi}\underline{X}(k) + \underline{\Psi}\underline{U}(k) + \underline{\Gamma}\underline{f}(k) \tag{6.3}$$

$$\underline{Z}(k+1) = \underline{H}\underline{X}(k+1) \tag{6.4}$$

where $\underline{X}(k)$, $\underline{U}(k)$, $\underline{f}(k)$, and $\underline{Z}(k)$ are the values of the corresponding continuous-time vectors sampled at the kth instant of time. The state transition matrix $\underline{\Phi}$, control transition matrix $\underline{\Psi}$, and residual transition matrix $\underline{\Gamma}$ have the same sizes as the corresponding continuous-time matrices. They are computed as follows:

$$\underline{\Phi} = \exp(\underline{A}T) \tag{6.5}$$

$$\underline{\Psi} = \left(\int_0^T \exp(\underline{A}\tau)\, d\tau\right)\underline{B} \tag{6.6}$$

$$\Gamma = \left(\int_0^T \exp(A\tau)\, d\tau\right) \tag{6.7}$$

Computation of Ψ and Γ assume that $U(k)$ and $f(k)$ remain constant over the interval T between successive time steps.

In Taylor's Series form, the three transition matrices are equal to

$$\Phi = I_n + (AT) + \frac{1}{2!}(AT)^2 + \frac{1}{3!}(AT)^3 + \ldots \tag{6.8}$$

$$\Gamma = I_n T + \frac{1}{2}(AT^2) + \frac{1}{3!}(A^2T^3) + \frac{1}{4!}(A^3T^4) + \ldots \tag{6.9}$$

$$\Psi = \Gamma B \tag{6.10}$$

Discrete-Time Kalman Filtering

Appendix B presents an adaptation of the state estimation theory presented in reference [83] to a form directly applicable to the present problem. The results shown on the Appendix will be used directly to design a filter that will estimate the state variables of an individual excitation or speed-governing system from given measurements under assumed levels of state disturbances and measurement noise. The state vector estimate at the (k + 1)th time step is given by

$$\hat{X}(k+1\,|\,k+1) = \hat{X}(k+1\,|\,k) + K(\infty)[Z(k+1) - H\hat{X}(k+1\,|\,k)] \tag{6.11}$$

where the predicted state estimate is

$$\hat{\underline{X}}(k+1\,|\,k) = \underline{\Phi}\hat{\underline{X}}(k\,|\,k) + \underline{\Psi}\underline{U}(k) + \underline{\Gamma}\hat{\underline{f}}(k) \tag{6.12}$$

and $\underline{Z}(k+1)$ is the vector of measurements at the (k+1)th time step.

$\underline{K}(\infty)$ is the steady-state solution to the following recursive formulas:

$$\underline{K}(k+1) = \underline{P}(k+1\,|\,k)\underline{H}^T\,[\underline{H}\underline{P}(k+1\,|\,k)\underline{H}^T + \underline{R}]^{-1} \tag{6.13}$$

$$\underline{P}(k+1\,|\,k) = \underline{\Phi}\underline{P}(k\,|\,k)\underline{\Phi}^T + \underline{\Gamma}\underline{Q}\underline{\Gamma}^T + \underline{I}_f \tag{6.14}$$

$$\underline{P}(k+1\,|\,k+1) = [\underline{I}_n - \underline{K}(k+1)\underline{H}]\,\underline{P}(k+1\,|\,k) \tag{6.15}$$

In Eqs.(6.13) and (6.14), the matrices $\underline{Q}$ and $\underline{R}$ are the positive-definite covariance matrices of the state disturbance and measurement noise vectors, respectively, in the corresponding continuous-time equations:

$$\dot{\underline{X}} = \underline{A}\underline{X} + \underline{B}\underline{U} + \underline{I}_n[\underline{f}(t) + \underline{\Omega}(t)] \tag{6.16}$$

$$\underline{Z} = \underline{H}\underline{X} + \underline{\nu}(t) \tag{6.17}$$

where $\underline{\Omega}(t)$ and $\underline{\nu}(t)$ are the vectors of state disturbance and measurement noise. The covariance matrices are

$$\underline{Q} = E[\underline{\Omega}(t)\underline{\Omega}^T(t)] = E[\underline{\Omega}(k)\underline{\Omega}^T(k)] \tag{6.18}$$

$$\underline{R} = E[\underline{\nu}(t)\underline{\nu}^T(t)] = E[\underline{\nu}(k)\underline{\nu}^T(k)] \tag{6.19}$$

Upon discretization in time,

$$\underline{X}(k+1) = \underline{\Phi X}(k) + \underline{\Psi U}(k) + \underline{\Gamma f}(k) + \underline{w}(k) \tag{6.20}$$

$$\underline{Z}(k+1) = \underline{H X}(k+1) + \underline{v}(k+1) \tag{6.21}$$

where

$$\underline{w}(k) = \underline{\Gamma \Omega}(k) \tag{6.22}$$

Thus, the discrete-time covariance matrices are given by

$$\begin{aligned} E[\underline{w}(k)\underline{w}^T(k)] &= E[\underline{\Gamma \Omega}(k)\underline{\Omega}^T(k)\underline{\Gamma}^T] \\ &= \underline{\Gamma} E[\underline{\Omega}(k)\underline{\Omega}^T(k)]\underline{\Gamma}^T \\ &= \underline{\Gamma Q}\underline{\Gamma}^T \end{aligned} \tag{6.23}$$

and

$$E[\underline{v}(k)\underline{v}^T(k)] = \underline{R} \tag{6.19}$$

Assuming time-invariant covariance matrices $\underline{Q}$ and $\underline{R}$, the above equations are true for all k = 0,1,2,... .

In Eq.(6.14), $\underline{J}_f$ is the assumed covariance matrix of the sum of the discrete-time filter input and residual terms. Applying the results of Appendix B,

$$\underline{J}_f = E\left[\underline{e}_r \underline{e}_r^T\right] \tag{6.24}$$

where

$$\underline{e}_r = [\underline{\Psi U}(k) + \underline{\Gamma}\hat{\underline{f}}(k)] - [\underline{\Psi U}(k) + \underline{\Gamma f}(k)] \tag{6.25}$$

and $\underline{U}(t)$ is the deterministic portion of the known input vector to the Kalman filter. Thus,

$$\begin{aligned} J_f &= E\left\{[\Gamma\hat{\underline{f}}(k) - \Gamma\underline{f}(k)][\Gamma\hat{\underline{f}}(k) - \Gamma\underline{f}(k)]^T\right\} \\ &= \Gamma E\left\{[\hat{\underline{f}}(k) - \underline{f}(k)][\hat{\underline{f}}(k) - \underline{f}(k)]^T\right\}\Gamma^T \end{aligned} \tag{6.26}$$

As assumed in Appendix B, $\underline{v}$ and $\underline{w}$ are independent stochastic processes with zero means, i.e.,

$$E[\underline{v}(k)\underline{w}^T(k)] = 0 \tag{6.27}$$

$$E[\underline{v}(k)] = 0 \tag{6.28}$$

$$E[\underline{w}(k)] = 0 \tag{6.29}$$

for all j,k = 0,1,2,.... The use of a constant gain matrix corresponding to the steady-state solution of the recursion formulas allows several advantages to be realized. Firstly, real-time computational requirements are reduced as the gain matrix need not be re-computed at every time step. Secondly, the conventional covariance Kalman filter as described by Eqs.(6.11)-(6.15) is susceptible to numerical instabilities and will have disastrous effects on controller performance if the instabilities occur in real time. Use of a constant gain matrix allows the numerical instabilities to be avoided in the off-line computations. More will be said about this in a latter section of this chapter.

Kalman Filtering on an Excitation System

This section will discuss necessary steps to carry out the computation of the filter gain matrix in the estimation of excitation system state variables.

As discussed in Chapter 4, the differential equations that apply to an excitation system are given by the following.

$$\dot{V}_y = \frac{1}{T_r}(E_t - V_y) \tag{6.30}$$

$$\dot{V}_r = \frac{1}{T_a}[-V_r + (-V_y - V_z + V_{\text{ref}} + V_s)K_a] \tag{6.31}$$

In situations where the regulator voltage is at its upper or lower limit,

$$\dot{V}_r = 0 \tag{6.32}$$

$$\dot{V}_z = \frac{1}{T_f}\left\{\frac{K_f}{T_e}[V_r - (S_e + K_e)E_{fd}] - V_z\right\} \tag{6.33}$$

$$\dot{E}_{fd} = \frac{1}{T_e}[V_r - (S_e + K_e)E_{fd}] \tag{6.34}$$

The introduction of random process and measurement noise will be considered later in this section. Prior to that, use of the deterministic Eqs.(6.30) to (6.34) does not affect the subsequent discussion.

Using incremental changes from prefault values as state variables,

$$\dot{X}^I = A^I X^I + B^I U^I + f^I + \text{higher-order terms} \tag{6.35}$$

where

$$A^I = \begin{bmatrix} \frac{-1}{T_r} & 0 & 0 & 0 \\ \frac{-K_a}{T_a} & \frac{-1}{T_a} & \frac{-K_a}{T_a} & 0 \\ 0 & \frac{K_f}{T_f T_e} & -\frac{1}{T_f} & \frac{-K_f}{T_f T_e}[K_e + S_e^I(1 + B_e \cdot E_{\text{fd}}^I)] \\ 0 & \frac{1}{T_e} & 0 & \frac{-1}{T_e}[K_e + S_e^I(1 + B_e \cdot E_{\text{fd}}^I)] \end{bmatrix} \tag{6.36}$$

$$B^I = [0 \ (\frac{K_a}{T_a}) \ 0 \ 0]^T \tag{6.37}$$

$$X^I = [\Delta V_y \ \Delta V_r \ \Delta V_z \ \Delta E_{\text{fd}}]^T \tag{6.38}$$

$$U^I = V_s \tag{6.39}$$

$$f^I = [(\frac{\Delta E_t}{T_r}) \ 0 \ 0 \ 0]^T \tag{6.40}$$

and S_o^I, E_{fd}^I are the prefault values of the saturation function and field voltages respectively. The superscript "I" for the matrices denotes quantities evaluated at the prefault operating point of the given generator.

Observability Analysis. Reference [94] formally proves the possibility of divergence of the Kalman filter if the matrix pair (A, H) from Eqs.(6.1)-(6.2) is not observable. References [89,96] state that for the system of Eqs.(6.1)-(6.2), the state vector X is observable from the given measurements Z (assuming known filter inputs and residual terms) if and only if the observability matrix M given by

$$M = [H^T \; A^T H^T \; (A^T)^2 H^T \; \ldots \; (A^T)^{n-1} H^T] \tag{6.41}$$

has rank n. In the present case,

$$A^T = A^{IT} = (A^I)^T \qquad H = [0 \; 0 \; 0 \; 1] \tag{6.42}$$

i.e., the field voltage E_{fd} is assumed to be the measured quantity. Since q = 1, it is sufficient to establish that M is nonsingular for observability. From the previous section,

$$A^I = \begin{bmatrix} a_{11} & 0 & 0 & 0 \\ a_{21} & a_{22} & a_{23} & 0 \\ a_{31} & a_{32} & a_{33} & a_{34} \\ a_{41} & a_{42} & 0 & a_{44} \end{bmatrix} \tag{6.43}$$

where a_{ij} denotes nonzero elements of the matrix. It is noted that

$$a_{21} = a_{23} = -\left(\frac{K_a}{T_a}\right) \tag{6.44}$$

The square of the matrix A^I is given by

$$(A^{IT})^2 = \begin{bmatrix} b_{11} & b_{12} & b_{13} & b_{14} \\ 0 & b_{22} & b_{23} & b_{24} \\ 0 & b_{32} & b_{33} & b_{34} \\ 0 & b_{42} & b_{43} & b_{44} \end{bmatrix} \tag{6.45}$$

where

$$\begin{aligned} b_{12} &= a_{11}a_{21} + a_{22}a_{21} \\ b_{32} &= a_{23}a_{22} + a_{33}a_{23} \\ b_{14} &= a_{21}a_{42} \\ b_{34} &= a_{23}a_{42} \end{aligned} \tag{6.46}$$

The last set of identities made use of direct matrix multiplication and took into account the existence of zero entries in the matrix A^I. The entries b_{ij} denote elements of the matrix $(A^{IT})^2$ which are not necessarily equal to zero. From the most recent results,

$$(A^{IT})^3 = \begin{bmatrix} c_{11} & c_{12} & c_{13} & c_{14} \\ 0 & c_{22} & c_{23} & c_{24} \\ 0 & c_{32} & c_{33} & c_{34} \\ 0 & c_{42} & c_{43} & c_{44} \end{bmatrix} \tag{6.47}$$

where, after once more taking into account the presence of zero entries,

$$\begin{aligned} c_{14} &= a_{21}a_{42}(a_{11} + a_{22} + 1) \\ c_{34} &= a_{23}a_{42}(a_{22} + a_{33} + 1) \end{aligned} \tag{6.48}$$

At this point, n = 4. The columns of the matrix M correspond simply to the fourth columns of I_4, A^{IT}, $(A^{IT})^2$, and $(A^{IT})^3$ as indicated by the measurement matrix H. Thus,

$$M = \begin{bmatrix} 0 & 0 & b_{14} & c_{14} \\ 0 & a_{42} & b_{24} & c_{24} \\ 0 & 0 & b_{34} & c_{34} \\ 1 & a_{44} & b_{44} & c_{44} \end{bmatrix} \tag{6.49}$$

and

$$\det M = (-1)(-a_{42})(b_{14}c_{34} - b_{34}c_{14}) = a_{42}(b_{14}c_{34} - b_{34}c_{14}) \tag{6.50}$$

Since $a_{21} = a_{23}$,

$$b_{14} = b_{34} = a_{21}a_{42} \tag{6.51}$$

Therefore,

$$\begin{aligned} \det \underline{M} &= a_{42}a_{21}a_{42}(c_{34} - c_{14}) = a_{42}^2 a_{21}a_{21}a_{42}(a_{33} - a_{11}) \\ &= a_{42}^3 a_{21}^2 (a_{33} - a_{11}) \end{aligned} \tag{6.52}$$

Thus, if $a_{33} = a_{11}$ (i.e., if $T_r = T_f$), $\underline{M}$ is singular and the excitation system state variables are not observable from the E_{fd} measurements only. From the excitation system data shown in Chapter 3, no generator satisfies this unobservability condition. Thus, the state variables of each excitation system are completely observable from the field voltage measurements.

Order Reduction and Scaling of Variables. At this point, it is worth mentioning that the state estimation scheme presented earlier in this chapter (conventional covariance filter) is susceptible to numerical instabilities [92]. The process of propagating the filter gain matrix $\underline{K}_f(k)$ and the covariance matrices $\underline{P}(k+1|k)$ and $\underline{P}(k+1|k+1)$ may yield grossly incorrect estimates as the value of estimation step k increases for an ill-conditioned estimation problem. The incorrect estimates, when used by the controller for feedback, amount to unstable operation. Thus, reliable estimator performance is of paramount importance.

The problem of numerical instability is mitigated for the most part by performing the computations of the filter gain matrix off-line (i.e., use of the steady-state solution). Measures to ensure convergence (such as scaling of variables) and convergence criteria check (such as the positive-definiteness of the covariance matrices) can all be enforced

in the off-line computations. The use of the actual state variables in the state estimator cause the largest and the smallest nonzero elements of the resulting feedback matrix to differ from each other by several orders of magnitude. It has been observed that this situation gives rise to serious numerical problems. This observation can be explained through Eqs.(6.13) to (6.15). References [92,93] state that for a matrix $\underline{\Sigma} = \underline{S}^T\underline{S}$, the condition number $\kappa(\underline{S})$ given by

$$\kappa(\underline{S}) = \frac{\sigma_1}{\sigma_n} \tag{6.53}$$

determines the stability of the inversion process of $\underline{\Sigma}$. In the expression for $\kappa(\underline{S})$, σ_1 is the largest eigenvalue of $\underline{\Sigma}$ while σ_n is the smallest eigenvalue of the same matrix. The higher the value of $\kappa(\underline{S})$, the greater the chances of numerical instabilities are in the computation of $\underline{\Sigma}^{-1}$. Inspection of Eqs.(6.13) to (6.15) shows how a large condition number for the state transition matrix Φ can easily lead to a correspondingly large condition number for the quantity $\left[\underline{H}\underline{P}(k+1\,|\,k)\underline{H}^T + \underline{R}\right]$. Use of a feedback matrix $\underline{A}$ with a large condition number in turn causes a similar behavior in the transition matrix Φ.

The use of scaled variables in the real-time estimation of actual state variables allows the use of a feedback matrix with improved numerical properties and amounts to a linear transformation of the original state variables.

Define the diagonal transformation matrix $\underline{\alpha}$ as

$$\underline{\alpha} = \begin{bmatrix} \alpha_1 & 0 & \dots & 0 & \dots & 0 \\ 0 & \alpha_2 & \dots & 0 & \dots & 0 \\ & & \cdot & & \cdot & \\ & & \cdot & & \cdot & \\ & & \cdot & & \cdot & \\ 0 & 0 & \dots & \alpha_i & \dots & 0 \\ & & \cdot & & \cdot & \\ & & \cdot & & \cdot & \\ & & \cdot & & \cdot & \\ 0 & 0 & \dots & 0 & \dots & \alpha_n \end{bmatrix} \tag{6.54}$$

where α_i = scale factor for x_i^I. Letting X_s denote the vector of scaled variables,

$$X_s = \underline{\alpha} X^I = [\alpha_1 x_1^I \;\; \alpha_2 x_2^I \;\; \dots \;\; \alpha_i x_i^I \;\; \dots \;\; \alpha_n x_n^I]^T \tag{6.55}$$

where X^I is the vector of original state variables. Assuming that the original differential equations are described by

$$\dot{X}^I = A^I X^I + B^I \underline{U} + \underline{f}^I \tag{6.56}$$

the corresponding equations for the scaled variables are given by

$$\begin{aligned} \dot{X}_s &= \underline{\alpha} A^I \underline{\alpha}^{-1} X^I + \underline{\alpha} B^I \underline{U} + \underline{\alpha} \underline{f}^I \\ &= A_s X_s + B_s U + \underline{f}_s \end{aligned} \tag{6.57}$$

With the original feedback matrix given by

$$A^I = \begin{bmatrix} a_{11} & a_{12} & \cdots & a_{1i} & \cdots & a_{1n} \\ a_{21} & a_{22} & \cdots & a_{2i} & \cdots & a_{2n} \\ & & \cdot & & \cdot & \\ & & \cdot & & \cdot & \\ & & \cdot & & \cdot & \\ a_{i1} & a_{i2} & \cdots & a_{ii} & \cdots & a_{in} \\ & & \cdot & & \cdot & \\ & & \cdot & & \cdot & \\ & & \cdot & & \cdot & \\ a_{n1} & a_{n2} & \cdots & a_{ni} & \cdots & a_{nn} \end{bmatrix} \tag{6.58}$$

the corresponding scaled feedback matrix is

$$A_s = \begin{bmatrix} a_{11} & \frac{\alpha_1}{\alpha_2} a_{12} & \cdots & \frac{\alpha_1}{\alpha_i} a_{1i} & \cdots & \frac{\alpha_1}{\alpha_n} a_{1n} \\ \frac{\alpha_2}{\alpha_1} a_{21} & a_{22} & \cdots & \frac{\alpha_2}{\alpha_i} a_{2i} & \cdots & \frac{\alpha_2}{\alpha_n} a_{2n} \\ \vdots & \vdots & & \vdots & & \vdots \\ \frac{\alpha_i}{\alpha_1} a_{i1} & \frac{\alpha_i}{\alpha_2} a_{i2} & \cdots & a_{ii} & \cdots & \frac{\alpha_i}{\alpha_n} a_{in} \\ \vdots & \vdots & & \vdots & & \vdots \\ \frac{\alpha_n}{\alpha_1} a_{n1} & \frac{\alpha_n}{\alpha_2} a_{n2} & \cdots & \frac{\alpha_n}{\alpha_i} a_{ni} & \cdots & a_{nn} \end{bmatrix} \tag{6.59}$$

Here, it is noted that the diagonal elements remain unchanged while the off-diagonal elements can be adjusted as needed through the use of appropriate scale factors.

The scale factors and an approximation used to improve the numerical characteristics of the excitation system feedback matrix will now be discussed. An observation can be made pertaining to the diagonal element a_{11} ($= \frac{-1}{T_r}$) of A^I. It is relatively large as T_r, the rectifier time constant is relatively low. Moreover, no amount of state variable scaling can change the value of this diagonal element. An examination of the excitation system model, however, reveals that the first state variable V_y lags the generator terminal voltage E_t by the small time constant T_r only. Thus, treating the variable ΔV_y as a measured input to to the state estimator (equal to ΔE_t) instead of a state variable appears to be a good approximation. The measurement and approximation errors intro-

duced by this step may be modelled as part of the state disturbances. Moreover, the order of the state estimator will be reduced (n = 3 instead of n = 4).

An observability analysis was performed on the fourth-order excitation system in the previous section. Since assuming $\Delta V_y = \Delta E_r$ amounts to making an additional measurement on the same excitation system, the third-order model of Eqs.(6.60)-(6.61) remains observable.

Non-unity scale factors were used to bring the non-zero elements of the feedback matrix within an order of magnitude from each other. Treating ΔV_y as a measured input and enforcing a renumbering of state variables and scale factors, the equations assumed in the design of the state estimator for the excitation system are

$$\dot{X} = AX + BU + f \tag{6.60}$$

$$Z = HX \tag{6.61}$$

The state vector is

$$X = [\alpha_1 \Delta V_r \;\; \alpha_2 \Delta V_z \;\; \alpha_3 \Delta E_{fd}]^T \tag{6.62}$$

with

$$\alpha_1 = 1.0 \quad , \alpha_2 = 100.0 \quad , \alpha_3 = 1.0 \tag{6.63}$$

The measurement vector is a scalar given by

$$Z = \Delta E_{fd} \tag{6.64}$$

Thus, the measurement matrix is given simply by

$$H = [0 \;\; 0 \;\; 1]^T \tag{6.65}$$

The modified feedback matrix is given by the equation

$$A = \underline{\alpha} A^{O} \underline{\alpha}^{-1} \tag{6.66}$$

where

$$\underline{\alpha} = \begin{bmatrix} \alpha_1 & 0 & 0 \\ 0 & \alpha_2 & 0 \\ 0 & 0 & \alpha_3 \end{bmatrix} \tag{6.67}$$

$$A^{O} = \begin{bmatrix} a_{22} & a_{23} & 0 \\ a_{32} & a_{33} & a_{34} \\ a_{42} & 0 & a_{44} \end{bmatrix} \tag{6.68}$$

The non-zero entries of A^{o} are identical to those of A^{I} shown in equation Eq.(6.43). The control input signal is assumed known to the estimator. Moreover, measurements on the generator terminal voltage magnitude are assumed to be available and equal to V_s (i.e., $\Delta V_s = \Delta E_t$). Thus,

$$\underline{U} = [V_s \;\; \Delta E_t]^T \tag{6.69}$$

The control matrix is therefore

$$\underline{B} = \begin{bmatrix} b_{IN} & b_{IN} \\ 0 & 0 \\ 0 & 0 \end{bmatrix} \tag{6.70}$$

where

$$b_{IN} = -\alpha_1 \frac{K_a}{T_a} \tag{6.71}$$

The residual vector $\underline{f}$ represents the higher-order terms in the Taylor's Series expansion of the nonlinear excitation system equations and inaccuracies in the computed feedback matrix due to changes in the operating point of the excitation system. It is determined in real time by subtracting from the known time derivatives of the state variables (based on the current value of the vector estimate) the corresponding terms determined by the linearized matrices.

Discrete-Time Equations. The next step in the determination of an appropriate filter gain matrix is the discretization in time of the continuous-time differential equations. This is accomplished through the application of Eqs.(6.5) to (6.10) to the continuous-time matrices of Eq.(6.60). It is pointed out at this point that if random state disturbances are present in the state equations, then the residual vector itself is a random quantity. This matter will be discussed next.

The deterministic continuous-time equations corresponding to the scaled variables of Eqs.(6.60)-(6.61), upon discretization in time as indicated by Eqs.(6.3)-(6.10), result in

$$\underline{X}(k+1) = \underline{\Phi X}(k) + \underline{\Psi U}(k) + \underline{\Gamma f}(k) \tag{6.72}$$

$$\underline{Z}(k+1) = \underline{H X}(k+1) \tag{6.73}$$

In the presence of random state disturbances and measurement noise,

$$\underline{X}(k+1) = \underline{\Phi X}(k) + \underline{\Psi U}(k) + \underline{\Gamma f}(k) + \underline{w}(k) \tag{6.74}$$

$$\underline{Z}(k+1) = \underline{H X}(k+1) + \underline{v}(k) \tag{6.75}$$

In the equations above, $\underline{w}(k)$ and $\underline{v}(k)$ are zero-mean gaussian random disturbances assumed to exist in the physical excitation system and field voltage measurement equipments. The random number $\underline{w}(k)$ also represents in part the small time-discretization errors introduced by Eqs.(6.8)-(6.10). These equations show the transition matrices to be exactly equal to their corresponding infinite series. Limitations imposed by actual computing devices, however, prevents this exact computations to be carried out. Moreover, the computation of Γ, the residual transition matrix, assumed a constant value of $\underline{f}(k)$ between t_k and t_{k+1}, which is not true for the corresponding continuous-time system. The random number $\underline{v}(k)$ represents the measurement noise that is expected to exist for any measurement device.

In the simulations, each of the nine excitation systems is assumed to have its own state estimator. The state disturbance covariance matrix is defined as

$$\begin{aligned} E[\underline{w}(k)\underline{w}^T(k)] &= \underline{Q} \\ E[\underline{w}(k)\underline{w}^T(k)] &= \Gamma \underline{Q} \Gamma^T \end{aligned} \tag{6.76}$$

and the measurement noise covariance matrix as

$$\underline{R} = E[\underline{v}(k)\underline{v}^T(k)] \tag{6.77}$$

Moreover,

$$\begin{aligned} \underline{J}_f &= E\left\{[\underline{\Gamma}\hat{\underline{f}}(k) - \underline{\Gamma}\underline{f}(k)][\underline{\Gamma}\hat{\underline{f}}(k) - \underline{\Gamma}\underline{f}(k)]^T\right\} \\ &= \underline{\Gamma}E\left\{[\hat{\underline{f}}(k) - \underline{f}(k)][\hat{\underline{f}}(k) - \underline{f}(k)]^T\right\}\underline{\Gamma}^T \end{aligned} \tag{6.78}$$

as shown earlier.

The simulation program assumed time-invariant and identical $\underline{Q}$'s and $\underline{J}$'s for all of the nine excitation systems. These were the diagonal and positive-definite matrices

$$\underline{Q} = \frac{1}{2}\begin{bmatrix} 1.0 \times 10^{-2} & 0 & 0 \\ 0 & 1.0 \times 10^{-2} & 0 \\ 0 & 0 & 3.0 \times 10^{-2} \end{bmatrix} \tag{6.79}$$

and

$$\underline{J}_f = \underline{\Gamma}\underline{Q}\underline{\Gamma}^T \tag{6.80}$$

i.e., it was assumed that

$$E\{[\hat{\underline{f}} - \underline{f}][\hat{\underline{f}} - \underline{f}]^T\} = \underline{Q} \tag{6.81}$$

Thus, the components of $\underline{w}(k)$ are assumed to be statistically independent of each other. Since only one measurement is performed for each excitation system, the matrix $\underline{R}$ also

contains only one element. Assumed values of measurement standard deviations for each of the nine excitation systems corresponded to about 4.5 per cent of the prefault large-signal field voltage per-unit value. Denoting this standard deviation by σ_{zi} for the ith generator and the element of $\underline{R}$ by σ_{zi}^2, the assumed measurement noise levels are

$$\sigma_{z1} = 8.9245 \times 10^{-2}$$

$$\sigma_{z2} = 1.1492 \times 10^{-1}$$

$$\sigma_{z3} = 1.1186 \times 10^{-1}$$

$$\sigma_{z4} = 1.0820 \times 10^{-1}$$

$$\sigma_{z5} = 1.4932 \times 10^{-1} \qquad (6.82)$$

$$\sigma_{z6} = 1.1096 \times 10^{-1}$$

$$\sigma_{z7} = 1.0674 \times 10^{-1}$$

$$\sigma_{z8} = 1.0127 \times 10^{-1}$$

$$\sigma_{z9} = 1.0624 \times 10^{-1}$$

As shown in the state estimate Eqs.(6.11) and (6.12), the predicted state estimate $\underline{X}(k+1\,|\,k)$ makes use of the present estimate $\underline{X}(k\,|\,k)$, the known input to the state estimator $\underline{U}(k)$ and a random residual vector $\hat{\underline{f}}(k)$. This residual vector is computed in real-time as

$$\hat{\underline{f}}(k) = \dot{\hat{X}}(t_k) - A\hat{X}(k \mid k) - \underline{BU}(k) \tag{6.83}$$

The derivative estimate $\dot{\hat{X}}(t_k)$ is computed using the continuous-time Eqs.(6.60)-(6.61) with $\underline{X}(t) = \hat{X}(k \mid k)$. Thus, the mean value of $\hat{\underline{f}}(k)$ is equal to $\underline{f}(t_k)$ and is non-zero.

Later in this chapter, results of simulated state estimation on the nine excitation systems of the test system using the assumed third-order model will be presented.

Kalman Filtering on a Speed-Governing System

The continuous-time differential equations of a third-order speed governor are shown in Chapter 4. Measurements on any of these three state variables will not be assumed thus ruling out the design of a third-order state estimator. This dilemma, however, can be resolved by incorporating one of the swing equations into the speed-governor equations and designing a fourth-order state estimator. The additional state variable in this scheme is the rotor speed with respect to a synchronously rotating frame of reference. It will also be assumed to be the measured quantity.

Thus, the initial system of equations to be considered for the state estimator would be

$$\dot{P}_W = \frac{1}{T_1}(C_G\omega - P_W) \tag{6.84}$$

$$\dot{P}_{GV} = \frac{1}{T_3}(P_S + P_{OG} - P_W - P_{GV}) \tag{6.85}$$

In cases where P_{GV} is at its upper or lower limit,

$$\dot{P}_{GV} = 0 \tag{6.86}$$

Physical constraints are also imposed on the time rate of change of P_{GV}. At these operating points, the time rate is constant, i.e.

$$\dot{P}_{GV} = \dot{P}_{GV}^{UP} \tag{6.87}$$

or

$$\dot{P}_{GV} = \dot{P}_{GV}^{DOWN} \tag{6.88}$$

whichever is applicable.

$$\dot{P}_{MECH} = \frac{1}{T_{CH}}(P_{GV} - P_{MECH}) \tag{6.89}$$

$$\dot{\omega} = \frac{1}{M}(P_{MECH} - P_E) - \frac{D}{M}(\omega - \omega_{qc}) \tag{6.90}$$

where ω_{qc} is the system center-of-angle. In matrix form,

$$\dot{X}^I = A^I X^I + B^I U + f^I \tag{6.91}$$

$$Z^I = H^I X^I \tag{6.92}$$

The equations above do not include the state disturbances and measurement noise which must be accounted for in the computation of the filter gain matrix. This simplification is justified in the early part of this section as the use of the deterministic equations above do not affect the subsequent observability analysis. Here, the residual vector $\underset{\sim}{f}^I$ is non-zero only for the cases where P_{GV} or its derivative assume their ceiling values and where the effective system frequency ω_{qc} is not equal to the system synchronous frequency. Otherwise, it will be shown shortly that the speed-governor model is basically linear if the electric power output is treated as a measured input to the estimator. In the equations above,

$$\underset{\sim}{X}^I = [\Delta P_W \;\; \Delta P_{GV} \;\; \Delta P_{MECH} \;\; \omega]^T \tag{6.93}$$

$$Z^I = \omega = [0 \;\; 0 \;\; 0 \;\; 1]\underset{\sim}{X}^I \tag{6.94}$$

$$\underset{\sim}{U} = [P_s \;\; \Delta P_E]^T \tag{6.95}$$

$$\underset{\sim}{A}^I = \begin{bmatrix} \frac{-1}{T_1} & 0 & 0 & \frac{C_G}{T_1} \\ \frac{-1}{T_3} & \frac{-1}{T_3} & 0 & 0 \\ 0 & \frac{1}{T_{CH}} & \frac{-1}{T_{CH}} & 0 \\ 0 & 0 & \frac{1}{M} & \frac{-D}{M} \end{bmatrix} \tag{6.96}$$

$$\underline{B}^I = \begin{bmatrix} 0 & 0 \\ \frac{1}{T_3} & 0 \\ 0 & 0 \\ 0 & \frac{-1}{M} \end{bmatrix} \tag{6.97}$$

$$H^I = [0 \ 0 \ 0 \ 1] \tag{6.98}$$

P_r is the known control input signal to the speed governor. ΔP_E may be computed from the results of (phasor) measurements on the generator terminals (voltage and current magnitudes and angles) or measured directly using present measuring devices. Moreover, ω, the relative speed of the generator rotor with respect to the synchronous system frequency can also be measured using phasor measurement technology.

Observability Analysis. The matrix pair (A^I, H^I) must satisfy the observability criterion before a fourth-order state estimator based on Eqs.(6.84)-(6.92) can be designed. Since n = 4 and q = 1 in this case, it is sufficient to establish that the observability matrix M is nonsingular where

$$M = [H^{IT} \ (A^{IT})H^{IT} \ (A^{IT})^2 H^{IT} \ (A^{IT})^3 H^{IT}] \tag{6.99}$$

Following the same general procedure of the preceding section,

$$A^I = \begin{bmatrix} a_{11} & 0 & 0 & a_{14} \\ a_{21} & a_{22} & 0 & 0 \\ 0 & a_{32} & a_{33} & 0 \\ 0 & 0 & a_{43} & a_{44} \end{bmatrix} \tag{6.100}$$

where the A_{ij}'s denote the nonzero elements of A^I. Also,

$$(A^{IT})^2 = \begin{bmatrix} b_{11} & b_{12} & b_{13} & 0 \\ 0 & b_{22} & b_{23} & b_{24} \\ b_{31} & 0 & b_{33} & b_{34} \\ b_{41} & b_{42} & 0 & b_{44} \end{bmatrix} \tag{6.101}$$

$$(A^{IT})^3 = \begin{bmatrix} c_{11} & c_{12} & c_{13} & c_{14} \\ c_{21} & c_{22} & c_{23} & c_{24} \\ c_{31} & c_{32} & c_{33} & c_{34} \\ c_{41} & c_{42} & c_{43} & c_{44} \end{bmatrix} \tag{6.102}$$

The b_{ij}'s and c_{ij}'s denote elements which are not necessarily zero. Therefore,

$$\underline{M} = \begin{bmatrix} 0 & 0 & 0 & c_{14} \\ 0 & 0 & b_{24} & c_{24} \\ 0 & a_{43} & b_{34} & c_{34} \\ 1 & a_{44} & b_{44} & c_{44} \end{bmatrix} \tag{6.103}$$

where

$$\begin{aligned} b_{24} &= a_{32}a_{43} \\ c_{14} &= b_{13}a_{43} \\ b_{13} &= a_{21}a_{32} \end{aligned} \tag{6.104}$$

The determinant of the matrix $\underline{M}$ is therefore

$$\begin{aligned}\det \underline{M} &= (-1)(a_{43})(-b_{24})(c_{14}) = a_{43}b_{24}c_{14} \\ &= (a_{43})(a_{32}a_{43})(b_{13}a_{43}) = a_{43}a_{32}a_{43}a_{21}a_{32}a_{43} \\ &= (a_{43})^3(a_{32})^2(a_{21})\end{aligned} \tag{6.105}$$

Using the known values of the initial feedback matrix,

$$\det \underline{M} = \left(\frac{1}{M}\right)^3\left(\frac{1}{T_{CH}}\right)^2\left(\frac{-1}{T_3}\right) \tag{6.106}$$

Thus, $\underline{M}$ is nonsingular and the speed-governing system state variables are observable from the speed measurements (assuming that P_r, ΔP_E, and f' are known).

Scaling of Variables. The following continuous-time equations are to be used by the state estimator of the speed-governor to improve the numerical characteristics of the feedback matrix.

$$\dot{\underline{X}} = \underline{A}\underline{X} + \underline{B}\underline{U} + \underline{f} \tag{6.107}$$

$$\underline{Z} = \underline{H}\underline{X} \tag{6.108}$$

The state vector is given by

$$\underline{X} = \underline{\alpha}\underline{X}^I \tag{6.109}$$

where

$$\underline{\alpha} = \begin{bmatrix} \alpha_1 & 0 & 0 & 0 \\ 0 & \alpha_2 & 0 & 0 \\ 0 & 0 & \alpha_3 & 0 \\ 0 & 0 & 0 & \alpha_4 \end{bmatrix} \tag{6.110}$$

The scale factors used are

$$\alpha_1 = 1.0 \ , \alpha_2 = 1.0 \ , \alpha_3 = 1.0 \ , \alpha_4 = 40.0 \tag{6.111}$$

The measured output for the estimator is

$$Z = \alpha_4 \omega \tag{6.112}$$

The scaled residual vector is

$$\underline{f} = \underline{\alpha} \underline{f}^I \tag{6.113}$$

Finally, the scaled matrices are

$$A = \underline{\alpha} A^I \underline{\alpha}^{-1} \tag{6.114}$$

$$B = \underline{\alpha} B^I \tag{6.115}$$

$$H = [0 \quad 0 \quad 0 \quad 1] = H^I \tag{6.116}$$

A discussion parallel to the previous section will now be followed. The continuous-time Eqs.(6.107)-(6.108) can be discretized in time, with random state disturbances and measurement noise introduced as

$$\underline{X}(k+1) = \underline{\Phi X}(k) + \underline{\Psi U}(k) + \underline{\Gamma f}(k) + \underline{w}(k) \tag{6.117}$$

$$\underline{Z}(k+1) = \underline{H X}(k+1) + \underline{v}(k) \tag{6.118}$$

The covariance matrices are defined as

$$\underline{Q} = E[\underline{w}(k)\underline{w}^T(k)] \tag{6.119a}$$

$$\underline{R} = E[\underline{v}(k)\underline{v}^T(k)] \tag{6.119b}$$

$$\underline{J}_f = \underline{\Gamma} E\left\{[\underline{\hat{f}}(k) - \underline{f}(k)][\underline{\hat{f}}(k) - \underline{f}(k)]^T\right\}\underline{\Gamma}^T \tag{6.119c}$$

Actual numerical values used in the simulations were

$$\underline{Q} = \begin{bmatrix} 1.0 \times 10^{-4} & 0 & 0 & 0 \\ 0 & 1.0 \times 10^{-3} & 0 & 0 \\ 0 & 0 & 1.0 \times 10^{-3} & 0 \\ 0 & 0 & 0 & 4.0 \times 10^{-5} \end{bmatrix} \tag{6.120}$$

$$\underline{R} = [5.2915 \times 10^{-3}] \tag{6.121}$$

$$J_f = \underline{0} \tag{6.122}$$

Use of a diagonal positive-definite matrix for $\underline{Q}$ once more assumes statistical independence between the components of the state disturbance vector $\underline{w}(k)$. The assumed covariance $\underline{R}$ of rotor speed measurements corresponds to a standard deviation of about 0.008 Hertz when the scale and conversion factors are both taken into account.

Results of simulated state estimation on the 9 speed-governing systems of the test system will be presented later in this chapter.

State Estimator Simulation Results

The results of the previous sections of this chapter are incorporated in the simulation program of Chapters 4 and 5 to test the behavior of the state estimator. Although the controller itself is centralized in function, smaller decentralized estimators (one for each excitation system and each speed governor system) have been designed to operate independently of each other. This is possible because an underlying assumption in the controller implementation is the availability of phasor measurement systems that measure power system state variables (generator terminal voltage and current phasors, internal machine voltage phasors, rotor speeds). Field voltage measurement schemes are also assumed.

A component of the centralized controller state vector corresponding to generator "i" is given by

$$X_i = \begin{bmatrix} \Delta E'_{qi} \\ \Delta\delta_{qi} - \Delta\delta_{q10} \\ \omega_i - \omega_{10} \\ \Delta V_{yi} \\ \Delta V_{ri} \\ \Delta V_{zi} \\ \Delta E_{fdi} \\ \Delta P_{Wi} \\ \Delta P_{GV,i} \\ \Delta P_{MECH,i} \end{bmatrix} \tag{6.123}$$

The first three state variables are made available either directly or indirectly by the phasor measurements. The next four variables belong to the ith excitation system and are estimated using the procedure presented in the section "Kalman Filtering on an Excitation System". The last three, together with the rotor speed ω_i which acts as a measured state, belong to the ith speed governing system and are estimated using a similar filtering algorithm.

The last two sections dealt with the continuous-time equations assumed by each of the Kalman filters. Scaled variables were defined and used to improve the numerical properties of the recursive computations. Observability of the defined states from the assumed measurements have also been established for the corresponding continuous-time equations. The existence of zero-mean gaussian random state disturbances and measurement noise were implicitly assumed although the equations were expressed in a deterministic way to carry out the observability analysis. Discretization of the continuous-time equations for the scaled variables then followed. Assumed state disturbance and measurement noise levels were also given. The computed steady-state filter

gain matrices using the recursive formulas were then presented with numerical stability of the computations established by checking the positive-definiteness of the resulting steady-state error covariance matrices. This section will present the results of the simulation program incorporating both the controller and estimator algorithms.

Computation of the control input signals from the control law actually makes use of the estimated state variables instead of the exact state variables. Thus, for the centralized controller,

$$\underline{U} = R^{-1}B^T[\hat{\underline{g}}_S(t_k) - K_S\hat{\underline{X}}(t_k)] \tag{6.124}$$

where $\hat{\underline{X}}(t_k) = \hat{\underline{X}}(k \mid k)$ and $\hat{\underline{g}}_S(t_k)$ is computed using Eq.(5.12) with $\underline{Y}_A(t) = \underline{Y}_A(t_k)$, $\underline{s}(t) = \hat{\underline{s}}(t_k)$ and $\underline{f}(t) = \hat{\underline{f}}(t_k)$. The controller residual estimates are determined by applying Eqs.(5.14) and (5.15) again with $\underline{X}(t) = \hat{\underline{X}}(t_k)$.

The cases to be studied in this section are aimed at determining the effects of decreasing the phasor measurement rate on the combined controller-estimator. At this point, three time rates will be defined. The first, the control rate, assumed constant in all of the study cases, is the rate at which the control input signals are updated. The assumed rate here is 200 Hz. In-between the instants of time at which the control input signals are updated, they are assumed to be constant. The second, the estimation rate, is the rate at which a state estimator updates the value of its corresponding state vector estimate based on the current estimate, known values of the control input signals, and the ***most recent*** results of the phasor measurements (which may have been obtained at a much slower rate). For the study cases, the estimation rate was also chosen to be 200 Hz. The third, the measurement rate is the rate with which the synchronized phasor measurement systems obtain new measurements for the state estimators. It is the effects

of the variations of this rate which will be presented in this section. Five cases will be considered as shown on Table 6.1.

Only the cases shown above will be considered as no noticeable change in the combined controller-estimator performance was observed for small changes in measurement rates.

Figures 6.1 to 6.3 show the time behavior of some excitation system variables and their estimates and some of the field voltage measurements as the phasor measurement rate is varied from 200 Hz to 10 Hz for a typical generator. Generator terminal voltage measurements, being part of the phasor measurements, are assumed to vary at the same rate. On the other hand, the field voltage measurement rate was assumed constant at 200 Hz.

Figures 6.4 to 6.9 show the time behavior of some speed-governor state variables and their estimates as the phasor measurement rate is varied from 200 Hz to 10 Hz for a typical generator. It is seen that as the measurement rate decreases, the state estimates which actually constitute part of the feedback to the controller, are effectively time-delayed representations of the corresponding actual state variables. This causes the combined controller-estimator to introduce growing oscillations in the power system, an undesirable effect of decreased phasor measurement rate.

Conclusions

This chapter presented the results of simulating the performance of the centralized controller as affected by the independent decentralized state estimators (Kalman filters). Feedback to the controller made use of the results of the phasor measurements and the state estimators. The phasor measurements were in fact used by the state estimator themselves. Thus, the phasor measurement rate directly affected the combined controller-estimator performance.

It has been shown that as the phasor measurement rate decreased below about 20 Hz, oscillations which grow with time began to appear in the power system, getting increasingly worse as the phasor measurement rate decreased. These results may point to the inadequacy of present measurement systems with rates of about 12.5 Hz. On the other hand, satisfactory controller performance, achieved at moderately large measurement rates, may provide an incentive to the development of faster measurement systems.

Table 6.1. Variation of Phasor Measurement Rate

Case Number	Phasor Measurement Rate
1	200 Hertz
2	40 Hertz
3	20 Hertz
4	13.333 Hertz
5	10.000 Hertz

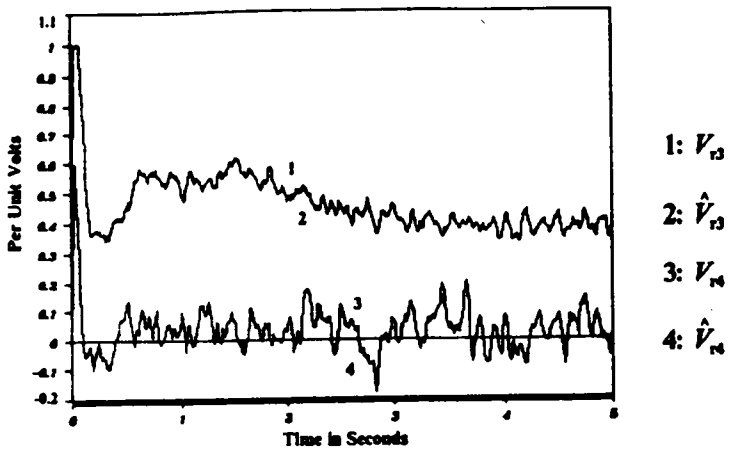

A.V_r and $\hat{V}_r$ (Generators 3 and 4)

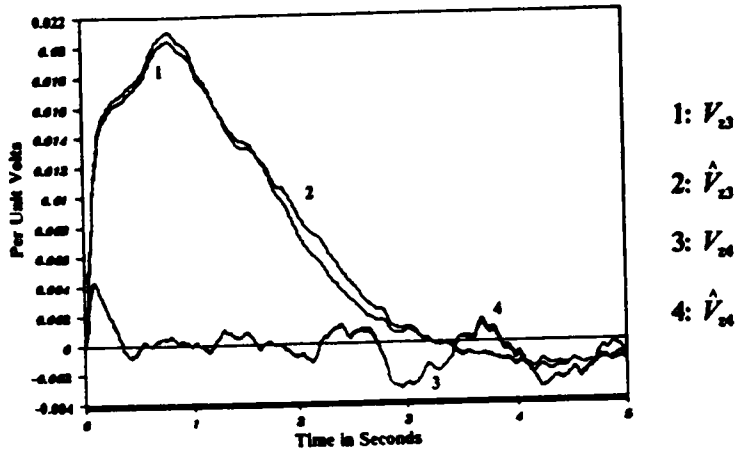

B.V_t and $\hat{V}_t$ (Generators 3 and 4)

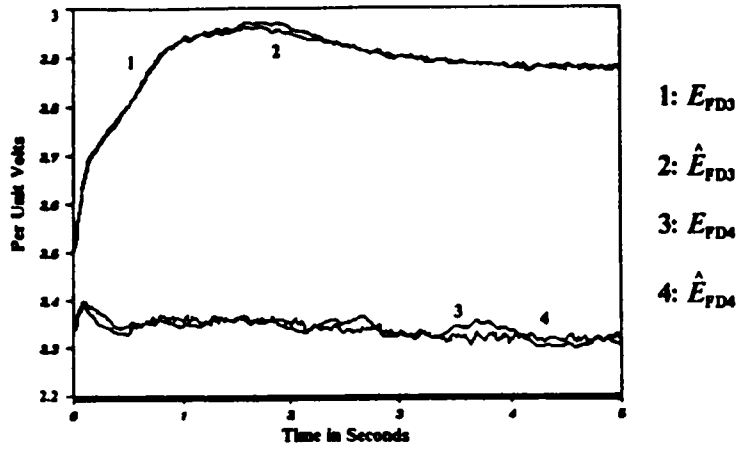

C.E_{FD} and $\hat{E}_{FD}$ (Generators 3 and 4)

Figure 6.1. Excitation System State Variables and Estimates (Case 1)

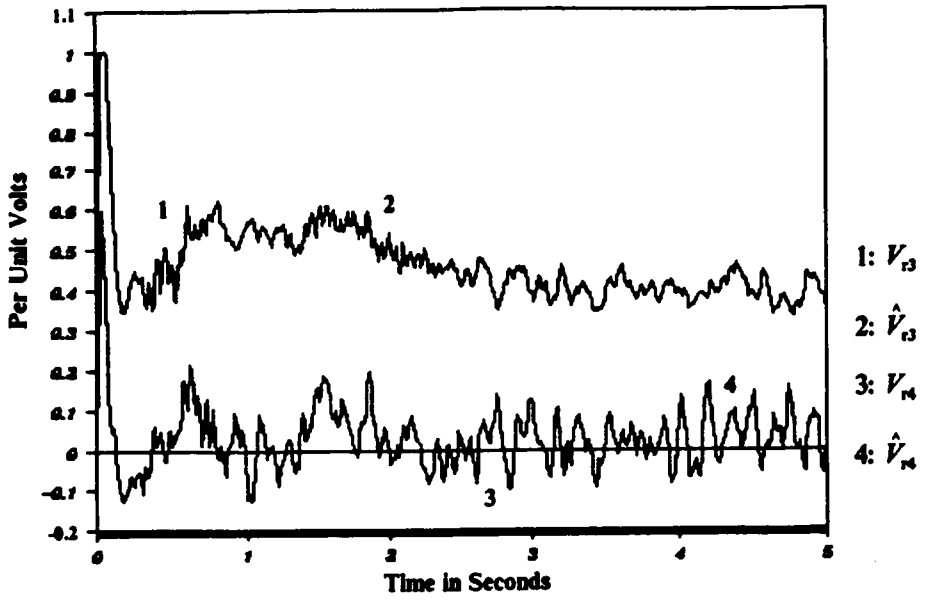

A. V_t and $\hat{V}_t$ (Generators 3 and 4)

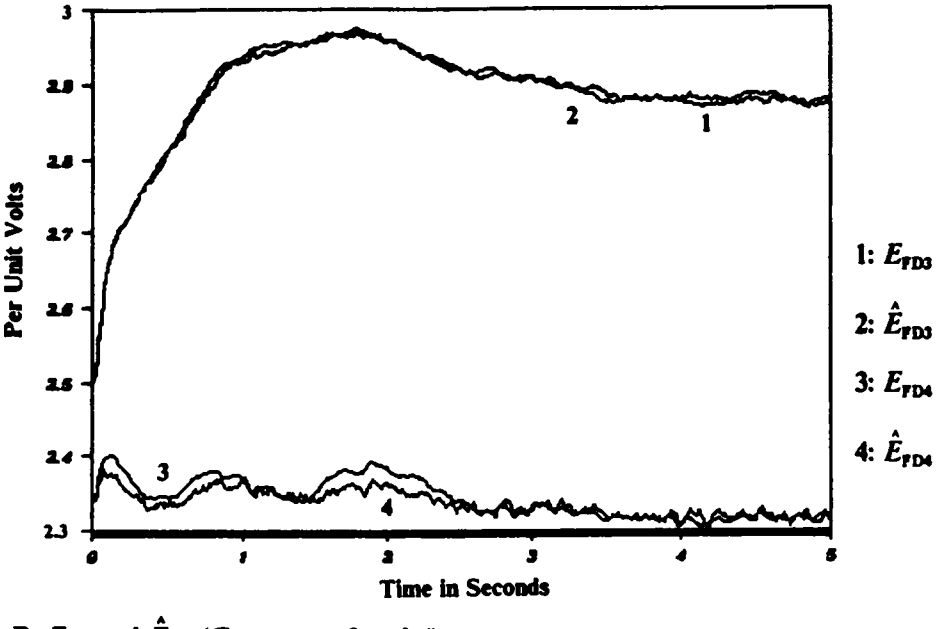

B. E_{FD} and $\hat{E}_{FD}$ (Generators 3 and 4)

Figure 6.2. Excitation System State Variables and Estimates (Case 3)

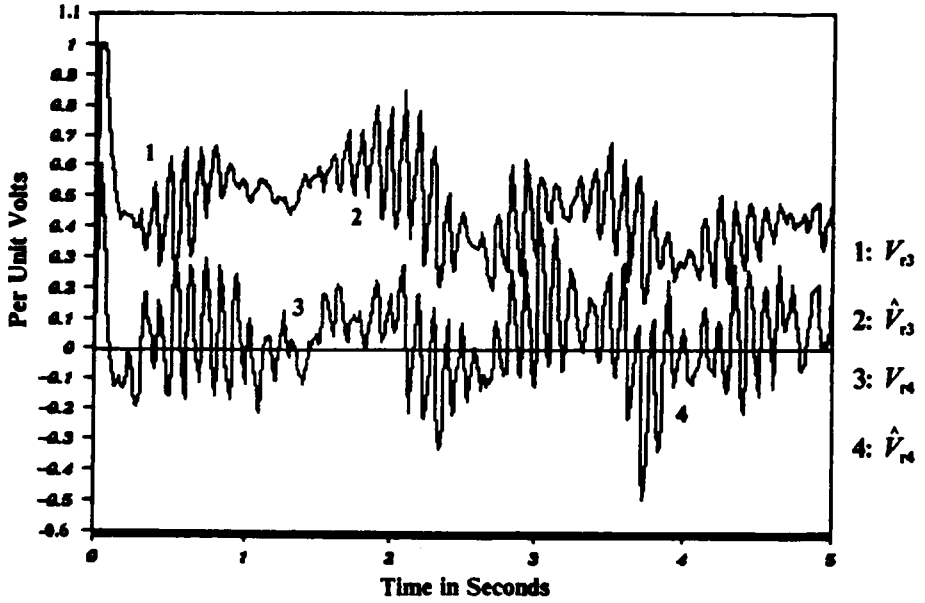

A. V_r and $\hat{V}_r$ (Generators 3 and 4)

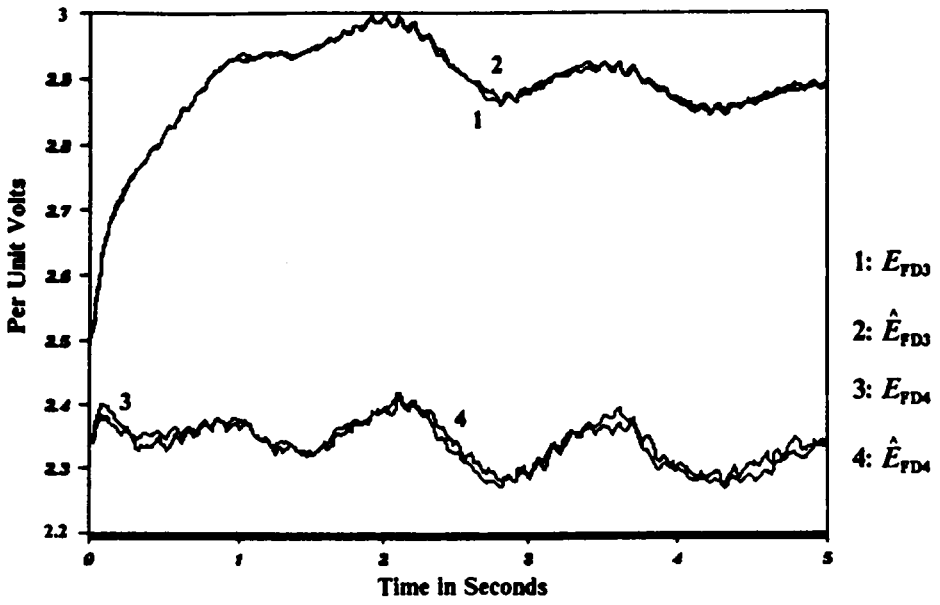

B. E_{FD} and $\hat{E}_{FD}$ (Generators 3 and 4)

Figure 6.3. Excitation System State Variables and Estimates (Case 5)

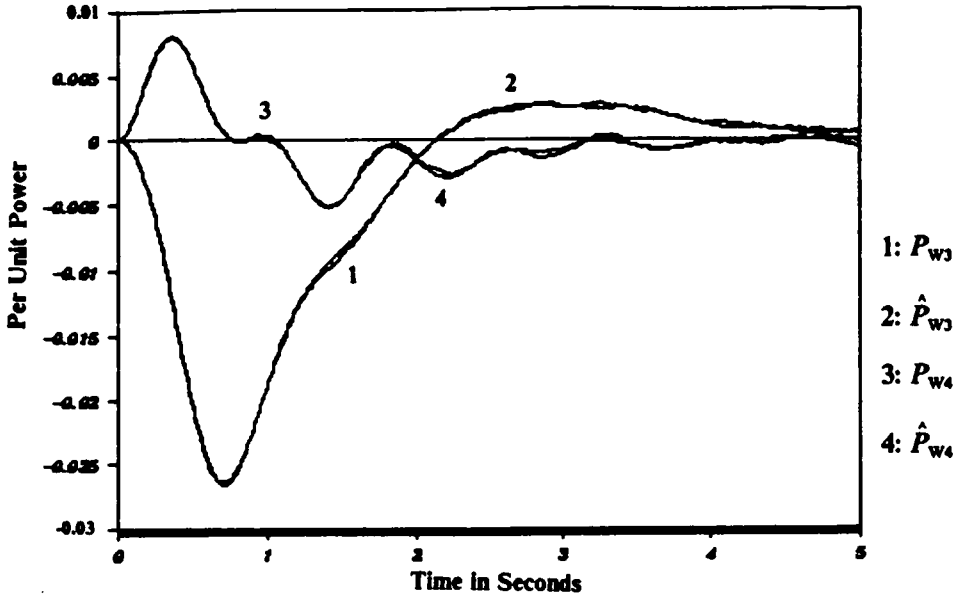

A. P_W and $\hat{P}_W$ (Generators 3 and 4)

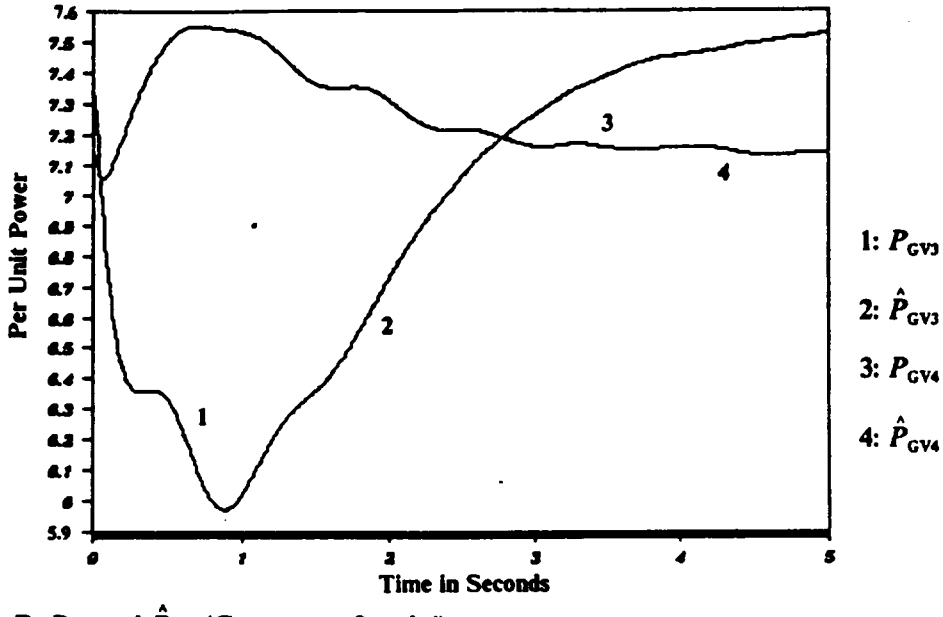

B. P_{GV} and $\hat{P}_{GV}$ (Generators 3 and 4)

Figure 6.4. Speed-Governor State Variables and Estimates (Case 1)

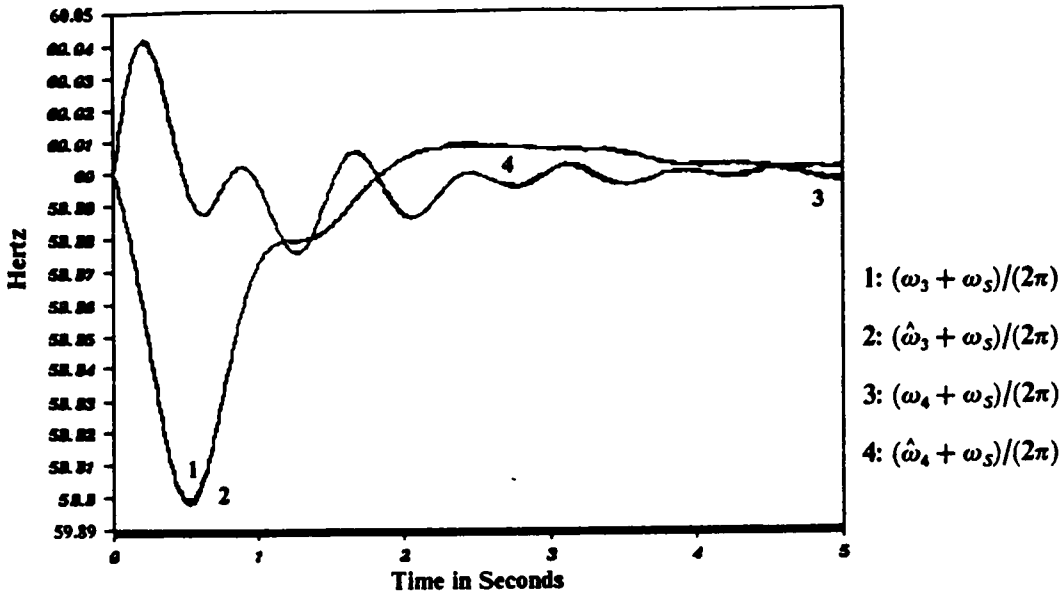

A. $(\omega + \omega_S)$ and $(\hat{\omega} + \omega_S)$ (Generators 3 and 4)

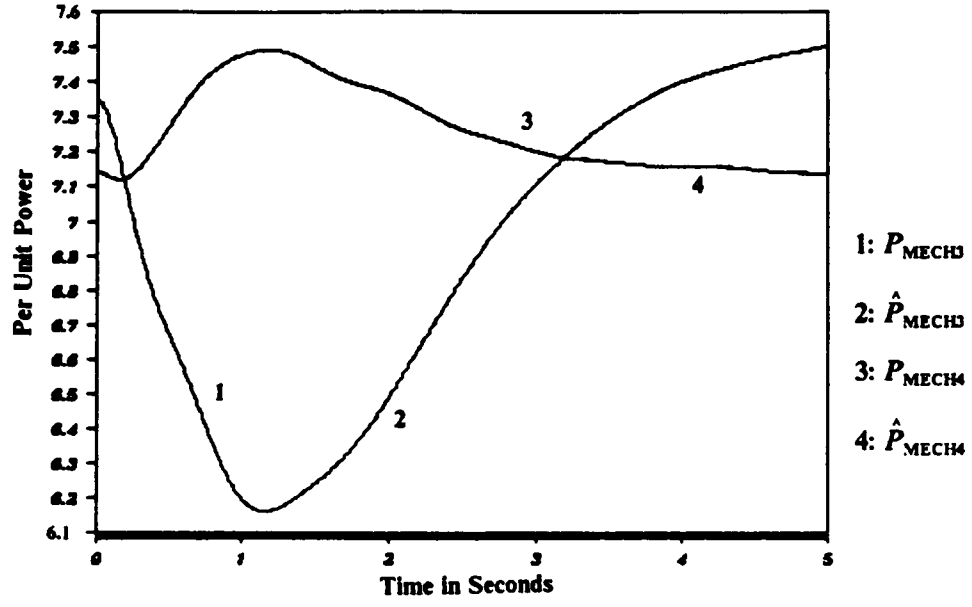

B. P_{MECH} and $\hat{P}_{MECH}$ (Generators 3 and 4)

Figure 6.5. Speed-Governor State Variables and Estimates (Case 1)

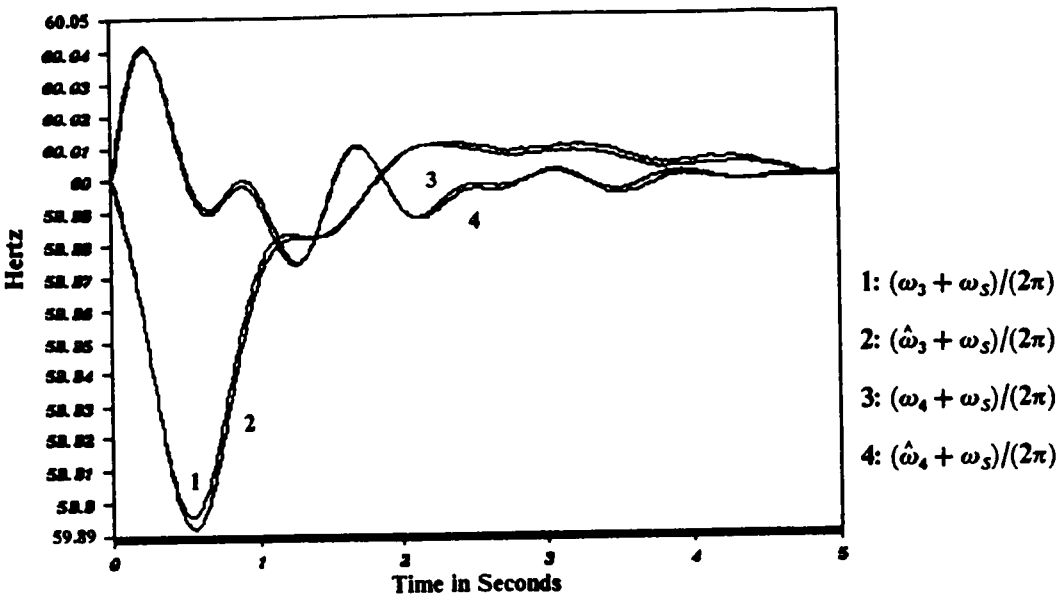

A. $(\omega + \omega_S)$ and $(\hat{\omega} + \omega_S)$ (Generators 3 and 4)

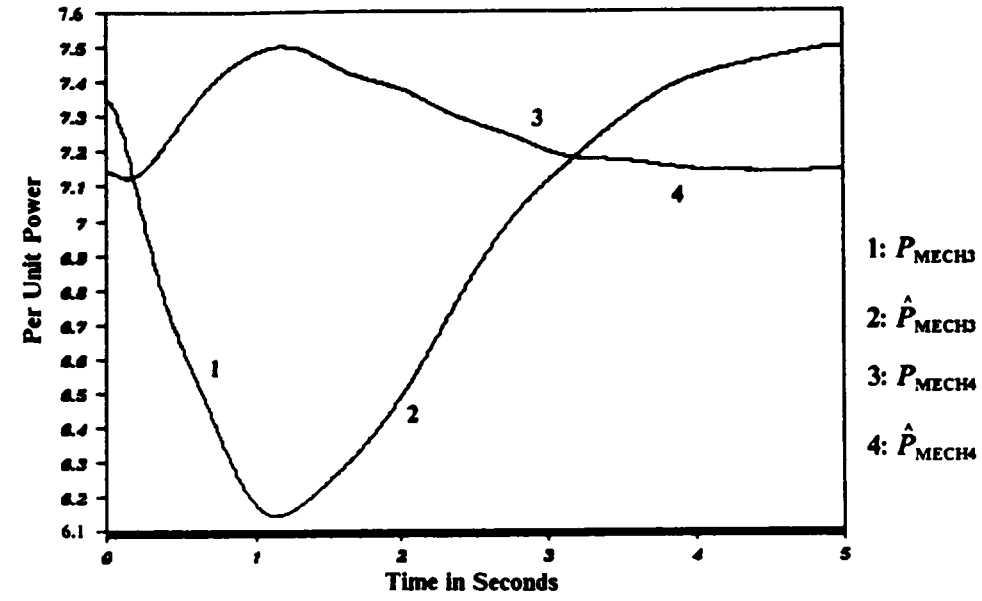

B. P_{MECH} and $\hat{P}_{MECH}$ (Generators 3 and 4)

Figure 6.6. Speed-Governor State Variables and Estimates (Case 2)

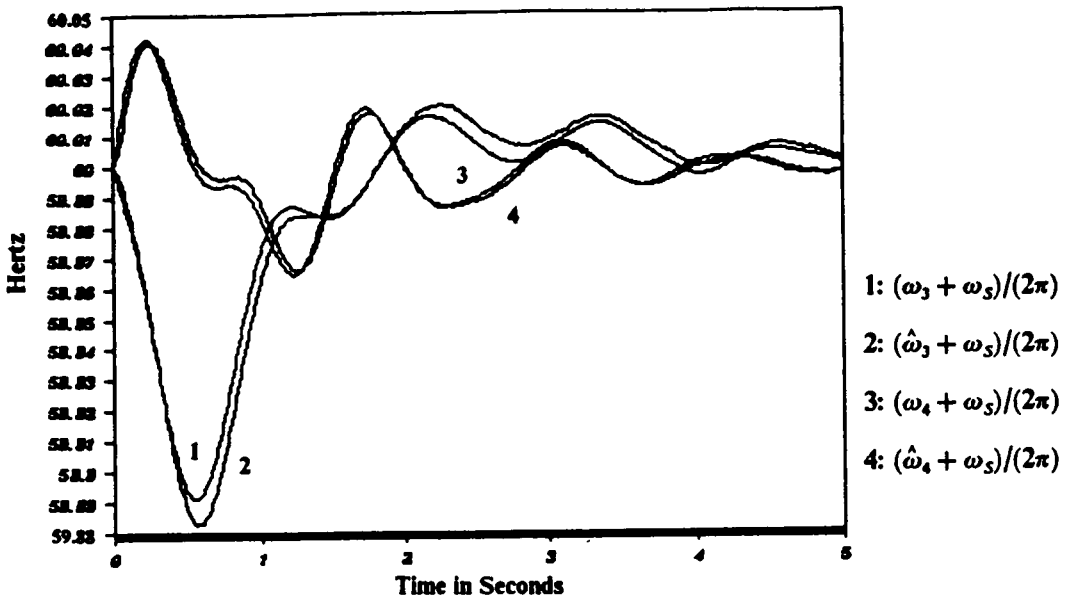

A. $(\omega + \omega_S)$ and $(\hat{\omega} + \omega_S)$ (Generators 3 and 4)

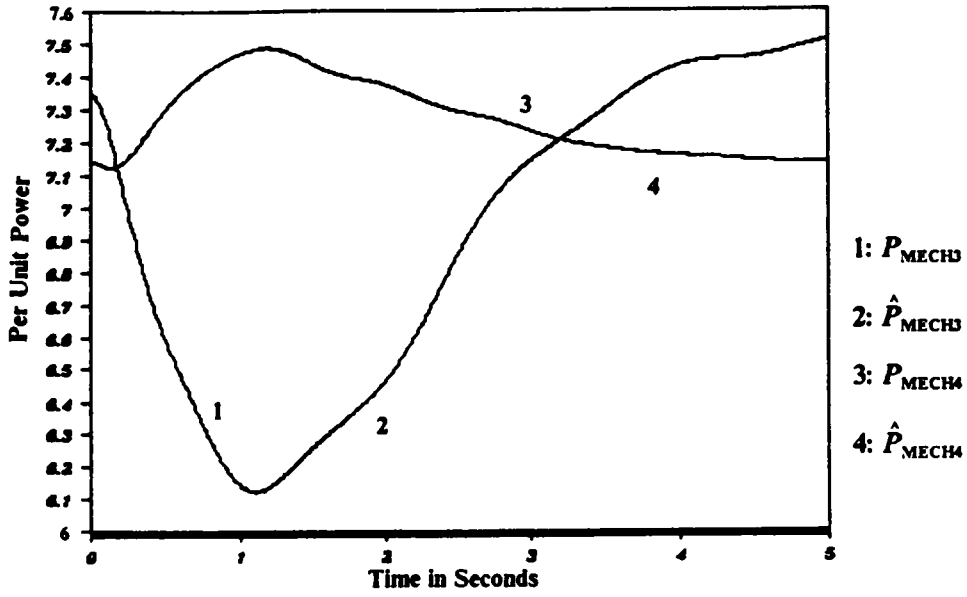

B. P_{MECH} and $\hat{P}_{MECH}$ (Generators 3 and 4)

Figure 6.7. Speed-Governor State Variables and Estimates (Case 3)

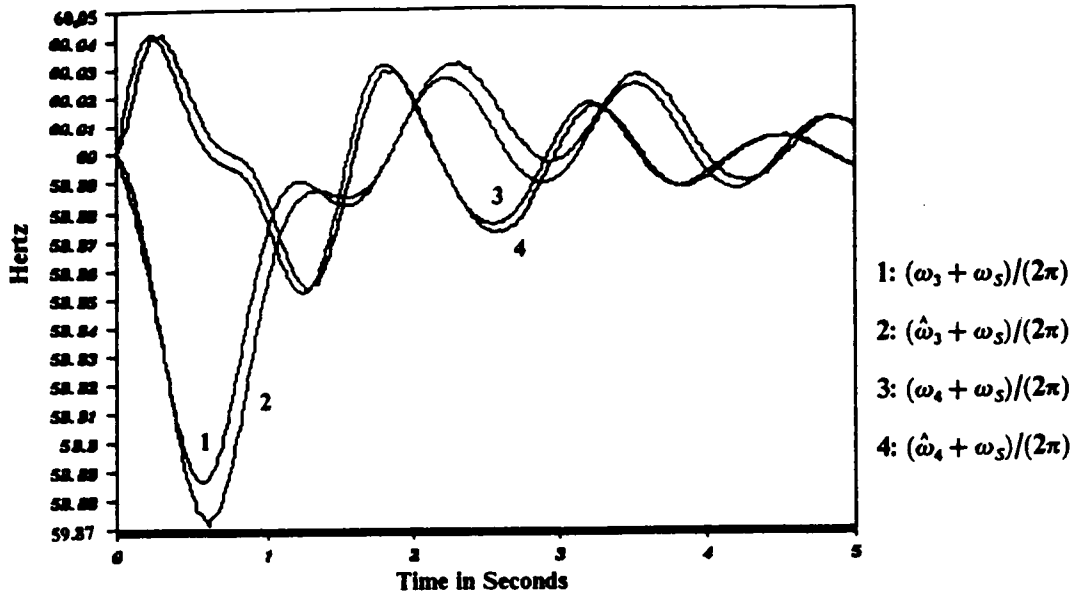

A. $(\omega + \omega_S)$ and $(\hat{\omega} + \omega_S)$ (Generators 3 and 4)

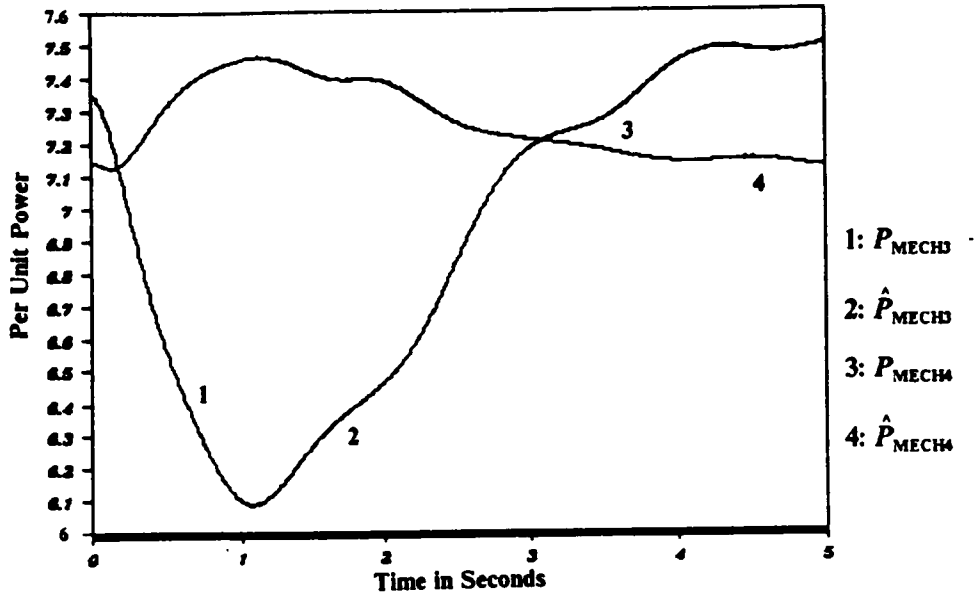

B. P_{MECH} and $\hat{P}_{MECH}$ (Generators 3 and 4)

Figure 6.8. Speed-Governor State Variables and Estimates (Case 4)

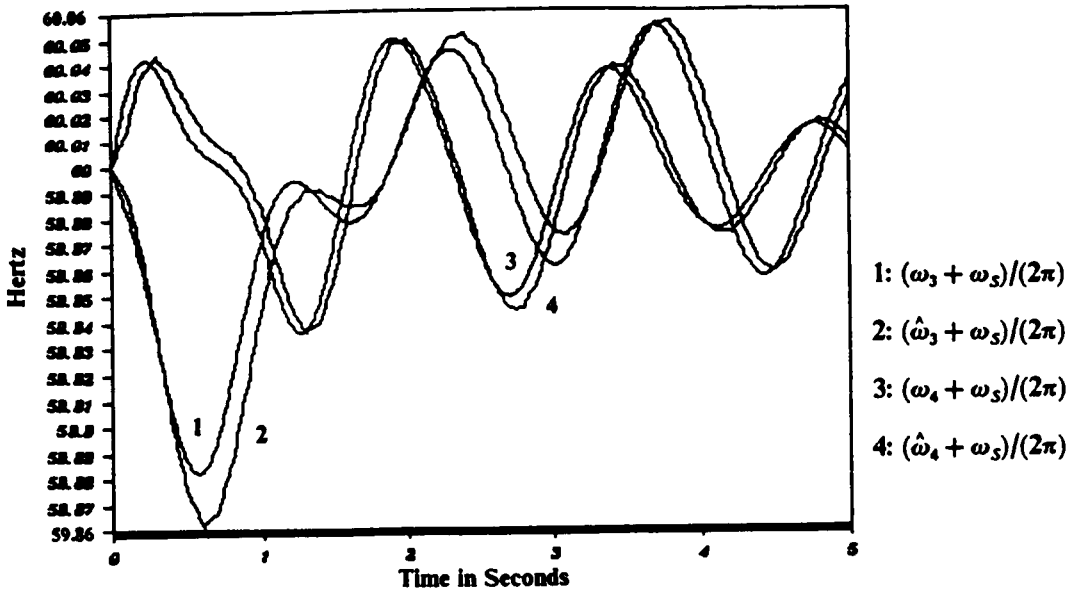

A. $(\omega + \omega_S)$ and $(\hat{\omega} + \omega_S)$ (Generators 3 and 4)

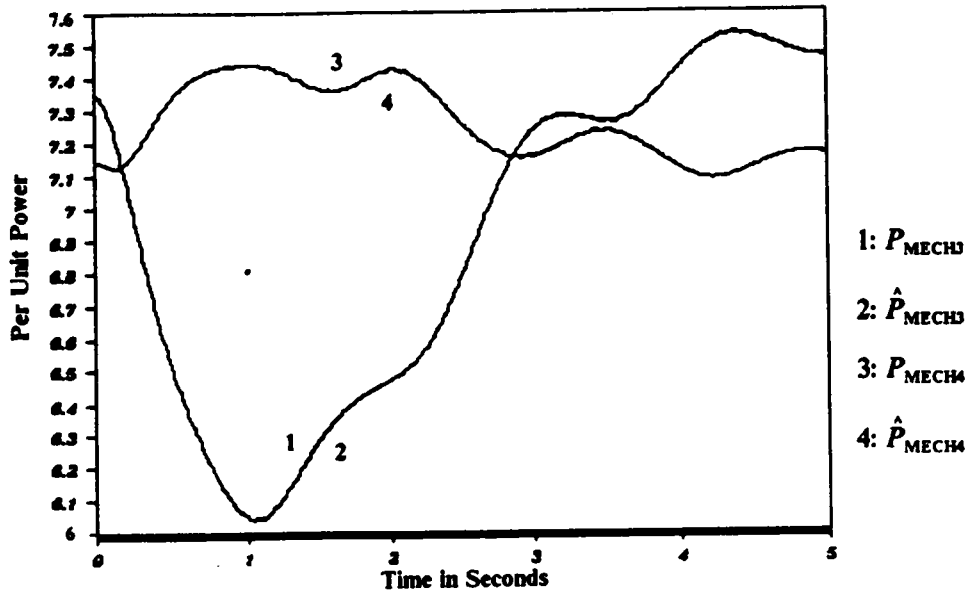

B. P_{MECH} and $\hat{P}_{MECH}$ (Generators 3 and 4)

Figure 6.9. Speed-Governor State Variables and Estimates (Case 5)

Chapter 7

Conclusions and Recommendations for Future Work

The first part of this chapter will restate some of the major conclusions of the chapters on the centralized controller and state estimators. The second and last part will be state some recommendations for future work related to the present work on optimal controllers.

From the simulation results of Chapter 5, it is concluded that the steady-state controller formulation ($t_f = \infty$) is highly acceptable especially in view of the time-invariant controller matrices.

Use of the approximate solution to the adaptive term $\underline{g}_s(t)$ shown in Eq.(5.12) which substantially reduces both the off-line and real-time computation requirements of the centralized controller, yields satisfactory controller performance.

In addition to the measurement of some power system state variables for feedback to the controller, the field voltages of the generators must also be measured as illustrated

in Case 3 (Chapter 5) where the solution to the Ricatti equation was very close to singularity.

In the presence of large state residuals, the effectiveness of the centralized controller is reduced. Control of buses away from the generators is practically impossible, and a trade-off is necessary between the controller sensitivity and its ability to reduce oscillation amplitudes in the early stages of controller operation.

Choice of elements for the weighting matrix $\underline{Q}$ (for a constant $\underline{R}$) in the cost function requires care and off-line simulation studies. Choice of very low values for $\underline{Q}$ results in poor controller performance while very large values do not necessarily improve controller performance and only makes the computation of $\underline{K}_s$ more difficult numerically.

Simulation results of Chater 6 show the need for faster phasor measurement systems. Infrequent measurements cause effective time delays to exist in the estimated and measured controller state variables, thus causing delayed feedback to the controller. The power system response gets worse as the delay increases, being characterized by undamped or even growing oscillations not present in the simulation studies of Chapter 5.

The simulation results of Chapter 6 show that the minimum requirement on the phasor measurement rate ($>$ 20Hertz) is not too far from presently existing measurement systems. Moreover, steady-state formulation (time step $k = \infty$) of the Kalman filters proved acceptable as long as the assumed process and measurement noise levels remained constant. Use of steady-state formulation has several advantages and justification :

1. Numerical instabilities can be avoided in the off-line precomputations of the filter matrices.

2. The recursion formulas yield the steady-state values after a fraction of a second.

3. Real-time computational requirements are reduced.

Recommendations for Future Work. The following recommendations are made regarding future work on optimal controllers :

1. Use of reduced-order models in the representation of power system components to minimize need for state estimators and to reduce the size of the controller.

2. Reformulation of the control problem such that the effective controller state variables are all measurable.

3. Study of the optimal centralized controller for a large AC/DC system.

4. Discrete-time formulation of the controller problem.

5. Reformulation of the control problem to include the system frequency in the output vector. This may necessitate attaching increased weights on the rotor speeds.

6. Study of controller performance subject to a more severe disturbance (e.g., one which involves "islanding" of the power system).

7. Study of estimator performance subject to time-varying state disturbance and measurement noise levels.

Bibliography

1. F.P.DeMello, C.Concordia, "Concepts of Synchronous Machine Stability as Affected by Excitation Control", *IEEE Transactions on Power Apparatus and Systems*, April 1969, pp.316-329

2. F.P.DeMello, L.N.Hannett, J.M.Undrill, "Practical Approaches to Supplementary Stabilizing from Accelerating Power", *IEEE Transactions on Power Apparatus and Systems*, Sept/Oct 1978, pp.1515-1522

3. E.V.Larsen, D.A.Swann, "Applying Power System Stabilizers, Part I: General Concepts", *IEEE Transactions on Power Apparatus and Systems*, June 1981, pp.3017-3024

4. E.V.Larsen, D.A.Swann, "Applying Power System Stabilizers, Part II: Performance Objectives and Tuning Concepts", *IEEE Transactions on Power Apparatus and Systems*, June 1981, pp.3025-3033

5. E.V.Larsen, D.A.Swann, "Applying Power System Stabilizers, Part III: Practical Considerations" , *IEEE Transactions on Power Apparatus and Systems*, June 1981, pp.3034-3046

6. K.E.Bollinger, M.V.Chapin, "Stability Tests and Tuning the PSS at Battle River Plant of Alberta Power Ltd.", *IEEE Transactions on Power Systems*, Vol.3, No.3, August 1988, pp. 956-962

7. K.E.Bollinger, A.F.Mistr, "PSS Tuning at the Virginia Electric and Power Co. Bath County Pumped Storage Plant", *IEEE Transactions on Power Systems*, Vol.4, No.2, May 1989, pp. 566-574

8. K.R.Padiyar, S.S.Prabhu, M.A.Pai, K.Gomathi, "Design of Stabilizers by Pole Assignment with Output Feedback", *Electric Power and Energy Systems*, Vol.2, July 1980, pp.140-146

9. J.H.Chow, J.J.Sanchez-Gasca, "Pole-Placement Designs of Power System Stabilizers", *IEEE Transactions on Power Systems*, Vol.4, No.1, February 1989, pp. 566-574

10. A.Ghandakly, P.Kronegger, "Digital Controller Design Method for Synchronous Generator Excitation and Stabilizer Systems , Parts I and II", *IEEE Transactions on Power Systems*, Vol.PWRS-2, No.3, August 1987, pp.633-644

11. K.Bollinger, A.Laha, R.Hamilton, T.Harras, "Power Stabilizer Design Using Root Locus Methods", *IEEE Transactions on Power Apparatus and Systems*, Sept/Oct 1975, pp.1484-1488

12. K.E.Bollinger, R.Winsor, A.Campbell, "Frequency Response Methods for Tuning Stabilizers to Damp Out Tie-Line Power Oscillations: Theory and Field Test Results", *IEEE Transactions on Power Apparatus and Systems*, Sept/Oct 1979, pp.1509-1515

13. F.P.DeMello, P.J.Nolan, T.F.Laskowski, J.M.Undrill, "Coordinated Application of Stabilizers in Multimachine Power Systems" , *IEEE Transactions on Power Apparatus and Systems*, May/June 1980, pp.892-901.

14. T.Hiyama, "Coherency-Based Identification of Optimum Site for Stabiliser Applications", *IEE Proceedings*, Vol.130, Part C, No.2, 1983, pp.71-74

15. O.H.Abdalla, S.A.Hassan, N.T.Tweig, "Coordinated Stabilization of a Multimachine Power System", *IEEE Transactions on Power Apparatus and Systems*, March 1984, pp.483-494

16. R.J.Fleming, M.A.Mohan, K.Parvatisam, "Selection of Parameters of Stabilizers in Multimachine Power Systems" , *IEEE Transactions on Power Apparatus and Systems*, May 1981, pp.2329-2333

17. H.B. Gooi, E.F. Hill, M.A. Mobarak, D.H. Thorne, T.H.Lee, "Coordinated Multi-Machine Stabilizer Settings Without Eigenvalue Drift", *IEEE Transactions on Power Apparatus and Systems*, August 1981, pp.3879-3887

18. A.Doi, S.Abe, "Coordinated Synthesis of Power System Stabilizers in Multimachine Power Systems", *IEEE Transactions on Power Apparatus and Systems*, June 1984, pp.1473-1479

19. C.M.Lim, S.Elangovan, "A New Stabilizer Design Technique for Multimachine Power Systems", *IEEE Transactions on Power Apparatus and Systems*, September 1985, pp.2393-2400

20. S.Lefebvre, "Tuning of Stabilizers in Multimachine Power Systems", *IEEE Transactions on Power Apparatus and Systems*, February 1983, pp.290-299

21. C.-L.Chen, Y.-Y.Hsu, "Coordinated Synthesis of Multimachine Power System Stabilizer Using an Efficient Decentralized Modal Control (DMC) Algorithm", *IEEE Transactions on Power Systems*, August 1987, pp.543-551

22. P.Kundur, M.Klein, G.J.Rogers, M.S.Zywno, "Application of Power System Stabilizers for Enhancement of Overall System Stability", *IEEE Transactions on Power Systems*, Vol.4, No.2, May 1989, pp. 614-626

23. D.A.Pierre, "A Perspective on Adaptive Control of Power Systems", *IEEE Transactions on Power Systems*, Vol.PWRS-2, No.2, May 1987, pp.387-396

24. J.Kanniah, O.P.Malik, G.S.Hope, "Excitation Control of Synchronous Generators Using Adaptive Regulators , Parts I and II", *IEEE Transactions on Power Apparatus and Systems*, May 1984, pp.897-910

25. S.-J.Cheng, Y.S.Chow, O.P.Malik, G.S.Hope, "An Adaptive Synchronous Machine Stabilizer", *IEEE Transactions on Power Systems*, Vol.PWRS-1, No.3, August 1986, pp.101-109

26. D.R.Romero, G.T.Heydt "An Adaptive Excitation System Controller in a Stochastic Environment" , *IEEE Transactions on Power Systems*, Vol.PWRS-1, No.1, February 1986, pp.168-175

27. O.P.Malik, G.S.Hope, S.J.Cheng, G.Hancock, " A Multi-Micro-Computer Based Dual-Rate Self-Tuning Power System Stabilizer", *IEEE Transactions on Energy Conversion*, Vol.EC-2, No.3, August 1987, pp.355-360

28. Y.-Y.-Hsu, K.-L.Liou, " Design of Self-Tuning PID Power System Stabilizers for Synchronous Generators", *IEEE Transactions on Energy Conversion*, Vol.EC-2, No.3, September 1987, pp.343-348

29. S.-J.Cheng, O.P.Malik, G.S.Hope, " Self-Tuning Stabiliser for a Multimachine Power System", *IEE Proceedings*, Vol.133, Part C, No.4, 1986, pp.176-185

30. C.-J.Wu, Y.-Y.Hsu, "Design of Self-Tuning PID Power System Stabilizer for Multimachine Power Systems", *IEEE Transactions on Power Systems*, Vol.3, No.3, August 1988, pp. 1059-1064

31. A.Chandra, O.P.Malik, G.S.Hope, "A Self-Tuning Controller for the Control of Multimachine Power Systems" , *IEEE Transactions on Power Systems*, Vol.3, No.3, August 1988, pp. 1065-1071

32. K.J.Astrom, P.Eykhoff, " System Identification - A Survey", *Automatica*, Vol.7, 1971 pp.123-162

33. D.W.Clarke, P.J.Gawthrop, " Self-Tuning Controller", *IEE Proceedings (Control & Science)*, Vol.122, No.9, Sept. 1975, pp.929-934

34. P.E.Wellstead, D.Prager, P.Zanker, "Pole Assignment Self-Tuning Regulator", *IEE Proceedings (Control & Science)*, Vol.126, No.8, August 1979, pp.781-787

35. A.Y.Allidina, F.M.Hughes, "Generalised Self-Tuning Controller with Pole Assignment", *IEE Proceedings*, Vol.127, Part D, No.1, January 1980, pp.13-18

36. N.Ramarao, D.K.Reitan, "Improvement of Power System Transient Stability Using Optimal Control: Bang-Bang Control of Reactance", *IEEE Transactions on Power Apparatus and Systems*, May/June 1970, pp.975-984

37. S.K.Biswas, N.U.Ahmed, "Optimal Voltage Regulation of Power Systems Under Transient Conditions" , *Electric Power Systems Research*, 6(1983), pp.71-77

38. S.M.Miniesy, E.V.Bohn, "Optimum Network Switching in Power Systems", *IEEE Transactions on Power Apparatus and Systems*, September/October 1970, pp.2118-2123

39. D.L.Lubkeman, G.T.Heydt, "The Application of Dynamic Programming in a Discrete Supplementary Control for Transient Stability Enhancement of Multimachine Power Systems" , *IEEE Transactions on Power Apparatus and Systems*, September 1985, pp.2342-2348

40. M.K.Musaazi, R.B.I.Johnson, B.J.Cory, "Multimachine System Transient Stability Improvement Using Transient Power System Stabilizers", *IEEE Transactions on Energy Conversion*, Vol.EC-1, No.4, December 1986, pp.34-38

41. C.D.Vournas, B.C.Papadias, "Power System Stabilization Via Parameter Optimization - Application to the Hellenic Interconnected System", *IEEE Transactions on Power Systems*, Vol.PWRS-2, No.3, August 1987, pp.615-623

42. H.A.M. Moussa, Y.-N.Yu, "Optimal Power System Stabilization Through Excitation And/Or Governor Control", *IEEE Transactions on Power Apparatus and Systems*, May/June 1972, pp. 1166-1173

43. B.Habibullah, Y.-N.Yu, "Physically Realizable Wide Power Range Optimal Controllers for Power Systems", *IEEE Transactions on Power Apparatus and Systems*, PAS-93(1974), pp. 1448-1506

44. B.Habibullah, "Optimal Governor Control of a Synchronous Machine", *IEEE Transactions on Automatic Control*, Vol.AC-26, No.2, April 1981

45. J.Y.H.Chen, G.L.Kusic, "Dynamic Stability and Excitation Control of Directly-Coupled Multimachine Systems", *IEEE Transactions on Power Apparatus and Systems*, February 1984, pp.389-397

46. O.A.Solheim, "Design of Optimal Control Systems with Prescribed Eigenvalues", *International Journal on Control*, 1972, Vol.15, No.1, pp.143-160

47. Y.-N. Yu, K.Vongsuriya, L.N.Wedman, "Application of an Optimal Control Theory to a Power System", *IEEE Transactions on Power Apparatus and Systems*, January 1970, pp. 55-62

48. C.E.Fosha,Jr., O.I.Elgerd, "The Megawatt-Frequency Control Problem - A New Approach Via Optimal Control Theory", *PICA '69 Conference Proccedings*, pp.123-132

49. Y.-N.Yu, C.Siggers, "Stabilization and Optimal Control Signals for a Power System", *IEEE Transactions on Power Apparatus and Systems*, July/August 1971, pp.1469-1481

50. Y.-N.Yu, H.A.M.Moussa, "Optimal Stabilization of a Multi-Machine System", *IEEE Transactions on Power Apparatus and Systems*, May/June 1972, pp. 1174-1182

51. E.J.Davison, N.S.Rau, F.V.Palmay, "The Optimal Decentralized Control of a Power System Consisting of a Number of Interconnected Synchronous Machines", *International Journal on Control*, 1973, Vol.18, No.6, pp.1313-1328

52. K.Ohtsuka, S.Yokokawa, H.Tanaka, H.Doi, "A Multivariable Optimal Control System for a Generator", *IEEE Transactions on Energy Conversion*, Vol.EC-1, No.2, June 1986, pp.88-98

53. W.J.Wilson, J.D.Aplevich, "Co-Ordinated Governor-Exciter Stabilizer Design in Multi-Machine Power Systems", *IEEE Transactions on Energy Conversion*, Vol.EC-1, No.3, September 1986, pp.61-67

54. A.Feliachi, "Optimal Decentralized Load Frequency Control", *IEEE Transactions on Power Systems*, Vol.PWRS-2, No.2, May 1987, pp.379-386

55. A.Feliachi, L.A.Belblidia, "Optimal Level Controller for Steam Generators in Pressurized Water Reactors", *IEEE Transactions on Energy Conversion*, Vol.EC-2, No.2, June 1987, pp.161-167

56. T.D.Younkins, J.R.Winkelman, J.J.Sanchez-Gasca, J.A.McGrady, "Output Feedback Multivariable Control for an Advanced Boiling Water Reactor", *IEEE Transactions on Energy Conversion*, Vol.EC-2, No.3, September 1987, pp.349-354

57. Y.L.Abdel-Magid, G.M.Aly, "Two-Level Optimal Stabilization in Multimachine Power Systems", *Electric Power Systems Research*, 6(1983), pp.33-41

58. Y.-Y.Hsu, C.-Y.Hsu, "Design of a Proportional Integral Power System Stabilizer", *IEEE Transactions on Power Systems*, May 1986, pp.46-53

59. C.-L.Chen, Y.-Y.Hsu, "Power System Stability Improvement Using Dynamic Output Feedback Compensators", *Electric Power Systems Research*, 12(1987), pp.37-39

60. A.Feliachi, X.Zhang, C.S.Sims, "Power System Stabilizers Design Using Optimal Reduced Order Models" , *IEEE Transactions on Power Systems*, November 1988, pp.1670-1684

61. W.S.Levine, M.Athans, "On the Determination of the Optimal Constant Output Feedback Gains for Linear Multivariable Systems", *IEEE Transactions on Automatic Control*, Vol.AC-15, No.1, February 1970, pp.44-48

62. S.S.Choi, H.R.Sirisena, "Computation of Optimal Output Feedback Gains for Linear Multivariable Systems", *IEEE Transactions on Automatic Control*, Vol.19, June 1974, pp.257-258

63. G.Kreisselmeier, "Stabilization of Linear Systems by Constant Output Feedback Using the Riccati Equation", *IEEE Transactions on Automatic Control*, Vol.20, August 1975, pp.556-557

64. H.Seraji, "Unattainability of Certain Pole Positions in Single-Input Systems with Output Feedback", *International Journal on Control*, 1975, Vol.22, No.1, pp.119-123

65. V.M.Raina, J.H.Anderson, "Optimal Output Feedback Control of Power Systems with High-Speed Excitation Systems", *IEEE Transactions on Power Apparatus and Systems*, March/April 1976, pp.677-686

66. W.-C.Chan, Y.-Y.Hsu, "An Optimal Variable Structure Stabilizer for Power System Stabilization", *IEEE Transactions on Power Apparatus and Systems*, June 1983, pp.1738-1746

67. N. Rostamkolai, A. G. Phadke, W. F. Long, and J. S. Thorp, "An Adaptive Optimal Control Strategy for Dynamic Stability Enhancement of AC/DC Power Systems", *IEEE Transactions on Power Systems*, August 1988, pp.1139-1145

68. V.I.Utkin, K.D.Yang, "Methods for Constructing Discontinuity Planes", *Automation and Remote Control*, Volume 39, No.9-12, Sept/Dec 1978, pp.1466-1470

69. Y.Y.-Hsu, W.C.-Chan, "Stabilization of Power Systems Using a Variable Structure Stabilizer" , *Electric Power Systems Research*, 6(1983), pp.129-139

70. A.S.Debs, R.E.Larson, "A Dynamic Estimator for Tracking the State of a Power System", *IEEE Transactions on Power Apparatus and Systems*, September/October 1970, pp.1670-1678

71. Z.Morvaj, "A Mathematical Model of an Electric Power System for Dynamic State Estimation", *Electric Power Systems Research*, 8(1984/85), pp.207-217

72. A.L.Leite da Silva, M.B.Do Coutto Filho, J.M.C.Cantera, "An Efficient Dynamic State Estimation Algorithm Including Bad Data Processing", *IEEE Transactions on Power Systems*, Nov.1987, pp.1050-1058

73. E.Handschin, F.D.Galiana "Hierarchical State Estimation for Real-Time Monitoring of Electric Power Systems", *Eighth PICA Conference*, Minneapolis, Minnesota, June 4-6, 1973

74. A.Keyhani, S.M.Miri, "Observers for Tracking of Synchronous Machine Parameters and Detection of Incipient Faults", *IEEE Transactions on Energy Conversion*, Vol.EC-1, No.2, June 1986, pp.184-192

75. E.Vaahedi, A.D.Noble, D.C.Macdonald, "Generator On-Line State Estimation and Optimal Control: Laboratory Implementation and Prospects for Development", *IEEE Transactions on Energy Conversion*, Vol.EC-1, No.3, September 1986, pp.55-60

76. M.C.Menelaou, D.C.Macdonald, "Supplementary Signals to Improve Transient Stability, On-Line Application to a Micro-Generator", *IEEE Transactions on Power Apparatus and Systems*, September 1982, pp.3543-3550

77. N. Rostamkolai, "Adaptive Optimal Control of AC/DC Systems", *Virginia Polytechnic Institute and State University*, Ph.D. Dissertation, 1986

78. R.T.Byerly, E.W.Kimbark (Editors), "Stability of Large Electric Power Systems", *IEEE Press*, New York, 1974

79. P.M.Anderson, A.A.Fouad, "Power System Control and Stability", *The Iowa State University Press*, 1977

80. D.E.Kirk, "Optimal Control Theory", *Prentice-Hall Inc.*, Englewood Cliffs, N.J.,1971

81. R.E.Kalman, "When Is a Linear Control System Optimal?", *Proc. Joint Automatic Control Conference*, Minneapolis, Minn., pp. 1-15, 1963

82. K.Ogata, "State Space Analysis of Control Systems", *Prentice-Hall Inc.*, Englewood Cliffs, N.J., 1967

83. P.B.Liebelt, "An Introduction to Optimal Estimation", *Addison-Wesley Publishing Company*, 1967

84. A.G.Phadke, J.S.Thorp, and M.G.Adamiak, "A New Measurement Technique for Tracking Voltage Phasors, Local System Frequency, and Rate of Change of Frequency", *IEEE Transactions on Power Apparatus and Systems*, May 1983, pp. 1025-1033

85. IEEE Committee Report, "Computer Representation of Excitation Systems", *IEEE Transactions on Power Apparatus and Systems*, June 1968, pp. 1460-1464

86. IEEE Committee Report, "Dynamic Models for Steam and Hydro-Turbines in Power System Studies" , *IEEE Transactions on Power Apparatus and Systems*, Nov/Dec 1973, pp. 1904-1915

87. M.A.Eggenberger, "A Simplified Analysis of the No-Load Stability of Mechanical-Hydraulic Speed Control Systems for Steam Turbine", *ASME Paper*, 60-WA-34

88. G.W.Stagg and A.H.El-Abiad, "Computer Methods in Power System Analysis", *McGraw Hill Inc.*, 1968

89. B.D.O.Anderson and J.B.Moore, "Linear Optimal Control", *Prentice Hall Inc.*, Englewood Cliffs, N.J., 1971

90. W.M.Wonham, "On a Matrix Riccati Equation of Stochastic Control", *SIAM Journal on Control*, Volume 6, Number 4, 1968, pp.681-697

91. T.Athay, et.al., "Transient Energy Stability Analysis", *Systems Engineering for Power: Emergency Operating State Control Conference*, DOE-CONF-790904-P1, Davos, Switzerland, Sept 30 - Oct 5, 1979

92. P.G.Kaminski, A.E.Bryson,Jr., and S.F.Schmidt, "Discrete Square Root Filtering: A Survey of Current Techniques", *IEEE Transactions on Automatic Control*, Vol.AC-16, No.6, December 1971, pp. 727-736

93. A.S.Householder, "The Theory of Matrices in Numerical Analysis", *Blaisdell Publishing Company*, 1964

94. R.J.Fitzgerald, "Divergence of the Kalman Filter", *IEEE Transactions on Automatic Control*, Vol.AC-16, No.6, December 1971, pp. 736-747

95. M.Athans, "The Role and Use of the Stochastic Linear-Quadratic-Gaussian Problem in Control System Design", *IEEE Transactions on Automatic Control*, Vol.AC-16, No.6, December 1971, pp. 529-552

96. J.S.Meditch, "Stochastic Optimal Linear Estimation and Control", *McGraw Hill Book Company*, New York, 1969

97. M.S.Sarma, "Synchronous Machines (Their Theory, Stability, and Excitation Systems)" , *Gordon and Breach Science Publishers*, 1979

98. P.C.Krause, F.Nozari, T.L.Skvarenina, D.W.Olive, "The Theory of Neglecting Stator Transients", *IEEE Transactions on Power Apparatus and Systems*, Vol.PAS-98, No.1, Jan/Feb 1979, pp.141-148

Appendix A

Synchronous Generator Formulas

This appendix will derive three formulas corresponding to the synchronous generator phasor diagram used in the paper. The subscript "i" denoting an individual generator will be dropped.

(1). E_I, the voltage proportional to field current, is given by

$$E_I = E'_q\left(\frac{x_d}{x'_d}\right) - \left(\frac{x_d}{x'_d} - 1\right)E_t\cos(\delta_q - \delta_t)$$

From the phasor diagram, neglecting the very small armature resistance,

$$E_I = E_t\cos(\delta_q - \delta_t) + x_d I_d \qquad (A.1)$$

Solving for I_d,

$$I_d = \frac{E_I - E_t \cos(\delta_q - \delta_t)}{x_d} \qquad (A.2)$$

From one of the algebraic equations,

$$E_I = E'_q + (x_d - x'_d) I_d \qquad (A.3)$$

Substituting Eq.(A.2) into Eq.(A.3) and simplifying yields

$$E_I = E'_q \left(\frac{x_d}{x'_d}\right) - \left(\frac{x_d}{x'_d} - 1\right) E_t \cos(\delta_q - \delta_t) \qquad (Q.E.D.)$$

(2). P_E, the generator real power output, is given by

$$P_E = \frac{E'_q E_t}{x_d} \sin(\delta_q - \delta_t) - \frac{E_t^2 (x_q - x'_d)}{2 x'_d x_q} \sin(2\delta_q - 2\delta_t)$$

The equivalent circuit shown on Figure A.1 is implied directly from the phasor diagram. Thus,

$$P_E = \frac{E_q E_t}{x_q} \sin(\delta_q - \delta_t) \qquad (A.4)$$

From one of the algebraic equations,

$$E_q = E'_q + (x_q - x'_d) I_d \qquad (A.5)$$

Solving for I_d,

$$I_d = \frac{(E_q - E'_q)}{(x_q - x'_d)} \tag{A.6}$$

From the phasor diagram, neglecting the very small armature resistance,

$$E_q = E_t \cos(\delta_q - \delta_t) + x_q I_d \tag{A.7}$$

Substituting Eq.(A.6) into Eq.(A.7) and solving the resulting equation for E_q yields

$$E_q = E'_q\left(\frac{x_q}{x'_d}\right) - \left(\frac{x_q - x'_d}{x'_d}\right) E_t \cos(\delta_q - \delta_t) \tag{A.8}$$

Substituting further Eq.(A.8) into Eq.(A.4), manipulating and using the trigonometric identity of Eq.(A.9) yields the desired expression for the real power output.

$$\sin\alpha \cdot \cos\alpha = \frac{1}{2}\sin(2\alpha) \tag{A.9}$$

$$P_E = \frac{E'_q E_t}{x_d} \sin(\delta_q - \delta_t) - \frac{E_t^2 (x_q - x'_d)}{2x'_d x_q} \sin(2\delta_q - 2\delta_t) \tag{Q.E.D.}$$

(3). Q_E, the generator reactive power output , is given by

$$Q_E = \frac{E'_q E_t}{x_d} \cos(\delta_q - \delta_t) - \frac{E_t^2}{x'_d x_q} [x_q \cos^2(\delta_q - \delta_t) + x'_d \sin^2(\delta_q - \delta_t)]$$

Using the equivalent circuit shown in Figure A.1,

$$Q_E = \frac{E_q E_t}{x_q} \cos(\delta_q - \delta_t) - \frac{E_t^2}{x_q} \tag{A.10}$$

Substituting the expression in Eq.(A.8) for E_q into Eq.(A.10), collecting like terms and using the trigonometric identity

$$1 - \cos^2\alpha = \sin^2\alpha \tag{A.11}$$

yields the desired expression for the generator reactive power output

$$Q_E = \frac{E'_q E_t}{x_d} \cos(\delta_{qi} - \delta_t) - \frac{E_t^2}{x'_d x_q} [x_q \cos^2(\delta_q - \delta_t) + x'_d \sin^2(\delta_q - \delta_t)] \tag{Q.E.D.}$$

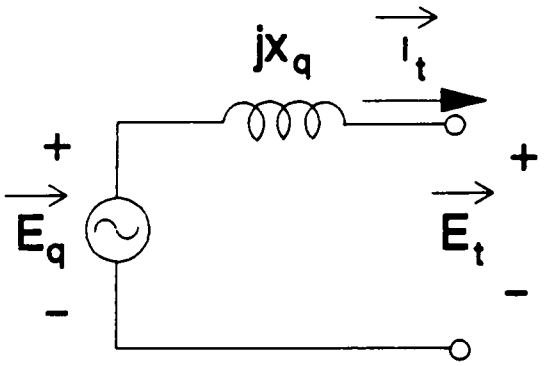

Figure A.1. Voltage Behind q-Axis Synchronous Reactance

Appendix B

Derivation of State Estimator (Discrete-Time) Formulas

The following derivations are based mainly on the theory presented in reference [83]. The derivations, particularly those in the earlier parts of this appendix, follow mainly the reference [83]. The latter part of the appendix is an adaptation and extension of the theory. A consistent notation will be used throughout Appendix B.

The Gauss-Markoff Fundamental Theorem

Reference [83] has proven the following basic theorem of state and parameter estimation. Let

$\underline{x}$ = n - state vector to be estimated

$\hat{\underline{x}}$ = estimate of the state vector

$\underline{\theta}$ = m - measurement or observation vector

Define the moment matrices as

$$\underline{C}_x = E(\underline{x}\underline{x}^T) \tag{B.1}$$

$$\underline{C}_{x\theta} = E(\underline{x}\underline{\theta}^T) \tag{B.2}$$

$$\underline{C}_\theta = E(\underline{\theta}\underline{\theta}^T) \tag{B.3}$$

and the error covariance matrix as

$$\underline{C}_e = E[(\hat{\underline{x}} - \underline{x})(\hat{\underline{x}} - \underline{x})^T] \tag{B.4}$$

Then, if $\underline{x}$ and $\underline{\theta}$ are random vectors with moment matrices $\underline{C}_x$, $\underline{C}_{x\theta}$, and $\underline{C}_\theta$ where $\underline{C}_\theta$ is nonsingular, the linear minimum mean square estimate $\hat{\underline{x}}$ of $\underline{x}$ given the measurement data $\underline{\theta}$ is equal to

$$\hat{\underline{x}} = \underline{C}_{x\theta}\underline{C}_\theta^{-1}\underline{\theta} \tag{B.5}$$

The associated error matrix $\underline{C}_e$ of the estimate is

$$\underline{C}_e = \underline{C}_x - \underline{C}_{x\theta}\underline{C}_\theta^{-1}\underline{C}_{x\theta}^T \tag{B.6}$$

If, in addition, it is true that

$$\underline{x} = \underline{C}_{x\theta}\underline{C}_{\theta}^{-1}E(\underline{\theta}) \tag{B.7}$$

then $\hat{\underline{x}}$ is the linear minimum variance unbiased estimate of $\underline{x}$.

Case of Linear Observations

If the observation vector $\underline{\theta}$ is related to $\underline{x}$ by

$$\underline{\theta} = \underline{B}\underline{x} + \underline{v} \tag{B.8}$$

where $\underline{B}$ is an m x n matrix, and the vector $\underline{v}$ represents the noise or error in the measurement process of $\underline{\theta}$ then,

$$\begin{aligned}\underline{C}_{x\theta} &= E[\underline{x}\underline{\theta}^T] = E[\underline{x}(\underline{B}\underline{x} + \underline{v})^T] \\ &= E[\underline{x}(\underline{x}^T\underline{B}^T + \underline{v}^T)] = E(\underline{x}\underline{x}^T)\underline{B}^T + E(\underline{x}\underline{v}^T) \\ \underline{C}_{x\theta} &= \underline{C}_x\underline{B}^T + \underline{C}_{xv}\end{aligned} \tag{B.9}$$

Also,

$$\begin{aligned}\underline{C}_{\theta} &= E[\underline{\theta}\underline{\theta}^T] = E[(\underline{B}\underline{x} + \underline{v})(\underline{B}\underline{x} + \underline{v})^T] \\ &= \underline{B}E(\underline{x}\underline{x}^T)\underline{B}^T + E(\underline{x}\underline{v}^T)^T\underline{B}^T + \underline{B}E(\underline{x}\underline{v}^T) + E(\underline{v}\underline{v}^T) \\ \underline{C}_{\theta} &= \underline{B}\underline{C}_x\underline{B}^T + \underline{C}_{xv}^T\underline{B}^T + \underline{B}\underline{C}_{xv} + \underline{C}_v\end{aligned} \tag{B.10}$$

Hence,

$$\hat{\underline{x}} = \underline{C}_{x\theta}\underline{C}_{\theta}^{-1}\underline{\theta}$$
$$= (\underline{C}_x\underline{B}^T + \underline{C}_{xv})(\underline{B}\underline{C}_x\underline{B}^T + \underline{C}_{xv}^T\underline{B}^T + \underline{B}\underline{C}_{xv} + \underline{C}_v)^{-1}\underline{\theta} \tag{B.11}$$

and

$$\underline{C}_e = \underline{C}_x - \underline{C}_{x\theta}\underline{C}_{\theta}^{-1}\underline{C}_{x\theta}^T$$
$$= \underline{C}_x - (\underline{C}_x\underline{B}^T + \underline{C}_{xv})(\underline{B}\underline{C}_x\underline{B}^T + \underline{C}_{xv}^T\underline{B}^T + \underline{B}\underline{C}_{xv} + \underline{C}_v)^{-1}(\underline{C}_x\underline{B}^T + \underline{C}_{xv})^T \tag{B.12}$$

State Vector and Noise Uncorrelated

If the observation error $\underline{v}$ is statistically independent from the state vector $\underline{x}$,

$$\underline{C}_{xv} = 0 \tag{B.13}$$

Thus, for the linear system $\underline{\theta} = \underline{B}\underline{x} + \underline{v}$,

$$\hat{\underline{x}} = (\underline{C}_x\underline{B}^T)(\underline{B}\underline{C}_x\underline{B}^T + \underline{C}_v)^{-1}\underline{\theta} \tag{B.14}$$

$$\underline{C}_e = \underline{C}_x - (\underline{C}_x\underline{B}^T)(\underline{B}\underline{C}_x\underline{B}^T + \underline{C}_v)^{-1}(\underline{C}_x\underline{B}^T)^T \tag{B.15}$$

Using the two matrix identities

$$\underline{A}\underline{B}^T(\underline{C} + \underline{B}\underline{A}\underline{B}^T)^{-1} = (\underline{A}^{-1} + \underline{B}^T\underline{C}^{-1}\underline{B})^{-1}\underline{B}^T\underline{C}^{-1} \tag{B.16}$$

and

$$(\underline{C}^{-1} + \underline{B}^T\underline{A}^{-1}\underline{B})^{-1} = \underline{C} - \underline{C}\underline{B}^T(\underline{B}\underline{C}\underline{B}^T + \underline{A})^{-1}\underline{B}\underline{C} \tag{B.17}$$

the estimate vector and error covariance matrix become

$$\hat{\underline{x}} = (\underline{C}_x^{-1} + \underline{B}^T\underline{C}_v^{-1}\underline{B})^{-1}\underline{B}^T\underline{C}_v^{-1}\underline{\theta} \tag{B.18}$$

$$\underline{C}_e = (\underline{C}_x^{-1} + \underline{B}^T\underline{C}_v^{-1}\underline{B})^{-1} \tag{B.19}$$

It can also be shown that $\hat{\underline{x}}$ is the vector $\underline{y}$ which minimizes the average distance of the data $\underline{\theta}$ from the linear form $\underline{B}\underline{y}$. Let the scalar quantity Q be the quadratic form

$$Q(\underline{y}) = (\underline{B}\underline{y} - \underline{\theta})^T\underline{C}_v^{-1}(\underline{B}\underline{y} - \underline{\theta}) + \underline{y}^T\underline{C}_x^{-1}\underline{y} \tag{B.20}$$

Expanding $Q(\underline{y})$,

$$Q(\underline{y}) = \underline{y}^T\underline{B}^T\underline{C}_v^{-1}\underline{B}\underline{y} - \underline{y}^T\underline{B}^T\underline{C}_v^{-1}\underline{\theta} - \underline{\theta}^T\underline{C}_v^{-1}\underline{B}\underline{y} + \underline{\theta}^T\underline{C}_v^{-1}\underline{\theta} + \underline{y}^T\underline{C}_x^{-1}\underline{y} \tag{B.21}$$

Since all terms are scalar,

$$Q(\underline{y}) = \underline{y}^T\underline{B}^T\underline{C}_v^{-1}\underline{B}\underline{y} - 2\underline{y}^T\underline{B}^T\underline{C}_v^{-1}\underline{\theta} + \underline{\theta}^T\underline{C}_v^{-1}\underline{\theta} + \underline{y}^T\underline{C}_x^{-1}\underline{y} \tag{B.22}$$

Differentiating with respect to $\underline{y}$,

$$\frac{dQ}{d\underline{y}} = 2\underline{B}^T\underline{C}_v^{-1}\underline{B}\underline{y} - 2\underline{B}^T\underline{C}_v^{-1}\underline{\theta} + 2\underline{C}_x^{-1}\underline{y} \tag{B.23}$$

Setting the right-hand side of the previous equation to zero,

$$\underline{B}^T\underline{C}_v^{-1}\underline{B}\underline{y} + \underline{C}_x^{-1}\underline{y} = \underline{B}^T\underline{C}_v^{-1}\underline{\theta} \tag{B.24}$$

or

$$\underline{y} = (\underline{B}^T \underline{C}_v^{-1} \underline{B} + \underline{C}_x^{-1})^{-1} \underline{B}^T \underline{C}_v^{-1} \underline{\theta} \tag{B.25}$$

Thus, the value of $\underline{y}$ which minimizes Q is identical to the estimate $\hat{\underline{x}}$ which minimizes the diagonal terms of $\underline{C}_{(\hat{x}-x)}$ provided the hypotheses of the set H, excluding $\underline{C}_x \to \infty$ are satisfied. The set H represents the following set of hypotheses:

1. The moment matrix $\underline{C}_v$ of the measurement noise $\underline{v}$ is available.
2. The inverse $\underline{C}_v^{-1}$ is nonsingular.
3. Knowledge of the true state $\underline{x}$ is unknown so that $\underline{C}_x \to \infty$.
4. The correlation between the measurement noise and the true state is zero so that $\underline{C}_{xv} = 0$.
5. The optimal estimate $\hat{\underline{x}}$ of $\underline{x}$ is the linear estimator which minimizes the diagonal elements of $\underline{C}_e = \underline{C}_{(\hat{x}-x)}$.
6. The measurements $\underline{\theta}$ are related to $\underline{x}$ by the linear equation $\underline{\theta} = \underline{B}\underline{x} + \underline{v}$.

Linear Observations With Unknown True States

If no information is available concerning the true state $\underline{x}$, it is reasonable to assume that the diagonal elements of the moment matrix of $\underline{x}$ are larger than any preassigned number. Thus,

$$\text{Cov}\,(\underline{x}) \to \infty \tag{B.26}$$

Since

$$\underline{C}_x = \mathrm{Cov}(\underline{x}) + \underline{\mu}\underline{\mu}^T \tag{B.27}$$

where $\underline{\mu}$ is the vector of mean values of $\underline{x}$,

$$\underline{C}_x \to \infty \tag{B.28}$$

from the fact that $\underline{\mu}\underline{\mu}^T$ is just a matrix of constants. Another way of stating this condition is that there is an infinite or unbounded uncertainty in the knowledge of the true state $\underline{x}$. The estimate vector and error covariance matrix then become

$$\hat{\underline{x}} = (\underline{B}^T \underline{C}_v^{-1} \underline{B})^{-1} \underline{B}^T \underline{C}_v^{-1} \underline{\theta} \tag{B.29}$$

$$\underline{C}_e = (\underline{B}^T \underline{C}_v^{-1} \underline{B})^{-1} \tag{B.30}$$

Use of A Priori Estimates

This section will present the derivation of formulas which combine an old estimate $\hat{\underline{x}}^r$ based upon r measurements, the old error matrix $\underline{C}_e^r$, with a new set $\underline{\theta}^s$ of measurements, s in number, to obtain an estimate $\hat{\underline{x}}^m$ which minimizes the variance terms of $\underline{C}_e^m$ where $m = r + s$. The following linear relationship will be assumed for the first r measurements :

$$\underline{\theta}^r = \underline{B}^r \underline{x} + \underline{v}^r \tag{B.31}$$

where $\underline{v}^r$ represents the uncertainty in the measurements. Assume that $(\underline{C}_v^r)^{-1}$ exists and that the correlation matrix $\underline{C}_{xv}^r$ vanishes. Assume further that nothing is known of the true state $\underline{x}$ so that $\underline{C}_x^{-1} = 0$. These are nothing more than the assumptions of the previous sections. The estimate $\hat{\underline{x}}^r$ which minimizes the diagonal terms of $\underline{C}_e^r$ is

$$\hat{\underline{x}}^r = [\underline{B}^{Tr}(\underline{C}_v^r)^{-1}\underline{B}^r]^{-1}\underline{B}^{Tr}(\underline{C}_v^r)^{-1}\underline{\theta}^r \tag{B.32}$$

The error matrix is

$$\underline{C}_e^r = \underline{C}_{(\hat{\underline{x}} - \underline{x})}^r = [\underline{B}^{Tr}(\underline{C}_v^r)^{-1}\underline{B}^r]^{-1} \tag{B.33}$$

Hence,

$$\hat{\underline{x}}^r = \underline{C}_e^r\underline{B}^{Tr}(\underline{C}_v^r)^{-1}\underline{\theta}^r \tag{B.34}$$

and

$$(\underline{C}_e^r)^{-1}\hat{\underline{x}}^r = \underline{B}^{Tr}(\underline{C}_v^r)^{-1}\underline{\theta}^r \tag{B.35}$$

Let an additional set of data $\underline{\theta}^s$ be available, i.e.,

$$\underline{\theta}^s = \underline{B}^s\underline{x} + \underline{v}^s \tag{B.36}$$

where

$$\underline{C}_{xv}^s = 0 \text{ and } \underline{C}_{vv}^{rs} = 0 \tag{B.37}$$

The last assumption ensures that the uncertainty in the first r measurements is uncorrelated to the uncertainty in the new set of s measurements. Let m = r + s. Then,

$$\begin{bmatrix} \underline{\theta}^r \\ \underline{\theta}^s \end{bmatrix} = \begin{bmatrix} \underline{B}^r \\ \underline{B}^s \end{bmatrix} \underline{x} + \begin{bmatrix} \underline{v}^r \\ \underline{v}^s \end{bmatrix} \tag{B.38}$$

or

$$\underline{\theta}^m = \underline{B}^m \underline{x} + \underline{v}^m \tag{B.39}$$

Also,

$$\underline{C}_v^m = E[\underline{v}^m \quad \underline{v}^{Tm}] = E\left[\begin{pmatrix} \underline{v}^r \\ \underline{v}^s \end{pmatrix} \quad (\underline{v}^{Tr} \quad \underline{v}^{Ts})\right]$$

$$= E\begin{bmatrix} \underline{v}^r \underline{v}^{Tr} & \underline{v}^r \underline{v}^{Ts} \\ \underline{v}^s \underline{v}^{Tr} & \underline{v}^s \underline{v}^{Ts} \end{bmatrix} = \begin{bmatrix} \underline{C}_v^r & \underline{C}_{vv}^{rs} \\ \underline{C}_{vv}^{rs} & \underline{C}_v^s \end{bmatrix} \tag{B.40}$$

Under the assumptions of Eqs.(B.37),

$$\underline{C}_v^m = \begin{bmatrix} \underline{C}_v^r & 0 \\ 0 & \underline{C}_v^s \end{bmatrix} \tag{B.41}$$

$$(\underline{C}_v^m)^{-1} = \begin{bmatrix} (\underline{C}_v^r)^{-1} & 0 \\ 0 & (\underline{C}_v^s)^{-1} \end{bmatrix} \tag{B.42}$$

The optimal estimate using the m measurements is

$$\begin{aligned}\hat{\underline{x}}^m &= \underline{C}_e^m[\underline{B}^{Tm}(\underline{C}_v^m)^{-1}\underline{\theta}^m] \\ &= [\underline{B}^{Tm}(\underline{C}_v^m)^{-1}\underline{B}^m]^{-1}[\underline{B}^{Tm}(\underline{C}_v^m)^{-1}\underline{\theta}^m]\end{aligned} \tag{B.43}$$

Hence,

$$\begin{aligned}(\underline{C}_e^m)^{-1} &= \left[\begin{pmatrix}\underline{B}^{Tr} & \underline{B}^{Ts}\end{pmatrix}\begin{pmatrix}(\underline{C}_v^r)^{-1} & 0 \\ 0 & (\underline{C}_v^s)^{-1}\end{pmatrix}\begin{pmatrix}\underline{B}^r \\ \underline{B}^s\end{pmatrix}\right] \\ &= \left[\begin{pmatrix}\underline{B}^{Tr} & \underline{B}^{Ts}\end{pmatrix}\begin{pmatrix}(\underline{C}_v^r)^{-1}\underline{B}^r \\ (\underline{C}_v^s)^{-1}\underline{B}^s\end{pmatrix}\right] \\ &= [\underline{B}^{Tr}(\underline{C}_v^r)^{-1}\underline{B}^r + \underline{B}^{Ts}(\underline{C}_v^s)^{-1}\underline{B}^s]^{-1}\end{aligned} \tag{B.44}$$

Also,

$$\begin{aligned}[\underline{B}^{Tm}(\underline{C}_v^m)^{-1}\underline{\theta}^m] &= [\underline{B}^{Tr} \quad \underline{B}^{Ts}]\begin{bmatrix}(\underline{C}_v^r)^{-1} & 0 \\ 0 & (\underline{C}_v^s)^{-1}\end{bmatrix}\begin{bmatrix}\underline{\theta}^r \\ \underline{\theta}^s\end{bmatrix} \\ &= \left[\begin{pmatrix}\underline{B}^{Tr} & \underline{B}^{Ts}\end{pmatrix}\begin{pmatrix}(\underline{C}_v^r)^{-1}\underline{\theta}^r \\ (\underline{C}_v^r)^{-1}\underline{\theta}^s\end{pmatrix}\right] \\ &= [\underline{B}^{Tr}(\underline{C}_v^r)^{-1}\underline{\theta}^r + \underline{B}^{Ts}(\underline{C}_v^s)^{-1}\underline{\theta}^s]\end{aligned} \tag{B.45}$$

Recalling that

$$\underline{C}_e^r = [\underline{B}^{Tr}(\underline{C}_v^r)^{-1}\underline{B}^r]^{-1} \text{ and } (\underline{C}_e^r)^{-1}\hat{\underline{x}}^r = \underline{B}^{Tr}(\underline{C}_v^r)^{-1}\underline{\theta}^r \tag{B.46}$$

we have

$$\underline{C}_e^m = [(\underline{C}_e^r)^{-1} + \underline{B}^{Ts}(\underline{C}_v^s)^{-1}\underline{B}^s]^{-1} \tag{B.47}$$

$$\hat{\underline{x}}^m = \underline{C}_e^m[(\underline{C}_e^r)^{-1}\hat{\underline{x}}^r + \underline{B}^{Ts}(\underline{C}_v^s)^{-1}\underline{\theta}^s] \tag{B.48}$$

Kalman Form Using A Priori Estimates

From the result shown as Eq.(B.48),

$$\hat{\underline{x}}^m = \underline{C}_e^m(\underline{C}_e^r)^{-1}\hat{\underline{x}}^r + \underline{C}_e^m\underline{B}^{Ts}(\underline{C}_v^s)^{-1}\underline{\theta}^s \tag{B.49}$$

Define the gain factor $\underline{K}$ as

$$\begin{aligned}\underline{K} &\equiv \underline{C}_e^m\underline{B}^{Ts}(\underline{C}_v^s)^{-1} \\ &= [(\underline{C}_e^r)^{-1} + \underline{B}^{Ts}(\underline{C}_v^s)^{-1}\underline{B}^s]^{-1}\underline{B}^{Ts}(\underline{C}_v^s)^{-1}\end{aligned} \tag{B.50}$$

Using the matrix identity shown as Eq.(B.16),

$$\underline{K} = \underline{C}_e^r\underline{B}^{Ts}[\underline{C}_v^s + \underline{B}^s\underline{C}_e^r\underline{B}^{Ts}]^{-1} \tag{B.51}$$

From the result shown as Eq.(B.47) and the matrix identity of Eq.(B.17),

$$\underline{C}_e^m = \underline{C}_e^r - \underline{C}_e^r\underline{B}^{Ts}[\underline{C}_v^s + \underline{B}^s\underline{C}_e^r\underline{B}^{Ts}]^{-1}\underline{B}^s\underline{C}_e^r \tag{B.52}$$

Combining Eqs.(B.51) and (B.52),

$$\underline{C}_e^m = \underline{C}_e^r - \underline{K}\underline{B}^s\underline{C}_e^r \tag{B.53}$$

From Eqs.(B.49) and (B.53),

$$\begin{aligned}\hat{\underline{x}}^m &= (\underline{C}_e^r - \underline{K}\underline{B}^s\underline{C}_e^r)(\underline{C}_e^r)^{-1}\hat{\underline{x}}^r + \underline{K}\underline{\theta}^s \\ &= \hat{\underline{x}}^r - \underline{K}\underline{B}^s\hat{\underline{x}}^r + \underline{K}\underline{\theta}^s\end{aligned} \tag{B.54}$$

Finally,

$$\hat{\underline{x}}^m = \hat{\underline{x}}^r + \underline{K}(\underline{\theta}^s - \underline{B}^s\hat{\underline{x}}^r) \tag{B.55}$$

Some Identities On The Moment Matrices

The following identities will be used in subsequent sections of this appendix.

Identity 1:

$$\begin{aligned}E(\hat{\underline{x}}\underline{\theta}^T) &= E(\underline{C}_{x\theta}\underline{C}_\theta^{-1}\underline{\theta}\underline{\theta}^T) \\ \underline{C}_{\hat{x}\theta} &= \underline{C}_{x\theta}\underline{C}_\theta^{-1}E(\underline{\theta}\underline{\theta}^T) \\ \underline{C}_{\hat{x}\theta} &= \underline{C}_{x\theta}\end{aligned} \tag{B.56}$$

Transposing,

$$\begin{aligned}\underline{C}_{\hat{x}\theta}^T &= \underline{C}_{x\theta}^T \\ E(\hat{\underline{x}}\underline{\theta}^T)^T &= \underline{C}_{x\theta}^T \\ E(\underline{\theta}\hat{\underline{x}}^T) &= \underline{C}_{x\theta}^T\end{aligned} \tag{B.57}$$

Identity 2:

$$E(\hat{\underline{x}}\hat{\underline{x}}^T) = E(\underline{C}_{x\theta}\underline{C}_{\theta}^{-1}\underline{\theta}\hat{\underline{x}}^T)$$
$$\underline{C}_{\hat{x}} = \underline{C}_{x\theta}\underline{C}_{\theta}^{-1}E(\underline{\theta}\hat{\underline{x}}^T) \quad \text{by Identity 1} \tag{B.58}$$
$$\underline{C}_{\hat{x}} = \underline{C}_{x\theta}\underline{C}_{\theta}^{-1}\underline{C}_{x\theta}^T$$

Identity 3:

$$E(\hat{\underline{x}}\underline{x}^T) = E(\underline{C}_{x\theta}\underline{C}_{\theta}^{-1}\underline{\theta}\underline{x}^T)$$
$$\underline{C}_{\hat{x}x} = \underline{C}_{x\theta}\underline{C}_{\theta}^{-1}E(\underline{\theta}\underline{x}^T) \tag{B.59}$$
$$\underline{C}_{\hat{x}x} = \underline{C}_{x\theta}\underline{C}_{\theta}^{-1}\underline{C}_{x\theta}^T$$

From Eq.(B.58) and Eq.(B.59),

$$\underline{C}_{\hat{x}x} = \underline{C}_{\hat{x}} \tag{B.60}$$

Discrete-Time Dynamic System Prediction (Special Case)

An important step in the linear Kalman filtering process is the prediction of the value of the state estimate at the next time step $\hat{\underline{x}}_{i+1}$ from the current value of state estimate $\hat{\underline{x}}_i$. This section of the appendix will deal with the above stated step. Current value of time step will be denoted by the subscript "i". The results will be invoked and extended in the section titled "Filtering for a Nonlinear System". Thus, given $\hat{\underline{x}}_i$, the current state estimate, and that

$$\underline{x}_{i+1} = \underline{S}(i+1,i)\underline{x}_i + \underline{w}_i \tag{B.61}$$

where

$\underline{S}(i+1,i)$ = transition matrix of the sequence

$\underline{x}_i$ = n-vector describing dynamic state at time t_i

$\underline{w}_i$ = random n-vector representing perturbation at t_i

$\underline{W}_i = E[\underline{w}_i \underline{w}_i^T]$

and the following correlation conditions and random vector characteristics:

$$\begin{aligned} E(\underline{w}_i) &= 0 \text{ , all i} \\ E(\underline{w}_i \underline{w}_j^T) &= 0 \text{ , } i \neq j \\ E(\underline{x}_i \underline{w}_j^T) &= 0 \text{ , } i \leq j \\ E(\underline{v}_i \underline{w}_i^T) &= 0 \text{ , all i} \end{aligned} \tag{B.62}$$

an appropriate expression for $\hat{\underline{x}}^p_{i+1}$, the state prediction, will be found.

Treating the given estimate $\hat{\underline{x}}_i$ as an observation of $\hat{\underline{x}}^p_{i+1}$,

$$\hat{\underline{x}}^p_{i+1} = \underline{C}_{x_{i+1}\hat{x}_i}(\underline{C}_{\hat{x}_i})^{-1}\hat{\underline{x}}_i \tag{B.63}$$

Thus,

$$\begin{aligned}\hat{\underline{x}}_{i+1}^{p} &= E(\underline{x}_{i+1}\hat{\underline{x}}_i^T)(\underline{C}_{\hat{x}_i})^{-1}\hat{\underline{x}}_i \\ &= E\big([\underline{S}(i+1,i)\underline{x}_i + \underline{w}_i]\hat{\underline{x}}_i^T\big)(\underline{C}_{\hat{x}_i})^{-1}\hat{\underline{x}}_i \\ &= [\underline{S}(i+1,i)E(\underline{x}_i\hat{\underline{x}}_i^T) + E(\underline{w}_i\hat{\underline{x}}_i^T)](\underline{C}_{\hat{x}_i})^{-1}\hat{\underline{x}}_i\end{aligned} \tag{B.64}$$

By hypotheses,

$$\begin{aligned}E(\underline{w}_i\hat{\underline{x}}_i^T) &= E(\hat{\underline{x}}_i\underline{w}_i^T) = E(\underline{A}\underline{\theta}_i\underline{w}_i^T) \\ &= \underline{A}E(\underline{\theta}_i\underline{w}_i^T) = \underline{A}E[(\underline{B}\underline{x}_i + \underline{v}_i)\underline{w}_i^T] \\ &= \underline{A}[\underline{B}E(\underline{x}_i\underline{w}_i^T) + E(\underline{v}_i\underline{w}_i^T)] \\ &= 0\end{aligned} \tag{B.65}$$

Hence,

$$\hat{\underline{x}}_{i+1}^{p} = \underline{S}(i+1,i)\underline{C}_{x_i\hat{x}_i}(\underline{C}_{\hat{x}_i})^{-1}\hat{\underline{x}}_i \tag{B.66}$$

However,

$$\underline{C}_{x_i\hat{x}_i} = \underline{C}_{\hat{x}_i x_i}^T = \underline{C}_{\hat{x}_i} \tag{B.67}$$

and therefore,

$$\begin{aligned}\hat{\underline{x}}_{i+1}^{p} &= \underline{S}(i+1,i)\underline{C}_{\hat{x}_i}(\underline{C}_{\hat{x}_i})^{-1}\hat{\underline{x}}_i \\ &= \underline{S}(i+1,i)\hat{\underline{x}}_i\end{aligned} \tag{B.68}$$

Error Covariance Matrix of Predicted State

The corresponding expression for the error matrix of the predicted state Eq.(B.68) of the preceding section is given by

$$
\begin{aligned}
\underline{C}_{i+1}^{p} &= E[(\hat{\underline{x}}_{i+1}^{p} - \underline{x}_{i+1})(\hat{\underline{x}}_{i+1}^{p} - \underline{x}_{i+1})^T] \\
&= E[(\underline{S}(i+1,i)\hat{\underline{x}}_i - \underline{S}(i+1,i)\underline{x}_i - \underline{w}_i)(\underline{S}(i+1,i)\hat{\underline{x}}_i - \underline{S}(i+1,i)\underline{x}_i - \underline{w}_i)^T] \\
&= E\big([\underline{S}(i+1,i)(\hat{\underline{x}}_i - \underline{x}_i) - \underline{w}_i][\underline{S}(i+1,i)(\hat{\underline{x}}_i - \underline{x}_i) - \underline{w}_i]^T\big) \\
&= E[(\underline{S}(i+1,i)\underline{e}_i - \underline{w}_i)(\underline{S}(i+1,i)\underline{e}_i - \underline{w}_i)^T] \\
&= \underline{S}(i+1,i)E(\underline{e}_i\underline{e}_i^T)\underline{S}^T(i+1,i) - E[\underline{w}_i\underline{e}_i^T\underline{S}^T(i+1,i)] \\
&\quad - E[\underline{S}(i+1,i)\underline{e}_i\underline{w}_i^T] + E(\underline{w}_i\underline{w}_i^T) \\
&= \underline{S}(i+1,i)\underline{C}_i\underline{S}^T(i+1,i) - E(\underline{w}_i\underline{e}_i^T)\underline{S}^T(i+1,i) - \underline{S}(i+1,i)E(\underline{e}_i\underline{w}_i^T) + \underline{W}_i
\end{aligned}
\tag{B.69}
$$

Reference [83] has shown that subject to the correlation conditions of Eqs.(B.57),

$$
\begin{aligned}
\underline{W}_i &= 0 \\
E(\underline{e}_i\underline{w}_i^T) &= 0 \\
E(\underline{w}_i\underline{e}_i^T) &= 0
\end{aligned}
\tag{B.70}
$$

Thus, finally,

$$
\underline{C}_{i+1}^{p} = \underline{S}(i+1,i)\underline{C}_i\underline{S}^T(i+1,i) + \underline{W}_i \tag{B.71}
$$

State Estimate for the Next Time Step

Using the most recent set of measurements, the predicted state estimate of Eq.(B.68) can be refined to yield the state estimate for the next time step. This is accomplished by using and adapting the Kalman form of Eq.(B.55) to suit the present objective. For convenience, Eq.(B.55) is repeated.

$$\hat{\underline{x}}^m = \hat{\underline{x}}^r + \underline{K}(\underline{\theta}^s - \underline{B}^s \hat{\underline{x}}^r) \qquad (B.55)$$

In the present problem, the following substitutions are applicable (with s = 1):

$$\hat{\underline{x}}_{i+1} = \hat{\underline{x}}^m$$

$$\hat{\underline{x}}^p_{i+1} = \hat{\underline{x}}^r$$

$$\underline{\theta} = \underline{\theta}^s \qquad (B.72)$$

$$\underline{B} = \underline{B}^s$$

where

$$\underline{\theta} = \underline{B}\underline{x}_{i+1} + \underline{v}_{i+1} \qquad (B.73)$$

$\underline{x}_{i+1}$ = state vector at next time step

$\underline{v}_{i+1}$ = random measurement noise q-vector at next time step

$\underline{\theta}$ = most recent measurement vector

$\hat{x}_{i+1}$ = state vector estimate for the next time step

$\hat{x}^p_{i+1}$ = predicted state estimate

Thus,

$$\hat{x}_{i+1} = \hat{x}^p_{i+1} + K(\underline{\theta} - B\hat{x}^p_{i+1}) \tag{B.74}$$

The matrix K is therefore computed at every time step as (following Eq.(B.51))

$$K = C^p_{i+1}B^T[V_{i+1} + BC^p_{i+1}B^T]^{-1} \tag{B.75}$$

where

$$V_{i+1} = E[\underline{\mu}_{i+1}\underline{\mu}^T_{i+1}]$$

From Eq.(B.53), the estimate error covariance matrix at the next time step is

$$C_{i+1} = C^p_{i+1} - KBC^p_{i+1} \tag{B.76}$$

Steady-State Solution for the Linear Filter

As the value of the time step "i" in the previous sections approaches a very large value, the covariance matrices C^p_i and C_i and the Kalman filter gain matrix K approach constant steady-state values if the state disturbance and measurement noise covariance matrices W_i and V_i are assumed constant. Therefore, for a system described by the state

transition Eq.(B.61), measurement Eq.(B.73), and estimate Eq.(B.74), the steady-state solutions for the matrices are given by

$$\underline{K}_{\infty} = \underline{C}_{\infty}^{p} \underline{B}^{T} [\underline{V} + \underline{B} \underline{C}_{\infty}^{p} \underline{B}^{T}]^{-1}$$

$$\underline{C}_{\infty}^{p} = \underline{S}(i+1,i) \underline{C}_{\infty} \underline{S}^{T}(i+1,i) + \underline{W} \qquad (B.77)$$

$$\underline{C}_{\infty} = \underline{C}_{\infty}^{p} - \underline{K}_{\infty} \underline{B} \underline{C}_{\infty}^{p}$$

following Eqs.(B.75),(B.71),and (B.76). Moreover, $\underline{W}$ and $\underline{V}$ are the assumed constant covariance matrices representing the state disturbances and noise measurements. The corresponding state estimate equation at steady-state is then

$$\hat{\underline{x}}_{i+1} = \hat{\underline{x}}_{i+1}^{p} + \underline{K}_{\infty} (\underline{\theta} - \underline{B} \hat{\underline{x}}_{i+1}^{p}) \qquad (B.78)$$

Filtering for a Nonlinear System

This last section of the appendix wiil consider the question of state estimation for a nonlinear system. The system state equations are assumed to be expressed as the sum of a linear term, a random residual vector the relationship of which to the state vector is unknown, and a random state disturbance vector which is distinct from the residual term. Moreover, a measured quantity at any time is assumed to represent the sum of a linear combination of the current state variables and the measurement noise. Use shall be made of some equations from the linear filter solution wherever applicable. Underlying assumptions which can represent limitations to optimal performance of the estimator will be brought out and related to the equations used for the estimator itself. In

this connection, a semi-rigorous approach will be used. The final resulting equations are used in this paper in the Chapter on state estimation.

The state transition equations are expressed as

$$\underline{x}_{i+1} = \underline{S}(i+1,i)\underline{x}_i + \underline{r}_i + \underline{w}_i \tag{B.79}$$

The measured quantities are given by the vector

$$\underline{\theta} = \underline{B}\underline{x}_{i+1} + \underline{v}_{i+1} \tag{B.80}$$

In the state transition equations, the quantity sum $\underline{w}_i$ represents the assumed total state disturbance. At each time step, the vector $\underline{r}_i$ is actually unknown and only the values of $\hat{\underline{r}}_i$ and $\hat{\underline{x}}_i$ are available. Assuming that the random variables $\underline{r}_i$ and $\underline{x}_i$ are uncorrelated (which may not be true in reality), and utilizing Eq.(B.68),

$$\hat{\underline{x}}^p_{i+1} = \underline{S}(i+1,i)\hat{\underline{x}}_i + \hat{\underline{r}}_i \tag{B.81}$$

The last equation makes use of the same noncorrelation and zero-mean assumptions for the components of the state disturbances. It was possible to decompose the predicted state into two components as a result of the assumed statistical independence between $\hat{\underline{x}}_i$ and $\hat{\underline{r}}_i$. At this point, it is noted that the refinement of the predicted state vector $\hat{\underline{x}}^p_{i+1}$ using the most recent set of measurements is identical to that of the linear filter (Eqs.(B.74) and (B.75)). It also follows that computation of the error covariance matrix for the next state estimates from the error covariance matrix for the predicted states should be identical to Eq.(B.76). The equations are repeated here for convenience.

$$\hat{\underline{x}}_{i+1} = \hat{\underline{x}}^p_{i+1} + \underline{K}(\underline{\theta} - \underline{B}\hat{\underline{x}}^p_{i+1}) \tag{B.74}$$

$$\underline{K} = \underline{C}_{i+1}^{p} \underline{B}^T [\underline{V}_{i+1} + \underline{B} \underline{C}_{i+1}^{p} \underline{B}^T]^{-1} \tag{B.75}$$

$$\underline{C}_{i+1} = \underline{C}_{i+1}^{p} - \underline{K} \underline{B} \underline{C}_{i+1}^{p} \tag{B.76}$$

At this point, the only step left to be determined in the state estimation of a nonlinear system is the computation of the error covariance matrix for predicted states from the current values of the filter matrices. This necessary equation will be determined by appealing to the basic definition of the covariance matrix. Thus,

$$\underline{C}_{i+1}^{p} = E[(\hat{\underline{x}}_{i+1} - \underline{x}_{i+1})(\hat{\underline{x}}_{i+1} - \underline{x}_{i+1})^T] \tag{B.82}$$

In the last equation,

$$(\hat{\underline{x}}_{i+1} - \underline{x}_{i+1}) = [\underline{S}(i+1,i)\hat{\underline{x}}_i + \hat{\underline{r}}_i] - [\underline{S}(i+1,i)\underline{x}_i + \underline{r}_i + \underline{w}_i] \tag{B.83}$$

After substituting the last expression into Eq.(B.82) and making use of the noncorrelation assumptions between $\underline{x}_i$, $\underline{r}_i$, and $\underline{w}_i$, Eq.(B.82) simplifies to

$$\underline{C}_{i+1}^{p} = E[\underline{S}(i+1,i)(\hat{\underline{x}}_i - \underline{x}_i)(\hat{\underline{x}}_i - \underline{x}_i)^T \underline{S}^T(i+1,i) + \underline{w}_i \underline{w}_i^T + (\hat{\underline{r}}_i - \underline{r}_i)(\hat{\underline{r}}_i - \underline{r}_i)^T] \tag{B.84}$$

$$\begin{aligned} \underline{C}_{i+1}^{p} &= \underline{S}(i+1,i) E[(\hat{\underline{x}}_i - \underline{x}_i)(\hat{\underline{x}}_i - \underline{x}_i)^T] \underline{S}^T(i+1,i) + E[\underline{w}_i \underline{w}_i^T] + E[\underline{e}_r \underline{e}_r^T] \\ &= \underline{S}(i+1,i) \underline{C}_i \underline{S}^T(i+1,i) + \underline{J}_i \end{aligned} \tag{B.85}$$

where

$$\begin{aligned} \underline{J}_i &= \underline{W}_i + E[\underline{e}_r \underline{e}_r^T] \\ \underline{e}_r &= (\hat{\underline{r}}_i - \underline{r}_i) \end{aligned} \tag{B.87}$$

The last equation is similar to Eq.(B.71) except for the addition of the term $E[\underline{e}_i\underline{e}_i^T]$ in Eq.(B.85). This term is the covariance matrix of the error in the estimate $\hat{\underline{x}}_i$. The four Eqs.(B.74),(B.75),(B.76), and (B.85) correspond to the following steady-state solution to the nonlinear filtering problem assuming non-time varying covariance matrices $\underline{W}$, $\underline{V}$, and $\underline{J}$:

$$\underline{K}_\infty = \underline{C}_\infty^p \underline{B}^T [\underline{V} + \underline{B}\underline{C}_\infty^p \underline{B}^T]^{-1}$$

$$\underline{C}_\infty^p = \underline{S}(i+1,i)\underline{C}_\infty \underline{S}^T(i+1,i) + \underline{J} \qquad (B.88)$$

$$\underline{C}_\infty = \underline{C}_\infty^p - \underline{K}_\infty \underline{B}\underline{C}_\infty^p$$

The state estimate equations are

$$\begin{aligned} \hat{\underline{x}}_{i+1} &= \hat{\underline{x}}_{i+1}^p + \underline{K}_\infty(\underline{\theta} - \underline{B}\hat{\underline{x}}_{i+1}^p) \\ \hat{\underline{x}}_{i+1}^p &= \underline{S}(i+1,i)\hat{\underline{x}}_i + \hat{\underline{L}}_i \end{aligned} \qquad (B.89)$$

The chapter on state estimation of this paper will present simulation results based on the formulas justified in this appendix. To reconcile the unidentical notation used in this appendix and in the Chapter on state estimation, equivalent expressions between the two notations are shown on Table B.1.

Table B.1. Equivalence of Chapter 6 and Appendix B Notations

Appendix B Notation	Chapter 6 Notation
$\underline{S}(i+1,i)$	$\underline{\Phi}$
$\underline{B}$	$\underline{H}$
$\underline{x}_i$	$\underline{X}(k\|k)$
$\underline{r}_i$	$\underline{\Psi U}(k) + \underline{\Gamma f}(k)$
$\underline{\theta}$	$\underline{Z}(k+1)$
$\hat{\underline{x}}_i$	$\hat{\underline{X}}(k\|k)$
$\hat{\underline{x}}_{i+1}$	$\hat{\underline{X}}(k+1\|k)$
$\hat{\underline{r}}_i$	$\underline{\Psi U}(k) + \underline{\Gamma}\hat{\underline{f}}(k)$
$\underline{w}_i$	$\underline{w}(k)$
$\underline{v}_i$	$\underline{v}(k)$
$\underline{W}_i$	$\underline{\Gamma Q \Gamma}^T$
$\underline{V}_i$	$\underline{R}$
$\underline{C}_{i+1}^p$	$\underline{P}(k+1\|k)$
$\underline{C}_{i+1}$	$\underline{P}(k+1\|k+1)$
$\underline{K}$	$\underline{K}(k+1)$
$\underline{K}_\infty$	$\underline{K}(\infty)$

Appendix C

Derivation of Control Equations

These derivations will be based mainly on the work done in references [77,80] utilizing the variational approach and Pontryagin's maximum principle. The general results of reference [80] will be invoked initially. The work in reference [77] will then be extended slightly to account for the residual term in the output equation.

Given the nonlinear system of differential equations

$$\dot{\underline{X}}(t) = \underline{F}(\underline{X}(t), \underline{U}(t), t) \tag{C.1}$$

and the cost function

$$J(\underline{U}) = \phi[\underline{X}(t_f), t_f] + \int_{t_o}^{t_f} \ell[\underline{X}(t), \underline{U}(t), t]\, dt \tag{C.2}$$

The Hamiltonian $\mathscr{H}$ is given by

$$\mathcal{H} = \ell[\underline{X}(t), \underline{U}(t), t] + \underline{P}^T(t)[\underline{F}(\underline{X}(t), \underline{U}(t), t)] \quad . \tag{C.3}$$

where $\underline{P}(t)$ is the costate vector of Lagrange multipliers. The optimal conditions are

$$\begin{aligned} \dot{\underline{X}}(t) &= \frac{\partial \mathcal{H}}{\partial \underline{P}(t)} \\ \dot{\underline{P}}(t) &= \frac{-\partial \mathcal{H}}{\partial \underline{X}(t)} \\ \underline{0} &= \frac{\partial \mathcal{H}}{\partial \underline{U}(t)} \end{aligned} \tag{C.4}$$

The final condition (at t_f) for the state and costate vector is

$$\frac{\partial \phi[\underline{X}(t_f), t_f]}{\partial \underline{X}(t_f)} - \underline{P}(t_f) = \underline{0} \tag{C.5}$$

In the present problem,

$$\underline{F}(\underline{X}(t), \underline{U}(t), t) = A\underline{X}(t) + B\underline{U}(t) + \underline{f}(t) \tag{C.6}$$

$$\ell[\underline{X}(t), \underline{U}(t), t] = \underline{U}^T(t)R\underline{U}(t) + [\underline{Y}(t) - \underline{Y}_d(t)]^T Q[\underline{Y}(t) - \underline{Y}_d(t)] \tag{C.7}$$

where

$$\underline{Y}(t) = C\underline{X}(t) + \underline{s}(t)$$

and

$$\phi[\underline{X}(t_f), t_f] = [\underline{Y}(t_f) - \underline{Y}_d(t_f)]^T H[\underline{Y}(t_f) - \underline{Y}_d(t_f)] \tag{C.8}$$

Thus, the Hamiltonian is given by

$$\mathcal{H} = \frac{1}{2}[C\underline{X}(t) + \underline{s}(t) - \underline{Y}_d(t)]^T Q[C\underline{X}(t) + \underline{s}(t) - \underline{Y}_d(t)]$$

$$+ \frac{1}{2}[\underline{U}^T(t) R \underline{U}(t)] + \underline{P}^T[A\underline{X}(t) + B\underline{U}(t) + \underline{f}(t)] \qquad (C.9)$$

$$\mathcal{H} = \frac{1}{2}[\underline{X}^T(t) C^T Q C \underline{X}(t) - \underline{X}^T(t) C^T Q \underline{Y}_d(t)]$$

$$- \frac{1}{2}[\underline{Y}_d^T(t) Q C \underline{X}(t) - \underline{Y}_d^T(t) Q \underline{Y}_d(t)]$$

$$+ \frac{1}{2}[\underline{X}^T(t) C^T Q \underline{s}(t)] - \frac{1}{2}[\underline{Y}_d^T(t) Q \underline{s}(t)]$$

$$+ \frac{1}{2}[\underline{s}^T(t) C^T Q C \underline{X}(t)] + \frac{1}{2}[\underline{s}^T(t) Q \underline{s}(t)]$$

$$- \frac{1}{2}[\underline{s}^T(t) Q \underline{Y}_d(t)] + \frac{1}{2}[\underline{U}^T(t) R \underline{U}(t)]$$

$$+ \underline{P}^T[A\underline{X}(t)] + \underline{P}^T[B\underline{U}(t)] + \underline{P}^T[\underline{f}(t)] \qquad (C.10)$$

Applying the necessary optimal conditions,

$$\dot{\underline{X}}(t) = \frac{\partial \mathcal{H}}{\partial \underline{P}(t)} = A\underline{X}(t) + B\underline{U}(t) + \underline{f}(t) \qquad (C.11)$$

$$\dot{\underline{P}}(t) = \frac{-\partial \mathcal{H}}{\partial \underline{X}(t)}$$

$$= -C^T Q C \underline{X}(t) + C^T Q \underline{Y}_d(t)$$

$$- \frac{1}{2} C^T Q \underline{s}(t) - \frac{1}{2} C^T Q \underline{s}(t) - A^T \underline{P}(t)$$

$$= - C^T Q C \underline{X}(t) + C^T Q \underline{Y}_d(t) - C^T Q \underline{s}(t) - A^T \underline{P}(t) \tag{C.12}$$

$$\underline{0} = \frac{\partial \mathcal{H}}{\partial \underline{U}(t)} = R\underline{U}(t) + B^T \underline{P}(t) \tag{C.13}$$

or

$$\underline{U}^*(t) = - R^{-1} B^T \underline{P}(t) \tag{C.14}$$

The augmented state and costate equations upon substitution of equation (C.14) into equation (C.11) results in

$$\begin{bmatrix} \dot{\underline{X}}(t) \\ \dot{\underline{P}}(t) \end{bmatrix} = \begin{bmatrix} A & - BR^{-1}B^T \\ - C^T Q C & - A^T \end{bmatrix} \begin{bmatrix} \underline{X}(t) \\ \underline{P}(t) \end{bmatrix} + \begin{bmatrix} \underline{f}(t) \\ C^T Q \underline{Y}_d(t) - C^T Q \underline{s}(t) \end{bmatrix} \tag{C.15}$$

The solution of the differential equation for $\underline{X}(t_f)$ and $\underline{P}(t_f)$ has the form

$$\begin{bmatrix} \underline{X}(t_f) \\ \underline{P}(t_f) \end{bmatrix} = \Phi(t_f, t) \begin{bmatrix} \underline{X}(t) \\ \underline{P}(t) \end{bmatrix} + \int_t^{t_f} \Phi(t_f, \tau) \begin{bmatrix} \underline{f}(t) \\ C^T Q \underline{Y}_d(t) - C^T Q \underline{s}_d(t) \end{bmatrix} d\tau \tag{C.16}$$

Applying the required final conditions,

$$\frac{\partial \{ \frac{1}{2} [C(t_f)\underline{X}(t_f) + \underline{s}(t_f) - \underline{Y}_d(t_f)]^T H [C(t_f)\underline{X}(t_f) + \underline{s}(t_f) - \underline{Y}_d(t_f)] \}}{\partial \underline{X}(t_f)} - \underline{P}(t_f) = \underline{0}$$

or

$$\underline{P}(t_f) = \frac{\partial}{\partial \underline{X}(t_f)} [\,\cdot\,] \tag{C.17}$$

where

$$[\,\cdot\,] = \frac{1}{2} X^T(t_f) C^T H C X(t_f) - \frac{1}{2} X^T(t_f) C^T H Y_d(t_f) - \frac{1}{2} Y_d(t_f) H C X_d(t_f)$$

$$+ \frac{1}{2} Y_d^T(t_f) H Y_d(t_f) + \frac{1}{2} X^T(t_f) C^T H s_d(t_f) - \frac{1}{2} Y_d(t_f) H s(t_f)$$

$$+ \frac{1}{2} s^T(t_f) H s(t_f) + \frac{1}{2} s^T(t_f) H C X(t_f) - \frac{1}{2} s^T(t_f) H Y_d(t_f)$$

Thus,

$$P(t_f) = C^T H C X(t_f) - \frac{1}{2} C^T H Y_d(t_f)$$

$$- \frac{1}{2} C^T H Y_d(t_f) + \frac{1}{2} C^T H s(t_f) + \frac{1}{2} C^T H^T s(t_f) \qquad (C.18)$$

For a symmetrical H matrix,

$$P(t_f) = C^T H C X(t_f) - C^T H Y_d(t_f) + C^T H s(t_f) \qquad (A-19)$$

Replacement of the integral term in equation (C.16) by two functions $f_1(t)$ and $f_2(t)$ and partitioning the state transition matrix results in:

$$\begin{bmatrix} X(t_f) \\ P(t_f) \end{bmatrix} = \begin{bmatrix} \phi_{11}(t_f,t) & \phi_{12}(t_f,t) \\ \phi_{21}(t_f,t) & \phi_{22}(t_f,t) \end{bmatrix} \begin{bmatrix} X(t) \\ P(t) \end{bmatrix} + \begin{bmatrix} f_1(t) \\ f_2(t) \end{bmatrix} \qquad (C.20)$$

or

$$X(t_f) = \phi_{11}(t_f,t) X(t) + \phi_{12}(t_f,t) P(t) + f_1(t) \qquad (C.21)$$

$$\underline{P}(t_f) = \phi_{21}(t_f,t)\underline{X}(t) + \phi_{22}(t_f,t)\underline{P}(t) + \underline{f}_2(t) \tag{C.22}$$

Substitution of $\underline{P}(t_f)$ as given by (C.19) into (C.22) results in:

$$C^T HC\underline{X}(t_f) - C^T H\underline{Y}_d(t_f) + C^T H\underline{s}(t_f) =$$

$$\phi_{21}(t_f,t)\underline{X}(t) + \phi_{22}(t_f,t)\underline{P}(t) + \underline{f}_2(t) \tag{C.23}$$

Substitution of (C.21) into (C.23) gives:

$$C^T HC[\phi_{11}(t_f,t)\underline{X}(t) + \phi_{12}(t_f,t)\underline{P}(t) + \underline{f}_1(t)] - C^T H\underline{Y}_d(t_f) + C^T H\underline{s}(t_f) =$$

$$\phi_{21}(t_f,t)\underline{X}(t) + \phi_{22}(t_f,t)\underline{P}(t) + \underline{f}_2(t) \tag{C.24}$$

Simplifying,

$$[C^T HC\phi_{12}(t_f,t) - \phi_{22}(t_f,t)]\underline{P}(t) = [\phi_{21}(t_f,t) - C^T HC\phi_{11}(t_f,t)]\underline{X}(t) +$$

$$[C^T H\underline{Y}_d(t_f) + \underline{f}_2(t) - C^T HC\underline{f}_1(t) - C^T H\underline{s}(t_f)] \tag{C.25}$$

$$\underline{P}(t) = K(t)\underline{X}(t) - \underline{g}(t) \tag{C.26}$$

where

$$K(t) = [C^T HC\phi_{12}(t_f,t) - \phi_{22}(t_f,t)]^{-1}[\phi_{21}(t_f,t) - C^T HC\phi_{11}(t_f,t)] \tag{C.27}$$

$$\underline{g}(t) = [C^T HC\phi_{12}(t_f,t) - \phi_{22}(t_f,t)]^{-1}$$
$$[-C^T H\underline{Y}_d(t_f) - \underline{f}_2(t) + C^T HC\underline{f}_1(t) + C^T H\underline{s}(t_f)] \tag{C.28}$$

Eq.(C.26) is the relationship needed for a direct solution approach. Substitution of Eq.(C.26) into Eq.(C.14) and simplifying,

$$\underline{U}^*(t) = -R^{-1}B^T[K(t)\underline{X}(t) - \underline{g}(t)] \tag{C.29}$$

$$\underline{U}^*(t) = R^{-1}B^T[\underline{g}(t) - K(t)\underline{X}(t)] \tag{C.30}$$

$$\underline{U}^*(t) = -R^{-1}B^TK(t)\underline{X}(t) + R^{-1}B^T\underline{g}(t) \tag{C.31}$$

To solve for K(t) and g(t), (19) is differentiated:

$$\dot{\underline{P}}(t) = \dot{K}(t)\underline{X}(t) + K(t)\dot{\underline{X}}(t) - \dot{\underline{g}}(t) \tag{C.32}$$

Then (C.11) is substituted into (C.32) and $\underline{U}(t)$ is replaced by the $\underline{U}^*(t)$ expression of (C.31):

$$\dot{\underline{P}}(t) = \dot{K}(t)\underline{X}(t) + K(t)[A\underline{X}(t) + B\underline{U}(t) + \underline{f}(t)] - \dot{\underline{g}}(t) \quad = \dot{K}(t)\underline{X}(t) +$$

$$K(t)\{A\underline{X}(t) + B[-R^{-1}B^TK(t)\underline{X}(t) + R^{-1}B^T\underline{g}(t)] + \underline{f}(t)\} - \dot{\underline{g}}(t) \tag{C.33}$$

Using Eqs.(C.12),(C.26),and (C.33),

$$-C^TQC\underline{X}(t) + C^TQ\underline{Y}_d(t) - C^TQ\underline{s}(t) - A^T[K(t)\underline{X}(t) - \underline{g}(t)] =$$

$$\dot{K}(t)\underline{X}(t) + K(t)[A\underline{X}(t) - BR^{-1}B^TK(t)\underline{X}(t)] +$$

$$K(t)BR^{-1}B^T\underline{g}(t) + K(t)\underline{f}(t) - \dot{\underline{g}}(t) \tag{C.34}$$

Rearranging terms,

$$[\dot{K}(t) + K(t)A - K(t)BR^{-1}B^T g(t) + C^T QC + A^T K(t)]\underline{X}(t) +$$

$$[K(t)BR^{-1}B^T \underline{g}(t) + K(t)\underline{f}(t) - \dot{\underline{g}}(t) - A^T \underline{g}(t) - C^T Q\underline{Y}_d(t) + C^T Q\underline{s}(t)]$$

$$= 0 \qquad (C.35)$$

The above equation is satisfied when the quantities inside each bracket is zero. Thus,

$$\dot{K}(t) = -A^T K(t) - K(t)A + K(t)BR^{-1}B^T K(t) - C^T QC \qquad (C.36)$$

$$\dot{\underline{g}}(t) = -[A^T - K(t)BR^{-1}B^T]\underline{g}(t) - C^T Q\underline{Y}_d(t) + C^T Q\underline{s}(t) \qquad (C.37)$$

From (C.26), at $t = t_f$,

$$\underline{P}(t_f) = K(t_f)\underline{X}(t_f) - \underline{g}(t_f) \qquad (C.38)$$

and from (C.19),

$$C^T HC\underline{X}(t_f) - C^T H\underline{Y}_d(t_f) + C^T H\underline{s}(t_f) = K(t_f)\underline{X}(t_f) - \underline{g}(t_f) \qquad (C.39)$$

Hence,

$$K(t_f) = C^T HC \qquad (C.40)$$

and

$$\underline{g}(t_f) = C^T H[\underline{Y}_d(t_f) - \underline{s}(t_f)] \qquad (C.41)$$

Appendix D

Matrices of Partial Derivatives

This appendix will show the elements of the partial derivative matrices used in the linearization process of Chapter 5. The notation to be used in Appendix 4 is consistent with the notation of Chapter 5.

Here,

NBUS = total number of buses in the power system = 39
NG = total number of generators in the system = 10

For a typical generator, there are 10 associated state variables. For the base case study (Case 1), the centralized controller has 91 state variables.

In the following, the sizes of the matrices of partial derivatives will be given together with their nonzero elements. All other elements not mentioned should be understood to be zero. The following subscripts will be adopted :

i to denote a generator $(1 \le i \le 10)$
j to denote a controller variable $(1 \le j \le 91)$
k to denote a power system bus $(1 \le k \le 39)$

The linearized controller state equation is given by

$$\dot{\underline{X}}(t) = \underline{G}_o + \left[\frac{\partial \underline{G}}{\partial \underline{\chi}} + \frac{\partial \underline{G}}{\partial \underline{E}_t} \frac{\partial \underline{E}_t}{\partial \underline{\chi}} + \frac{\partial \underline{G}}{\partial \underline{\delta}_{tr}} \frac{\partial \underline{\delta}_{tr}}{\partial \underline{\chi}} \right] \underline{X}(t) + + \frac{\partial \underline{G}}{\partial \underline{U}} \underline{U}(t) + \underline{f}(\underline{\chi}(t))$$

where

$$\dot{\underline{\chi}}(t) = \underline{G}(\, \underline{\chi}(t), \underline{U}(t), \underline{E}_t(\underline{\chi}(t)), \underline{\delta}_{tr}(\underline{\chi}(t)) \,)$$

$$\underline{E}_t = [E_{t1} \;\; E_{t2} \;\; \cdots \;\; E_{ti} \;\; \cdots \;\; E_{t10}]^T$$

$$\underline{\delta}_{tr} = [(\delta_{t1} - \delta_{q10}) \;\; (\delta_{t2} - \delta_{q10}) \;\; \cdots \;\; (\delta_{ti} - \delta_{q10}) \;\; \cdots \;\; (\delta_{t10} - \delta_{q10})]^T$$

(1).Let $\underline{L} = \dfrac{\partial \underline{G}}{\partial \underline{\chi}}$, a 91 x 91 matrix.

Nonzero elements of $\underline{L}$ are given by (i = 1, 2, ...,9):

$$\underline{L}[10*(i-1)+1,\; 10*(i-1)+1] = \frac{-1}{T_{do,i}} \left(\frac{x_{di}}{x'_{di}} \right)$$

$$\underline{L}[10*(i-1)+1,\; 10*(i-1)+2] = \frac{1}{T_{do,i}} \left(\frac{x_{di}}{x'_{di}} - 1 \right) E_{ti} \sin(\delta_{tr,i} - \delta_{qr,i})$$

$$\underline{L}[10*(i-1)+1,\; 10*(i-1)+7] = \frac{1}{T_{do,i}}$$

$$\underline{L}[10*(i-1)+2,\; 10*(i-1)+3] = 2\pi \times 60.0$$

$$L[10*(i-1)+3,\ 10*(i-1)+1] = \frac{-1}{M_i}\left(\frac{E_{ti}}{x'_{di}}\right)\sin(\delta_{qr,i} - \delta_{tr,i})$$

$$L[10*(i-1)+3,\ 10*(i-1)+2] = \frac{-1}{M_i}\left[\frac{E'_{qi}E_{ti}}{x'_{di}}\cos(\delta_{qr,i} - \delta_{tr,i})\right] + \frac{1}{M_i}\left[\frac{E_{ti}^2}{x'_{di}x_{qi}}(x_{qi} - x_{di})\cos[2(\delta_{qr,i} - \delta_{tr,i})]\right]$$

$$L[10*(i-1)+3,\ 10*(i-1)+3] = \frac{-D_i}{M_i} \quad \text{(approximation)}$$

$$L[10*(i-1)+3,\ 10*(i-1)+10] = \frac{1}{M_i}$$

$$L[10*(i-1)+4,\ 10*(i-1)+4] = \frac{-1}{T_{ri}}$$

$$L[10*(i-1)+5,\ 10*(i-1)+4] = \frac{-K_{ai}}{T_{ai}}$$

$$L[10*(i-1)+5,\ 10*(i-1)+5] = \frac{-1}{T_{ai}}$$

$$L[10*(i-1)+5,\ 10*(i-1)+6] = \frac{-K_{ai}}{T_{ai}}$$

$$L[10*(i-1)+6,\ 10*(i-1)+5] = \frac{K_{fi}}{T_{fi}T_{Ei}}$$

$$L[10*(i-1)+6,\ 10*(i-1)+6] = \frac{-1}{T_{fi}}$$

$$L[10*(i-1)+6,\ 10*(i-1)+7] = \frac{-K_{fi}}{T_{fi}T_{Ei}}[S_{Ei}(1 + B_{ei}E_{fd,i}) + K_{Ei}]$$

$$L[10*(i-1)+7,\ 10*(i-1)+5] = \frac{1}{T_{Ei}}$$

$$L[10*(i-1)+7,\ 10*(i-1)+7] = \frac{-1}{T_{Ei}}[S_{Ei}(1 + B_{ei}E_{fd,i}) + K_{Ei}]$$

$$L[10*(i-1)+8,\ 10*(i-1)+3] = \frac{C_{Gi}}{T_{1i}} \quad \text{(approximation)}$$

$$L[10*(i-1)+8,\ 10*(i-1)+8] = \frac{-1}{T_{1i}}$$

$$L[10*(i-1)+9,\ 10*(i-1)+8] = \frac{-1}{T_{3i}}$$

$$L[10*(i-1)+9,\ 10*(i-1)+9] = \frac{-1}{T_{3i}}$$

$$L[10*(i-1)+10,\ 10*(i-1)+9] = \frac{-1}{T_{CH,i}}$$

$$L[10*(i-1)+10,\ 10*(i-1)+10] = \frac{-1}{T_{CH,i}}$$

For i = 10,

$$L[91, 91] = -\frac{1}{T_{do,10}}\left(\frac{x_{d10}}{x'_{d10}}\right)$$

(2).Let $M = \frac{\partial G}{\partial U}$, a 91 x 18 matrix.

Its nonzero elements are given by (i = 1, 2, ...,9) :

$$M[10*(i-1)+5,\ 2*(i-1)+1] = \frac{K_{ai}}{T_{ai}}$$

$$M[10*(i-1)+9,\ 2*(i-1)+2] = \frac{1}{T_{3i}}$$

(3).Let $N = \frac{\partial G}{\partial E_t}$, a 91 x 10 matrix.

Its nonzero elements are given by (i = 1, 2, ..., 9) :

$$N[10*(i-1)+1,\ i] = \frac{1}{T'_{do,i}}\left(\frac{x_{di}}{x'_{di}} - 1\right)\cos(\delta_{qr,i} - \delta_{tr,i})$$

$$N[10*(i-1)+3,\ i] = \frac{-1}{M_i}\frac{E'_{qi}}{x'_{di}}\sin(\delta_{qr,i} - \delta_{tr,i}) + \frac{1}{M_i}\frac{E_{ti}}{x'_{di}x_{qi}}(x_{qi} - x'_{di})\sin[2(\delta_{qr,i} - \delta_{tr,i})] \quad \text{(approximation)}$$

For i = 10,

$$N[91,\ 10] = \frac{1}{T'_{do,10}}\left(\frac{x_{d10}}{x'_{d10}} - 1\right)\cos(\delta_{qr,10} - \delta_{tr,10})$$

(4).Let $T = \frac{\partial G}{\partial \delta_{tr}}$, a 91 x 10 matrix.

Its nonzero elements are given by (i = 1, 2, ..., 9) :

$$T[10*(i-1)+1,\ i] = \frac{1}{T'_{do,i}}\left[\left(\frac{x_{di}}{x'_{di}} - 1\right)E_{ti}\right]\sin(\delta_{qr,i} - \delta_{tr,i})$$

$$I[10*(i-1)+3,\ i] = \frac{-1}{M_i}\left[\frac{-E'_{qi}E_{ti}}{x'_{di}}\cos(\delta_{qr,i}-\delta_{tr,i})\right] - \frac{1}{M_i}\left[\frac{E_{ti}^2}{x'_{di}x_{qi}}(x_{qi}-x_{di})\cos[2(\delta_{qr,i}-\delta_{tr,i})]\right]$$

For i = 10,

$$I[91,\ 10] = \frac{1}{T'_{do,10}}\left[\left(\frac{x_{d10}}{x'_{d10}}-1\right)E_{t10}\right]\sin(0-\delta_{tr,10})$$

(5).Let $\underline{V} = \frac{\partial E_t}{\partial \underline{\chi}}$ and $\underline{W} = \frac{\partial \underline{\delta}_{tr}}{\partial \underline{\chi}}$, both 10 x 91 matrices.

As stated in Chapter 5, nonzero elements of $\underline{V}$ and $\underline{W}$ are contained in the $\underline{C}_1$ matrix where

$$\underline{C}_1 = -\underline{J}_A^{-1}\underline{J}_B$$

and

$$\begin{bmatrix}\Delta\underline{P}\\ \Delta\underline{Q}\end{bmatrix} = \underline{J}_A\begin{bmatrix}\Delta\underline{V}_L\\ \Delta\underline{\delta}_{Lr}\end{bmatrix} + \underline{J}_B\begin{bmatrix}\Delta\underline{E'}_q\\ \Delta\underline{\delta}_{qr}\end{bmatrix}$$

In the above equation, $\underline{J}_A$ is (2*NBUS) x (2*NBUS), $\underline{J}_B$ is (2*NBUS) x 19, and $\underline{C}_1$ is (2*NBUS) x 19. Upon computation of $\underline{C}_1$, the elements of $\underline{V}$ and $\underline{W}$ are extracted as follows :

For i = 1, 2, ..., 10 ,

$\underline{V}[i, 10*(i-1)+1] = \underline{C}_1[NBUS - NG + i, i]$

$\underline{W}[i, 10*(i-1)+1] = \underline{C}_1[2*NBUS - NG + i, i]$

For i = 1, 2, ..., 9 ,

$\underline{V}[i, 10*(i-1)+2] = \underline{C}_1[NBUS - NG + i, NG+i]$

$\underline{W}[i, 10*(i-1)+2] = \underline{C}_1[2*NBUS - NG + i, NG+i]$

The vita has been removed from the scanned document